STRUCTURAL PROPERTY IMPROVEMENTS TO AEROSPACE SANDWICH COMPOSITES USING Z-PINS

A thesis submitted in fulfilment of the requirements for
the degree of Doctor of Philosophy (Aerospace)

Asintha Medini Nanayakkara
B. Eng (Aero) (Hon 1st Class) (RMIT University)

School of Aerospace, Mechanical and Manufacturing Engineering
RMIT University
January 2013

DECLARATION

I certify that except where due acknowledgement has been made, the work is that of the author alone; the work has not been submitted previously, in whole or in part, to qualify for any other academic award; the content of the thesis is the result of work which has been carried out since the official commencement date of the approved research program; and, any editorial work, paid or unpaid, carried out by a third party is acknowledged.

Asintha Medini Nanayakkara
January 21st 2013

ACKNOWLEDGEMENTS

Firstly, I would like to thank Professor Adrian Mouritz for his unwavering direction and commitment towards this PhD thesis, his technical expertise, and his constant support and encouragement throughout my research career. Thank you for being ever supportive and understanding and for being a real inspiration. I have learnt many invaluable lessons from you. Secondly, I would like to thank Dr. Stefanie Feih for her constant support and invaluable input towards this PhD and also being consistently supportive and understanding. Thank you for all your valuable technical guidance and assistance. I would also like to thank the other staff at RMIT University for their support and guidance.

This project would not have been possible without the funding provided by the CRC-ACS (Cooperative Research Centre for Advanced Composite Structures) and RMIT University (Australian Postgraduate Award). I would also like to acknowledge the grant provided by the Australian Microscopy and Microanalysis Research Facility (AMMRF) for access to the micro-CT equipment at the University of Sydney.

I would like to thank Mr. Peter Tkatchyk and Mr. Robert Ryan for the technical assistance and expertise throughout the course of this project, for being ever helpful and accommodating during the seemingly endless hours of sample manufacturing and testing.

I would like to thank the Composites Team for their valuable input and support, and especially my fellow colleagues and friends at RMIT, specifically, Tze Min Koh.

I would like to thank my best friend Naadia Nawaz for being the rock that I could always lean on and the person that I can always talk to.

I would like to thank my friends Mohammed Al Fzari and Leeva Sheidaee for being incredibly supportive these past few years and for believing that I could accomplish this.

I would like to thank Vijay Balasingam for making this journey an easier one.

Finally I would like to thank my parents and my brother, especially my amazing parents without whom I would not be here today. Thank you for all your sacrifices and for your love.

Dedicated to my parents, Aruni and Nalaka Nanayakkara.

ABSTRACT

The general aim of this PhD project is to advance the science and technology of z-pinned sandwich composites by performing an in-depth investigation into their mechanical properties, strengthening mechanisms and damage modes. The PhD thesis presents a comprehensive and critical review of the published scientific literature into z-pinned sandwich composites. While past studies often report large improvements to the mechanical performance of sandwich composites due to z-pinning, the research is incomplete and gaps exist in the characterisation of these materials. The identification of these gaps in the characterisation of z-pinned sandwich composites provides the basis for the original research work performed in this PhD project.

The PhD thesis presents a study into the through-thickness compression properties, strengthening mechanisms and damage modes of a sandwich composite structure reinforced with orthogonal z-pins. It was found that less than 4% in z-pin volume content was required to increase greatly the compression modulus (up to 300%), strength (700%) and strain energy absorption capacity (500%). While the compression properties were found to be highly sensitive to the z-pin content, the properties were much less dependent on the end constraint (i.e. built-in column or unsupported column) and diameter of the pins. An investigation into the compressive failure mechanisms of the z-pins within the foam core using acoustic emission monitoring, scanning electron microscopy and x-ray computed microtomography revealed for the first time that the fibrous z-pins failed during both elastic and plastic deformation of the core foam via a complex damage process involving splintering, kinking and fragmentation. It is shown that existing models fail to accurately determine the compression properties due to the complex failure mechanism of the z-pins, which are not accounted for in the existing models.

The PhD thesis presents a comprehensive experimental study into the impact damage resistance, post-impact mechanical properties of z-pinned sandwich composites and localised loading behaviour, which has not been previously investigated to any great detail. The research showed that there was no improvement to the impact damage

resistance of the z-pinned sandwich composite at low impact energies (when damage was confined to the impacted face skin). The post-impact compressive stiffness and failure load for the z-pinned sandwich composite remained the same (within experimental scatter) as the unpinned material. Z-pinning was found to be only marginally effective at increasing the damage resistance when the impact energy was high enough to cause core crushing. This study showed that under a localised impact load, z-pins were not particularly effective at increasing the damage resistance or post-impact mechanical properties of sandwich composites and this is attributed to the small number of pins available to resist a localised (point) impact load. It was discovered that increasing the loading area improved the indentation stiffness and crush strength, and this was due to the increased number of z-pins resisting indentation. The experimental indentation results were further analysed against predictions using an indentation model for z-pinned sandwich composites.

As a final novel study, the effect of z-pinning on the mechanical performance of T-shaped bonded sandwich joints was investigated. Experimental testing revealed that the stiffness, ultimate load and absorbed energy capacity of the sandwich composite joint was improved by z-pinning. The failure load and energy absorption were increased by the z-pins suppressing skin-to-core failure by generating bridging traction loads through the foam core. Pin pull-out tests revealed that z-pins generated high mode I bridging traction loads during frictional pull-out from the face skins, and this increased the load capability and stabilised the fracture process of the sandwich joint. The improvements to the mechanical properties of the T-joint are discussed using mechanical models for the bridging laws of z-pins in composite materials. This research revealed for the first time that z-pinning could be used an as alterative to mechanical fastening for the high strength joining of T-section sandwich composite components.

The PhD thesis concludes with a summary of the major research findings, a discussion of future research directions into z-pinned sandwich composite panels and joints, and the remaining challenges in the certification of z-pinned sandwich composites for use in aircraft structures.

PUBLICATIONS

The following publications and conference presentations have resulted from the research performed as part of the PhD project:

Nanayakkara, A., Feih, S. and Mouritz, A.P., 'Improving the through-thickness compression properties of aerospace sandwich composites by z-pinning', Proceedings of the 21st Australasian Conference on the Mechanics of Structures and Materials, December 7-10 2010, Melbourne, Australia.

Nanayakkara, A., Feih, S. and Mouritz, A.P., 'Experimental analysis of the through-thickness compression properties of z-pinned sandwich composites', Composites Part A, Volume 42, Issue 11, pp. 1673-1680, 2012.

Nanayakkara, A., Feih, S. and Mouritz, A.P., 'Experimental impact damage study of z-pinned sandwich composites', Journal of Sandwich Structures and Materials, Volume 14 (4) , pp. 469-486, 2012.

Nanayakkara, A., Feih, S. and Mouritz, A. P., 'Improving the mechanical properties of sandwich composite T-joints by z-pinning', Composite Structures, Volume 96, pp. 207-215, 2013.

Nanayakkara, A., Feih, S. and Mouritz, A.P., 'Improving the mechanical properties of sandwich composite T-joints by z-pinning', Proceedings of the 8th Asian-Australasian Conference on Composite Materials, November 6-8 2012, Kuala Lumpur, Malaysia.

TABLE OF CONTENTS

List of Figures

List of Tables

Chapter 1 INTRODUCTION

1.1 SANDWICH COMPOSITES FOR AEROSPACE STRUCTURES

A sandwich composite consists of a lightweight core material combined with high strength and stiffness face skins. The core is a low density material intended to provide weight saving and carry shear loads. A range of materials can be used in sandwich construction to create a desired set of structural properties depending on the design criteria. Common cores include polymer foams and honeycomb materials, and they are covered with thin face skins which are usually a metal sheet or fibre-reinforced polymer laminate.

Sandwich composites have been used in aerospace structures for about 60 years. The first sandwich construction by the aerospace industry was during World War II when sections of the de Havilland Mosquito were constructed using plywood skins combined with a balsa wood core [1]. The industry has evolved into using metallic or polymer foam cores having honeycomb or cellular structures. As examples, the Boeing 747 aircraft uses honeycomb core sandwich composites in a few structural applications such as the fore flap, and many aircraft use sandwich construction for fuselage applications such as the Beech Starship (Nomex honeycomb core/graphite epoxy skins), Cirrus SR20 (PVC foam core/E-glass epoxy skins) and Hawker Horizon (Nomex honeycomb core/graphite epoxy skins). Sandwich composites are increasingly being used in the airframe and rotor blades of helicopters. For example, the Eurocopter NH90 uses Nomex/glass epoxy sandwich composites for secondary structures [2]. Eurocopter also uses sandwich materials in for some of its helicopter rotor blades such as the EC135 rescue helicopter [3]. Figure 1-1 shows the uses of sandwich composite materials in secondary structures on the Citation III business jet and in the blades and secondary structure of the EC135 helicopter. The utilization of these materials is typical for current aircraft structural applications.

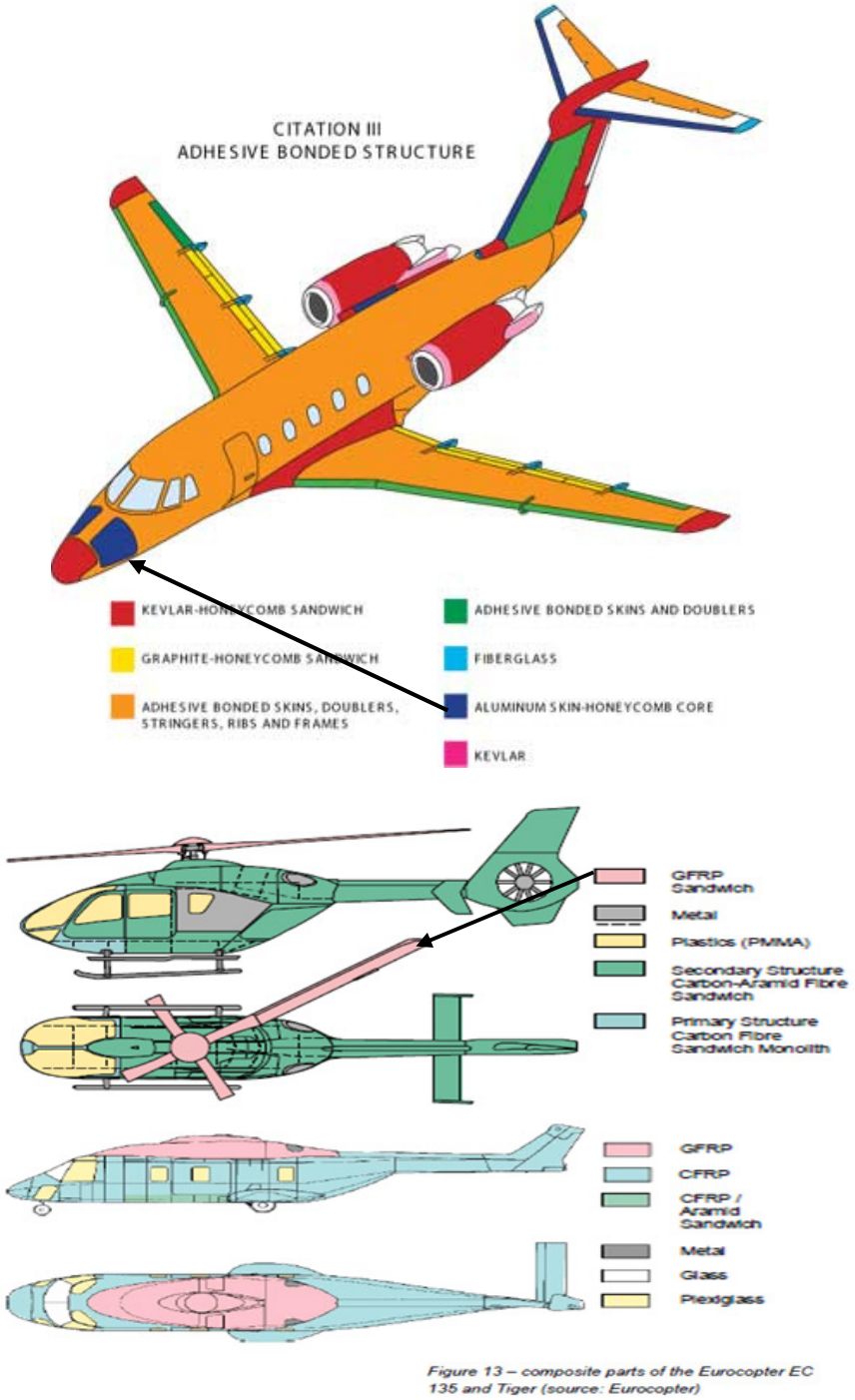

Figure 1-1: Sandwich Composite Applications in Aircraft (e.g. Citation III) and Helicopters (e.g EC135). Arrows point to the sandwich composite applications in the above image.

The low through-thickness mechanical properties of sandwich composites - such as low stiffness, strength and impact damage tolerance - are a long standing problem. Sandwich materials also have weak skin-to-core peel strength. For these reasons, sandwich composites are rarely used in primary (safety-critical) structures, and monolithic laminates or metal alloys are used instead. The conventional approach to increase the mechanical

properties of the core material is to increase its density. Properties such as the shear and compressive strengths are directly proportional to the bulk density of the core material. However, increasing the density adds to the weight of the sandwich composite, which is undesirable when used in large quantities on aircraft and somewhat defeats the purpose of using these materials in the first place. Alternative solutions to increase the mechanical properties of the core, without incurring significant cost and weight penalties, is an important and challenging goal for the aerospace industry. These problems have led to a growing field of research to investigate the reinforcement of sandwich composites in the through-thickness direction by stitching, weaving, tufting and z-pinning.

1.2 INTRODUCTION TO Z-PINNING

Z-pin technology emerged in the 1970's where small metal pins were investigated for their potential use in reinforcing composite laminates in the through-thickness direction [4]. The first z-pins were used in carbon/epoxy prepreg laminates to improve the interlaminar shear strength. Steel pins were inserted by Huang and co-workers [4] at +/-45° to the orthogonal direction to prevent delamination cracking and thereby improve the interlaminar shear strength. At the time, however, the technology did not exist to manufacture large quantities of this z-pinned material.

Following a period of apparent inactivity during the 1980s, z-pinning technology reemerged in the early 1990s when Aztex Inc (a small US-based technology company)[1] developed fine pins known as Z-Fibers®, which can be inserted through a stack of prepreg composite plies creating three-dimensional fibre reinforcement. Z-Fibers® and their method of insertion was patented by Aztex Inc in 1998 [5]. Z-pinning is the only method that can reinforce laminates and sandwich composites with carbon/epoxy prepreg skins in commercial quantities for aerospace applications. Z-pins are most commonly made with unidirectional carbon fibre composite for high stiffness and strength (see Figure 1-2), although other high performance materials (such as titanium alloy) are also used. Tomashevskii and co-workers [6-8] also developed a process for inserting thin metal wires in the through-thickness direction of composite materials to increase the interlaminar

[1] Aztex Inc was acquired by Albany Engineered Composites who are the manufacturer of Z-Fibers®.

fracture toughness. Unlike the Z-Fibers® technology developed by Aztex Inc., however, the process developed by Tomashevskii did not advance to commercialization.

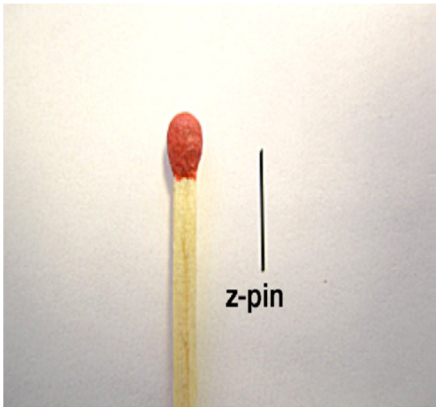

Figure 1-2: Photograph showing the size of a typical fibrous z-pin [9]

Conventional sandwich composites have high bending stiffness and in-plane mechanical properties, and (as mentioned) are widely used in structural applications because of their light weight. However, the core material has low mechanical properties, requiring reinforcement or a new design enhancement, especially in the through-thickness direction. Z-pins have been one of several methods investigated to reinforce sandwich composites in the through-thickness direction. Other methods include 3D weaving, stitching, tufting and Tycore® [9-33]. However, these methods are only suitable for sandwich composites with non-prepreg face skins, whereas many aircraft sandwich structures use prepreg-based laminate skins for higher structural performance.

Z-pins increase the through-thickness compression and flexural properties of sandwich composites [10, 34-38]. The z-pins are often arranged in an X-shaped configuration to maximize the in-plane shear properties of the core, although it is possible to use other configurations such as an orthogonal pattern whereby the pins are aligned parallel to the through-thickness direction [34, 37, 39-41]. Aztex Inc. developed two types of structural sandwich composites known as X-Cor™ (Figure 1-3) and K-Cor™ (Figure 1-4). The z-pins are inserted through both the face skins and core (X-cor™) or inserted through the core only with the skins being unpinned and the pins folded over the core (K-Cor™) [42].

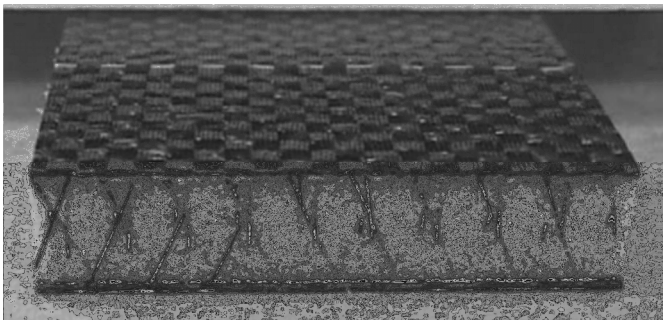

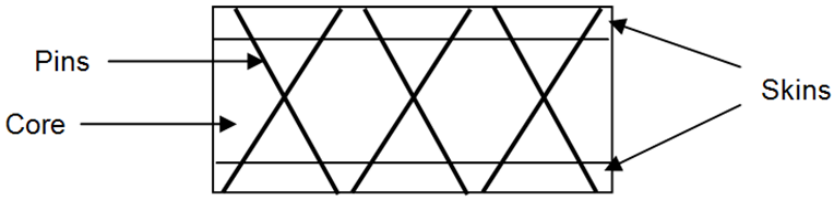

Figure 1-3: X-Cor^{IM} [43]

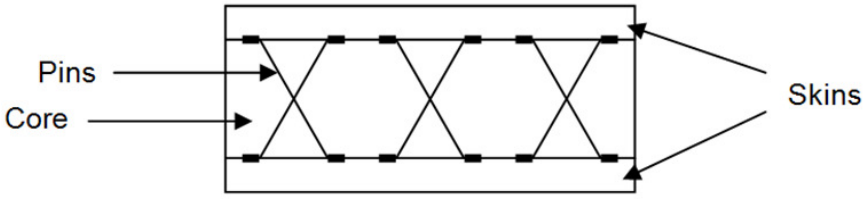

Figure 1-4: Schematic of K-Cor

Large improvements to the mechanical properties of sandwich composites have been achieved using z-pin reinforcement, including increased impact damage resistance, in-plane shear properties, and skin-to-core delamination strength [34, 37-41, 44-46]. Z-pins also increase the transverse (or through-thickness) compressive properties of sandwich composites, which can improve their crush resistance under impact loads [26, 32, 45, 47]. Large improvements to the through-thickness compressive modulus, strength and absorbed energy of sandwich composites were found when reinforced with titanium pins [34]. The effect of z-pin reinforcement on the structural and damage tolerant properties of sandwich materials is reviewed in greater detail in the next chapter.

Z-pins are also useful to replace fasteners and bolts in structural joints, leading to weight savings. Currently z-pins are used instead of the titanium fasteners in the air inlet ducts and bay doors of the F/A-18 E/F Superhornet aircraft, which are made using carbon fibre/epoxy laminate [42, 48] (Figure 1-5). The use of z-pins in the F/A-18 Hornet results

in a cost saving of about US$83,000 and a weight saving of 17 kg for each fighter [43]. Z-pins are also used in the cargo doors of the C17 Globemaster, which are also made of carbon/epoxy laminate (Figure 1-6). The only publicly disclosed aerospace application of z-pinned sandwich composites is the UH60M Black Hawk, which uses X-cor™ composite components in its tail cone that provides a weight saving of 21 kg compared to conventional sandwich construction (Figure 1-7). Z-pins are also used in the composite roll-over bars of Formula One racing cars [49].

Figure 1-5: F/A-18 E/F Superhornet use z-pinned laminates in the air inlet ducts

Figure 1-6: C17 Globemaster uses z-pinned laminates in the cargo bay doors

Figure 1-7: UH60M Black Hawk uses z-pinned sandwich composites in the tail cone

The use of z-pinned laminates and sandwich materials by the aerospace industry, despite being limited, has the benefit of practically demonstrating the advantages of using these materials, and this may lead to more applications in the future. The aerospace industry is traditionally conservative in the use of new materials due to cost, certification, manufacturing, and safety issues. Z-pinned sandwich composites are still not fully understood by many parts of the industry. Z-pinned sandwich composites are a relatively new class of advanced materials that require significant research into their properties before the industry is likely to gain confidence and understanding of their benefits over traditional sandwich materials.

1.3 AIM OF PhD RESEARCH

The general aim of this PhD project is to investigate the effect of z-pins on the structural properties, strengthening mechanisms and failure modes of sandwich composite structures and their joints. The z-pins are embedded in the orthogonal direction of a typical aerospace sandwich composite consisting of face skins made of carbon fibre/epoxy laminate and a lightweight core of polymer foam.

An objective of this project is to critically review published scientific and technical studies in z-pinned sandwich composites to assess the current state-of-the art as well as identify important gaps in the characterisation of these materials which require further investigation. Some of the gaps that are identified are then researched as part of this project. Specifically, the research performed as part of this PhD aims to assess the effect of z-pinning on the through-thickness mechanical properties, in-plane mechanical properties, and impact damage tolerance of sandwich composites. The PhD also aims to evaluate the effect of z-pinning on the structural properties of sandwich composite joints. Thus far, the influence of orthogonal pins on the through-thickness stiffness, strength and strain energy properties; in-plane stiffness and failure strength properties; impact damage resistance and post-impact mechanical properties; and joint properties of sandwich composites has been investigated to a limited extent only or not investigated at all.

The stiffening and strengthening mechanisms of z-pins will be investigated and mechanical models for predicting the stiffness and strength properties of z-pinned sandwich

composites will be assessed. Therefore, the PhD aims to collate a large body of experimental data to undertake a rigorous validation of mechanical models to ascertain whether they are capable of accurately predicting the properties of z-pinned sandwich composites. This PhD also aims to clearly identify the strengthening and failure mechanisms of z-pins under different loading conditions (including impact) with the aim to develop mechanical models which are more mechanistically-based than many existing models.

It is expected that this PhD work will make a significant and original contribution to the field of z-pinned sandwich composites which will bring these materials closer to aerospace applications.

1.4 STRUCTURE OF PhD THESIS

Following this chapter, the PhD thesis is structured into chapters which each deal with separate aspects of z-pinned sandwich composites.

Chapter 2 provides a comprehensive literature review of published research on z-pinned sandwich composites and, where relevant, z-pinned laminates and other reinforcement techniques. The literature review summarizes the findings of the behaviour of sandwich composites under compression loading, impact and indentation loading and post-impact mechanical properties, including the analytical models available thus far to predict the properties of z-pinned composites. The limited literature available on joining sandwich structures is also reviewed and the manufacturing techniques utilized to z-pin laminates and sandwich structures are described.

Chapter 3 presents a research investigation into the through-thickness stiffness, strength and absorbed energy of z-pinned sandwich composites with different parameters such as z-pin volume content and z-pin diameter. Non-destructive inspection techniques, microstructural analysis and finite element modelling are used to identify the failure mechanisms of z-pins under compression loading. In addition, mechanical and finite element models are used to predict the compression properties. A complete

characterisation of the existing mechanical models to predict the through-thickness stiffness and strength of z-pinned sandwich composites is undertaken.

Chapter 4 investigates the static indentation resistance, impact resistance, and post-impact mechanical properties of sandwich composites. The indentation resistance of z-pinned sandwich composites under three different contact conditions (spherical, cylindrical and flat plate) is investigated and analysed using existing mechanical models. Two impact energy regimes are investigated; low (<25J) and high energy (>25J). The damage sustained, the absorbed energy characteristics and failure modes of z-pinned composites under in-plane loading conditions are investigated.

Chapter 5 investigates the effect of z-pinning on the mechanical properties and strengthening mechanics of sandwich T-joints. The strengthening and failure mechanisms of z-pinned T-joints (z-pinned along the bondline) are investigated, and compared against an unpinned joint. The bridging traction mechanics of z-pinned sandwich panels are determined (both experimentally and analytically) to explain the strengthening effect of z-pins within a sandwich T-joint.

This PhD thesis concludes with several recommendations for future work and a discussion of the design processes and certification requirements of using z-pins in aerospace sandwich structures.

Chapter 2 LITERATURE REVIEW

ABSTRACT

The chapter presents a comprehensive and critical review of the published scientific literature into z-pinned sandwich composites. The objective of this chapter is to identify research progress towards the modelling and experimental characterisation of z-pinned sandwich materials. Another aim is the identification of gaps in the current body of knowledge pertaining to z-pinned sandwich composites, which then establishes the direction for the research studies performed as part of the PhD project.

The literature review examines the manufacturing processes, microstructure and mechanical properties of z-pinned sandwich composites and, when relevant, z-pinned laminates. Certain studies conducted on z-pinned laminates provide useful insights into the manufacture of z-pinned sandwich materials and other studies into the microstructure, interlaminar toughness and mechanical properties of the z-pinned face skins. Studies of the through-thickness mechanical properties of z-pinned sandwich composites are thoroughly reviewed, including the effect of z-pins on properties such as the stiffness, strength and strain energy capacity. Studies conducted on the impact damage properties and the indentation resistance of z-pinned sandwich composites are also reviewed. Mechanical models for calculating the through-thickness properties of z-pinned sandwich composites are described and their accuracy assessed. Lastly, research into the effect of z-pinning on the structural properties of bonded composite joints is reviewed. The identification of gaps in the mechanical characterisation of z-pinned sandwich composites provides the basis for the research work performed in this PhD project.

2.1 MANUFACTURING PROCESSES FOR Z-PINNED COMPOSITES

There are two production methods for inserting z-pins into a composite preform; whether the preform is a laminate or sandwich material. One method to insert the z-pins uses an autoclave and the other method is called the Ultrasonically Assisted Z-Fiber® process.

In the autoclave process (Figure 2-1), a foam carrier containing the required volume content of z-pins is placed over the assembled, uncured prepreg laminate or sandwich composite structure, secured in place, and then compressed under the overpressure applied by the autoclave [50]. The z-pins are driven into the uncured composite under the applied pressure. The pressure must be below the crush pressure of the core material when z-pinning a sandwich material to avoid damage. Because the overpressure must be reasonably low, it is then difficult (if not impossible) to drive the z-pins through the entire thickness of a sandwich composite, which is often very thick. The heat within the autoclave ensures that the uncured laminate face skins are pliable (due to viscous softening of the uncured polymer matrix) which eases the insertion of the z-pins. Any excess carrier foam is then removed and protruding z-pins can be shaved or sanded off. This method of manufacturing z-pinned composites is not widely used and is not currently applied to the manufacture of z-pinned sandwich composites.

The second method for fabricating z-pinned laminates and sandwich composites is the Ultrasonically Assisted Z-Fiber® (UAZ®) process, which was developed and patented by Aztex Inc. [36, 51-53]. The z-pinning process starts by placing a foam carrier containing the z-pins over the uncured composite. The z-pins are arranged in a grid pattern inside the foam carrier to the specific volume content, as shown in Figure 2-2a. The foam is used to ensure an even spacing between the z-pins and to provide them with lateral support during insertion. The foam carrier does not form part of the final composite product, and is discarded after the z-pins have been inserted. The z-pins are driven from the foam carrier into the uncured sandwich material using an ultrasonic tool (Figure 2-2b) that generates high frequency compressive waves (~20 kHz). The device can be hand-held and operated manually or incorporated into an automated process. The foam carrier collapses under the acoustic pressure that drives the z-pins into the uncured composite. Z-pins are inserted progressively by moving the ultrasonic tool over the foam carrier several times until all the pins have fully penetrated the sandwich composite. The compressed foam carrier and any excess length of z-

pins protruding from the face skins are then shaved off to provide a smooth surface finish. After z-pinning the composite, a final ply is often laid on the outer surfaces of the material which is then cured inside an autoclave. The main steps of the UAZ® process are shown sequentially in Figure 2-3.

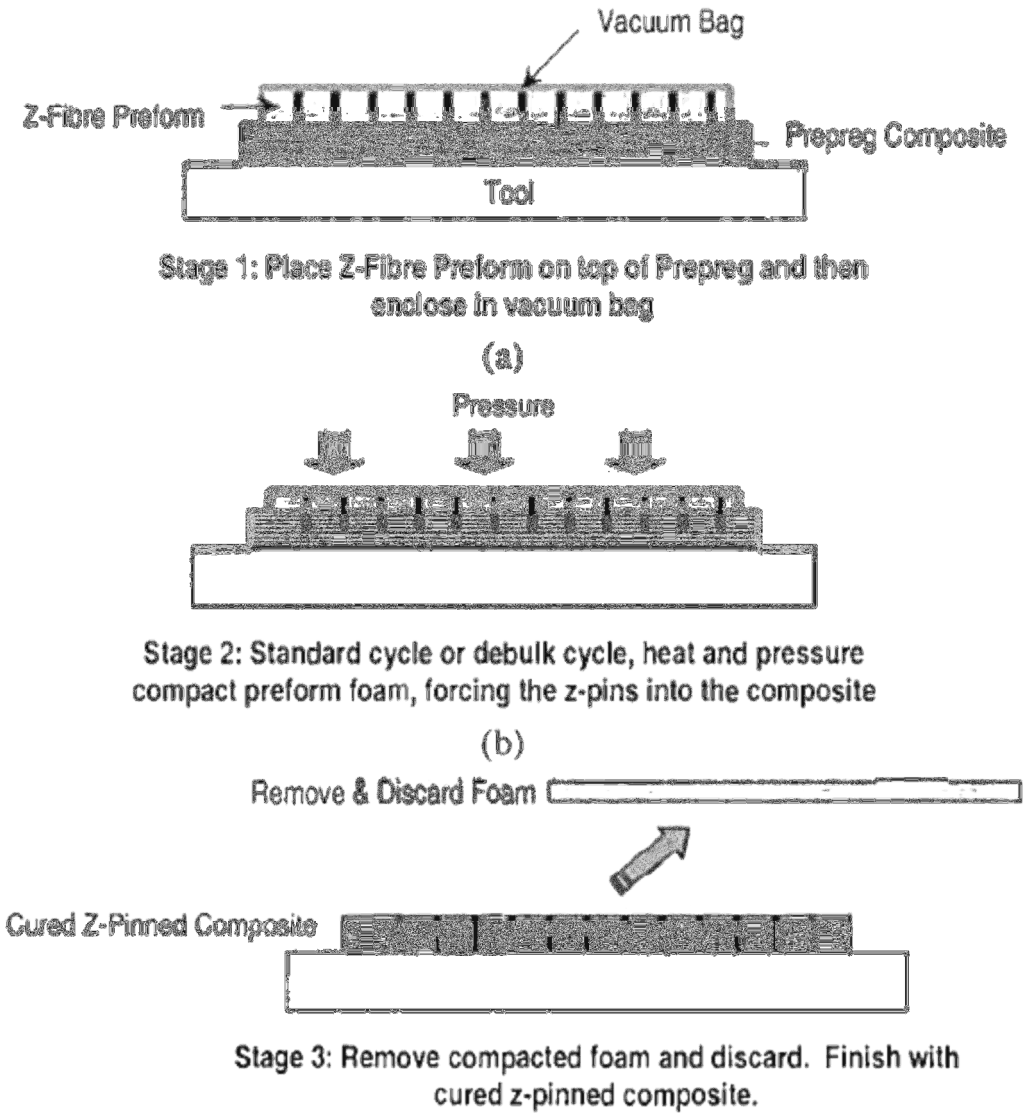

Figure 2-1: Schematic of autoclave process for z-pinning [42]

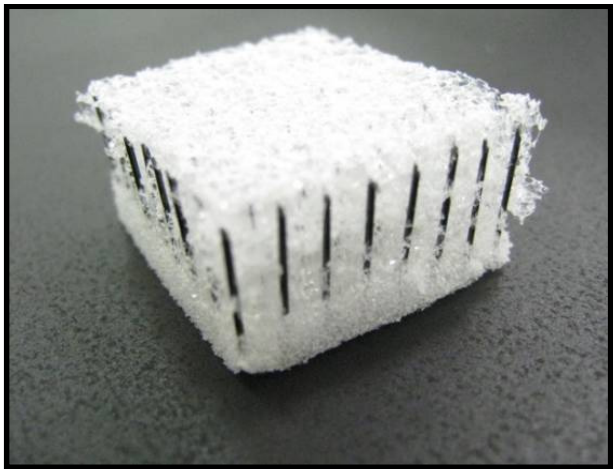

(a)

(b)

Figure 2-2: (a) Collapsible foam carrier containing z-pins and (b) Hand-held ultrasonic tool

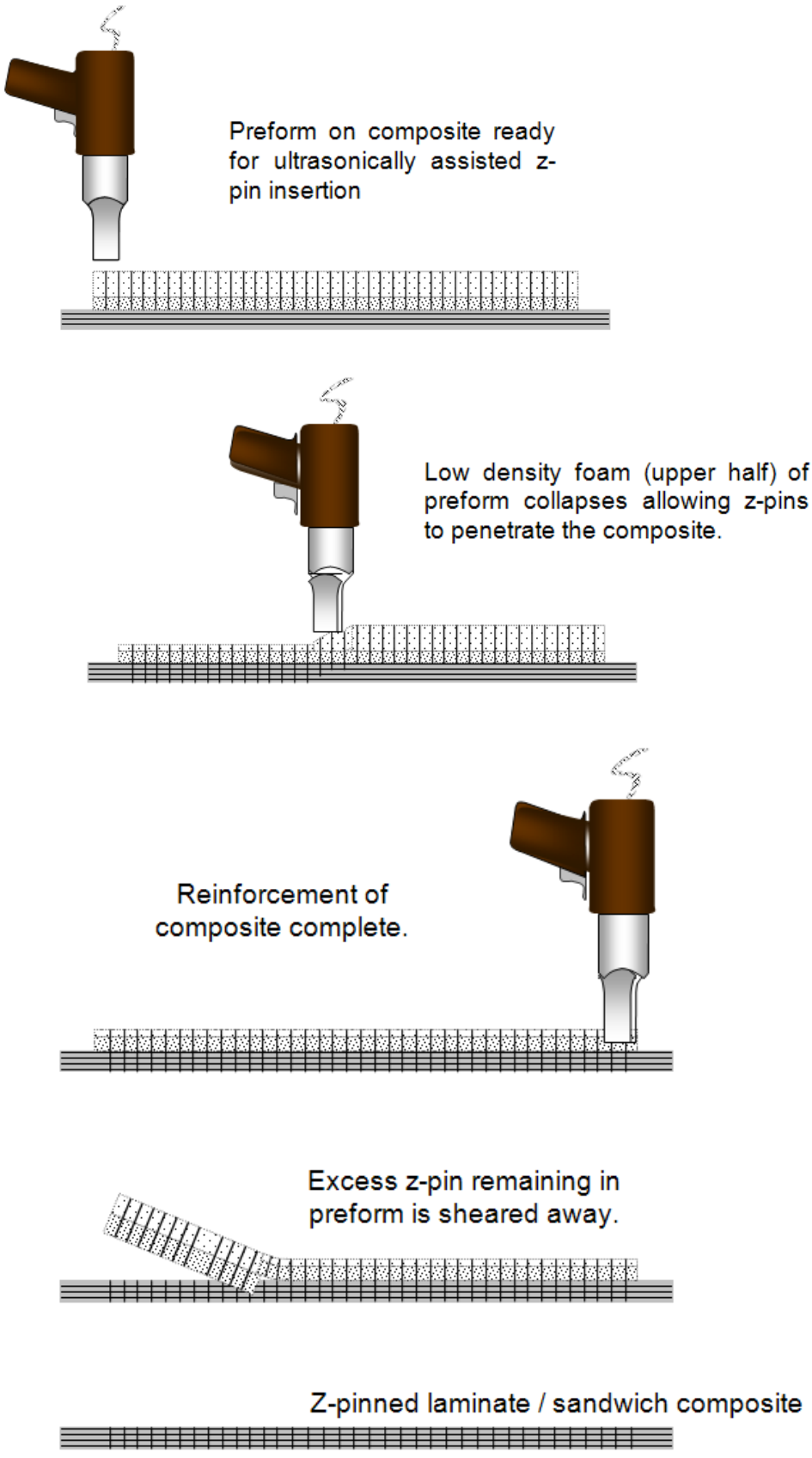

Figure 2-3: Schematic of the UAZ® process for z-pinning. [9]

Both the autoclave and UAZ® methods require the uncured composite to be debulked before z-pinning, otherwise porosity can occur. It is difficult to remove voids after z-pinning due to the presence of the high stiffness pins now embedded in the composite. Also, with both the manual and automated processes it becomes difficult to insert the pins with increasing pin thickness and pin volume content. (The process for the manufacture of z-pinned sandwich composites used in this PhD project is explained in Chapter 3).

2.2 MICROSTRUCTURE OF Z-PINNED SANDWICH COMPOSITES

To gain a better understanding of the mechanical behaviour of z-pinned composite materials, a thorough investigation into the microstructural changes caused by z-pinning is required. The effect of z-pinning on the microstructure of sandwich composites has not been characterized. However, research into the microstructural defects caused by the z-pinning of laminates provides an understanding into how the face skins are likely to be affected [9, 35, 36, 43, 54-57]. From the microstructural characterisation work on laminates, it can be summarised that the most significant effects of z-pinning are fibre waviness and crimp, broken fibres, resin-rich zones, misaligned pins, and interfacial cracks between the pins and composite. There is no published information on the microstructural damage caused to core materials by z-pinning.

2.2.1 Fibre Waviness Caused by Z-Pins

Fibre waviness is defined as the in-plane crimp of straight fibres by a z-pin [54]. Fibre waviness is a common microstructural defect in z-pinned laminates and may be expected in the face skins to sandwich composites. Fibre waviness occurs in a region around the z-pin where the laminate fibres are pushed aside during pin insertion, which can also cause another type of microstructural defect known as resin-rich zone, which is explained later. The angle of fibre waviness, θ, is reported to be highest along the flanks of the resin-rich region around a z-pin, as seen in Figure 2-4 [9, 54]. The angle of fibre waviness and the length of the wavy region increase with the pin diameter [54]. The angle is also dependent on the type of fabric or prepreg, with the fibre stiffness and fibre packing density both affecting the extent of waviness [9]. For example, Figure 2-6 shows planar views of z-pins within unidirectional

tape and woven fabric laminates. Fibre waviness around the z-pins in tape laminates is usually symmetric due to the near uniform areal distribution of fibres whereas in fabric laminates the fibre waviness is non-symmetric due to pre-existing waviness and the non-uniform fibre distribution (due to the tows) [58]. Fibre waviness is also seen in other types of three-dimensional fibre composites such as stitched and tufted composites [42].

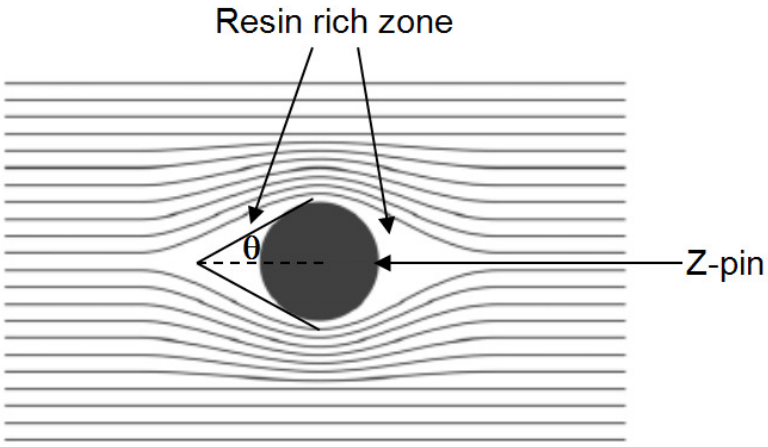

Figure 2-4: Fibre waviness angle around a z-pin (adapted from [54])

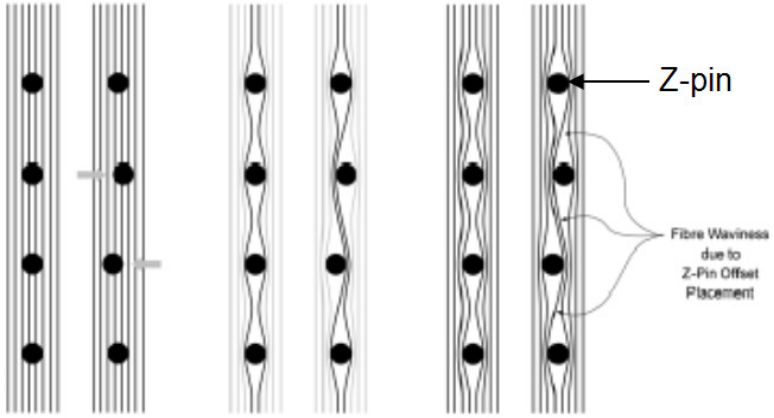

Figure 2-5: Continuous fibre waviness [54]

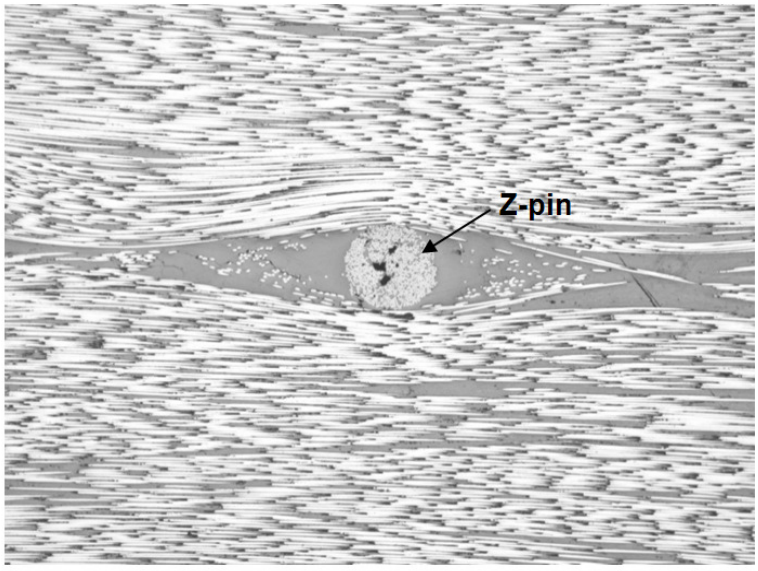

(a)

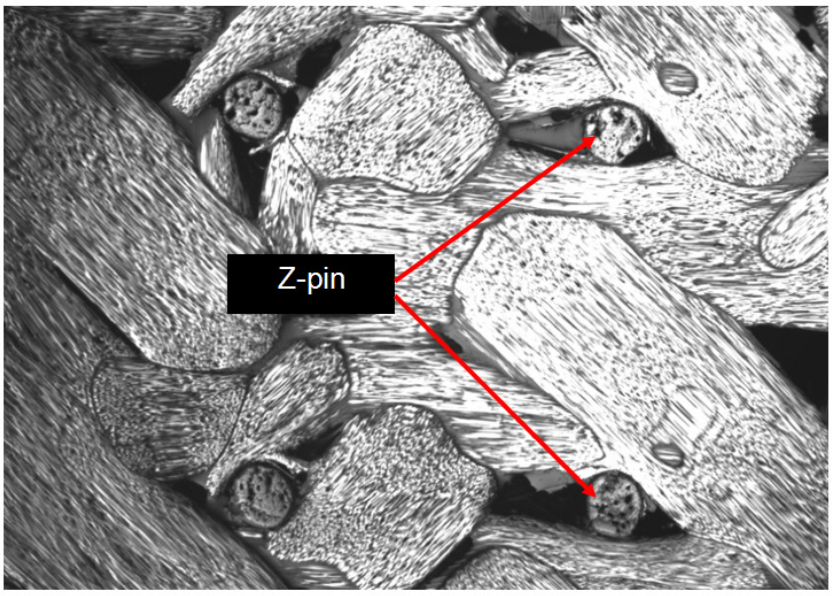

(b)

Figure 2-6: Examples of (a) symmetric and (b) non-symmetric fibre waviness caused by z-pins in unidirectional and woven laminates, respectively.

2.2.2 Fibre Crimp Caused by Z-pins

Fibre crimp is created when the insertion of z-pins results in fibre misalignment in the out-of-plane (or through-thickness) direction, as shown schematically in Figure 2-7. When z-pins are inserted they create both in-plane waviness and out-of-plane crimp of the prepreg ply fibres. Steeves and Fleck [58] report that crimped fibres may break when bent excessively

through a tight angle, and that the lay-up pattern (such as cross-ply) may help inhibit the crimping effect [59].

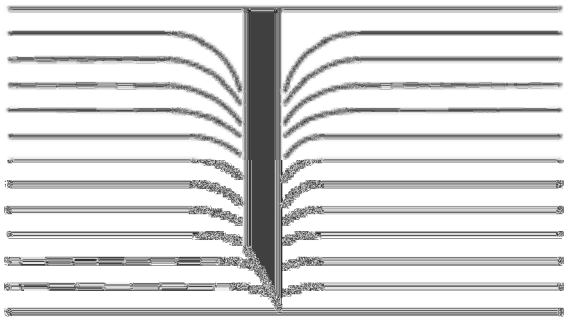

Figure 2-7: Fibre crimp [54]

2.2.3 Resin-Rich Zones Caused by Z-pins

Resin-rich zones are common in z-pinned laminates where the pins have pushed aside or crimped the fibres which creates a small gap that is filled with polymer resin during curing (Figure 2-8). The zones have an eyelet shape which is elongated in the fibre direction. Resin-rich zones can be quite large relative to the fibre diameter, and are dependent on the pin diameter. Higher pin volume content also results in a larger number of resin-rich zones, which may then result in a continuous resin-rich channel where the zones have coalesced along a row of pins aligned along the fibre direction [56].

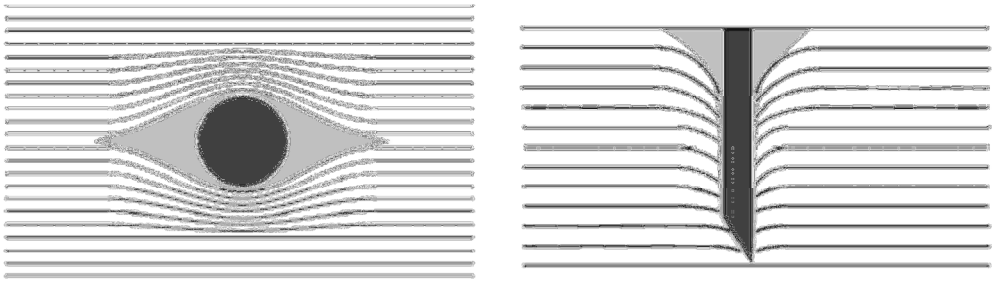

(a) (b)

Figure 2-8: Fibres deflected by pin insertion, creating resin-rich zones represented by the grey area. (a) In-plane fibre waviness (b) Out-of-plane fibre crimp [54]

2.2.4 Broken Fibres Caused by Z-pins

Broken or damaged fibres can occur during the z-pinning process. The insertion of z-pins generates sliding friction at the pin-laminate interface that can damage fibres in the prepreg plies. The insertion process, pin diameter, resin viscosity and fibre packing density are factors controlling the amount of fibre damage. During insertion, the z-pins are forced through a stack of uncured prepreg plies under a moderately high force which can result in the pin leading edge pushing on fibres which may then bend and break [36, 54, 58].

2.2.5 Misaligned Z-Pins

The UAZ® process is designed to ensure that all z-pins are embedded in the orthogonal direction of the composite material. However, z-pins are often inclined from the orthogonal direction over a range of angles up to as high as 30^{o}. For example, Figure 2-9 shows an inclined z-pin in a carbon-epoxy laminate and a histogram showing the population distribution of z-pins offset at various angles from the orthogonal direction. Chang et al. [57] performed an investigation into the causes for z-pin offset in carbon-epoxy laminates, and found that the two main causes were the trimming of segments of the pins protruding from the surface after insertion and the pressure applied during consolidation of the z-pinned preform in the autoclave. Trimming applies a lateral force on the z-pins which causes them to be displaced from the orthogonal direction while the consolidation pressure compacts the uncured preform which forces the pins to be displaced at an angle. Chang et al. [57] also found that the average inclination angle of the z-pins increased with their diameter.

While the misalignment of z-pins in laminates has been thoroughly studied, the offset of pins in sandwich composites has not been investigated. Despite this, the study of laminates provides some insight into the offset of z-pins within the laminate skins to a sandwich composite due to similarities in the z-pinning and curing processes.

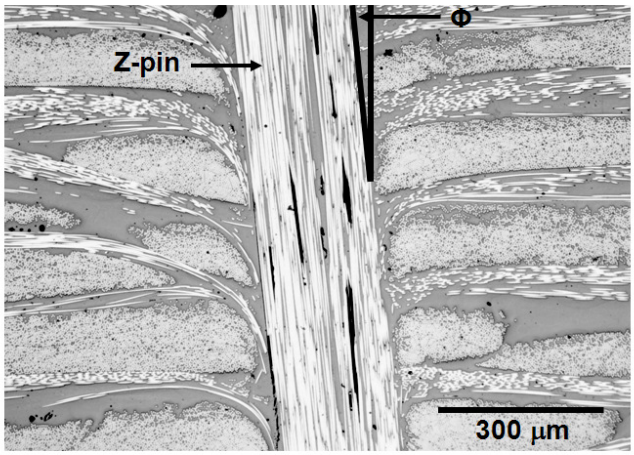

(a)

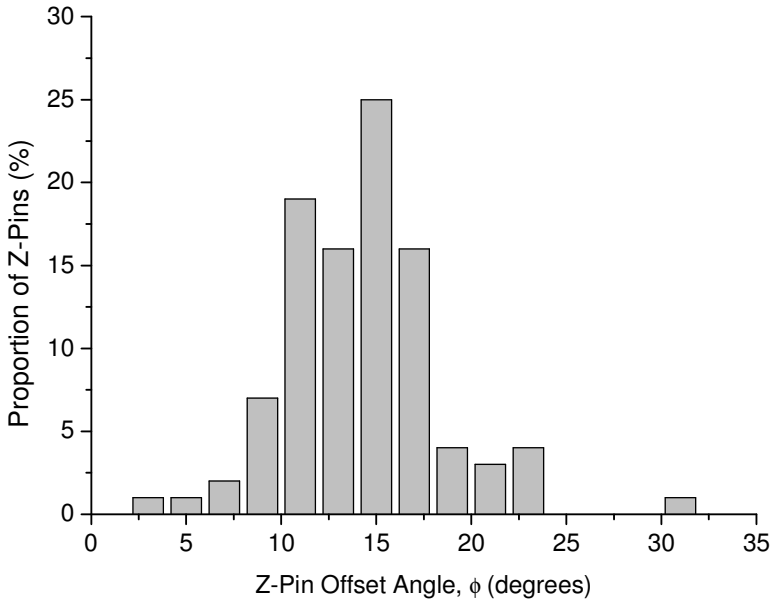

(b)

Figure 2-9: (a) Pin offset and (b) histogram showing the pin distribution angles for a carbon-epoxy laminates [55]

2.2.6 Interfacial Cracks Caused by Z-pins

Interfacial cracking between the z-pins and laminate can occur due to differences in their thermal expansion coefficients (Figure 2-10). Z-pins have a lower thermal expansion coefficient in the through-thickness direction of the laminate and therefore undergo smaller changes in length during the heating and cooling phases of the cure process. Upon cooling

from the cure temperature, the laminate experiences a larger contraction resulting in an axial compression stress in the pins and tensile stresses in the laminate. This tensile stress can be greater than the failure stress of the polymer matrix and therefore cracking occurs at or near the z-pin/laminate interface [60]. Interfacial cracking is often found in z-pinned laminates, but has not been investigated for z-pinned sandwich composites. It is possible that cracks may occur between the z-pins and laminate skins and between the pins and core material, although this has not been researched.

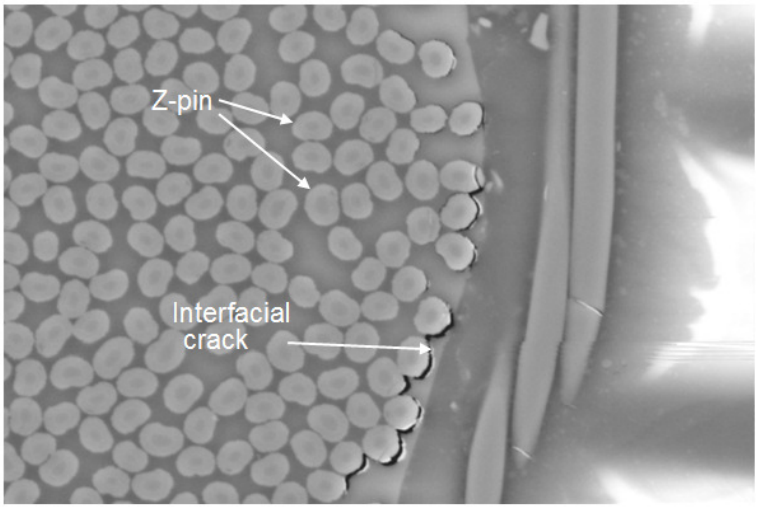

Figure 2-10: Cracking at the z-pin/laminate interface [60]

2.2.7 Volumetric Swelling Caused by Z-Pins

The insertion of z-pins can result in volumetric swelling of the laminate and thereby cause a reduction in the average fibre volume content [43, 55, 61]. This effect becomes more pronounced with increasing z-pin content. A study conducted by Chang [54] reports that the swelling can occur due to the laminate expanding to accommodate the z-pins and the prepreg plies resisting compaction during cure due to the stiff pins propping the mould surfaces. To prevent volumetric swelling, particular care must be taken during the manufacturing and cure processes.

2.3 MECHANICAL PROPERTIES OF Z-PINNED COMPOSITES

The mechanical properties of z-pinned sandwich composites have been investigated to some extent over the past ten years, although a complete characterisation of these materials is lacking. The effect of z-pins on the through-thickness mechanical properties of sandwich composites has been investigated more thoroughly than other properties such as the in-plane mechanical properties and impact damage resistance. The effect of z-pinning of bonded sandwich joints has not been investigated at all. This section presents a review of published research work into the mechanical properties of z-pinned sandwich composites and, when relevant, z-pinned laminates (which can provide an understanding into the mechanical behaviour of the face skins).

2.3.1 Delamination resistance

Z-pins can increase greatly the delamination resistance by raising the interlaminar fracture toughness of laminates [51, 53, 62-66]. Delamination is one of the major contributors to the degradation of the mechanical properties (particularly compression and interlaminar shear strengths) of composite structures, and therefore a large amount of research into the interlaminar toughness properties and delamination toughening mechanisms using z-pins has been performed. The delamination resistance of the skins to z-pinned sandwich composites has not been investigated, although the work on laminates provides an understanding of the interlaminar toughening effect caused by pins.

Z-pins are highly effective in retarding the growth of long delamination cracks (typically above 5-20 mm) in laminates, but are not as effective against short cracks [36, 67-69]. Z-pinning improves the interlaminar fracture toughness under mode I, mode II and mixed mode I/II load conditions. The delamination toughness of laminates usually increases linearly with the volume content of z-pins, as shown for example in Figure 2-11. In this example the mode I delamination toughness doubles for every 0.5% increase in the pin content whereas the increase in mode II toughness is less rapid but still significant. This difference occurs because orthogonal z-pins are more efficient at restricting crack opening (mode I) than crack sliding (mode II) displacements. It has also been found that z-pins slow the delamination crack growth rate under mode I interlaminar cyclic stress loading [53]. This is an advantage for aerospace structures where many structural components undergo fatigue loading.

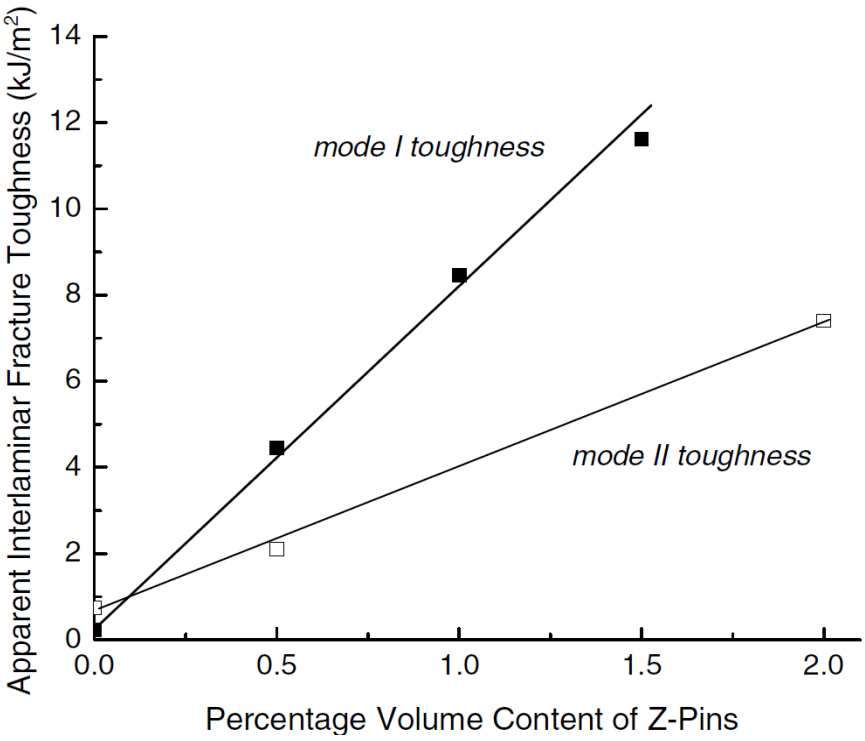

Figure 2-11: Effect of volume content of z-pins on the modes I and II interlaminar fracture toughness of a carbon-epoxy laminate [9]

The increase to the mode I interlaminar fracture toughness and fatigue resistance is attributed to the following crack bridging toughening mechanisms: elastic deformation, debonding and frictional pull-out of the z-pins. As a delamination grows in length a pin bridging zone is created along the crack wake, as shown in Figure 2-12. Z-pins generate traction loads that lower the stress at the crack tip and thereby increase the interlaminar toughness and fatigue resistance. The traction load is generated by the resistance of the z-pins against elastic deformation until they debond from the laminate, and then the traction load is generated by friction stresses as the pins are pulled from the laminate under increasing crack opening displacement. The pins stop generating traction loads when they are pulled completely from the laminate, as shown in Figure 2-13. In some cases the pins are broken, rather than pulled out, and this occurs when the tensile failure stress of the pin is less than the friction pull-out stress. This rarely occurs in thin laminates, although pin fracture becomes increasing more common when the thickness of the laminate is increased [70]. Z-pins are only effective when the crack is large enough for the bridging traction zone to be fully developed, which is typically between 5 and 20 mm long (depending on the pin content).

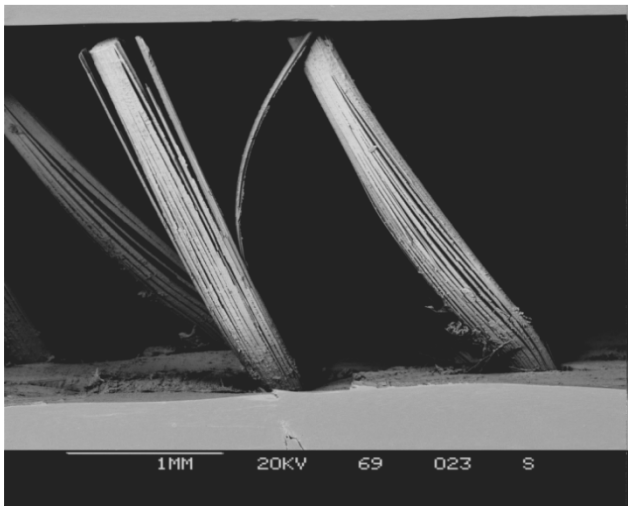

Figure 2-12: Z-pins bridging a delamination crack

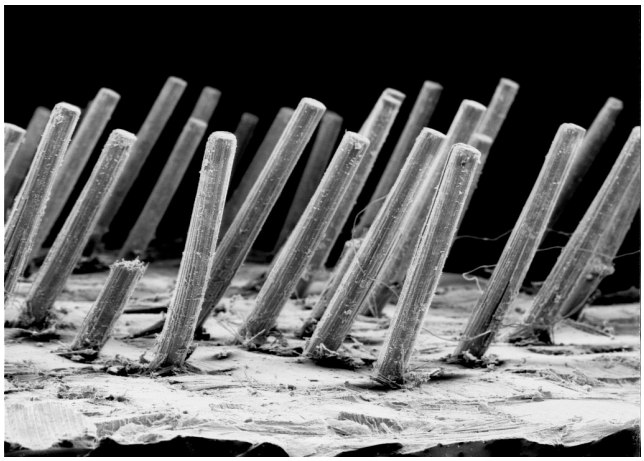

Figure 2-13: Pull-out failure of z-pins

The mode II interlaminar toughness properties of z-pinned laminates have also been extensively studied [65, 66, 71-73], and the main toughening mechanisms are elastic shear deformation, debonding, snubbing, and shear induced pull-out of the pins. Snubbing is a toughening process where crack sliding displacements become large enough to force the z-pins to press into the laminate near the crack plane [74] resulting in a large increase (typically 3-10 times) to the friction stress opposing pin pull-out.

The interlaminar toughening that is achieved by z-pinning can be related directly to the bridging traction loads, which can be determined by measuring the pull-out force for a z-pin under mode I or II loading conditions. The typical traction load-crack opening displacement response of a z-pin under mode I loading is presented in Figure 2-14. The bridging traction

load is determined by the experimental testing of one or several z-pins in a pull-out event. Experimental studies have been conducted and theoretical models have been developed to calculate the bridging traction loads [62, 72, 75, 76]. However, no studies have been conducted into the bridging traction loads and laws of z-pins in a sandwich composite, where the core and two face skins contribute to the interlaminar toughening effect.

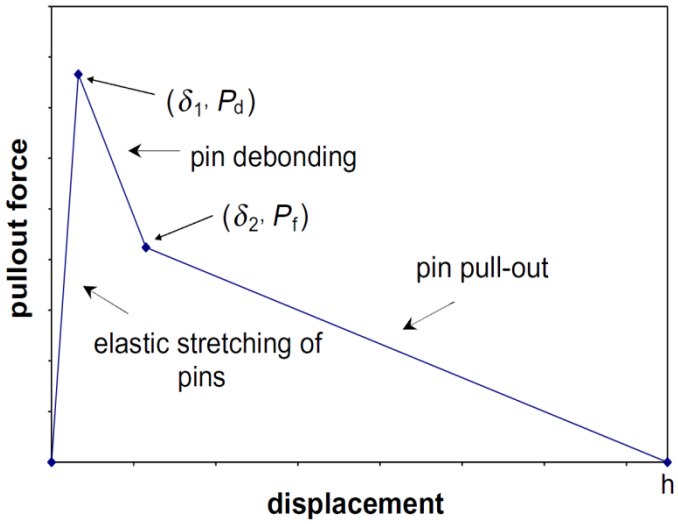

Figure 2-14: Simplified z-pin traction load curve for pin pull-out under mode I interlaminar loading [76]

2.3.2 Impact damage properties

The low impact damage resistance and post-impact mechanical properties of laminates and sandwich composites has been a long-standing problem with aircraft structures due to bird strike and other impact events. The most insidious type of impact-induced damage is often delamination cracking because it is difficult to observe visually and can reduce the in-plane properties. Z-pinning significantly improves the delamination toughness properties of composites which thereby improves resistance against delamination cracks caused by impact loading. The effect of z-pinning on the impact damage resistance of laminates has been studied to a much greater extent than for sandwich composites. Research has shown that z-pinning reduces the delamination damage to laminates caused by low speed objects, ballistic projectiles and hail damage [9, 32, 43, 50, 62, 67, 69]. Impact damage to a z-pinned laminate is often lower than the unpinned material, particularly when the delaminations are long

enough to allow the formation of a long bridging traction zone. Damage area reductions of about 20% to 65% have been reported by Zhang et al [32] for z-pinned carbon-epoxy laminate subjected to low-energy impacts. For hailstone impact the damage area is reduced by between 30% and 50% due to z-pinning [50]. Isa et al. [78] reported that the impact damage resistance increases with the volume content of z-pins, as shown for example in Figure 2-15 for barely visible impact loading of a carbon-epoxy laminate. In all cases, the reduction in damage area is due to bridging traction loads generated by z-pins. The total traction load increases with the z-pin content resulting in a corresponding reduction to the amount of delamination damage caused by an impact event. As mentioned, z-pinning is not effective at increasing the interlaminar toughness of materials containing short delaminations (less than ~5-20 mm), and consequently z-pins do not improve the damage resistance for short cracks but are highly effective at resisting large-scale cracking (as shown in Figure 2-15), which causes the greatest reduction to the post-impact properties.

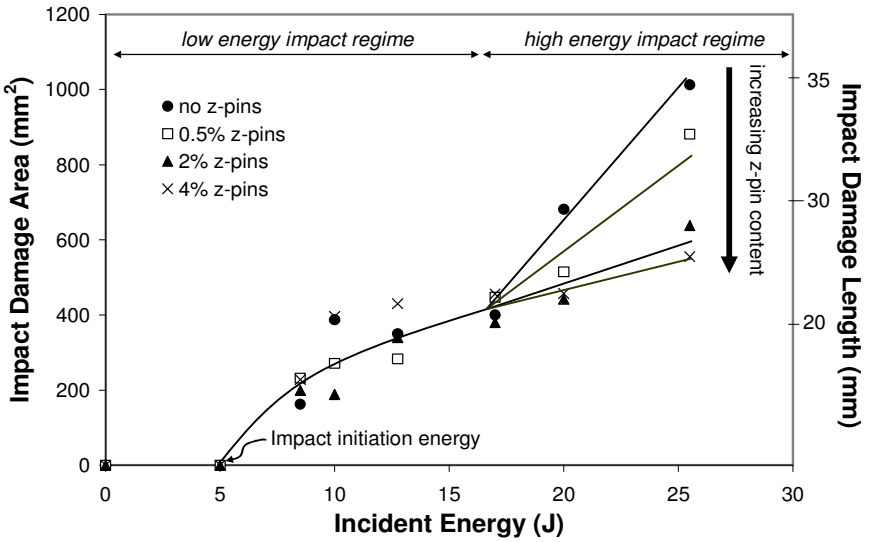

Figure 2-15: Effect of increasing impact energy and z-pin content on the amount of the delamination damage to a carbon-epoxy laminate [77].

The improvement to the impact damage resistance due to z-pinning often results in improved post-impact mechanical properties of laminates [32, 36, 64, 69]. For instance, Figure 2-16 shows that z-pinning increases the post-impact residual compressive strength of a carbon-epoxy laminate, with the improvement increasing with the z-pin content. This is a result of the reduction to the delamination damage caused by impact loading due to the z-pins

generating bridging traction loads. The traction loads also resist compressive buckling of the delaminated plies in the z-pinned laminate which increases the compressive failure stress.

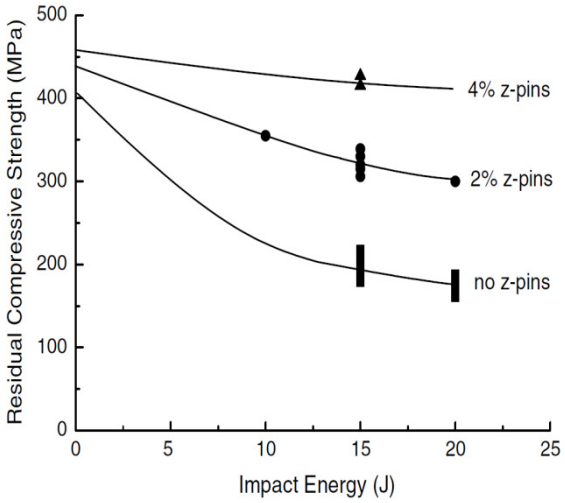

Figure 2-16: Post-impact mechanical properties [69]

In the study of the impact damage resistance of z-pinned materials, laminates have been more extensively studied than sandwich composites. Only two studies have been conducted on the impact damage resistance of z-pinned sandwich composites, and it was found that z-pinning reduces the amount of impact damage [26, 46]. Furthermore, it was found that z-pinning improves the crush resistance and absorbed energy of sandwich composites under impact loading [34, 46]. However, the effects of increasing impact energy and z-pin content on the impact damage resistance of z-pinned sandwich composites has not been determined. Also, there is a lack of published experimental data on the post-impact mechanical properties of z-pinned sandwich composites, and their impact damage properties and mechanisms need to be more thoroughly assessed before these materials can be considered for damage tolerant aircraft structures.

2.3.3 Elastic properties of z-pinned laminates and sandwich composites

Numerous numerical and experimental studies have shown that z-pinning reduces the in-plane tensile, compressive or bending moduli of laminates, albeit by a small amount in most materials [57, 67, 78, 79]. Finite element models, analytical models and experimental studies have all shown that the in-plane modulus properties decrease at a linear rate with increasing volume content of z-pins. The reduction to the in-plane modulus properties also increases

with the z-pin diameter, as shown in Figure 2-17 [9]. The loss in the in-plane modulus is due to the microstructural defects caused by z-pinning, such as fibre waviness, resin-rich zones and swelling of the laminate (which reduces the fibre volume content and thereby the stiffness properties). The percentage reduction in modulus is greatest when the fibre orientation is aligned in the load direction. In other words, z-pinned unidirectional laminates suffer a greater percentage loss in modulus compared with a z-pinned quasi-isotropic material. Average maximum reductions of about 10% have been reported [9]. While it is known that the elastic properties of laminates decrease gradually with increasing volume content and diameter of z-pins, the effect of z-pinning on the in-plane elasticity of sandwich materials is not known.

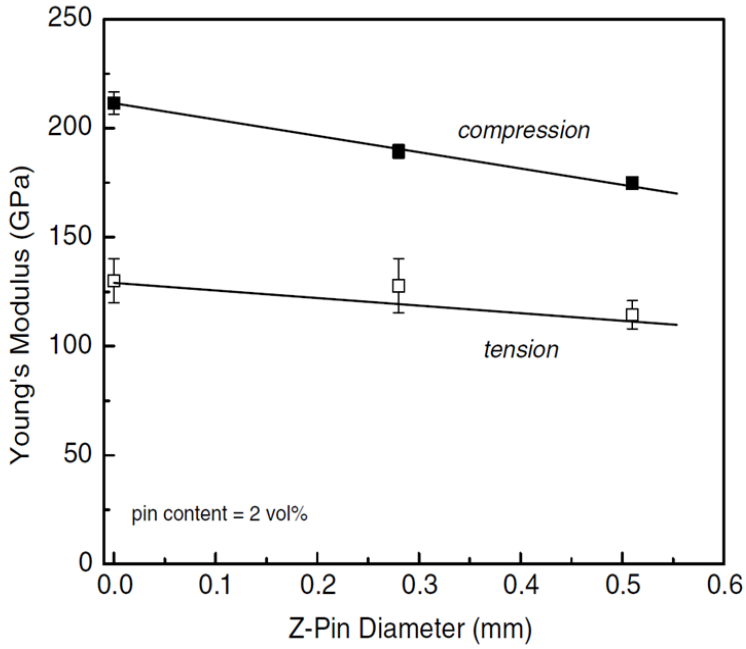

Figure 2-17: Reduction in in-plane tension and compression modulus of a unidirectional carbon-epoxy laminate with increasing z-pin diameter [9]

Z-pinning is a highly effective method for increasing the through-thickness compressive modulus of z-pinned sandwich composites [34, 38]. For example, Figure 2-18 shows the effect of increasing volume content of z-pins on the through-thickness modulus of a foam core sandwich composite structure [38]. A study by Cartié and Fleck [34] reports large improvements to the through-thickness compressive modulus of sandwich composites when reinforced with titanium pins. The modulus increases rapidly due to the high stiffening effect of the z-pins, which have elastic modulus values many times greater than the foam core.

In addition to the through-thickness stiffness, z-pins are also effective at improving the shear properties of sandwich composites, with the z-pins carrying most of the compression and shear loads [43, 80, 81]. In a study conducted by Partridge et al. [43] on the mechanical properties of commercial z-pinned sandwich composites (X-cor™ and K-cor™), it was found that changing the angle between the z-pins affected the compression and shear properties. To improve the shear loading resistance of X-cor™ or K-cor™, the z-pins need to be inserted at a larger offset angle. Therefore, the shear and compression properties of a z-pinned sandwich composite can be controlled.

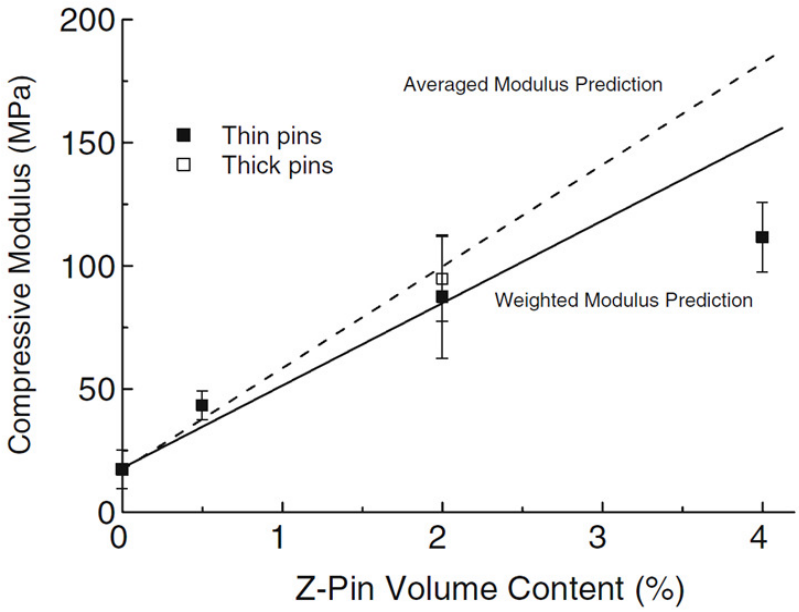

Figure 2-18: Effect of volume content of z-pins on the through-thickness compression modulus of a glass fibre/PVC foam core sandwich composite [38]

Mouritz [38] proposed a simple mechanical model to calculate the through-thickness elastic modulus of a z-pinned sandwich composite (E_c) based on the rule-of-mixtures:

$$E_c = E_f f_f + E_p f_p \qquad [2\text{-}1]$$

The first and second terms account for the stiffness contributions of the core and z-pins, respectively. E_f and E_p are the elastic modulus of the foam core and z-pins, respectively, and f_f and f_p are the volume fractions of foam material and z-pins in the core, respectively. E_p is related to the pin offset angle via the expression;

$$E_p(\theta) = \left[\frac{\cos^4\theta}{E_x} + \frac{\sin^4\theta}{E_y} + \left(\frac{1}{G_{xy}} - \frac{2\nu_{xy}}{E_x} \right) \sin^2\theta \cos^2\theta \right]^{-1} \quad [2\text{-}2]$$

The subscripts x and y refer to the directions parallel and normal to the z-pin axis. G_{xy}, τ_{xy}, and ν_{xy} are the shear modulus, shear strength and Poisson's ratio values for the z-pin, respectively. θ is the inclination angle of the z-pin from the compression load direction. However, because the z-pins are inclined over a range of angles, E_p can be calculated using a weighted analysis of the different angles [38]:

$$E_p\left(\sum\theta\right) = \sum_{\theta=0}^{\theta=90} f_p(\theta).E_p(\theta) \quad [2\text{-}3]$$

where $f_p(\theta)$ and $E_p(\theta)$ are the volume fraction and compression modulus of the z-pins at a given angle, (θ).

The results of this model are presented in Figure 2-18 for the conditions where it is assumed that all the z-pins are inclined at the same angle ("average modulus prediction") or inclined over a range of angles ("weighted modulus prediction"). It is seen that the modulus is predicted with better accuracy using the weighted modulus method, and the compression modulus increases linearly with z-pin content at a similar rate to the experimental data.

2.3.4 Strength properties of z-pinned laminates and sandwich composites

Similar to the in-plane elastic properties, the z-pinning of laminates reduces their in-plane tensile [36, 55, 61, 67, 82], compressive [36, 38, 58, 82-84] and bending strengths [85]. Typical reductions to the in-plane tension and compression properties of a carbon-epoxy laminate with increasing volume fraction of z-pins are shown in Figure 2-19 [86]. The reduction is due to microstructural damage caused by z-pinning such as the fibre waviness, fibre breakage, resin-rich zones, and reduced fibre content caused by swelling. Such defects result in a loss in the load-carrying capacity of laminates. The effect of z-pinning on the in-plane strength properties of sandwich composite structures has not been investigated.

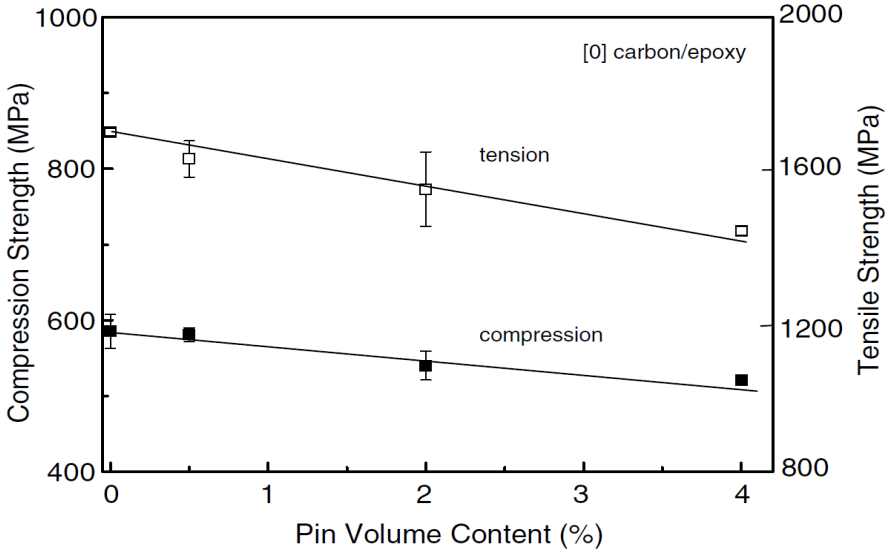

Figure 2-19: Tensile and compressive strengths of z-pinned undirectional carbon/epoxy composite [86]

Z-pinning increases the through-thickness compressive strength of sandwich composites. The z-pins are much higher in strength than the core, and consequently there is a substantial improvement in the compressive strength properties due to pinning. These results have been experimentally and theoretically proven for a variety of pin configurations in sandwich composites [34, 38]. The core acts as a support which allows the z-pins to resist buckling, further improving the through-thickness compression properties [34, 38]. Cartié and Fleck [34] found that the compressive strength and energy absorption capacity of z-pinned sandwich materials is much greater than the individual contributions of the core and unsupported z-pins (Figure 2-20). This was due to the synergistic strengthening process occurring when the core and z-pins are used in combination. The through-thickness compressive properties are improved due to an increase to the elastic buckling load of the z-pins caused by the foam behaving as an elastic Winkler foundation in supporting the pins. In other studies, Mouritz [38] also measured large improvements to the through-thickness compressive strength of a sandwich composite with increasing volume fraction of fibrous z-pins.

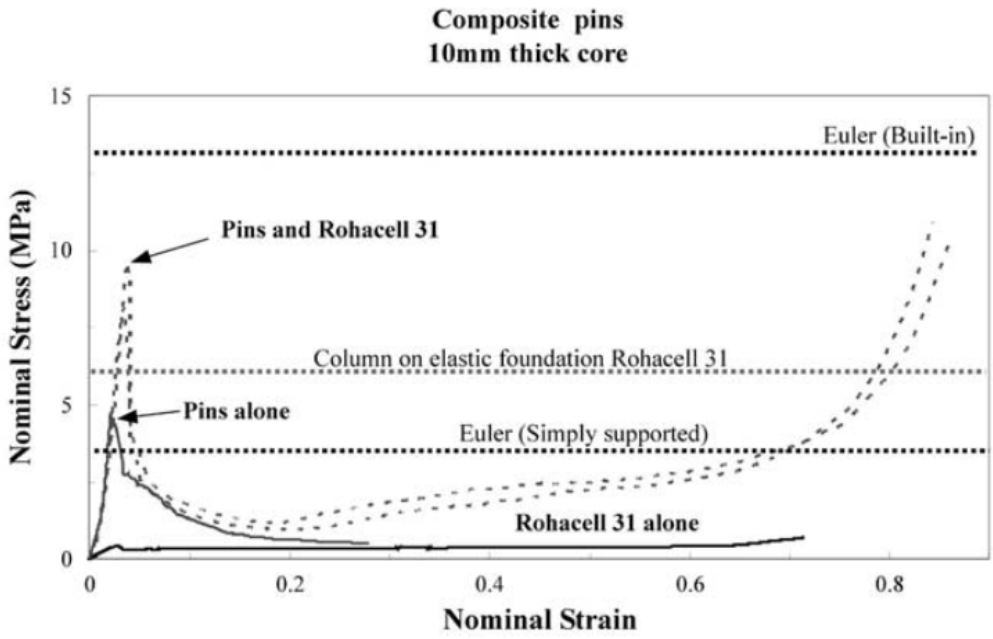

Figure 2-20: Stress vs strain for composite pins in 10 mm thick foam core. In each figure, the dotted horizontal lines refer to the predicted compressive strength due to elastic buckling of the pin reinforcement with different boundary conditions [34]

Mechanical models have been developed to calculate the through-thickness compression strength of z-pinned sandwich composites. The models are based on the deformation behaviour of metal or fibrous pins in a sandwich material subjected to through-thickness compressive stress [34, 38, 87]. The buckling model by Cartié and Fleck [34] assumes pin failure occurs via a buckling process and the strength-based model by Mouritz [38] assumes axial crushing of the pins.

The strength model (like the stiffness model described in the previous section) uses rule-of-mixtures to calculate the through-thickness compressive strength of a z-pinned sandwich composite [38]:

$$\sigma_c = \sigma_f f_f + \sigma_p f_p \qquad [2\text{-}4]$$

where σ_f and σ_p are the compressive strengths of the foam core and z-pins, respectively. σ_p is related to the pin offset angle, θ, via the expression:

$$\sigma_p(\theta) = \left[\frac{\cos^2\theta(\cos^2\theta - \sin^2\theta)}{\sigma_x^2} + \frac{\sin^4\theta}{\sigma_y^2} + \frac{\cos^2\theta\sin^2\theta}{\tau_{xy}^2} \right]^{-\frac{1}{2}} \quad [2\text{-}5]$$

σ_x and σ_y represent the axial and transverse strengths of the z-pin, respectively, and τ_{xy} is the in-plane shear strength of the pin. To account for the variability in pin offset angle, the strength is weighted to the volume fraction of the pins at each angle using:

$$\sigma_p\left(\sum\theta\right) = \sum_{\theta=0}^{\theta=90} f_p(\theta).\sigma_p(\theta) \quad [2\text{-}6]$$

Figure 2-21 shows the strength predictions by Mouritz [38] for a z-pinned sandwich composite, and significant improvements are seen with increasing pin volume content. The agreement between the calculated (data points) and measured (curve) strengths is good when the variable pin offset angles are considered in the analysis.

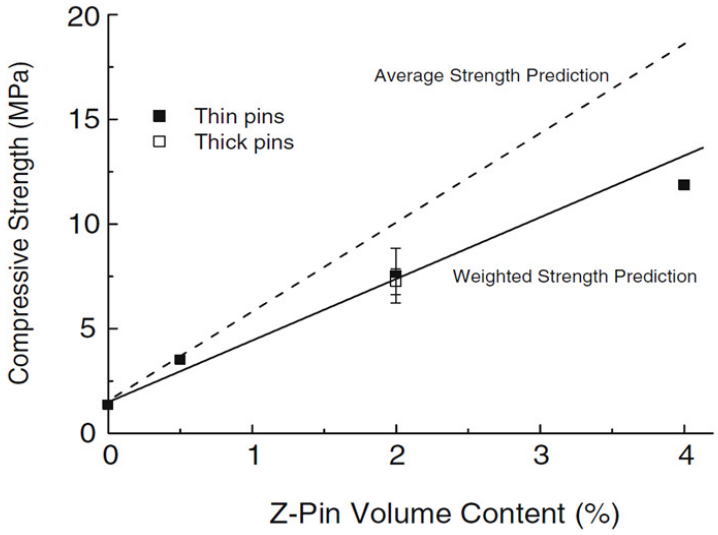

Figure 2-21: Compressive yield strength of z-pinned sandwich composite [38]

Cartié and Fleck [34] formulated a buckling model for metal pins that assumes they collapse by elastic (Euler) buckling. The compressive strength of a z-pinned sandwich composite can be calculated using the expression [34]:

$$\sigma_c = f\sigma_p \cos^2 \omega + \alpha_f \quad [2\text{-}7]$$

where α_f is the average stress in the foam, σ_p is the buckling stress of the pins, and θ is the pin offset angle. σ_f and σ_p are calculated using:

$$\alpha_f = \frac{4E_f P_{buc}}{\pi d_p^2 E_p \cos\omega} \quad [2\text{-}8]$$

$$\sigma_p = \frac{\pi^2 E_p I}{A_p (\mu l)^2}\left(m^2 + \frac{\beta l^4}{m^2 \pi^4 E_p I}\right) \quad [2\text{-}9]$$

where E_pI is the flexural stiffness, l is the pin length, m is the number of half sine waves when the pin buckles (assumed to be 1), β is the foundation modulus of the foam, A_p is the pin cross-sectional area, P_b is the pin buckling load, and E_f and E_p are the elastic modulus of the foam and z-pin, respectively. Cartié and Fleck [34] found that the failure strengths calculated using their buckling model were lower than the measured values (Figure 2-20). This discrepancy was attributed to the rotational constraint in the pins ends [34]. A similar study was undertaken by Long et al. [87] for titanium and carbon pins within a sandwich composite, and reported the same trend in results.

2.3.5 Indentation resistance of z-pinned sandwich composites

While several studies have studied the compressive properties and strengthening mechanics of z-pinned sandwich composites under a distributed (wide-area) load encompassing a large number of pins [34], less has been reported on the compressive response under localised (point) impact loading involving a small number of pins. Long and Guiqiong [40] report that z-pinning increases the indentation resistance of sandwich composites under point loading. Long and Guiqiong [40] performed an experimental and theoretical investigation into the quasi-static indentation resistance of z-pinned foam core sandwich panels under a spherical indenter, and they measured a large improvement to the indentation resistance due to the stiffening and strength effect of the pins as shown in Figure 2-22. Long and Guiqiong [40] also found that under elastic loading conditions, indentation damage initiated at the

interfaces between the z-pins and indented face sheet and between the z-pins and foam core. At higher indentation forces the z-pins immediately under the indenter collapsed by buckling, and this was accompanied by a reduction in the indentation strength.

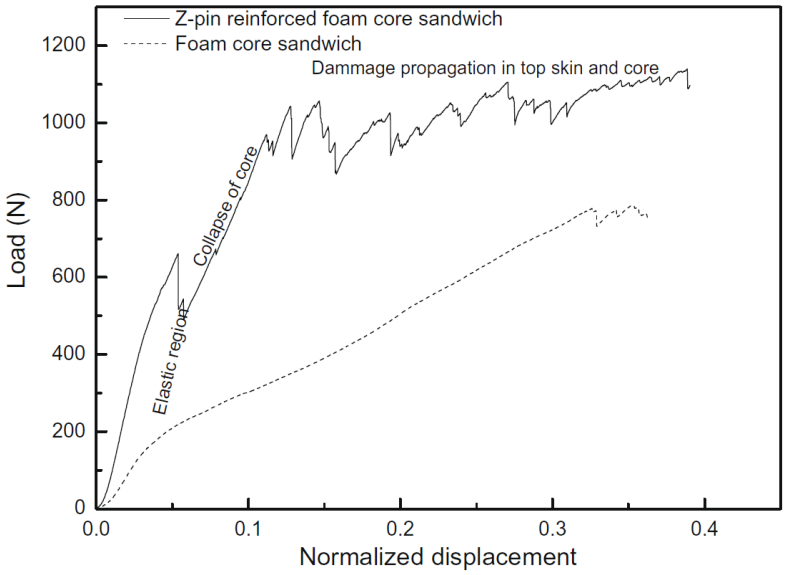

Figure 2-22: Improved indentation resistance of a foam core sandwich composite due to z-pinning (improved load carrying capacity) [40]

Mechanical models have been developed to analyse the indentation response of z-pinned sandwich composites [40, 88]. Long and Guiqiong [40] derived an approximate theoretical solution using the principle of minimum potential energy that was based on the system illustrated in Figure 2-23 in order to analyse the indentation response of z-pinned sandwich composites. The hemispherical indenter is treated as a flat-nose indenter where the radius then becomes constant, R_{in}, and is assumed to equal 0.4R where R is the indenter radius.

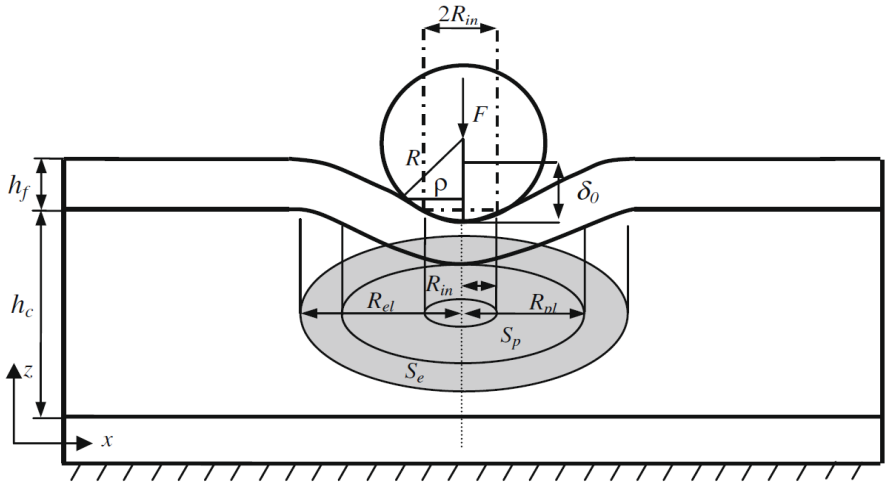

Figure 2-23: Quasi-static indentation by Long and Guiqiong [40]

The plastic work absorbed by the sandwich composite under an indentation force is defined by:

$$D_{pl} = \int_{S_p} \sigma_c \delta dS_p = \pi \sigma_c \delta_0 R_{in}^2 + \frac{4}{9} \sigma_c \delta_0 (R_{el} - R_{in})^2 \left[1 - \left(1 - \frac{R_{pl} - R_{in}}{R_{el} - R_{in}} \right)^3 \right]^2 \quad [2\text{-}10]$$

Where σ_c is the collapse stress of the sandwich composite. R_{pl} is the radius of the plastic zone in the foam core and is determined by:

$$R_{pl} = R_{el} - \sqrt{\frac{\delta^*}{\delta_0}} \frac{R_{el} - R_{in}}{\left[1 + \frac{R_{in}}{R_{el} - R_{in}} \right]} \quad [2\text{-}11]$$

δ_0 is the indentation depth. δ^* is the out-of-plane displacement of the z-pinned foam core, and is dependent to the pin modulus (E_p), pin strength (σ_p) and pin offset angle (ω) according to;

$$\delta^* = \frac{\sigma_p h_c}{E_p \cos^2 \omega} = \frac{\pi^5 m^4 E_p d_p^4 + 64\beta l_p^4}{16\pi^3 m^2 \mu^2 E_p l_p d_p^2 \cos \omega} \qquad [2\text{-}12]$$

where l_p is the pin length and d_p is the pin diameter.

The collapse resistance of the sandwich composite is based on the analysis by Du et al. [89] and Cartié and Fleck [34], and predicts the compressive strength, $\sigma_{c,}$ of a z-pinned sandwich composite (equation 2-7 discussed in detail in section 2.3.4) with the assumption that the z-pins fail by Euler buckling under the indentation load.

2.3.6 Z-Pinned Composite Joints

Composite aircraft structures are joined using adhesives and then usually reinforced with bolts, rivets or some other type of mechanical fastener. Problems with conventional joints are that the adhesives are often too weak to carry high out-of-plane stresses and the fastener holes introduce concentrated stresses that lower the ultimate strength of the laminate adherends. Z-pins can be an attractive option to reinforce joints by raising the bond-line toughness and potentially reducing or eliminating the need for fasteners. Figure 2-24 shows various designs of sandwich joints that could potentially benefit from z-pinning, including T-shaped joints, U-channel joints, bonded fillet designs and bolted connections [90-94]. However, no studies have been reported on the structural properties and damage resistance of sandwich T-joints reinforced with z-pins.

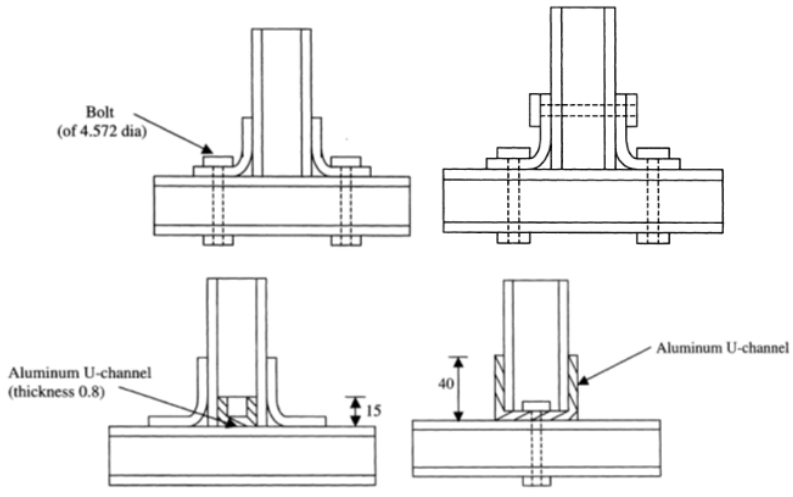

Figure 2-24: Types of sandwich T-joints [94]

Recent studies have shown that z-pins increase the mechanical properties of bonded joints (lap joints, L-shaped joints, T-stiffened panels and T-joints) made of carbon-epoxy laminate [61, 63, 66, 73, 95-98]. Several studies show that the z-pin reinforcement of T-joints improves the ultimate strength, delamination toughness and absorbed energy capacity [63, 99-101]. This is because the z-pins toughen the joint bond-line by resisting large-scale cracking due to bridging traction loads generated by the z-pins [99]. For example, Figure 2-25 shows the typical effect of z-pinning on the strength of a laminate T-joint [64]. A study conducted by Toral-Vazquez et al. [102] reported a 200% increase in the pull-out strength of T-joints reinforced by z-pins. A more comprehensive study conducted by Koh et al. [99] found that the strengthening and toughening effect of laminate T-joints increases with the volume content of z-pins. The studies on laminate joints indicate that z-pinning may also be an effective strengthening method for sandwich joints, although this has not been investigated.

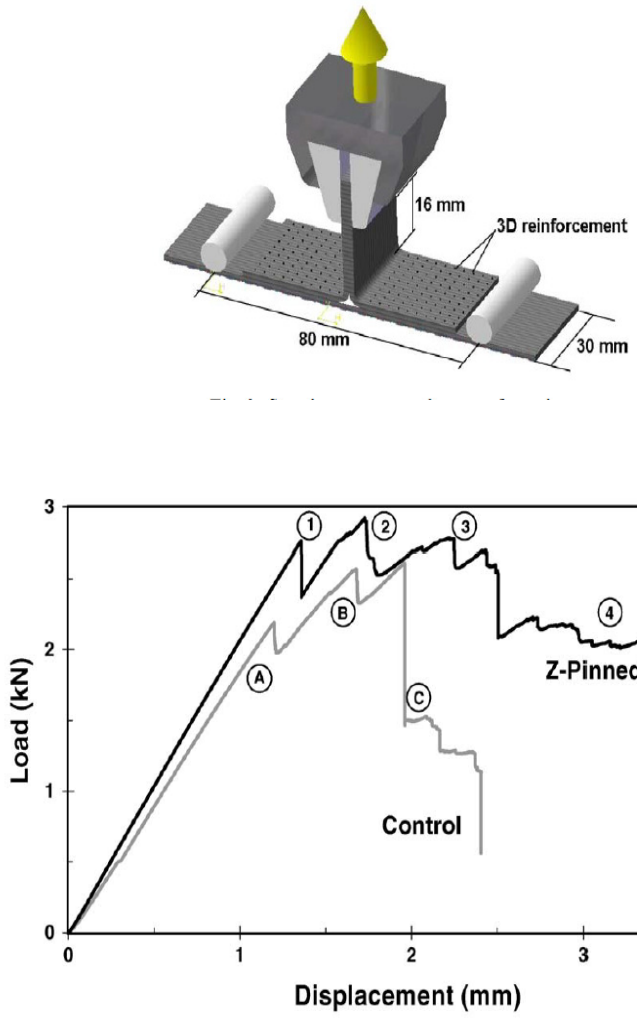

Figure 2-25: Effect of pull-off loading to the stiffener (upper diagram) and the load-displacement response of unpinned and z-pinned laminate T-joints [64]

2.4 CONCLUSIONS

This chapter has presented a comprehensive review of published research into the manufacturing, microstructural characterisation, and mechanical properties of z-pinned laminates and z-pinned sandwich composite structures. The review revealed that a complete study of the microstructure of z-pinned sandwich composites, including defects, has not been undertaken. However, characterisation work conducted on the microstructure of z-pinned laminates provides insights into the defects caused by the z-pinning of the laminate face skins to sandwich materials. The main types of microstructural defects are in-plane fibre waviness and crimp, broken fibres, pin-offset, resin-rich zones, interfacial cracks, and volumetric swelling which lowers the average fibre volume content.

The mechanical properties of sandwich composites have only been investigated to a limited extent, and a complete analysis and experimental assessment of the properties is lacking. Again the mechanical properties of z-pinned laminates were reviewed when relevant to the face skins of sandwich composites. The delamination behaviour, stiffness, strength, impact, indentation response and joint properties of z-pinned sandwich composites were reviewed. While there has been research conducted on the through-thickness properties of z-pinned sandwich composites, information is lacking on the effect of orthogonal fibrous pins on the mechanical properties; the effect of pin end restraint conditions; and the effect of varying z-pin volume content. There is also a significant amount of information lacking on the impact and dynamic properties of sandwich composites reinforced with orthogonal pins. The post-impact mechanical properties of sandwich composites have also not been investigated. Mechanical models to calculate through-thickness compression stiffness, strength and indentation resistance of z-pinned sandwich composite have been reviewed in this chapter. A complete characterisation of these models is lacking. The review also revealed that there is no published research on the strengthening and toughening of sandwich T-joints reinforced with z-pins.

This PhD project aims to address several gaps in the science and technology of z-pinned sandwich composite panels and joints. A series of experimental research studies are conducted to determine the effects of orthogonal pins on the microstructure; through-thickness and in-plane mechanical properties and strengthening mechanisms; indentation and

impact damage resistance; and the joint strength of foam core sandwich composites. The experimental research is used to further the current level of knowledge into z-pinned sandwich composites as well as validate existing mechanical models and develop new models which can be used in the design of high performance sandwich materials for aerospace structures.

Chapter 3 THROUGH-THICKNESS COMPRESSION PROPERTIES AND STRENGTHENING MECHANICS OF Z-PINNED SANDWICH COMPOSITES

ABSTRACT

This chapter presents an experimental and theoretical investigation into the through-thickness compression properties, strengthening mechanisms and failure modes of sandwich composite structures reinforced with orthogonal z-pins. The compression modulus of the polymer foam core sandwich composite was found to increase rapidly with the volume content of z-pins due to their high longitudinal stiffness. However acoustic emission monitoring and X-ray computed tomography reveal that some z-pins are damaged during elastic loading. The compression stress to induce core crushing is increased greatly by z-pinning (up to nearly 700%), although a large percentage of the z-pins fail close to the elastic stress limit by longitudinal splitting and/or kinking. The total absorbed compressive strain energy of the sandwich composite is also improved greatly by z-pinning (more than 600%) due to the z-pins resisting core crushing, even though they are severely damaged.

The experimental results are compared to predicted mechanical properties for the z-pinned sandwich composite calculated. A comprehensive study conducted on existing mechanical models shows that they lack the capacity to accurately predict the properties of sandwich materials reinforced with brittle z-pins, due to the complex and stochastic nature of the pin failure process. A finite element study conducted on the stress fields within a fibrous z-pin under buckling loads provides an insight into regions of potential failure in a z-pin. While it is difficult to accurately pinpoint the exact location of pin failure because of the stochastic nature of the z-pin failure and due to naturally occurring flaws within the pin itself, the current study and previous studies indicate that z-pins are likely to have larger stress concentrations at the skin/z-pin interface.

Part of the research presented in this chapter has been published in the following articles:

Nanayakkara, A., Feih, S. and Mouritz, A.P., 'Experimental analysis of the through-thickness compression properties of z-pinned sandwich composites', Composites, 42A, (2011), 1673-1680, 2012.

Nanayakkara, A., Feih, S. and Mouritz, A.P., 'Improving the through-thickness compression properties of aerospace sandwich composites by z-pinning', Proceedings of the 21st Australasian Conference on the Mechanics of Structures and Materials, December 7-10 2010, Melbourne, Australia.

3.1 INTRODUCTION

Large improvements to the mechanical properties of foam core sandwich composites have been achieved using z-pin reinforcement, including increased impact damage resistance, in-plane shear properties, and delamination fracture toughness (as discussed in the literature review conducted in Chapter 2). For example, Cartié and Fleck [34] measured large improvements to the through-thickness compressive modulus, strength and absorbed energy of sandwich composites when reinforced with titanium pins. Cartié and Fleck [34] found that the compressive strength and energy absorption capacity of z-pinned sandwich materials is much greater than the individual contributions of the core and unsupported z-pins; with a synergistic strengthening process occurring when the core and z-pins are used in combination. The through-thickness compressive properties are improved by an increase to the elastic buckling load of the z-pins due to the foam behaving as an elastic Winkler foundation in supporting the pins. Mouritz [38] measured large improvements to the through-thickness compressive modulus and strength of a sandwich composite with increasing volume fraction of fibrous z-pins.

Finite element and analytical models have been developed to calculate the mechanical properties of sandwich composites reinforced with z-pins, including the through-thickness compressive properties and indentation resistance [34, 38, 40, 103]. These models are based on fundamental assumptions about the elastic and inelastic deformation behaviour of the z-pins to external loading which determines the elastic modulus and strength of the z-pinned sandwich composite. While the deformation behaviour of metal pins to external loading has been determined experimentally and then used in the formulation of a mechanistic-based mechanical model for z-pinned composites [34, 87], similar information for fibrous z-pins is not complete. Z-pins made of carbon fibre composite are the most common type of pin reinforcement, however information on their deformation behaviour in sandwich materials under through-thickness compression loading is lacking. Such information is essential for the development of mechanical models which accurately predict the through-thickness compression, indentation and impact properties of sandwich composites strengthened with fibrous z-pins. In particular, information is lacking on the influences of the volume content, diameter and end constraint of z-pins on the compression properties.

This chapter presents an experimental and modelling investigation to demonstrate the improvement to the through-thickness compression properties of an aerospace sandwich composite structure reinforced with z-pins made of unidirectional carbon filament rod. The research determines the influences of the volume content (up to 4%), diameter and end constraint of orthogonal z-pins on the compressive stiffening, strengthening and strain energy absorption of sandwich composites. The chapter determines the elastic, inelastic and failure behaviour of fibrous z-pins under through-thickness compression loads using scanning electron microscopy, acoustic emission, X-ray computed tomography and FE analysis. This chapter also aims to assess the accuracy of existing mechanical models in predicting the through-thickness mechanical properties of z-pinned sandwich composites. A critical assessment of the mechanical models is conducted using the mechanical properties and strengthening mechanics of the z-pinned sandwich material determined from the experimental research.

3.2 SANDWICH MATERIALS AND EXPERIMENTAL METHODOLOGY

3.2.1 Sandwich Composites

Sandwich composite specimens were made with thin face skins of carbon-epoxy laminate covering a low density core of polymer foam. This material is representative of the polymer foam core sandwich composites used in modern aircraft structures. The skins were made using unidirectional prepreg tape (VTM 264 supplied by Advanced Composites) stacked in a quasi-isotropic ply pattern with a thickness of 2 mm. The core material was closed-cell polymethacrylimid (PMI) foam with a density of 52 kg/m^3 and 75 kg/m^3 and thickness of 6 mm (ROHACELL Type 51RIST or 71RIST respectively supplied by Evonik GmbH). The material properties for ROHACELL 51 and 71RIST are given in Table 3-1. All samples tested in this study were made of these materials.

Table 3-1: Mechanical properties of ROHACELL foam core

Property	ROHACELL 51RIST	ROHACELL 71RIST
Elastic Modulus	75 MPa	105 MPa
Density	52 kg/m^3	75 kg/m^3
Shear Modulus	24 MPa	42 MPa
Tensile Strength	1.6 MPa	2.2 MPa
Compressive Strength	0.8 MPa	1.7 MPa
Shear Strength	0.8 MPa	1.3 MPa
Poisson's Ratio	0.33	0.33

A preliminary study conducted on z-pinning three densities of RIST type foams (51, 71 and 110RIST) revealed that the 110RIST type was too dense (110kg/m^3) to z-pin effectively (especially the high pin volume contents) without causing severe damage to the specimens. Z-pinning the 51RIST type proved to be the easiest but because of its low density, the foam was prone to crushing unless cured in an autoclave at low pressure. Therefore the 71RIST type foam proved to be ideal, and the studies conducted in this thesis were mainly on this core material. However, results from the 51RIST type foam are also presented.

Two types of z-pinned sandwich materials were produced for flat-wise compression testing:

- Type I: sandwich composite containing z-pins in both the face skins and core.
- Type II: sandwich composite containing z-pins only in the core, with the face skins not reinforced with the pins.

The geometry and size of the flat-wise specimens made using these two types of sandwich composite are shown schematically in Figure 3-1.

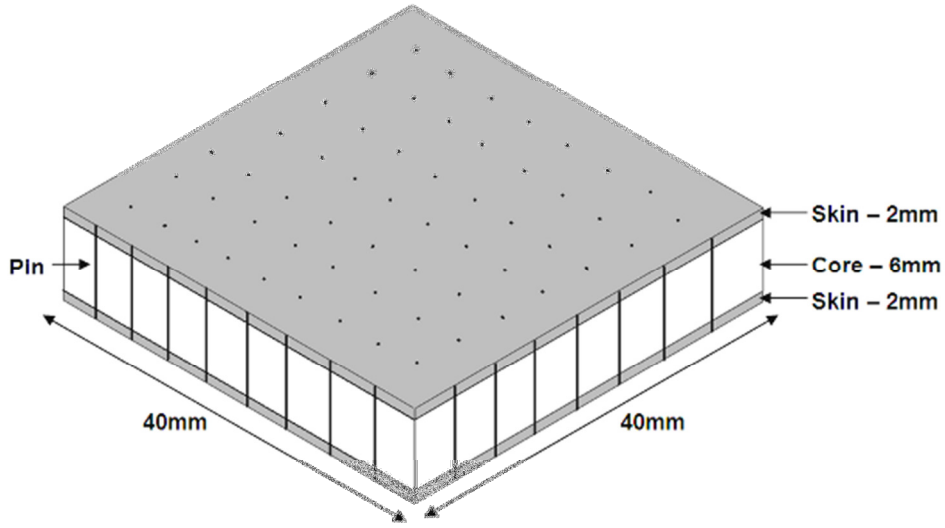

(a)

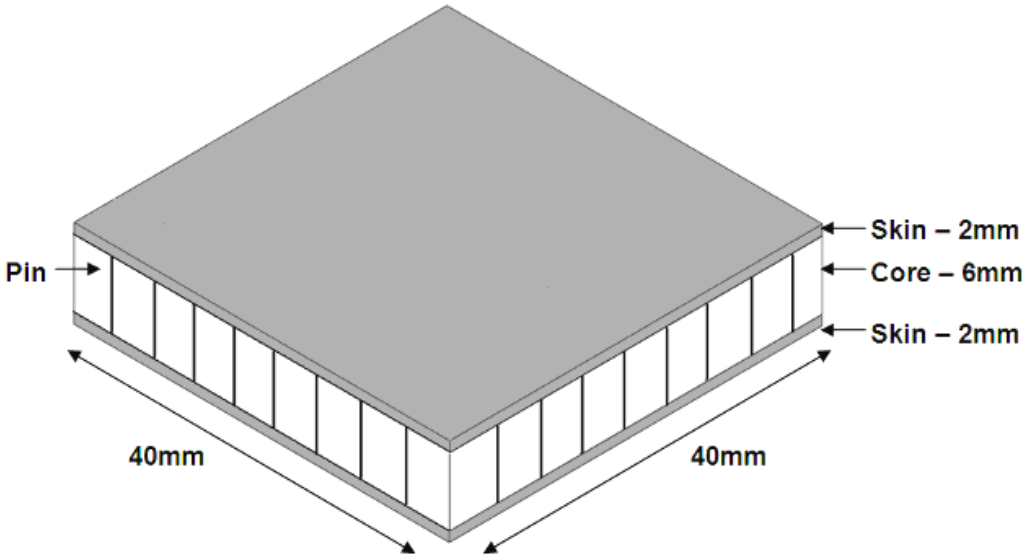

(b)

Figure 3-1: Sandwich composite flat-wise specimens containing z-pins: (a) pins through the skins and core (Type I) or (b) pins through the core only (Type II). Note that the z-pins are arrayed in a square grid pattern.

The Types I and II sandwich materials are similar to commercially available X-cor™ and K-cor™, respectively, with the important difference being that the z-pins are arranged in an orthogonal rather than X-configuration pattern, the z-pins are undercured and K-cor™ also contains an adhesive layer. The ends of the z-pins in the Type I specimen are embedded within the face skins, and this replicates the boundary condition of a built-in column. The z-

pin ends in the Type II specimen are not embedded in the skins, and this more closely replicates the boundary condition for a simply supported column, as illustrated in Figure 3-2.

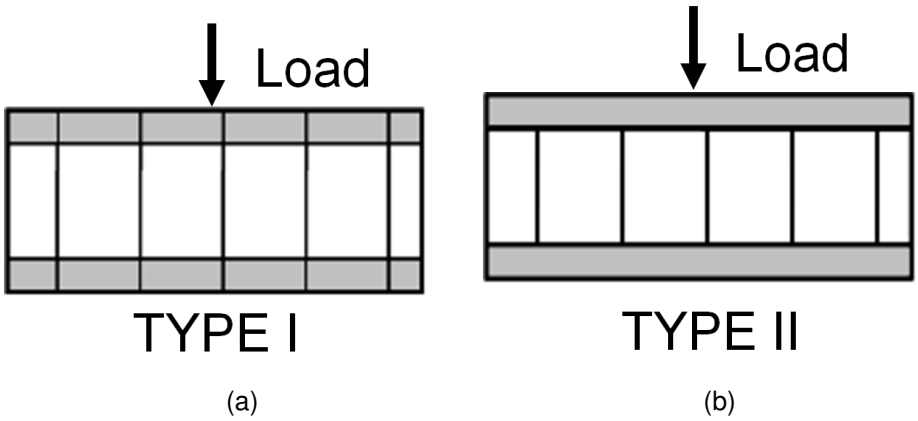

Figure 3-2: Boundary conditions for (a) Built-in Type I z-pinned sandwich composite and (b) Simply supported Type II z-pinned sandwich composite

The z-pins were inserted into the sandwich composite using a process similar to the z-pinning of fibre-polymer laminates, which was described in detail in Chapter 2. The manufacture of the Type I sandwich composite consisted of several steps which are illustrated sequentially in Figure 3-3 and described as follows.

1. Laminate skins were cut precisely to panel size in varying fibre orientations (0,+45, -45/90).
2. Sandwich skins (top and bottom) were laid-up separately in a quasi-isotropic pattern. The ply stack was debulked at every fourth ply to eliminate porosity. It must be noted that the last ply (0) was not included in the lay-up and was saved for post-z-pinning.
3. The sandwich core was introduced as a separate piece and the skins were placed on both sides of the core and further debulked. This final debulking process ensures that the sandwich skins stick to the core and remove any trapped air along the interfacial region.
4. The uncured sandwich is placed on the z-pinning table and is protected with several layers of non-stick polymer film. The film ensures minimal contamination of the sandwich composite during the z-pinning process and also protects the external plies of the sandwich skins from abrasion when the excess length of the z-pins are sanded to produce a smooth surface finish.

5. The z-pins (in their foam carrier) are placed on top of the film protecting the sandwich composite and then secured in place with adhesive tape.
6. The z-pinning process begins with the hand-held ultrasonic device (operated at the frequency of 20 kHz) being pressed slowly and firmly down on the z-pin preform and moved over the entire z-pin region till all z-pins have completely penetrated the sandwich composite.
7. Any excess length of z-pins protruding from the sandwich composite is then shaved and sanded off and the protective film can be removed from the top of the sandwich composite.
8. The final 0 ply is laid on the top and bottom surfaces of the sandwich composite and debulked one final time before the cure. A caul plate is used to ensure a smooth surface finish on the cured sandwich composite.

The manufacture of the Type II sandwich composite varied slightly to the manufacture of the Type I material (Figure 3-4), and involved the following processing steps.

1. Laminate skins were cut precisely to panel size in varying fibre orientations (0,+45, -45/90).
2. Sandwich skins (top and bottom) were laid-up separately in a quasi-isotropic pattern. The ply stack was debulked at every fourth ply. All of the plies were included in the skin lay-up at this stage, and none were saved for post-z-pinning.
3. The sandwich core was introduced as a separate piece and z-pinned prior to the assembly of the sandwich composite. Several layers of film were utilized to protect the core from contamination during z-pinning.
4. The z-pins (in their foam carrier) were placed on top of the film protecting the sandwich core and then secured in place.
5. The foam core was z-pinned using the hand-held ultrasonic device.
6. Any excess length of z-pins protruding from the sandwich core is then shaved and sanded off and the protective film then removed from the core.
7. The uncured sandwich skins were placed on both sides of the z-pinned core and then debulked.
9. The Type II sandwich composite is then ready for cure. A caul plate is used to ensure a smooth surface finish on the cured sandwich composite.

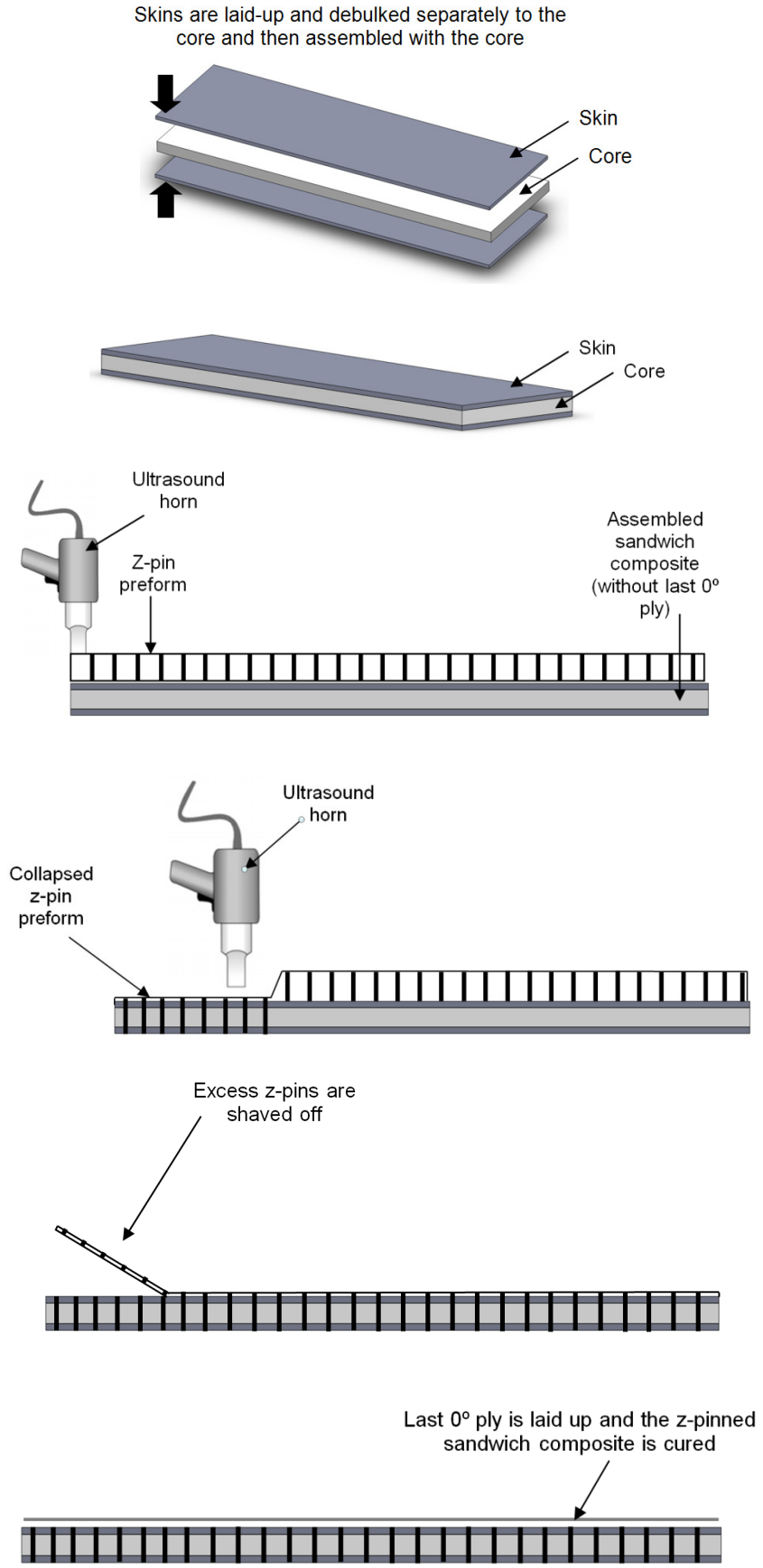

Figure 3-3: Manufacture of Type I z-pinned sandwich composite

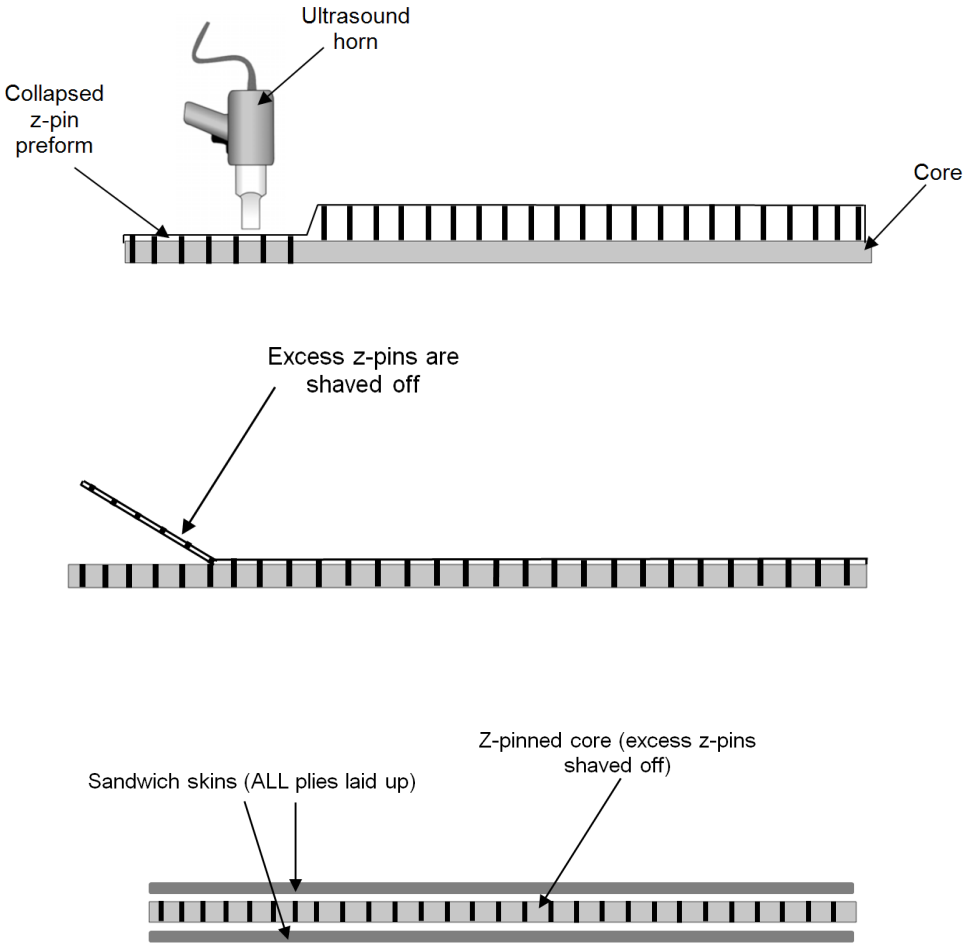

Figure 3-4: Manufacture of Type II z-pinned sandwich composite

As mentioned, the main difference in the manufacturing processes was that the z-pins in the Type I material were inserted through both the uncured carbon/epoxy face skins and PMI foam core, whereas the pins in the Type II material were inserted through the core only, and then the uncured skins were applied to core. After z-pinning the sandwich composites were cured inside an autoclave at 276 kPa and 120°C for one hour. No adhesive was used for bonding the face skins to the foam core. The epoxy within the skins was used for bonding with the core during the curing process in the autoclave.

Sandwich composite specimens were produced using thin z-pins (0.28 mm diameter) at volume contents of 0.5%, 1%, 2% or 4% or thick z-pins (0.51 mm diameter) at the volume content of 2%. The thin z-pins are pultruded rods of unidirectional T300 carbon fibre-bismaleimide (Albany Engineered Composites) with a longitudinal elastic modulus of 135 GPa and axial compressive strength of 1.6 GPa. The thick z-pins are rods of unidirectional T600 carbon fibre-bismaleimide (also produced by Albany Engineering Composites). The

manufacturer (Albany Engineered Composites) of the z-pins did not disclose the fibre content of the thin and thick z-pins. However, the fibre content is expected to be similar for both pin types because the same process (pultrusion) is used in their manufacture. It is estimated that the fibre volume content is within the range of 60-65%, which is typical for pultruded composite products. The mechanical properties of the thick and thin z-pins are given in Table 3-2 [38]. Control sandwich composite specimens without z-pins were also produced.

Table 3-2: Mechanical properties of Z-pins

Property	Thin Pins T300 carbon/bismaleimide	Thick Pins T600 carbon/bismaleimide
Axial Compression Modulus, E_x	135 GPa	150 GPa
Transverse Compression Modulus, E_y	8.3 GPa	8.3 GPa
Shear Modulus, G_{xy}	125 MPa	125 MPa
Axial Compression Strength, σ_x	1.59 GPa	1.77 GPa
Transverse Compression Strength, σ_y	60 MPa	60 MPa
Shear Strength, τ_{xy}	70 MPa	70 MPa
Poisson's Ratio, ν_{xy}	0.24	0.24

The z-pins were arranged in a near-orthogonal pattern in both types of sandwich material. It was extremely difficult to insert all of the z-pins in a perfect orthogonal pattern using the manual z-pinning process, and instead the pins are inclined over a narrow range of shallow angles close to the orthogonal direction. This is a microstructural feature of z-pinned composites, as discussed for laminates in chapter 2. Figure 3-5 shows X-ray computed images of z-pinned sandwich material (core material digitally removed), and it is seen that the z-pins were inclined at various angles. Figure 3-6 presents histograms showing the distribution of inclined angles for the z-pins in the Types I and II sandwich composites for all pin volumes from 0.5% to 4%. All visible offset angles were recorded for Types I and II sandwich composites (at each pin volume content). This was done via a visual measuring method whereby all visible faces of the sandwich specimen were photographed and the offset angle was measured from the orthogonal direction as seen in Figure 3-7. For both types of sandwich composite about 80% of the z-pins have an offset angle less than 5°.

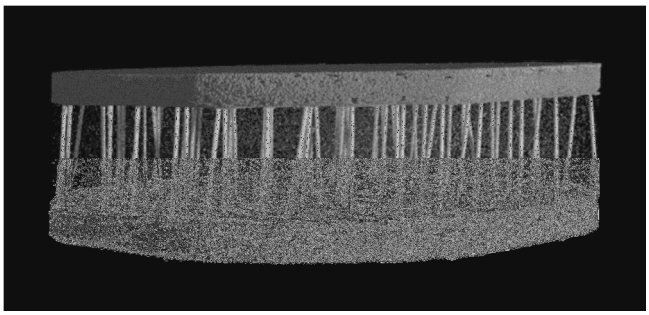

(a)

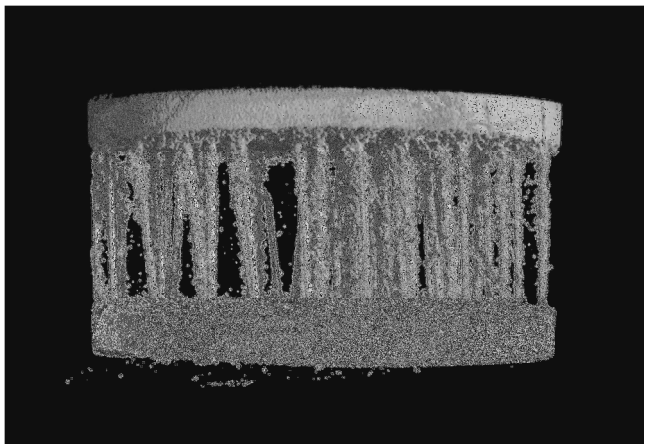

(b)

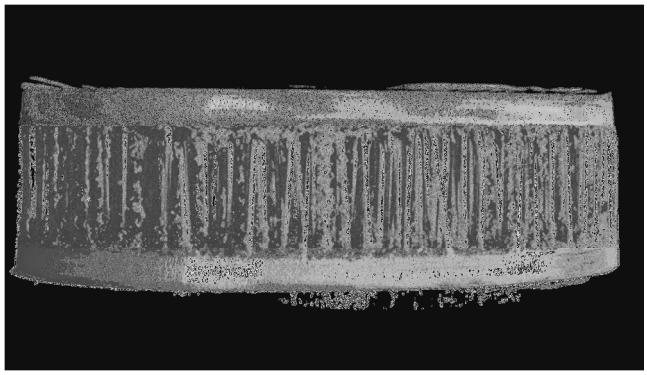

(c)

Figure 3-5: X-ray computed tomography image of z-pinned sandwich composite specimens at different pin offset angles (a) 0.5% thin pins (b) 2% thin pins and (c) 4% thin pins showing that the pins are inclined at various angles.

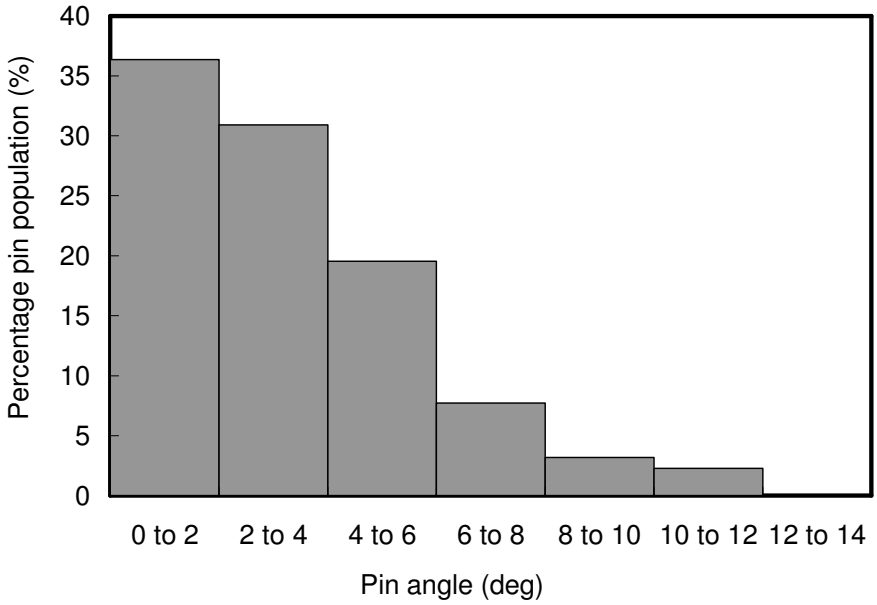

(a)

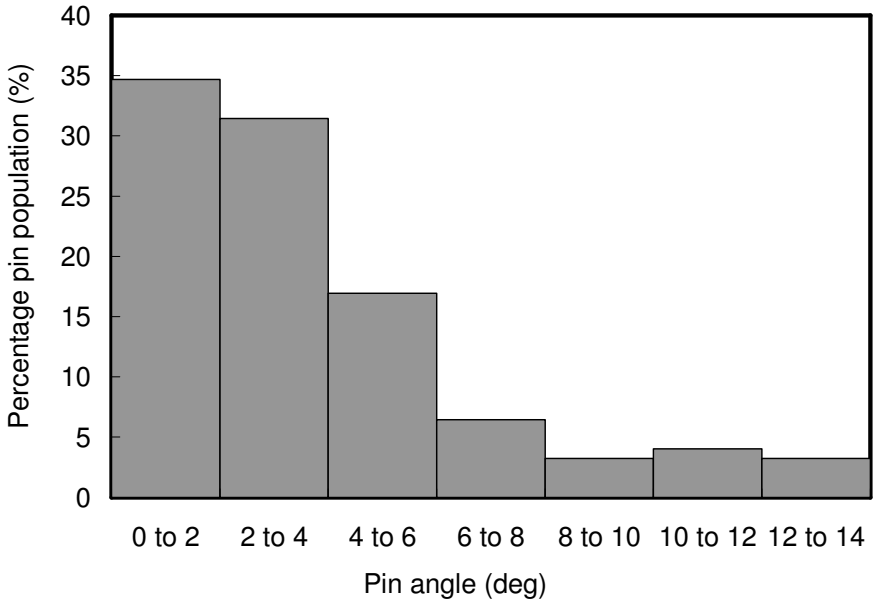

(b)

Figure 3-6: Histograms of z-pin population against inclination angle for the (a) Type I and (b) Type II sandwich materials.

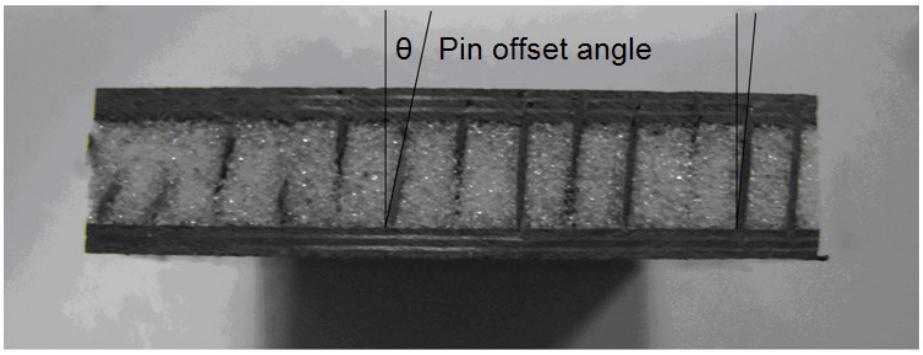

Figure 3-7: Measuring pin offset angles in sandwich specimens

3.2.2 Flat-Wise Compression Testing of Sandwich Composites

The through-thickness compression properties of the unpinned and z-pinned sandwich composites were determined using the flat-wise test method specified in ASTM C393. The specimens were 40 mm long, 40 mm wide and 10 mm thick, as shown in Figure 3-1. A compression load was applied evenly over the face skins in the through-thickness direction using a 50 kN Instron machine. The tests were performed under ambient conditions (~20^{o}C and 55% relative humidity). The samples were compressed at a constant displacement rate of 0.5 mm/min until their original thickness was reduced by 40% (i.e. compressed from 10 mm down to 6 mm), at which point significant densification occurs due to core crushing. It can be said that compression takes place mostly in the core, resulting in a higher percentage reduction in core thickness. The compression modulus was determined by calculating the gradient of linear (elastic deformation) region of the graph as indicated by Figure 3-9a. For example, in the 4% pin volume content category in Figure 3-9d, the compression modulus was measured over the strain range of 4% to 7%. Ten samples of each type of sandwich material were tested under identical flat-wise compression conditions to quantify the variability in material properties.

3.2.3 Damage Analysis of Sandwich Composites

The deformation and failure of the z-pins under flat-wise compression loading was studied using scanning electron microscopy, acoustic emission monitoring, and X-ray computed tomography. The scanning electron microscopy was conducted using a Phillips XL 30 using backscattered electron imaging. The acoustic emission was performed using a single wide-

band piezoelectric sensor (WD sensor) mounted on the compression plate of the Instron machine. The sensor was connected to the 2/4/6 Preamplifier and PCI-2 AE system (Pacific Acoustics Corporation), and the signal was analysed using AEwin software. The X-ray computed tomography was performed using a SkyScan 1172, which is a Desktop X-ray microtomograph (Figure 3-8). A source voltage of 49 kV and current of 167 μA were used. Image pixel size was set to 17.23 μm. The samples were rotated at 0.2° steps with an exposure time of 1770 ms allowing for accurate and complete image capture.

Figure 3-8: SkyScan 1172, X-ray tomography equipment

3.3 RESULTS AND DISCUSSION

3.3.1 Compression Stress-Strain Response of the Z-Pinned Sandwich Composites

The typical resistance of a z-pinned sandwich composite to through-thickness compression loading is shown in Figure 3-9a. Compression stress-strain curves are presented for the Type I sandwich composite that is z-pinned through both the face skins and core for foam type 51RIST (Figure 3-9b) and foam type 71RIST (Figure 3-9c) and the Type II material in which only the core is z-pinned (Figure 3-9d). The Type II material for 51RIST type foam was not investigated after determining that the most suitable foam for this study was the 71RIST type foam (due to the poor crush resistance of the low density 51RIST type foam). The curves

show an initial elastic response which defines the through-thickness compressive modulus, before reaching the yield point where the sandwich composite begins to experience irreversible deformation. The curve for the unpinned composite shows a small load drop immediately following the yield point due to crushing of the foam core. The load drop following the yield point is more pronounced in the z-pinned sandwich composites. Despite the z-pinned sandwich composites generally experiencing a larger load drop than the unpinned composite following the yield point, the pinned materials retain higher compression load-bearing capacity for the entire strain range. Similar observations to these were made by Cartié and Fleck [34] for sandwich composites reinforced with titanium pins. The compression stress-strain curves were used to determine the effect of z-pins on the following material properties: compression modulus, yield stress and absorbed energy.

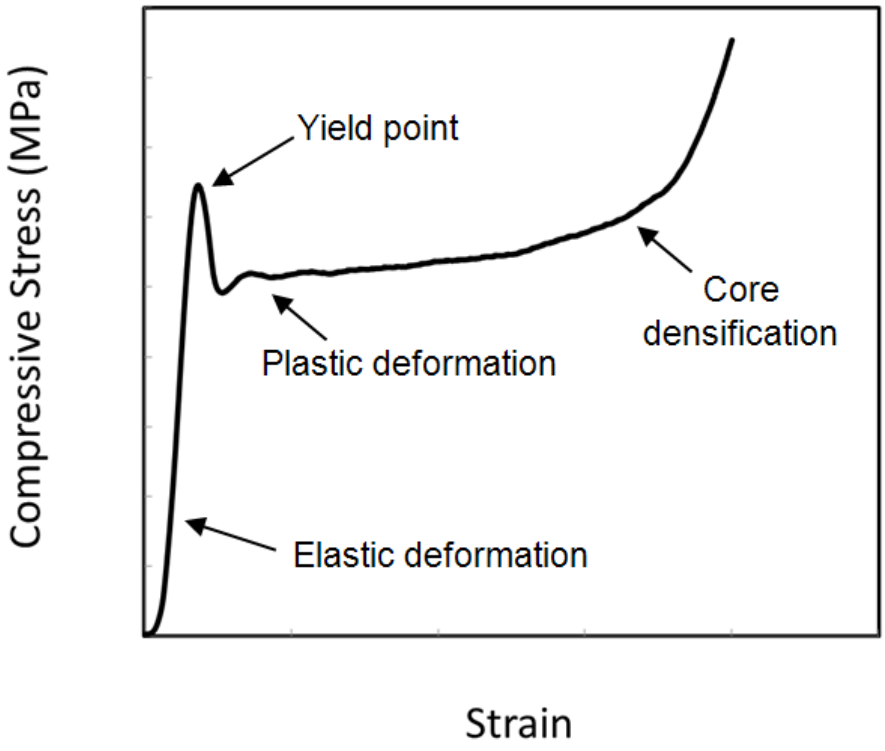

(a)

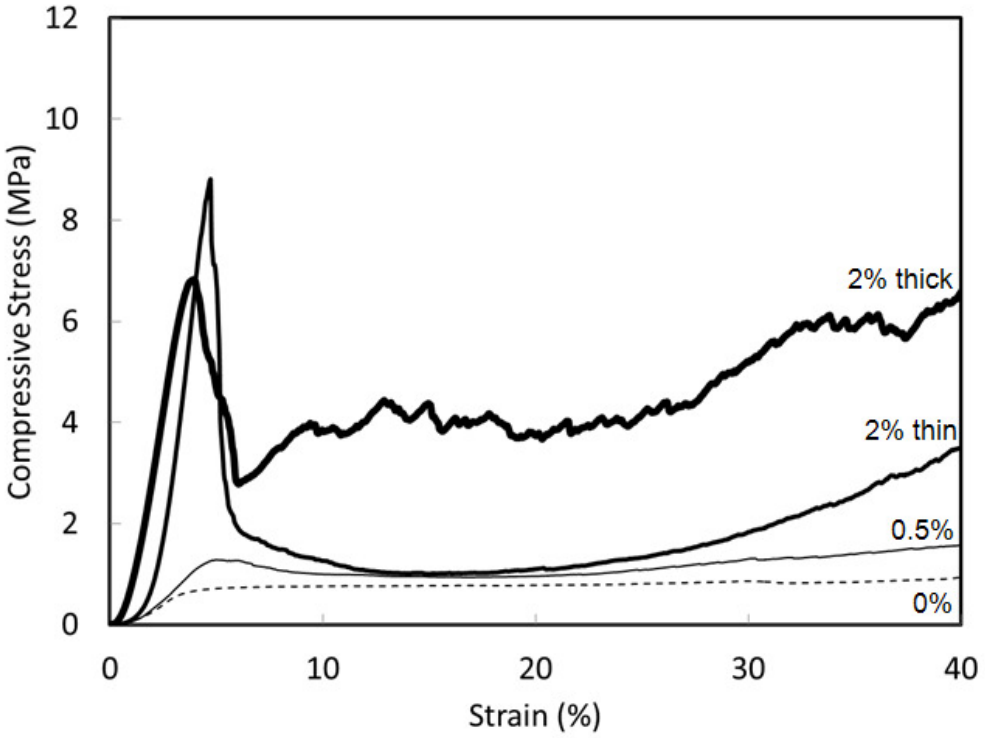
Compressive Stress (MPa)
Strain (%)
2% thick
2% thin
0.5%
0%

(b)

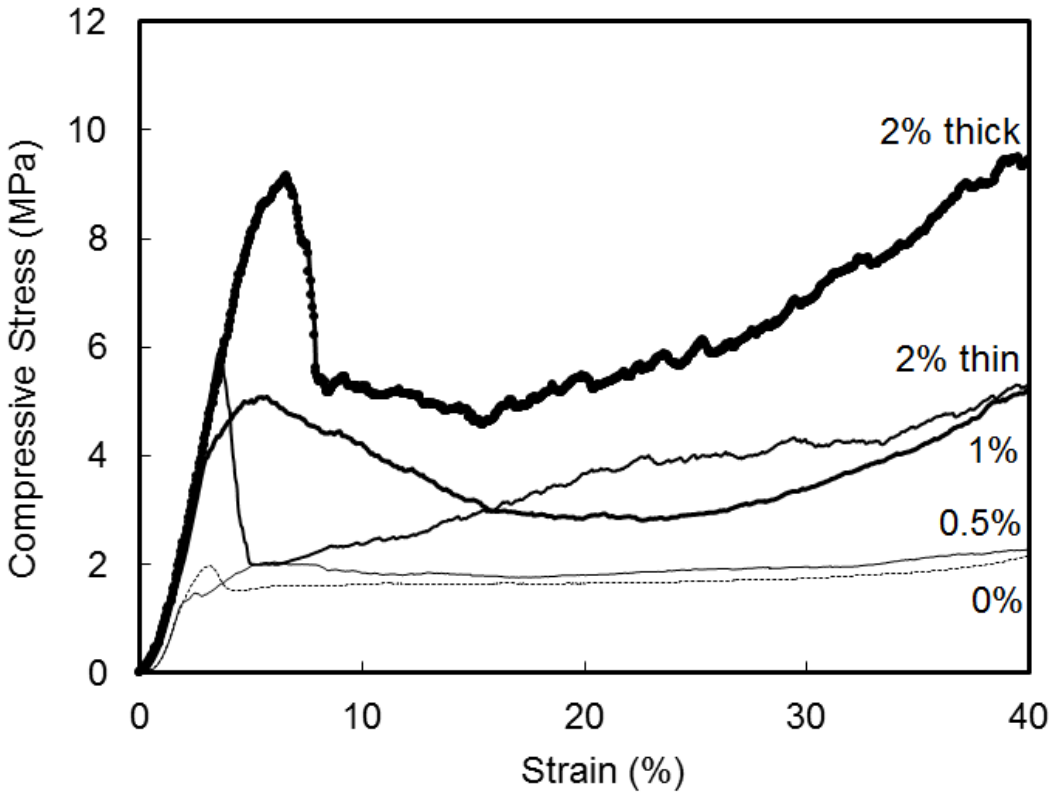
Compressive Stress (MPa)
Strain (%)
2% thick
2% thin
1%
0.5%
0%

(c)

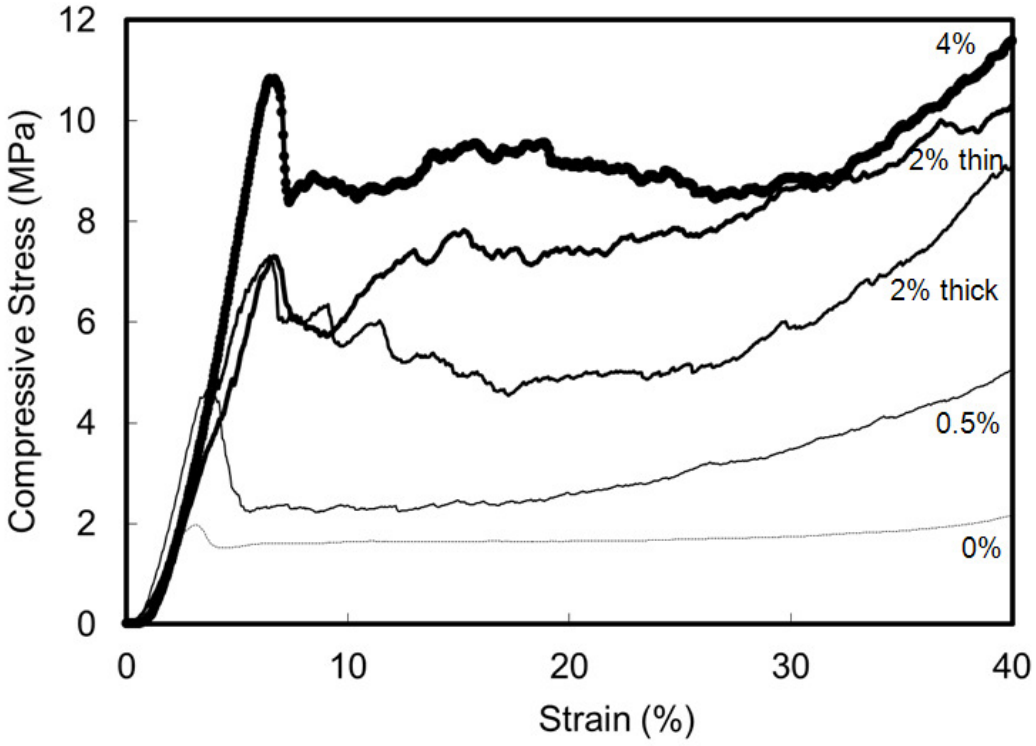

(d)

Figure 3-9: Flat-wise compression stress-strain curves: (a) Typical behaviour for a z-pinned sandwich composite, (b) z-pins through both the skins and the core (Type I) and foam type 51RIST, (c) z-pins through both the skins and core (Type I) and foam type 71RIST, and (d) z-pins through the core only (Type II) and foam type 71RIST

3.3.2 Compression Modulus and Stiffening Mechanisms of Z-Pinned Sandwich Composites

The effects of volume content, diameter and end restraint condition of the z-pins on the compression modulus of the sandwich composite is shown in Figure 3-10. Despite large scatter in the data (the cause of which will be discussed later in this chapter), there is a progressive increase to the compressive stiffness with the volume content of z-pins. The compression properties are improved by several hundred percent with just a few percent of z-pins for both foam types, which show the strong stiffening effect provided by z-pins when aligned in the orthogonal direction. Mouritz [38] measured similar improvements to the through-thickness compressive modulus of a fibreglass sandwich composite with increasing z-pin content, as reported in Chapter 2. The increase in the compression modulus is due to the z-pins behaving as a highly rigid elastic foundation. The z-pins are much stiffer than the

foam core (by about 1500 times), and therefore increasing their volume content by a small amount results in a large increase to the elastic properties of the sandwich material.

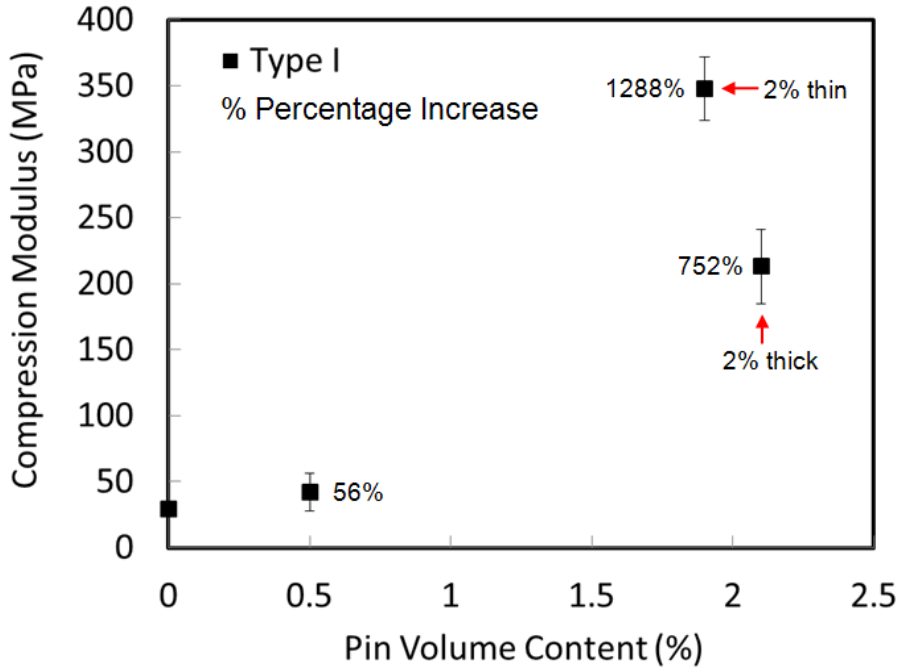

(a)

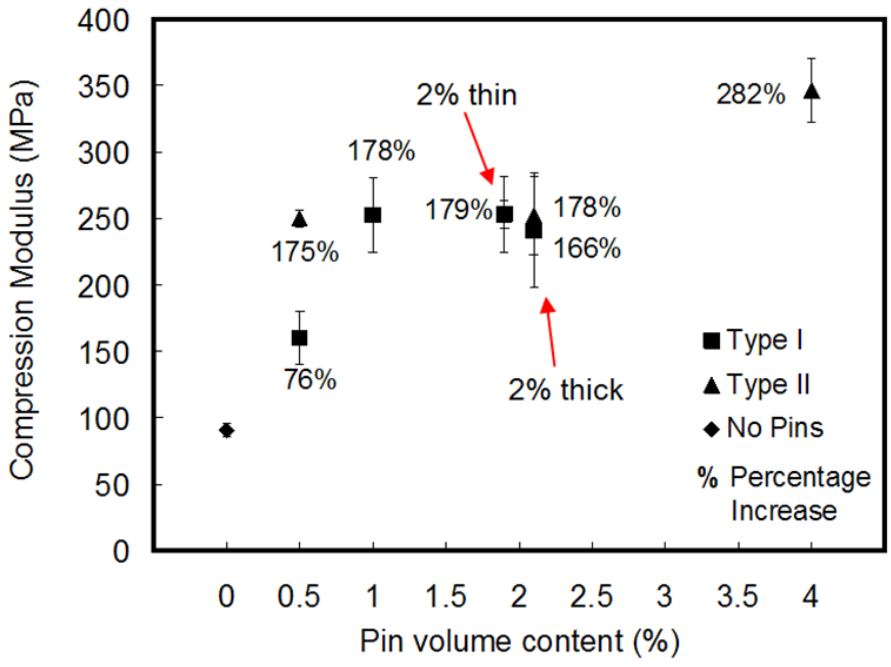

(b)

Figure 3-10: Effects of the volume content and diameter of z-pins on the through-thickness compression modulus. The error bars represent one standard deviation. The percentage values indicate the increase in compression modulus of the z-pinned sandwich composite compared to the unpinned material with the same core density. Results for foam type (a) 51RIST and (b) 71RIST

A study of the lower density foam revealed that a large improvement in the modulus occurred with a 2% volume content of z-pins when compared to the 0.5% volume content (Figure 3-10a). This improvement, though significant for the 71RIST type foam, was not as pronounced due to the combined stiffness of the core and z-pins. The 71RIST type foam has a compressive strength that is 112% greater than that of the 51RIST type foam. The combined compressive strength of the z-pins and the foam is therefore greater for higher density foam (71RIST). The results in Figure 3-10b show that the compressive modulus properties are similar for the Types I and II materials, indicating that the z-pin boundary condition (i.e. built-in column or simply supported column, respectively) does not have a large influence on the stiffness properties. The stiffness of an elastic column is not affected by its boundary condition, and therefore the elastic properties for the Types I and II sandwich composites should be the same for fixed z-pin content provided the misalignment is similar. Figure 3-10 also shows the elastic properties of the sandwich composites with the same volume content of thin or thick z-pins are similar. This is because the stiffening effect of z-pins is not determined by their size, but only by their volume fraction and elastic modulus.

The compression modulus of a sandwich composite is related to the volume content of z-pins via the rule-of-mixtures expression (below, equation 3-1) developed by Mouritz [38] and described in detail in chapter 2 (equations 2-1 to 2-3).

$$E_c = E_f f_f + E_p f_p \qquad [3\text{-}1]$$

The first and second terms account for the stiffness contributions of the core and z-pins, respectively. E_f and E_p are the elastic modulus of the foam core and z-pins, respectively, and f_f and f_p are the volume fractions of foam material and z-pins in the core, respectively. E_p is related to the pin offset angle via the expression;

$$E_p(\theta) = \left[\frac{\cos^4\theta}{E_x} + \frac{\sin^4\theta}{E_y} + \left(\frac{1}{G_{xy}} - \frac{2\nu_{xy}}{E_x} \right) \sin^2\theta \cos^2\theta \right]^{-1} \qquad [3\text{-}2]$$

The subscripts x and y refer to the directions parallel and normal to the z-pin axis. G_{xy}, τ_{xy}, and v_{xy} are the shear modulus, shear strength and Poisson's ratio values for the z-pin, respectively. θ is the inclination angle of the z-pin from the compression load direction.

This model was solved for the different types of z-pinned material, and the calculated compression modulus values are compared against the experimental results in Table 3-3. In the calculation the average pin inclination angle (θ) measured for each pin volume content category was used. The analysis reveals that the theoretical elastic modulus increases linearly with the volume content of the z-pins for the same misalignment angle. The elastic modulus then decreases with an increasing average pin offset angle, which is expected. The results are very sensitive to the offset angle. However, despite accounting for the offset angle, the theoretical modulus values were much higher than the experimental values in most cases. Reasonable predictions were only achieved for pin volume fractions of 0.5% and samples with large offset angles.

Table 3-3: Experimental and theoretical compressive modulus values for the z-pinned sandwich composite with the 71RIST foam core. The average pin offset values, which were measured, were used in the calculation of the theoretical modulus

Composite (I) - Type I (II) - Type II	Measured Average pin offset angle (deg)	Experimental Modulus (MPa)	Theoretical Modulus (MPa)
0.5% (I)	6.1°	160	156
1% (I)	3.5°	252	371
2% Thin (I)	1.6°	253	1547
2% Thick (I)	4.9°	241	412
0.5% (II)	2.7°	250	305
2% Thin (II)	2.1°	253	1194
2% Thick (II)	5.7°	252	342
4% (II)	2.1°	346	2372

The theoretical compressive modulus of the z-pinned sandwich composites was also calculated using finite element (FE) modelling. A FE model was created using Abaqus (Version 6.1) to analyse the through-thickness modulus of a z-pinned sandwich composite. The carbon/epoxy prepreg skins were not included in this analysis because deformation occurs in the z-pins and the foam core region only. The foam core was modelled using three-

dimensional solid elements. The z-pins were modelled using three node quadratic truss elements (T3D2) using the embedded element function in Abaqus to include the pins within the foam. The quadratic truss element was able to account for the orthotropic properties of the z-pins. Figure 3-11 shows the FE model in which all of the z-pins are perfectly orthogonal in the foam core. The analysis aimed at establishing the linear stiffness of the material, and a quasi-static analysis approach was therefore chosen.

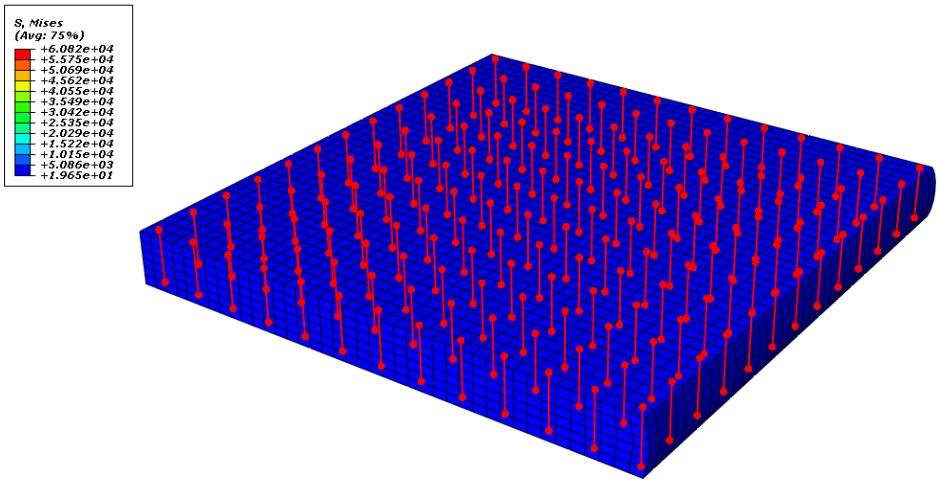

Figure 3-11: FE model showing 2% thick pins embedded in 71RIST foam core

Figure 3-12 compares the measured modulus values against the modulus calculated using the FE model and the analytical model by Mouritz [38]. Two data sets are represented in the analytical model; the orthogonal and the weighted analysis, where the orthogonal model assumes perfectly orthogonal pins and the weighted analysis considers the distribution of pin offset angles in that sample category. The experimental modulus values are much lower than the calculated values for all z-pin contents whereas the FE analysis and the theoretical model are in much better agreement. This agreement is due to the similar approaches to calculate the stiffness of the sandwich core using the elastic properties, volume content and the misalignment angle of the z-pins. To investigate the disagreement between the experiment and the calculated values, the FE model was changed so that the z-pins were inclined at various angles up to 14^{o} (Figure 3-13), which is the maximum measured offset angle (Figure 3-6) for each pin volume content category. The effect of offsetting the z-pins on the compression modulus calculated using the FE model is shown in Figure 3-12. An FE analysis was conducted whereby the z-pins were perfectly orthogonal and also offset;

however, the consideration of offset pins in the FE analysis only provides a small reduction in modulus. Despite the reduction in modulus, it was not significant enough to match the measured experimental values, showing that the inclination of the pins is not the reason for the reduced modulus. It should be noted that the two data points at the 2% pin volume content are 2% thin pins and 2% thick pins.

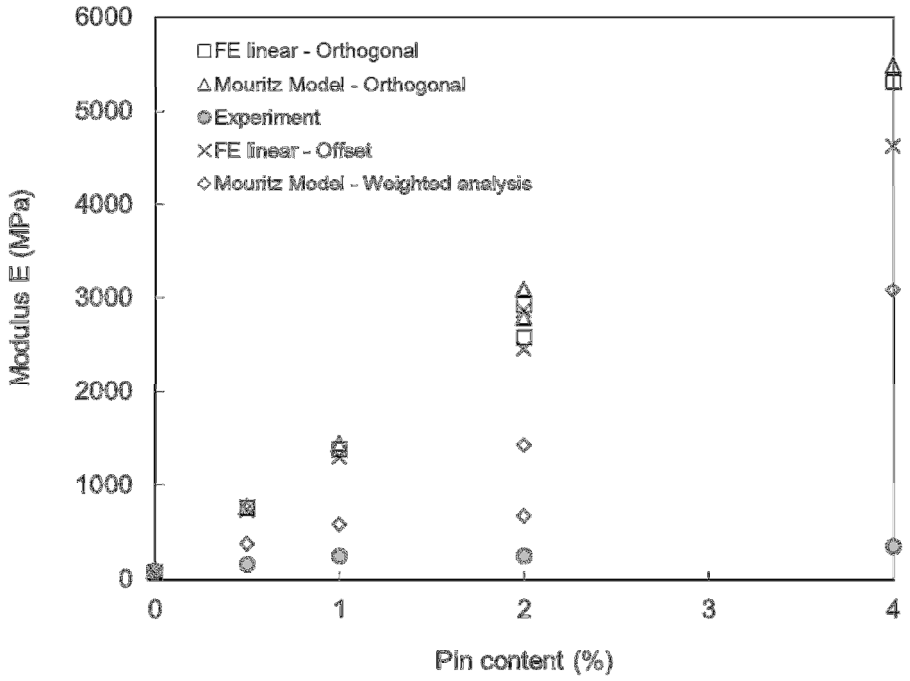

Figure 3-12: Modulus improvement with increasing z-pin content; analytical and finite element methods

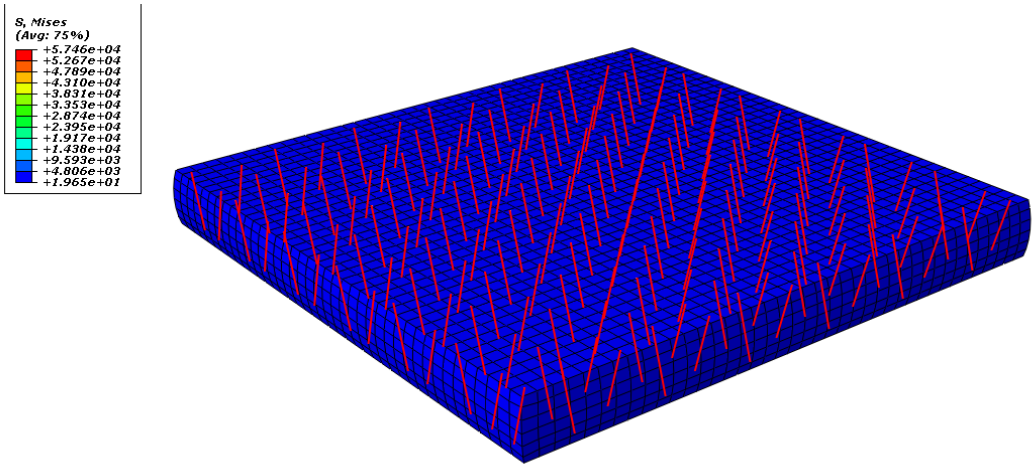

Figure 3-13: FE model with offset z-pins

A sensitivity study conducted on the impact of the z-pin offset angle on the stiffness prediction by the model shows that the value of the elastic modulus reduces rapidly with the z-pin offset angle (Figure 3-14).

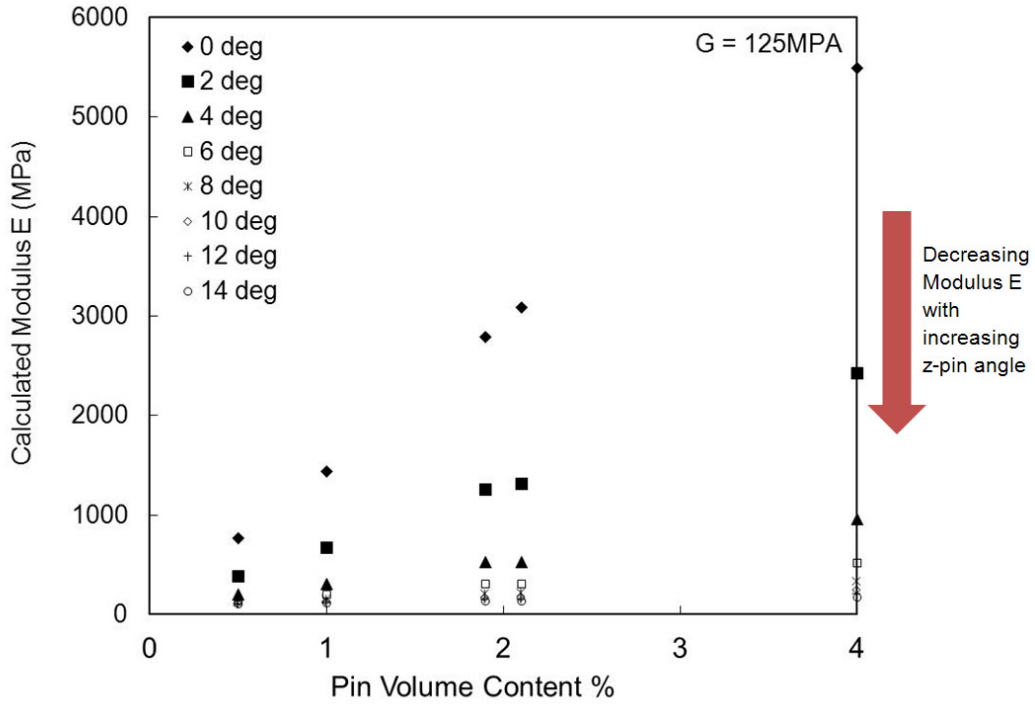

Figure 3-14: Sensitivity of calculated stiffness (Mouritz Model [38]) to the z-pin modulus E_p with increasing offset angle

The variation in the modulus values between Figure 3-12 and Figure 3-14 for a 14^o pin offset angle is due to different shear modulus values in the analysis and is explained in detail below. The mechanical model predicting the through-thickness modulus of the z-pinned sandwich composite is sensitive to the shear modulus of the z-pin. Equation 3-2 shows the calculation of the z-pin modulus based on the pin offset angle. If the pin offset angle was to remain constant, the z-pin modulus would be then dependent on z-pin material properties such as the z-pin transverse modulus or the shear modulus. The model shows sensitivity to the shear modulus. The shear modulus was investigated due to the lack of published information on z-pin material properties. The only available published shear modulus (as shown in Table 3-2) appears to be rather low, when compared to the generic shear modulus of unidirectional carbon, which is in the order of 5GPa. Figure 3-15a shows the calculated modulus (Equation 3-1) with increasing pin volume content for a variety of z-pin shear modulus values (with the z-pin offset angle fixed at 10deg). It can be seen from the figure

that doubling the z-pin shear modulus roughly doubles the calculated modulus for the sandwich composite.

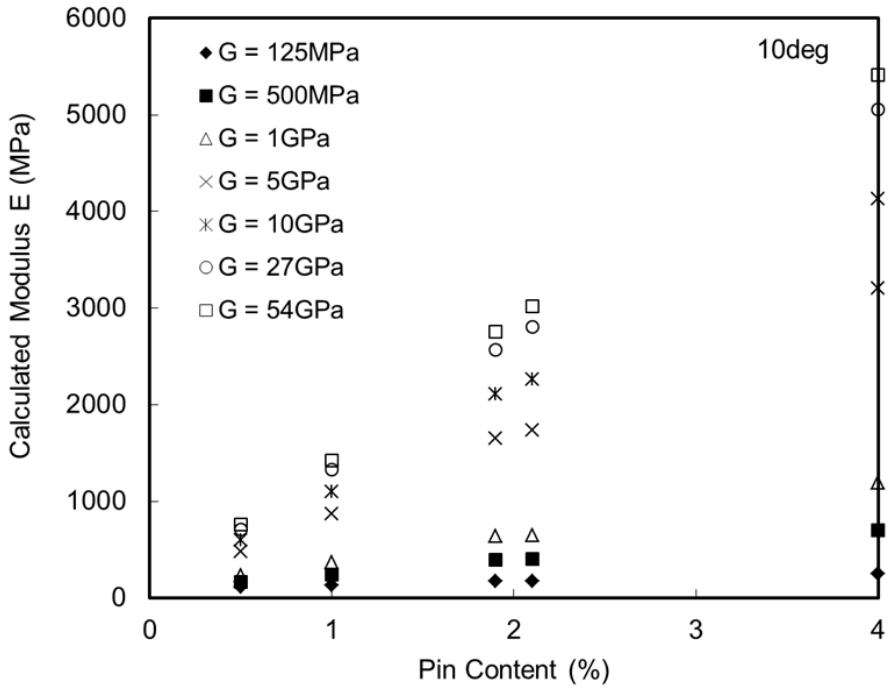

(a)

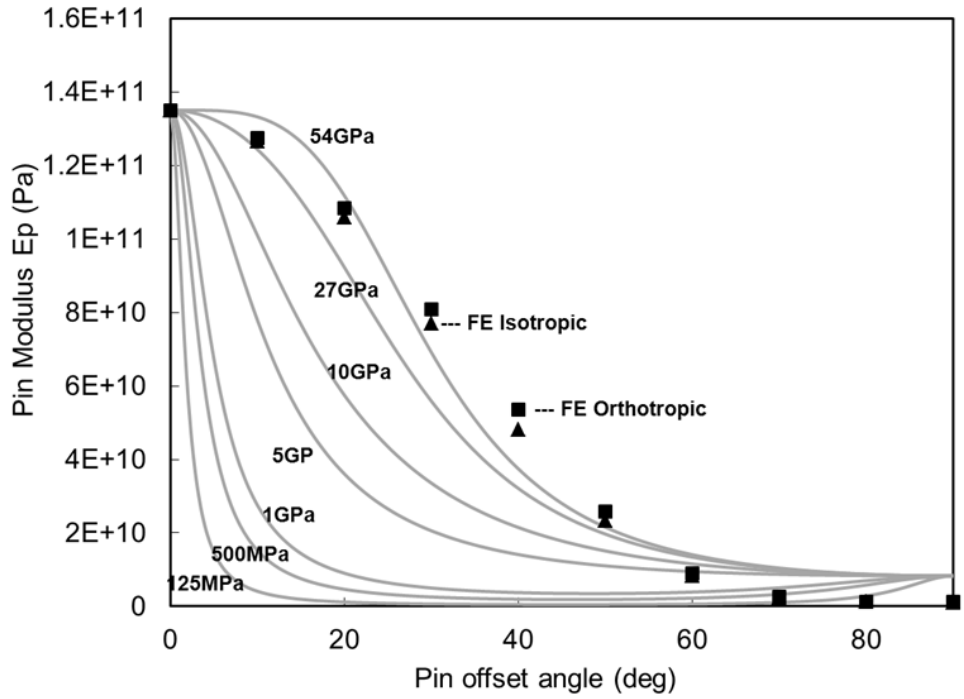

(b)

Figure 3-15: (a) Sensitivity of z-pin shear modulus to the calculated modulus E and (b) Sensitivity of z-pin modulus to the shear modulus of the pin G, with increasing offset angle

The modulus of the z-pin E_p is highly sensitive to its shear modulus for all offset angles (Equation 3-2). Figure 3-15b shows this sensitivity of the pin modulus to a variety of shear modulus values ranging from the published 125MPa value to the value of 54GPa, which has been the shear modulus that is deduced through finite element method, in an elastic and isotropic analysis. The shear modulus (G) of an elastic beam element is deduced by the Young's modulus (E) and the Poisson's ratio (ν) using the following equation;

$$G = \frac{E}{2(1+\nu)} \qquad [3\text{-}3]$$

An orthotropic finite element study showed a similar response to the isotropic study. The analytical model presented for predicting the modulus of the z-pin (Equation 3-2) is also in agreement with the finite element study when a value of 54GPa is used for the shear modulus, validating the theoretical principles that govern the analytical model.

The inabilities of the stiffness model by Mouritz [38] and the FE model to accurately predict the elastic modulus was examined by investigating the compressive response of the z-pins as the sandwich composite was subjected to increasing compression loading within the elastic regime of the stress-strain curve. Acoustic emission was performed on z-pinned specimens to monitor the damage and failure of z-pins, which is characterised by an acoustic event with high amplitude (80-100 dB) and energy (20 – 100 kJ). Three acoustic emission studies were conducted to characterize and isolate pin failure:

- investigate the acoustic energy events emitted by the unpinned sandwich composite
- identify the AE properties of damage to z-pins in a sandwich composite
- capture the acoustic energy hits of a fully z-pinned sandwich

In the first study, a sandwich composite sample without z-pins was compressed and the corresponding acoustic energy events were recorded. Shown in Figure 3-16 are data points which indicate discrete acoustic emission events and a linear curve which shows the cumulative acoustic emission counts with increasing compressive strain. Most of the acoustic emission events for the unpinned sandwich composite under elastic loading conditions had low energy levels (below 5-10 kJ). A few higher energy acoustic emissions (between 20kJ

and 30kJ) were detected when the yield stress was reached, and this was attributed to core crushing.

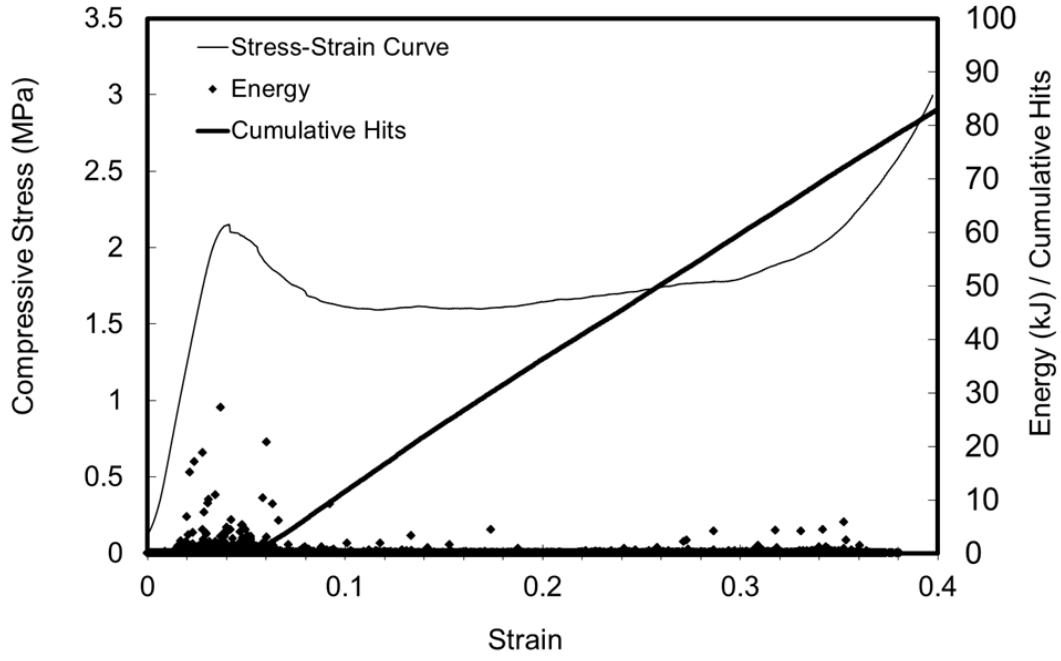

Figure 3-16: Acoustic emission monitoring of the unpinned sandwich composite. The data points indicate discrete acoustic emission events and the thick curve shows the cumulative number of emission events with increasing strain.

In the second study, a sandwich composite test (Type I) was z-pinned over an area of 10 mm x 10 mm, as shown in Figure 3-17a. The sample only contained nine z-pins (each with a diameter of 0.51 mm) within the central region. Figure 3-17b shows the load-strain and acoustic emission results for this sample. There were just nine high energy acoustic emission hits (15-60 kJ) which were recorded at the strain region as the onset of core yielding in the sandwich composite began. That is, each hit corresponded to one of the z-pins being damaged at about the strain at which the core started to permanently deform. Using this method (whereby there are fewer and a known number of pins), the event of pin failure can be successfully isolated to the elastic and yield regions of the graph.

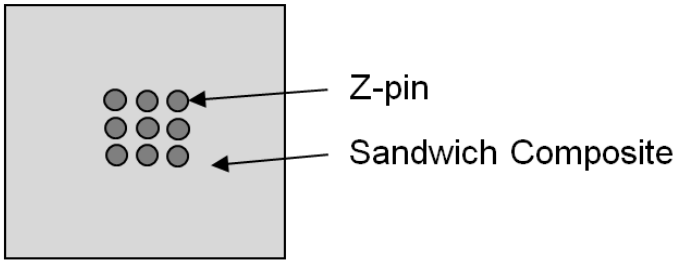

(a)

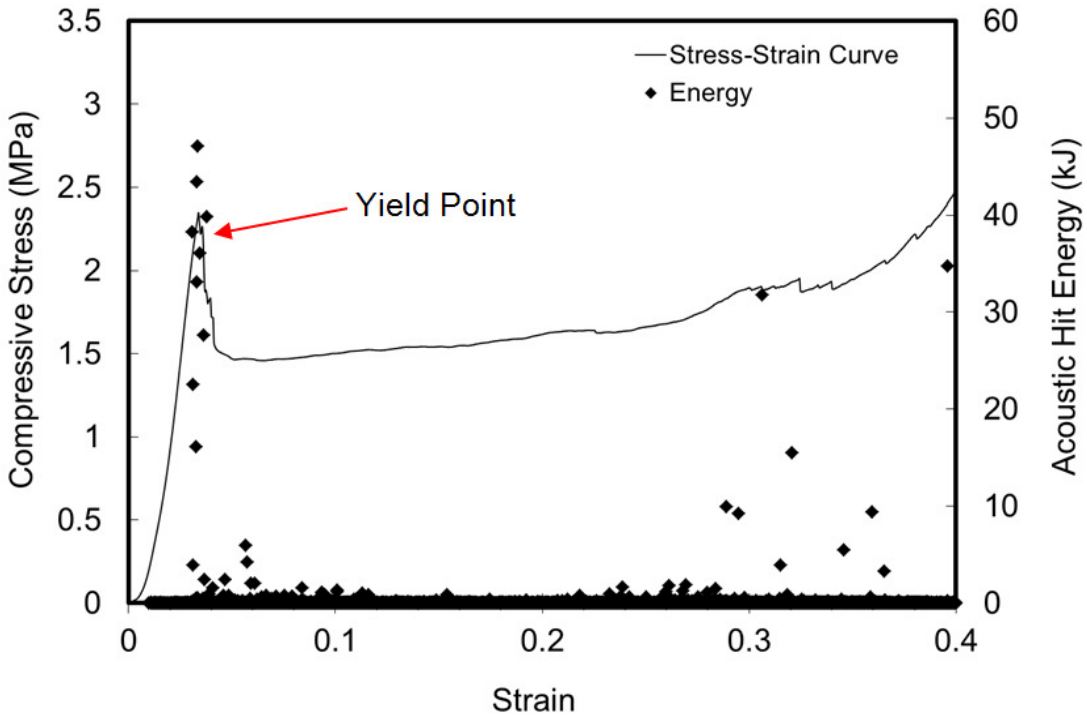

(b)

Figure 3-17: (a) Centralized pin configuration to determine pin failure acoustic signal (b) Acoustic energy result for compression test of the sandwich composite containing nine z-pins

The acoustic response of a fully z-pinned sandwich composite sample was investigated in the third study. A large number of high energy acoustic emission events were detected in the elastic regime, even at very low strain (Figure 3-18). The total number of acoustic events increased rapidly with the applied stress up to the yield stress of the z-pinned sandwich composite. This reveals that the z-pins are damaged (despite their high stiffness and strength) during elastic deformation of the foam core.

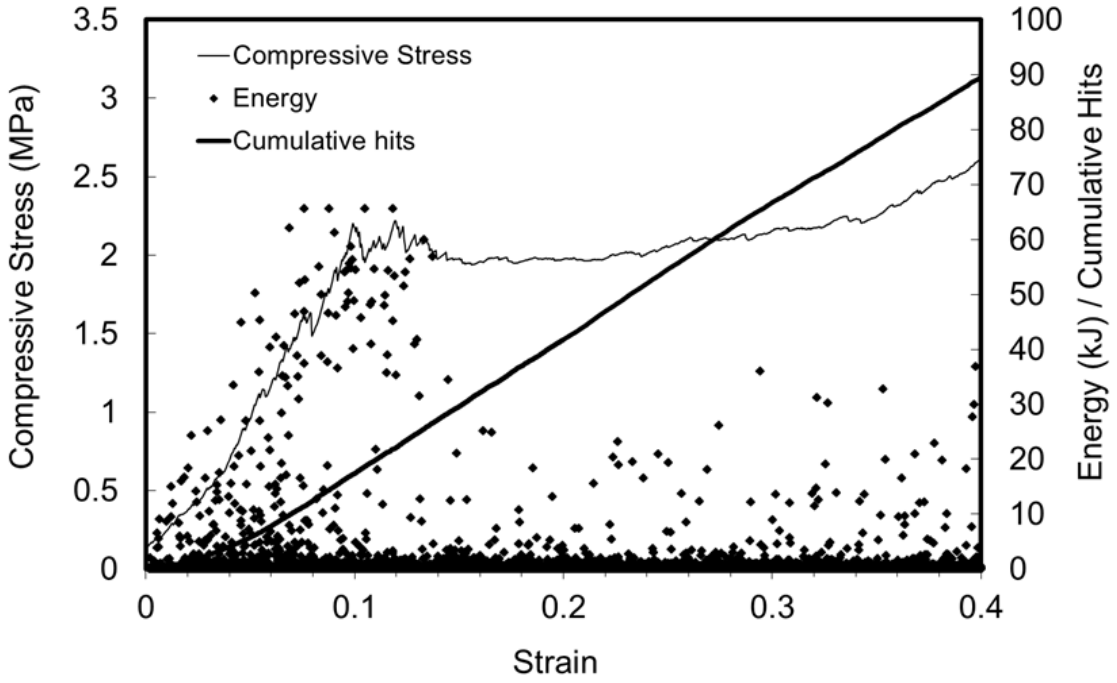

Figure 3-18: Acoustic emission monitoring of the z-pinned sandwich composite containing 2% thick z-pins. The data points indicate discrete acoustic emission events and the thick curve shows the cumulative number of emission events with increasing strain.

To investigate the failure of z-pins in the elastic regime, z-pinned sandwich specimens which had been loaded within the elastic regime (and then unloaded) were examined using X-ray computed tomography. Figure 3-19 shows the z-pins following elastic loading to the strain of 2.5%, and numerous pins had failed by longitudinal splitting and kinking. This indicates that the acoustic emission events recorded during elastic loading are caused by this splitting and microbuckling damage to the z-pins.

Examination of the z-pins before insertion in the sandwich composites revealed the presence of voids, as shown in Figure 3-20. The voids are caused by incomplete wetting of the carbon fibres with the BMI resin matrix during the pultrusion process used to manufacture the z-pins. The voids are elongated in shape and are aligned along the z-pin axis. It is believed that the voids induce longitudinal splitting of the z-pins under elastic compressive loading. The splitting then causes the z-pins to collapse by kinking. This damage causes a large loss in stiffness to the z-pins, and it is almost certainly responsible for the measured compression modulus values being lower than the calculated modulus (Table 3-3). Furthermore, given that the partial failures of the pins occur in both the elastic and plastic regions of the graph, the measurement of the experimental modulus cannot be truly represented as elastic.

Therefore the elastic limit of the z-pinned sandwich structure cannot be accurately determined due to the stochastic nature of failure in the z-pins.

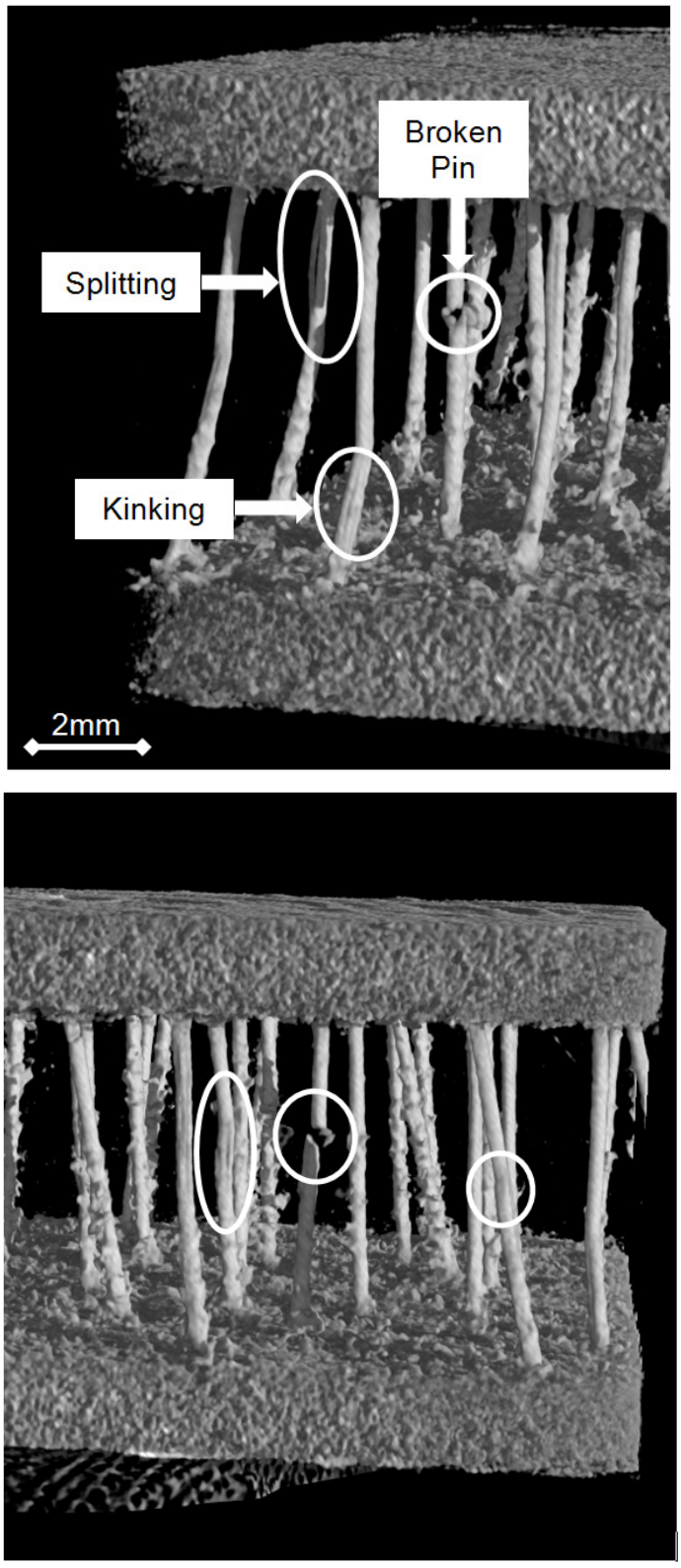

Figure 3-19: X-ray computed tomography image of a z-pinned sandwich composite (0.5% thin z-pins) following elastic compression loading. Some z-pins have failed by longitudinal splitting and kinking.

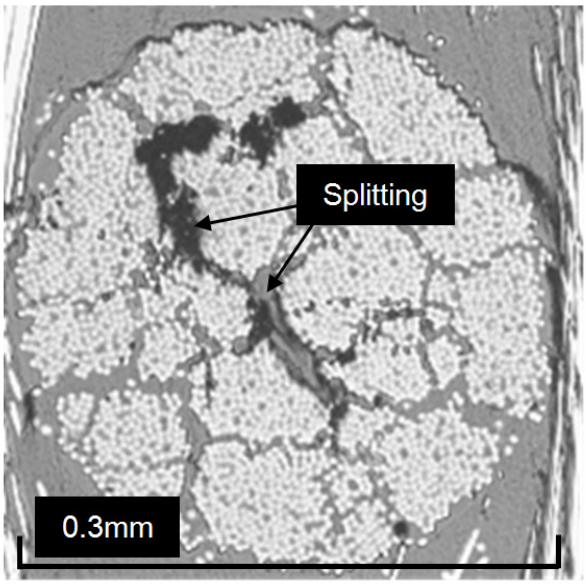

(a)

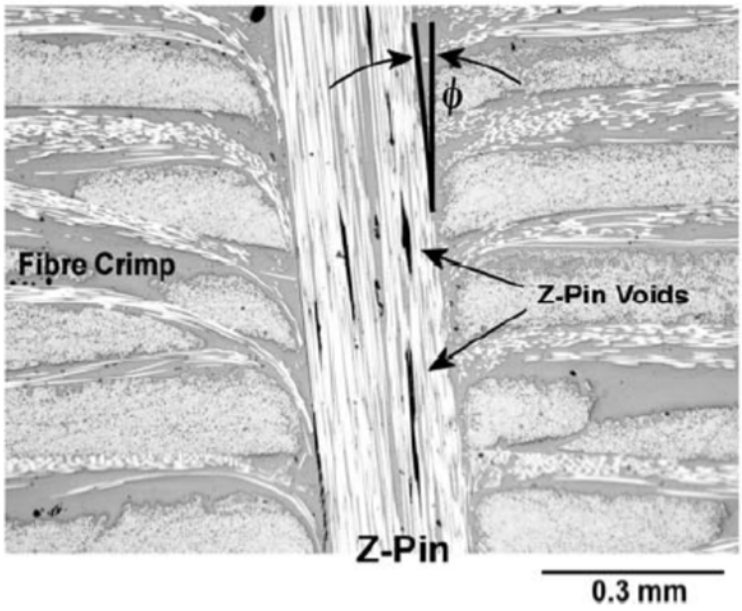

(b)

Figure 3-20: Voids in an as-manufactured z-pin. (a) The view is taken across the width (load-bearing area) of the pin. (b) View along the length of the pin in a carbon/epoxy laminate similar to the material used in the face skins to the sandwich composite. Photographs from Chang [54]

Damage to the z-pins during elastic loading occurs over a range of stress levels due to the stochastic nature of the pre-existing defects. Not all the z-pins contain voids, and those pins that do have voids of different sizes and volume contents. As a result, the compressive stress to induce longitudinal splitting and kinking varies between the z-pins, and this accounts for the large amount of scatter in the measured elastic modulus values for the z-pinned sandwich

composites shown in Figure 3-10. The offset angle of the pin may also play a role in the specific failure method of the pin, i.e. kinking or splitting.

A FEA study was conducted on a unit pin model (single z-pin) to investigate the failure of z-pins under compressive loads. A previous FE modelling study by Kocher et. al. [104] investigated the stresses generated within sandwich composites containing z-pins arranged in a truss-type structure where the pins are inclined at 45° or 60° from the orthogonal direction. The model determined the stresses within the z-pins and face skins under through-thickness compression loading of the sandwich material. The FE analysis revealed that the highest stresses are concentrated at the interfacial region between the z-pins and face skins. Failure is expected to occur by damage to the z-pins in this region and by penetration of the z-pins into the skin laminate.

To further investigate the stresses in a z-pin under compressive loads, a single z-pin was modelled in Abaqus using solid elements. The pin was offset at different angles and embedded within the top and bottom face skins. The foam was neglected in the model due to the relatively small contribution it has towards the through-thickness properties. Kocher et al. [104] also found that the foam does not result in a significant improvement in strength. Figure 3-21 shows the FE model for the single z-pin in orthogonal and several offset directions up to 12°. A concentrated load of 1 kN was applied in the z- (through-thickness) direction. The maximum stress generated within the z-pinned material system and the failure load of the z-pin was calculated for the different pin angles.

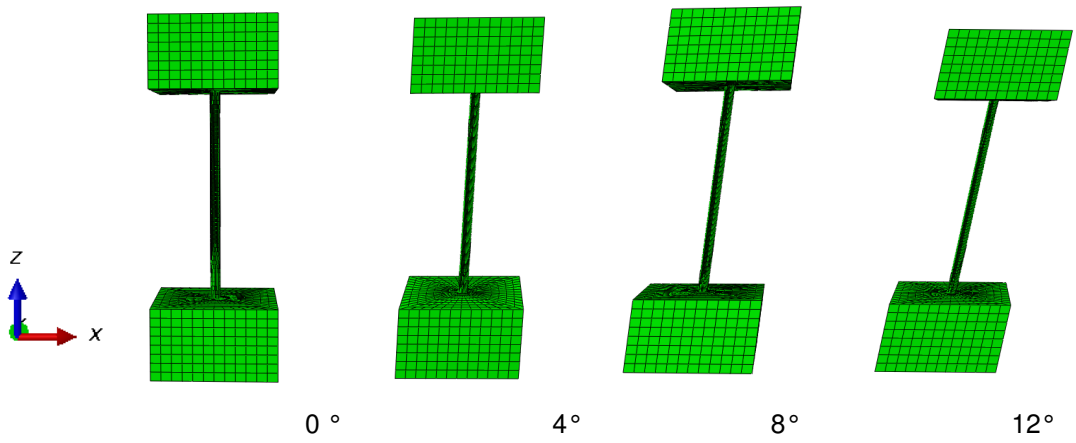

Figure 3-21: FE model showing a single z-pin at different offset angles before through-thickness compression loading

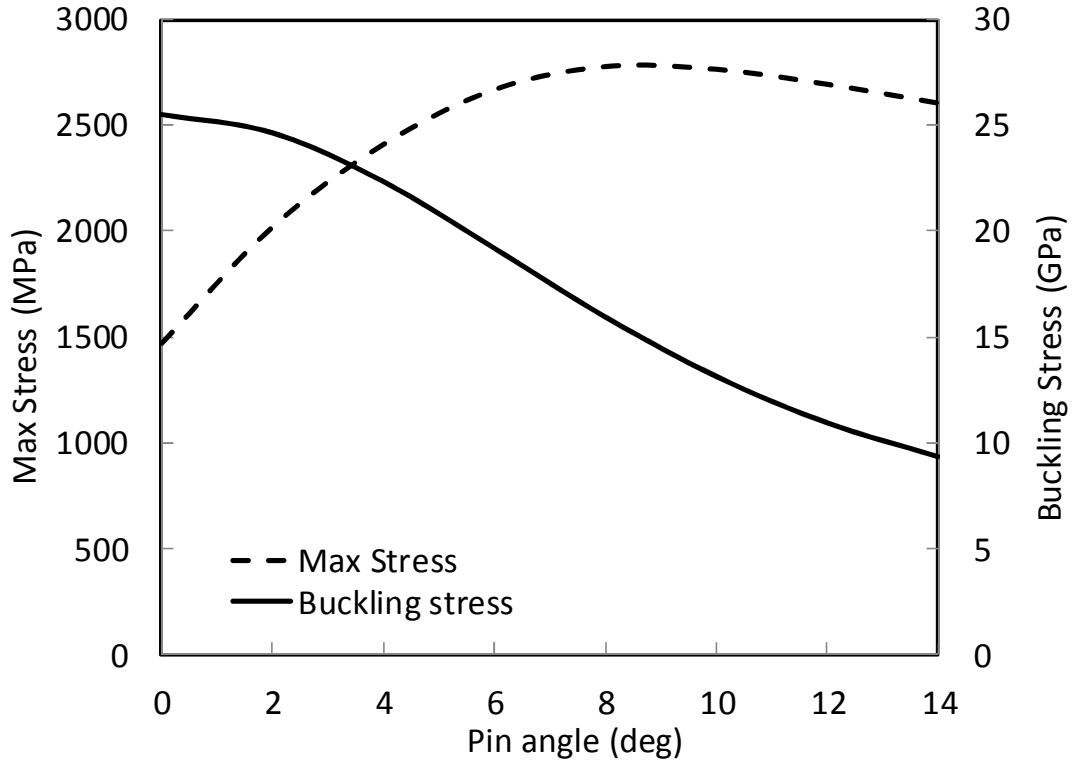

Figure 3-22: Effect of z-pin offset angle of the maximum stress (load) generated within the pin

The FE analysis revealed that the z-pin buckling load decreased (which was indicated by a static buckling analysis) with increasing pin offset angle, which is expected (Figure 3-22). The maximum stress was determined by recording the maximum Mises Stress value in the FE analysis. It was also found that the locations of concentrated stress (maximum Mises stresses) in the z-pin were dependent on the offset angle. At 0°, the maximum stress was concentrated in the middle of the z-pin at the point of maximum lateral displacement due to the buckle, as seen in Figure 3-23a. This indicates that at 0° the z-pin is likely to fail via Euler-type buckling in the form of a half-sine wave. With increasing offset angle, the maximum stress shifted closer to the interfacial region between the z-pin and face skins and this suggests that the pin will fail close to the interface. This shift in the stress concentration location is shown in Figure 3-23b to Figure 3-23d. This agrees with the study by Kocher et al. [104] where the stress concentrations were calculated to occur the z-pin and skin interface at large offset angles of the truss structure (45° or 60°). It can also be seen in Figure 3-23 that the stresses in the z-pin are not just concentrated in one location, but there a several regions of high stress along the pin length. This is representative of the multiple failures observed in the z-pin using x-ray computed microtomography. Despite providing theoretical accuracy

and verification, the FE study does not accurately represent the experimental finding whereby the z-pin failure process involves splitting, kinking and microbuckling rather than pure buckling. A far more detailed analysis is required whereby the voids within the z-pin should be modelled.

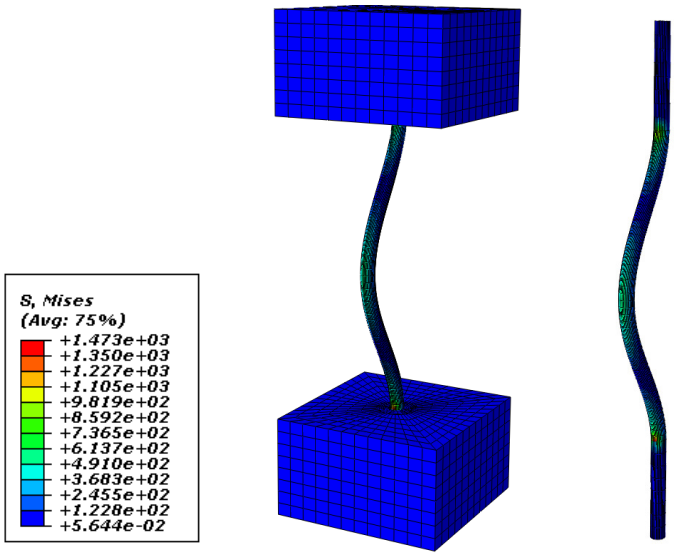

(a) 0°

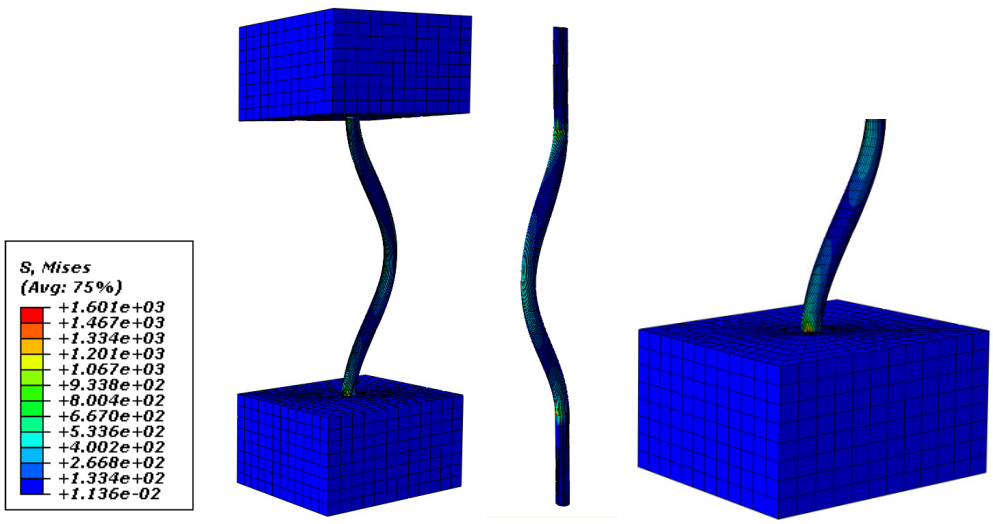

(b) 4°

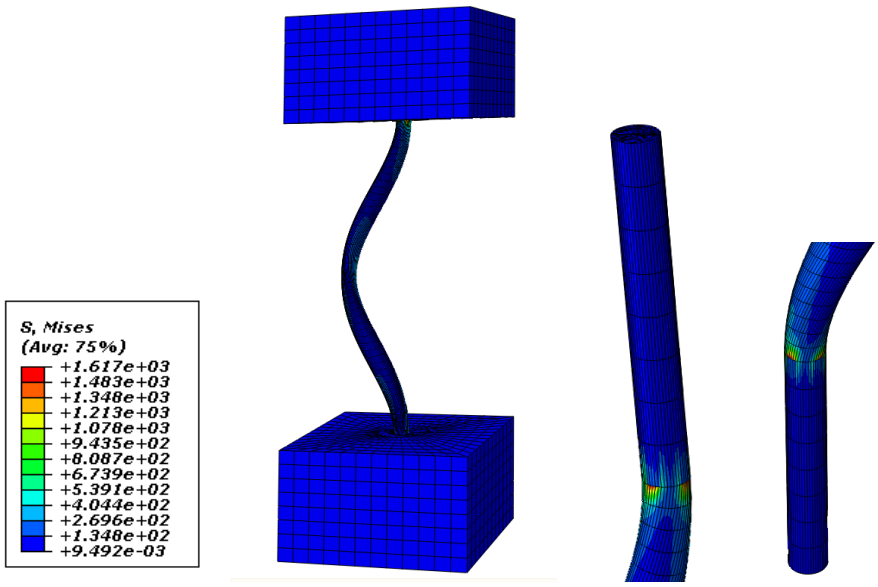

(c) 8°

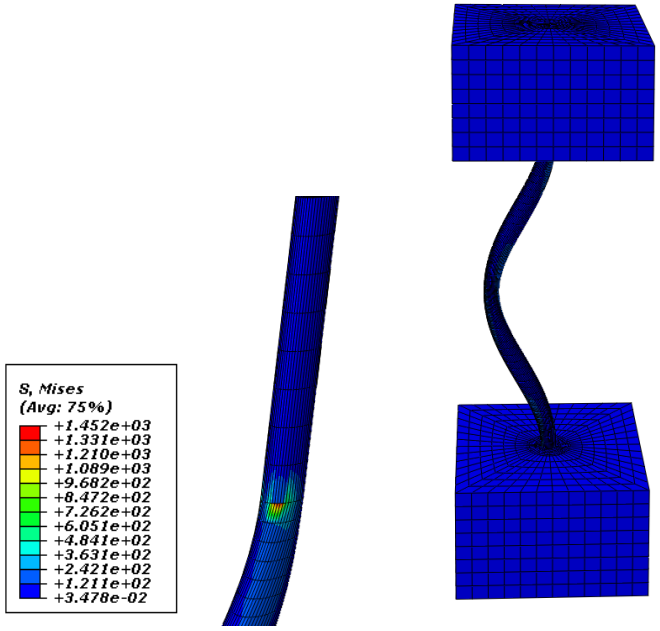

(d) 12°

Figure 3-23: Stress concentrations with increasing z-pin offset angle

The experimental research presented in this section has clearly shown that the through-thickness compression modulus of the sandwich composite increases with the z-pin content. The z-pins are denser than the foam core, and therefore there is some weight penalty incurred when reinforcing the core with pins. Figure 3-24 shows the calculated effect of increasing z-pin content on the percentage weight gain of the foam material. Material selection charts (also called Ashby plots) for the modulus-density and strength-density relationships of engineering materials are presented in Figure 3-25. Included in these charts are the property-density relationships of the foam core material with and without z-pins. It is seen that both the modulus and strength of the foam are greatly increased (by at least one order of magnitude) with only a small increase in density. These large improvements in the specific properties makes z-pinning an effective method for the stiffening and strengthening of light-weight structural materials used on aircraft.

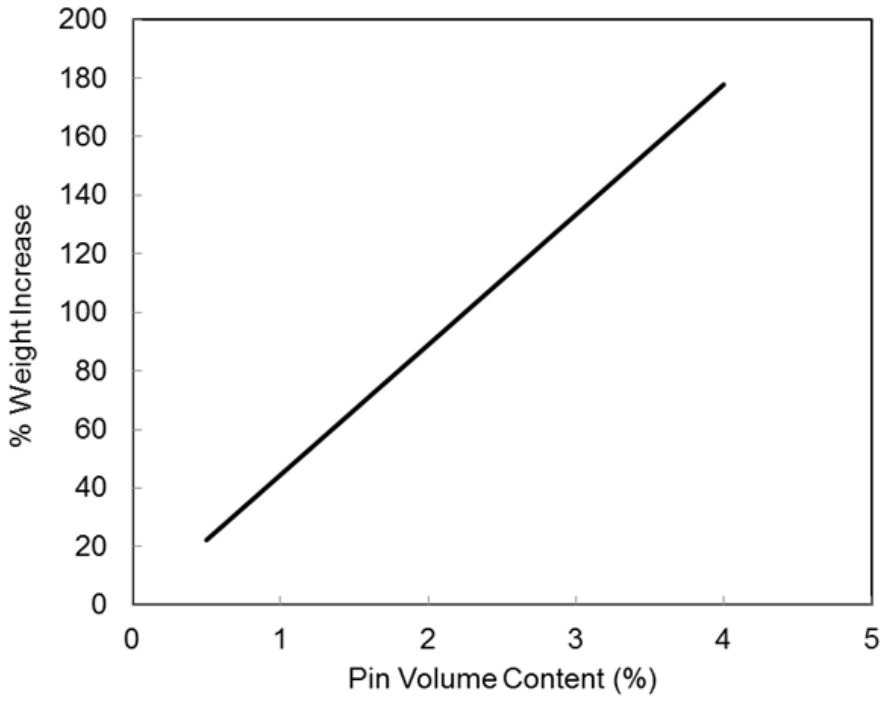

Figure 3-24: Percentage weight increase to the RIST71 core material with increasing pin volume content

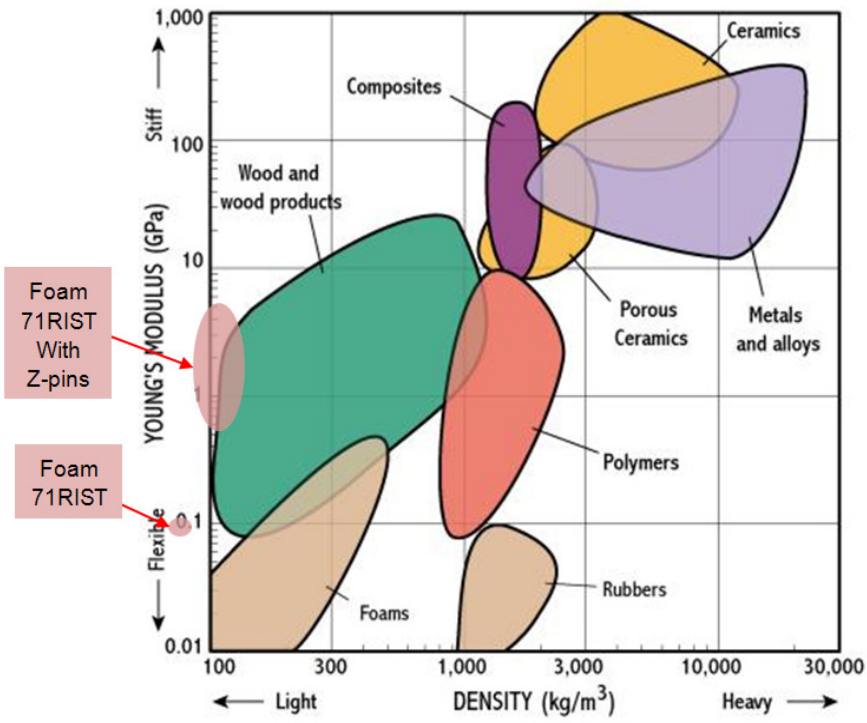

(a)

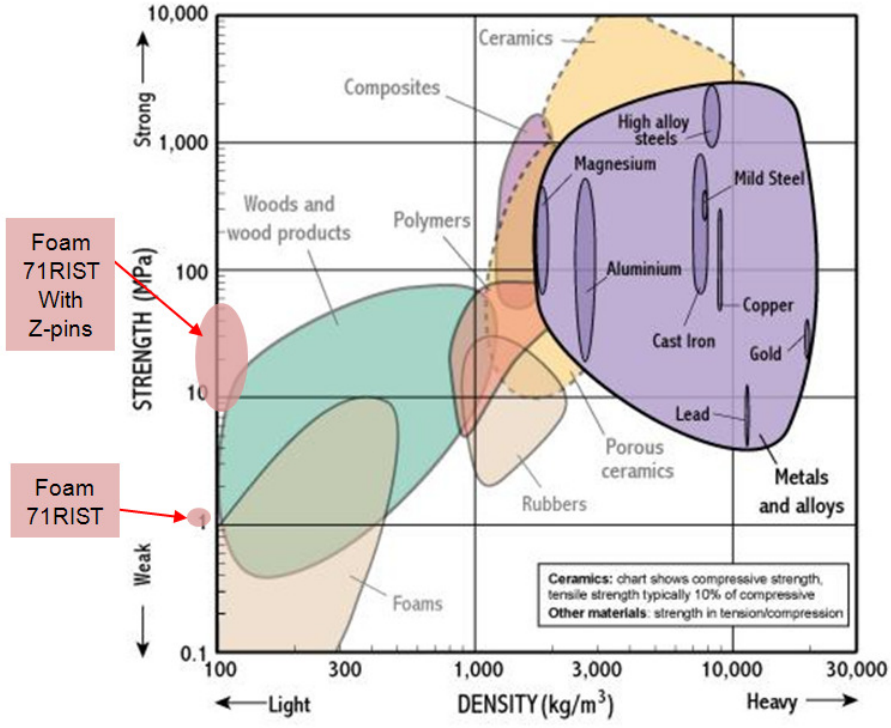

(b)

Figure 3-25: Ashby plots for 71RIST foam with and without z-pins (a) Young's modulus – Density and (b) Strength – Density

This study has shown that the stiffening effect by the z-pins is controlled mostly by the volume content, elastic modulus and orientation of the z-pins, and that the diameter and boundary condition of the pins are less important. The efficacy of the z-pins in stiffening of the foam core will increase with the ratio of E_p/E_f, where E_p and E_f are the Young's modulus of the z-pin and core material, respectively. The ratio will increase with the volume content and modulus of the z-pins as well as reduction of the misalignment angle of the pins from the orthogonal direction. Figure 3-26 shows predicted increase in the through-thickness compressive modulus of a sandwich composite with increasing E_p/E_f ratio for different z-pin contents (for the Mouritz model). This ratio was based on the stiffness of the two foams studied in this thesis. The dashed line shows the existing E_p/E_f ratio for both the 51RIST and the 71RIST type foams. The figure shows that the composite stiffness increases at a linear rate with increasing E_p/E_f. This increase is pronounced when the pin volume content is increased. The trends for the 51RIST foam are nearly the same as the 71RIST foam, and this is because the difference in stiffness of the two foams is not significant.

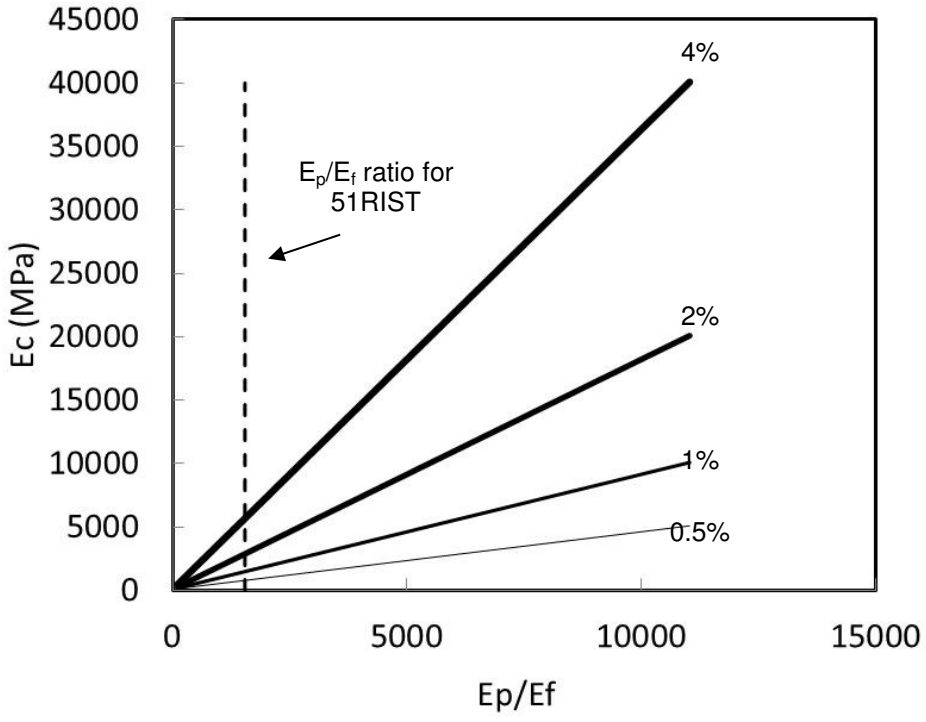

(a)

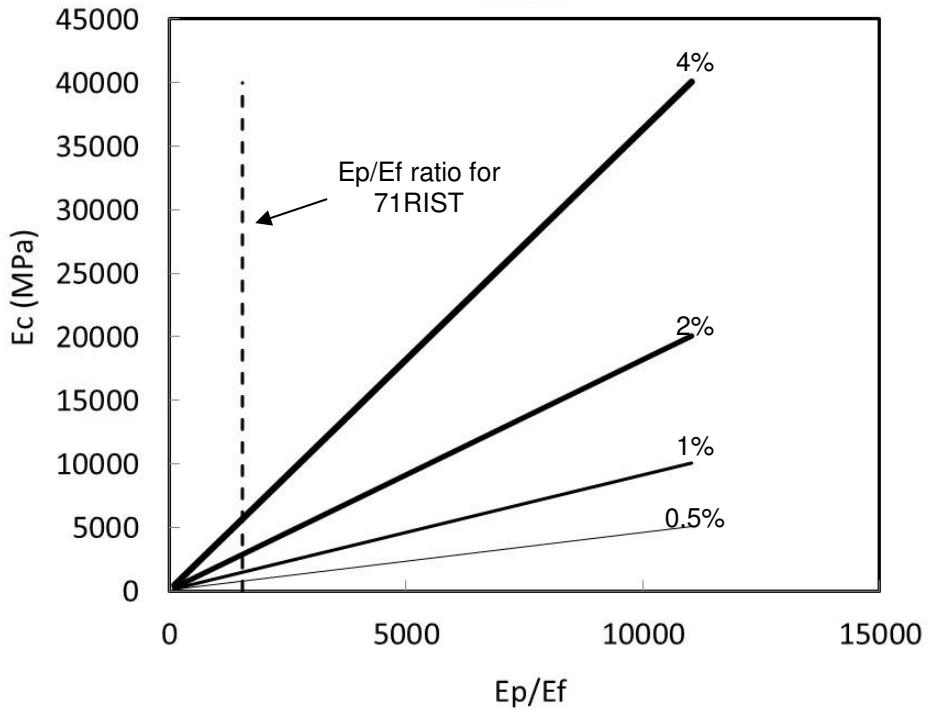

(b)

Figure 3-26: Increase in the stiffness of the sandwich composite (E_c) with increasing E_p/E_f ratio for (a) 51RIST foam and (b) 71RIST foam core materials

3.3.3 Compression Strengthening, Energy Absorption Capacity and Strengthening Mechanisms of Z-Pinned Sandwich Composites

Figure 3-27 and Figure 3-28 show the measured effects of increasing volume content and diameter of z-pins on the compressive yield strength and compressive strain energy absorption capacity of the sandwich composite. The yield strength is the stress level at which the sandwich material begins to undergo bulk plastic deformation, and is taken from the compressive stress-strain curve as the peak stress immediately following the elastic region and immediately before the load drop. The compressive strain energy absorption is the amount of strain energy needed to deform the sandwich material over the test strain range (40% deformation), and is determined from the total area under the compressive stress-strain curve. Both the yield strength and strain energy absorption capacity increase rapidly with the volume content of z-pins. At the highest z-pin content (4%), the yield strength is increased by nearly 700% and the absorbed strain energy by about 600%. The improvement to these properties is not affected significantly by the z-pin diameter (for the two sizes that were studied) or by the end constraint on the z-pin (built-in column or simply supported column). This reveals that improvements to the through-thickness compressive properties (modulus,

strength and absorbed strain energy) are determined primarily by the volume content of the z-pins, and other pin parameters (such as diameter and end constraint) are less influential.

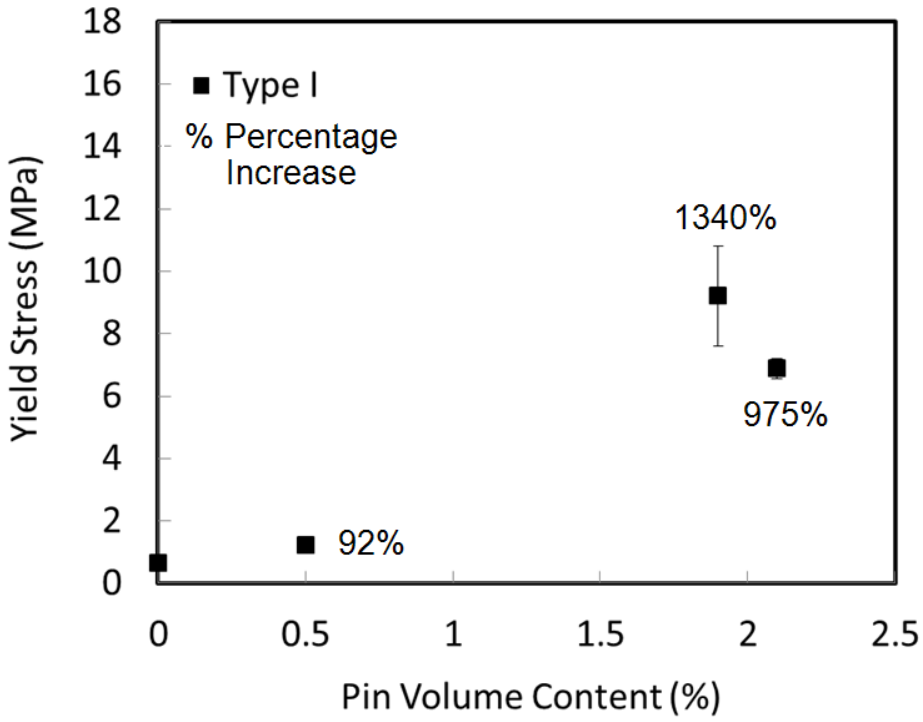

(a)

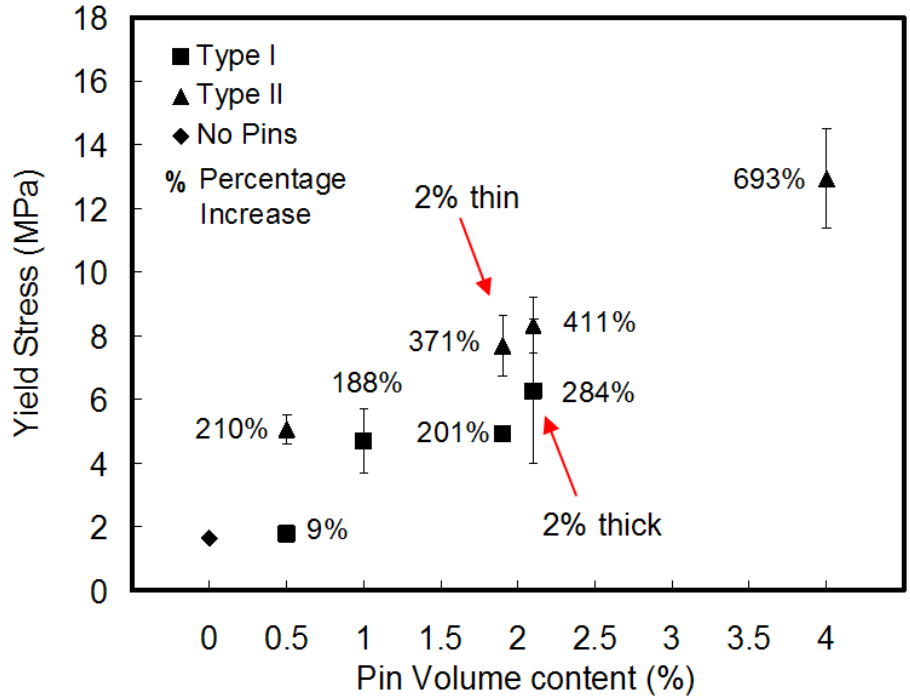

(b)

Figure 3-27: Effects of the volume content and diameter of z-pins on the through-thickness compression yield stress. The error bars represent one standard deviation. (a) 51RIST foam and (b) 71RIST foam core sandwich composites

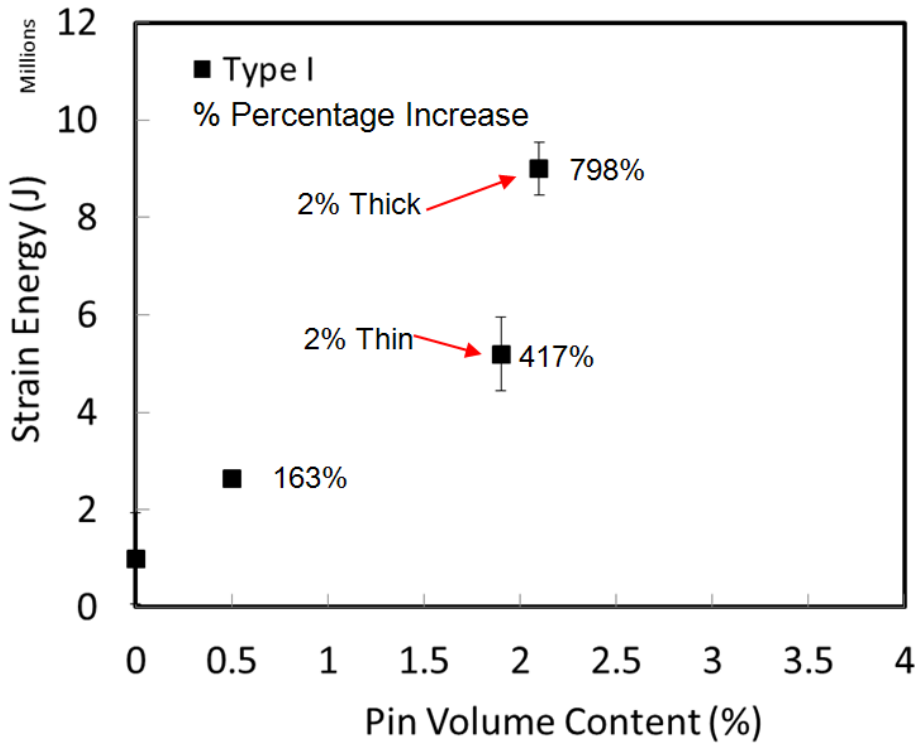

(a)

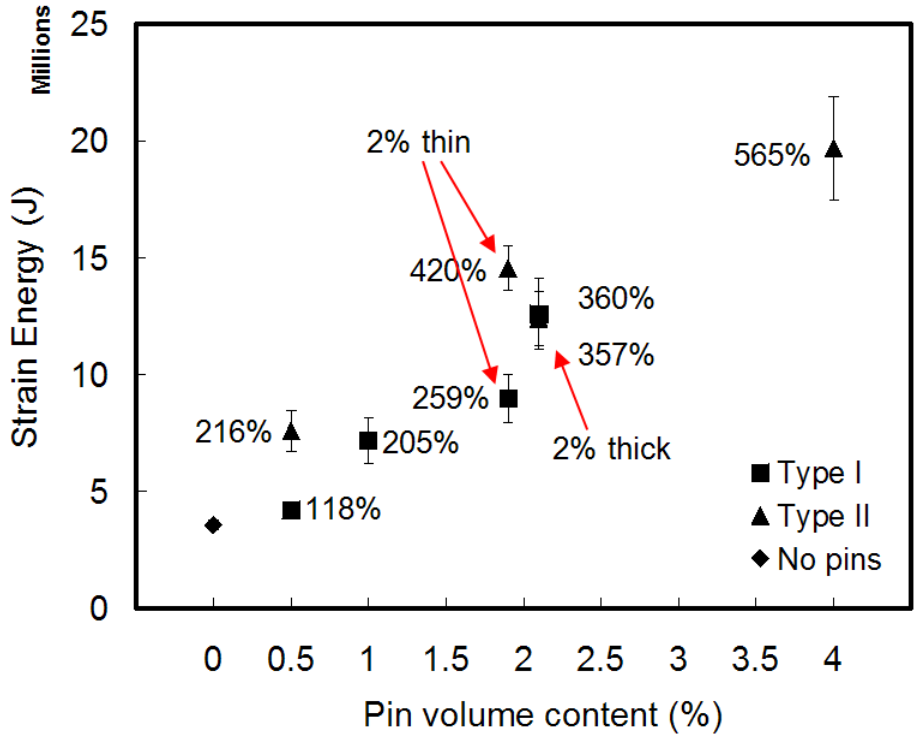

(b)

Figure 3-28: Effects of the volume content and diameter of z-pins on the compressive strain energy absorption capacity. The error bars represent one standard deviation. (a) 51RIST foam and (b) 71RIST foam core sandwich composites

The compressive stress-strain curves for the z-pinned sandwich composites show an abrupt load drop immediately following the yield point (Figure 3-9). This is due to a sudden loss in pin stiffness and strength. The compressive failure behaviour of the z-pins between the yield stress point and the end of the compression test (at 40% deformation) was determined using acoustic emission monitoring, X-ray computed tomography and scanning electron microscopy. Figure 3-16 shows that a high density of low energy acoustic events (most below 10 kJ) were recorded for the unpinned material at the compressive yield point, and this is due to initial plastic crushing of the foam core. The number and energy of the acoustic events in this material then remains relatively low with increasing compressive strain until about 30% when the material begins to work-hardened due to densification of the crushed core. In contrast, the z-pinned sandwich composite emitted both low energy (under 10 kJ) and higher energy acoustic signals (~20-60 kJ) due to core crushing and z-pin damage, respectively. The high energy acoustic events occur over the entire strain region which indicates that z-pins fail over the entire strain range.

Figure 3-29 presents a sequence of X-ray computed tomography images of a z-pinned sandwich composite taken at increasing levels of compressive strain between the yield point and the end of the flat-wise compression test. Buckling of the z-pins is not evident, which is the dominant failure mode for metal pins in sandwich composites [34]. Instead, increasing the compressive strain caused an increasing number of z-pins to fail by longitudinal splitting and kinking and also at multiple locations along the length of the pins. The z-pins failed over a range of compressive strain values due to their variable strength and inclined angles, although a large percentage of the pins fail close to the yield point, as shown in Figure 3-29a and by the acoustic emission monitoring results presented in Figure 3-18. Increasing the compressive strain beyond the yield point causes further damage to the z-pins by crushing and fragmentation.

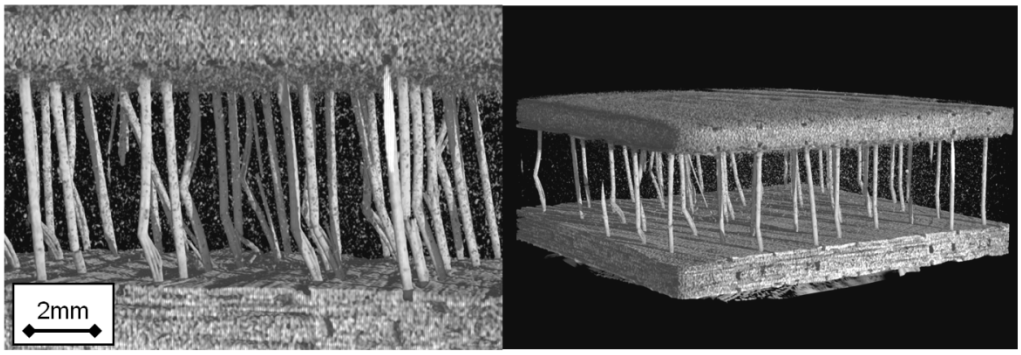

(a)

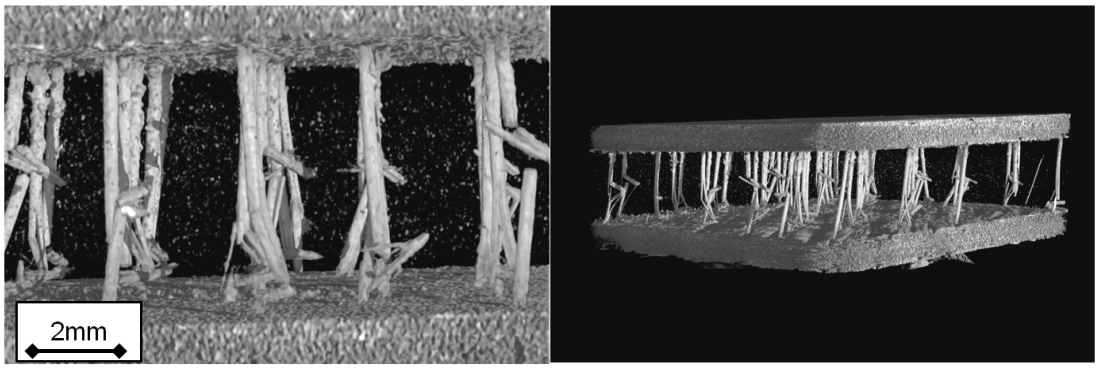

(b)

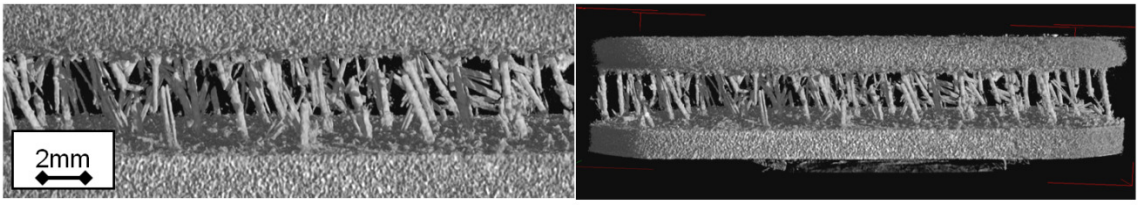

(c)

Figure 3-29: High (left-hand side) and low (right-hand side) magnification x-ray computed tomography images of a z-pinned sandwich composite (0.5% thin pins) taken after loading at increasing levels of compressive strain: (a) 8% (yield point), (b) 18% and (c) 40% (end of test).

Even though most of the z-pins failed close to the yield point, the residual strength and absorbed energy capacity of the z-pinned sandwich composites remained much higher than the unpinned material. It appears that even after the z-pins break they do not completely lose their load-bearing capacity. Instead, the fractured ends of the z-pins are pressed into the core material which acts as a stress transfer medium (Figure 3-30). The fractured ligaments of the z-pins were forced into the foam core with a mechanical response similar to a cylindrical punch at an inclined angle being pressed into a plastic medium (i.e. core material). The resistance against this process increases the further the fractured ligaments of the z-pins are pressed into the core, thereby increasing the compressive strength and strain energy absorption capacity above that of the unpinned sandwich material. The total force needed to

press the fractured z-pins into the core increases with their volume fraction, and this accounts for the increase to the compressive strength and strain energy absorption of the z-pinned sandwich composites at high compressive strain levels.

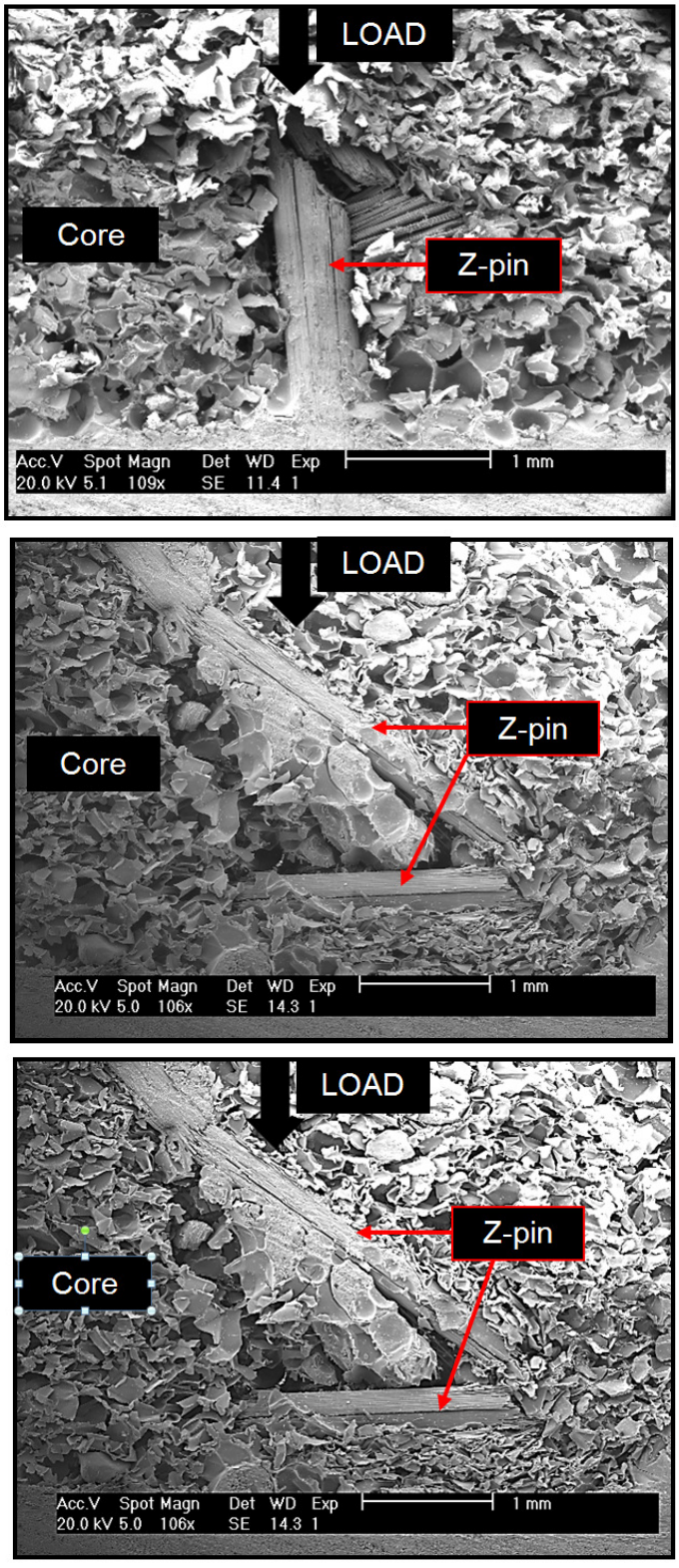

Figure 3-30: Scanning electron micrographs showing examples of indentation of the foam core by fractured z-pins.

Several models have been developed to calculate the flat-wise compressive strength of z-pinned composites, including a buckling model proposed by Cartié and Fleck [34] and a strength-based model by Mouritz [38]. The compressive strength of a sandwich composite reinforced with z-pins that fail by buckling is calculated using [34]:

$$\sigma_c = f_p \sigma_p \cos^2 \theta + \sigma_f \qquad [3\text{-}4]$$

where σ_f is the average stress in the foam, f_p is the volume fraction of z-pins, θ is the pin offset angle and σ_p is the buckling stress of the pins. σ_f and σ_p are calculated using:

$$\sigma_f = \frac{4E_f P_b}{\pi d_p^2 E_p \cos\theta} \qquad [3\text{-}5]$$

and

$$\sigma_p = \frac{\pi^2 E_p I}{A_p (\mu l)^2}\left(m^2 + \frac{\beta l^4}{m^2 \pi^4 E_p I}\right) \qquad [3\text{-}6]$$

where E_pI is the flexural stiffness, l is the pin length, β is the foundation modulus of the foam, m is the number of half sine waves the pin buckles (assumed to be 1), μ is a value of 0.5 or 1 depending on the end restraint condition of the z-pin and E_f and E_p are the elastic modulus of the foam and z-pin, respectively.

When the z-pins fail by crushing rather than buckling then the compressive strength is calculated using [38]:

$$\sigma_p\left(\sum\theta\right) = \sum_{\theta=0}^{\theta=90} V_p(\theta).\sigma_p(\theta) \qquad [3\text{-}7]$$

where the compressive strength of the pins at the inclined angle (θ) is determined using:

$$\sigma_p(\theta) = \left[\frac{\cos^2\theta(\cos^2\theta - \sin^2\theta)}{\sigma_x^2} + \frac{\sin^4\theta}{\sigma_y^2} + \frac{\cos^2\theta\sin^2\theta}{\tau_{xy}^2} \right]^{-\frac{1}{2}} \quad [3\text{-}8]$$

σ_x and σ_y represent the axial and transverse strengths of the z-pin, respectively, and τ_{xy} is the shear strength of the pin.

Table 3-4 shows the calculated increase to the compressive strength of the sandwich composite with increasing volume content of z-pins when it is assumed that pin failure occurs by buckling (Equation 3-4) or crushing (Equation 3-2). Strength calculations for both models used the average value of the measured z-pin offset angles for each pin volume content category. The agreement of the models with the measured strength values is poor, and this is because neither model has the capacity to analyse the complex failure process of fibrous z-pins which involves longitudinal splitting, kinking and fragmentation. Modelling is also difficult because of the presence of voids within fibrous z-pins which influence their failure stress. Therefore, existing mechanical models are unable to predict the compressive strength of composites reinforced with these fibrous z-pins, and the development of a strength-based model is challenging due to the complexity of the failure mechanisms and the stochastic strength properties of the pins. However, such a model is needed for the design of z-pinned composite structures for aerospace and other applications.

Table 3-4: Experimental and theoretical compressive yield strength.

Composite (I) - Type I (II) - Type II	Average pin offset angle (deg)	Experimental Compressive Strength (MPa)	Strength Model [38] (MPa)	Buckling Model [34] (MPa)
0.5% (I)	6.1°	1.8 +/- 0.1	3.8	1.5
1% (I)	3.5°	4.7 +/- 1	8.4	2.8
2% Thin (I)	1.6°	4.9 +/- 0.1	24.3	5.4
2% Thick (I)	4.9°	6.3 +/- 2.3	11.9	19.8
0.5% (II)	2.7°	5.1 +/- 0.5	5.8	1.1
2% Thin (II)	2.1°	7.7 +/- 1	21.2	3.8
2% Thick (II)	5.7°	8.3 +/- 0.9	10.6	13.7
4% (II)	2.1°	12.9 +/- 1.6	41.4	7.4

3.4 KINKING STRENGTH MODELLING OF Z-PINS

In light of the discovery that z-pin failure is a complex process involving several damage mechanisms, including kinking, the Budiansky-Fleck [105, 106] model for compressive failure of fibre composites via plastic kinking was adapted to determine pin strength. Figure 3-31 shows x-ray tomography images of z-pins in a sandwich composite kinking under compressive loads.

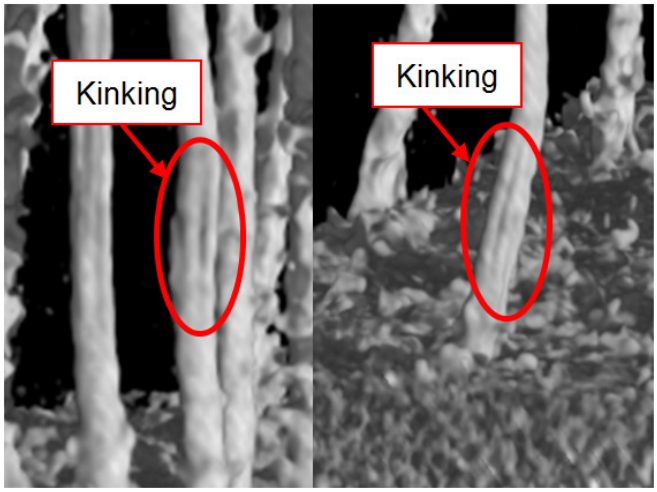

Figure 3-31: Examples of kinking failure of z-pins in a sandwich composite

Kinking can be defined as a process whereby the fibres undergo micro-buckling collectively in a narrow band, as shown schematically in Figure 3-32. Kink bands in unidirectional carbon fibre composites typically have a β value (which is the rotation angle normal to the fibre orientation) of 10° to 30° and a width of about 10 fibre diameters. If kinking is assumed to be an elastic bifurcation buckling problem and β is 0°, then the kinking stress (σ_c) is determined by:

$$\sigma_c = \frac{G_m}{1-\nu_f} \qquad [3\text{-}9]$$

Where G_m is the shear modulus of the matrix and ν_f is the volume fraction of the fibres. An equation for kinking in the plastic regime was developed by Argon [107] and modified by Budiansky and Fleck [105, 106]:

$$\sigma_k = \frac{\tau_\gamma}{\gamma_Y + \bar{\phi}} = \frac{G}{1 + \frac{\bar{\phi}}{\gamma_Y}} \quad ; \; \gamma_Y = \frac{\tau_Y}{G} \qquad [3\text{-}10]$$

Whereby τ_y is the longitudinal shear stress, γ_y is the yield shear strain and $\bar{\phi}$ is the initial misalignment angle. Busiansky and Fleck [105, 106] state that if the elastic-ideally plastic constitutive law is assumed, then the limit point buckling occurs at a particular ratio of kinking stress to shear modulus for fibrous materials that obey the Ramberg-Osgood shear stress relationship:

$$\sigma_k / G = \left[1 + n \left(\frac{3}{7} \right)^{\frac{1}{n}} \left\{ \frac{\bar{\phi} / \gamma_Y}{n-1} \right\}^{\frac{n-1}{n}} \right]^{-1} \qquad [3\text{-}11]$$

where $\gamma_\gamma = \frac{\tau}{\tau_Y} + \frac{3}{7}\left(\frac{\tau}{\tau_Y} \right)^n$ (Ramberg-Osgood shear stress relationship)

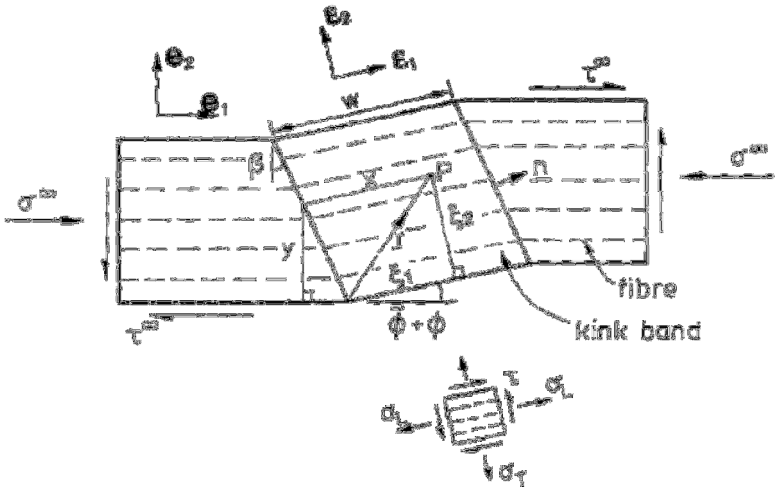

Figure 3-32: Kink band geometry and notation, adapted from Budiansky and Fleck [105, 106]

With the assumption that the initial fibre misalignment angle is 2° (which is a typical value for unidirectional tape laminate) and for all values of n within the range $3<n<\infty$, then the

variation of σ_k/G with $\bar{\phi}/\gamma_Y$ is the same. For $\bar{\phi}/\gamma_Y$ the values range from 3 to 4 and σ_k/G for range from 0.2 to 0.25 [105, 106]. Therefore, based on this relationship, the kinking stress, σ_k, can be determined for z-pins offset at different misalignment angles. This kinking stress can then be applied to the strength model developed in the Mouritz model [38] (Equation 3-1), replacing the term for z-pin strength σ_p, and thereby creating a new model for the prediction of through-thickness strength of a z-pinned sandwich composite. This assumes that the main mode of z-pin failure is kinking. The new model with the kinking relationship is described by:

$$\sigma_c = \sigma_f f_f + \sigma_k f_p \qquad [3\text{-}12]$$

Figure 3-33 shows the variation in the failure strength calculated using the new kinking stress model with the pin offset angle for two z-pin volume contents. Figure 3-33 shows the Mouritz [38] strength model with crushing failure assumptions and the newly introduced kinking stress model. The strength of the z-pinned sandwich composite decreases with increasing pin offset angle for both the crushing and the kinking failure mechanisms. However, the original crushing failure assumption shows large over-predictions in the strength in comparison to the experimental strength for both 0.5% and 2% pin volume contents, which are 1.8 MPa and 4.9 MPa respectively. However, with the introduction of the kinking stress to the Mouritz model [34], the strength predictions for a z-pinned sandwich composite are much lower and in closer agreement with the experimental values, although they are now under-predicting the experimental results. However, sensitivity to the pin offset angle is now reduced. Table 3-5 shows the predictions made by the kinking stress model on the strength of a z-pinned sandwich composite with varying pin volume content. The new model takes in to account the average offset angle recorded and also conducts a weighted analysis for every pin volume content category. It should be noted that the kinking stress model does not account for the z-pin end restraint condition. The values calculated by the kinking model, both with average angle and a weighted prediction are in closer agreement with the experimental values. Despite the under-prediction of strength values, the model shows that introducing the concept of z-pin kinking as a failure mode is a more realistic and accurate than the assumption of crushing based on the tomography results. The

incorporation of other failure modes such as splitting can provide a more accurate representation of the actual complex failure of z-pins under compressive loads.

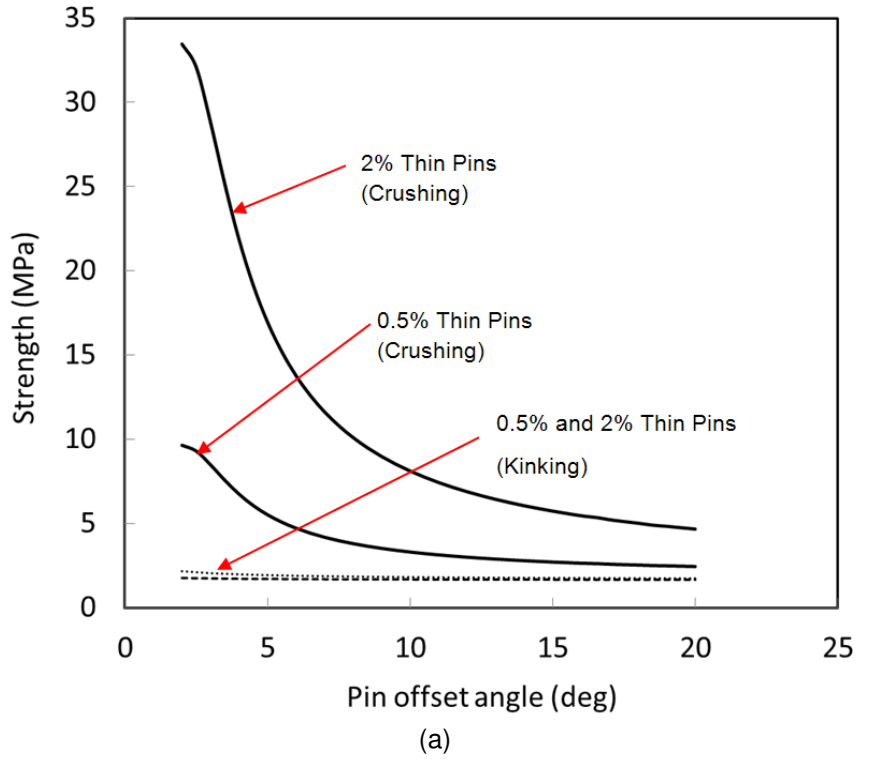

(a)

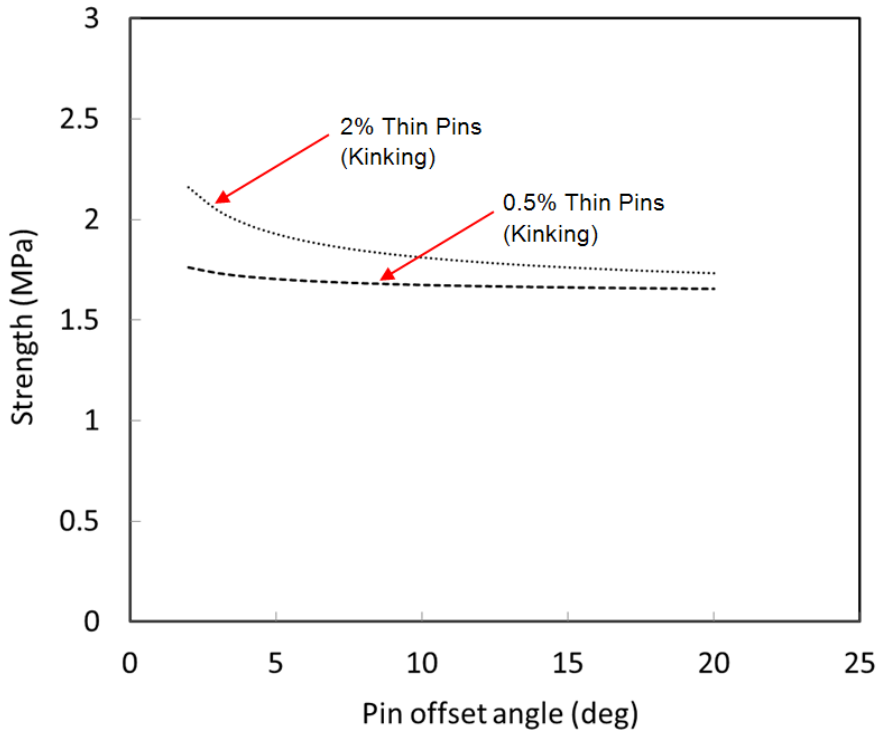

(b)

Figure 3-33: New model for predicting z-pinned sandwich composite strength using kinking stress (a) in comparison with the Mouritz model [34] with pin crushing and (b) expanded view of new kinking model

Table 3-5: Strength of a z-pinned sandwich composite with z-pin crushing failure and z-pin kinking failure assumptions

Composite (I) - Type I (II) – Type II	Average pin offset angle (deg)	Experimental Compressive Strength (MPa)	Strength Model Mouritz [34] (MPa)	New Model with Kinking Stress using average offset angle (MPa)	New Model with Kinking Stress using weighted analysis (MPa)
0.5% (I)	6.1º	1.8 +/- 0.1	3.8	1.7	1.7
1% (I)	3.5º	4.7 +/- 1	8.4	1.8	2
2% Thin (I)	1.6º	4.9 +/- 0.1	24.3	2.2	2.7
2% Thick (I)	4.9º	6.3 +/- 2.3	11.9	1.9	2.2
0.5% (II)	2.7º	5.1 +/- 0.5	5.8	1.7	1.8
2% Thin (II)	2.1º	7.7 +/- 1	21.2	2.1	2.4
2% Thick (II)	5.7º	8.3 +/- 0.9	10.6	1.9	2.1
4% (II)	2.1º	12.9 +/- 1.6	41.4	2.7	3.5

3.5 CONCLUSIONS

Z-pinning is an effective method for improving the through-thickness compressive properties of sandwich composites. Z-pins inserted in an orthogonal configuration increase the compression modulus, strength and absorbed strain energy capacity of foam core sandwich composites. The compressive properties increase rapidly with the volume fraction of z-pins, and only a small amount of pins (under a few percent) is needed to improve the properties by several hundred percent. The improvement to the properties is controlled strongly by the z-pin content, and is not influenced significantly by the pin diameter (for the two sizes studied) or the pin end constraint (built-in column or simply supported column).Fibrous z-pins fail during both elastic and plastic deformation of the foam core via a complex process of splintering, kinking and fragmentation. However, even after the z-pins have failed, the collapsed pin segments can promote significant strengthening because the foam core behaves as a Winkler elastic foundation which allows stress transfer. Also, the fractured ligaments of the z-pins are pressed into the foam core under increasing compressive strain which strengthens the sandwich material. Failure of the fibrous z-pins is initiated by voids created during pin manufacturing, and as a result they do not respond to compressive loading in the same way as metal pins. Existing mechanical models for calculating the through-thickness properties of z-pinned sandwich composites are not accurate for the materials studied here, because they do not account for the splintering and kinking of the z-pins.

Chapter 4 INDENTATION AND IMPACT PROPERTIES OF Z-PINNED SANDWICH COMPOSITES

ABSTRACT

This chapter assesses the indentation and impact properties of sandwich composites when the core was reinforced with through-thickness z-pins. Low-speed point loading (indentation) and high-speed point loading (impact) experiments were conducted to investigate the effect of localised loading conditions on the mechanical response of z-pinned sandwich materials. The low-speed tests involved indenting the composites with a hemispherical ball, cylindrical rod and flat plate to induce different surface contact conditions. An increase in contact area by changing the type of indenter resulted in an increase in the through-thickness stiffness and absorbed energy properties of the z-pinned sandwich composite. The increase was attributed to the increase in contact area where an increasing number of z-pins resist the indentation load. The experimental results were compared with theoretical results calculated using an indentation model for z-pinned sandwich composites, and the agreement was poor. It was established that the existing model lacks the fidelity to mechanistically analyse the indentation process involving splintering, kinking and fragmentation of the z-pins.

There was no improvement to the impact damage resistance and post-impact mechanical properties of the z-pinned sandwich composite at low impact energies (when damage was confined to the impacted face skin). Z-pins were only marginally effective at increasing the damage resistance when the impact energy was high enough to cause core crushing. Z-pins absorbed high impact energy via splitting, microbuckling and fragmentation during core crushing, and these processes increased slightly the impact damage resistance of the sandwich composite.

Part of the research presented in this chapter has been published in the following article:

Nanayakkara, A., Feih, S. and Mouritz, A.P., 'Experimental impact damage study of z-pinned sandwich composites', *Journal of Sandwich Structures and Materials*, Vol. 14, pp. 469-486, 2012.

4.1 INTRODUCTION

Problems with conventional sandwich composites (with an unreinforced core material) include poor resistance against through-thickness compression, crushing and impact loads, as previously mentioned. The low stiffness and strength of the core material provide little resistance against crushing of the sandwich composite when subjected to indentation or impact loading. Furthermore, cracking between the face skins and core can occur under indentation or impact loads due to the low interfacial bond strength. Both core crushing and skin-core cracking can reduce the in-plane properties of sandwich composites, particularly the compressive strength and fatigue life. A potential solution to the low indentation and impact resistance of sandwich composites is stiffening and strengthening of the core material with through-thickness pins.

As mentioned in Chapters 2 and 3, through-thickness reinforcement of the core material can increase the flatwise compression stiffness, strength and energy absorption of sandwich composites. For example, Rice et al [41] measured an increase of over 2500% to the peak flatwise compressive strength of a sandwich composite when its core was reinforced with z-pins. Recent research by Long and Guiqiong [40] has shown that the surface indentation strength of sandwich composites under quasi-static loading is improved greatly by z-pins. The large improvements to the compression properties and indentation strength of sandwich composites suggest that their impact damage resistance may also be increased with through-thickness reinforcement.

While there is a large body of theoretical and experimental research which proves that the through-thickness reinforcement of sandwich materials increases the core properties under quasi-static loading conditions, there is little published work into the impact and dynamic properties. Vaidya and colleagues [26, 46] experimentally studied the low-velocity impact response of z-pinned sandwich composites, and found that the z-pins reduced the amount of damage. Fan and Xioa-qing [108] found that through-thickness stitching of foam core

sandwich composites also increased the impact resistance. In related studies, Vaidya et al. [46] and Cartié and Fleck [34] showed that z-pinning was effective at increasing the crush strength and absorbed energy capacity of sandwich materials under high-speed compression loading. Despite these studies, much remains unknown about the impact damage resistance of sandwich composites with through-thickness core reinforcement, including the crush resistance and damage resistance mechanisms. Furthermore, no information is available on the post-impact mechanical properties of sandwich composites with through-thickness reinforcement.

This chapter presents an experimental investigation into the indentation resistance and impact damage properties of z-pinned sandwich composites. Previous work conducted on the analytical modelling of the indentation resistance of sandwich composites is compared to new experimental indentation results. An experimental and theoretical investigation conducted by Long and Guiqiong [40] on the quasi-static indentation of z-pinned foam core sandwich panels using a spherical indenter reports that the insertion of z-pins can stiffen the sandwich composite significantly. An approximate theoretical solution is presented using the principle of minimum potential energy. Experimental indentation results reported in this chapter are compared to this study and further developed by investigating the effect of contact area on the indentation of z-pinned sandwich composites.

The effect of z-pins on the impact damage resistance and post-impact mechanical properties of sandwich composites was assessed for two impact energy regimes that created different types of damage: low impact energy loading which caused damage to the impacted face skin only and high impact energy loading which caused damage to both the impacted skin and foam core. The two types of impact damage are important in the assessment of the impact performance of sandwich materials because both occur in practical situations.

4.2 SANDWICH MATERIALS AND RESEARCH METHODOLOGY

4.2.1 Sandwich Composites

Indentation and impact tests were performed on unpinned and z-pinned sandwich composite panels consisting of two face skins of carbon fibre-epoxy laminate covering a low density

core of polymer foam. Each skin was made using unidirectional prepreg tape (VTM 264) stacked in a quasi-isotropic ply pattern with a thickness of 2 mm. The core material was closed-cell polymethacrylimid (PMI) foam (Rohacell Type 71RIST supplied by Evonik GmbH) with a thickness of 6 mm. The foam had an elastic modulus of 105 MPa, compressive strength of 1.7 MPa and shear strength of 1.3 MPa when measured at a quasi-static loading rate. The material was the same as that used to study the flatwise compression properties as described in chapter 3.

The z-pins used to reinforce the sandwich composite in the through-thickness direction were pultruded rods of T300 carbon/bismaleimide (Albany Engineered Composites Pty. Ltd) with a diameter of 0.28 mm and 0.51 mm, used respectively in the impact and indentation studies. The z-pins were inserted into the sandwich composite using a process similar to the z-pinning of fibre-polymer laminates, which is described in detail by Mouritz [9] and Chang et al. [55] and outlined in Chapters 2 and 3. The sandwich composite was reinforced to the z-pin volume content of 2%, with the pins being arranged in a square grid pattern. The z-pins were inserted in the orthogonal direction, although the fully embedded pins were inclined over a range of shallow angles as revealed by X-ray computed tomography and discussed in Chapter 3. The majority of z-pins were aligned within 5-6^{o} of the orthogonal direction, and the average offset angle was 2.1^{o}. Theoretical analysis by Long and Guiqiong [40] indicates that this shallow range of z-pin angles is unlikely to significant change the through-thickness properties compared to all the pins being perfectly aligned in the orthogonal direction.

After the z-pinning process was complete, the sandwich composite was cured inside an autoclave at 276 kPa and 120°C for one hour. The laminate face skins were bonded to the foam core during curing without the use of polymer adhesive. A control sandwich composite without z-pins was produced under identical conditions as the bench-mark material to assess the effect of z-pins on the indentation and impact properties. The z-pinned sandwich structures used in this study are all of the Type I variety as described in Chapter 3.

4.2.2 Indentation Testing

Indentation testing was conducted by applying low-speed compression loads (0.5 mm/min) using a 25mm diameter hemispherical steel ball and a 25mm diameter steel rod on to the face skin of the sandwich panels, as shown schematically in Figure 4-1. The panel samples were

40 mm wide, 40mm long and 10mm thick, and they were indented to about 70% strain (i.e. to a depth of ~ 7 mm), and four samples of each category were tested.

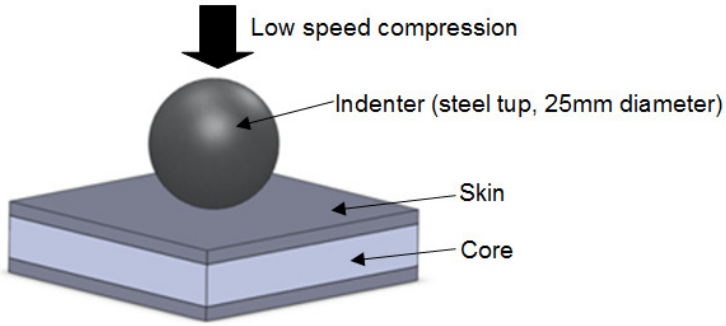

(a)

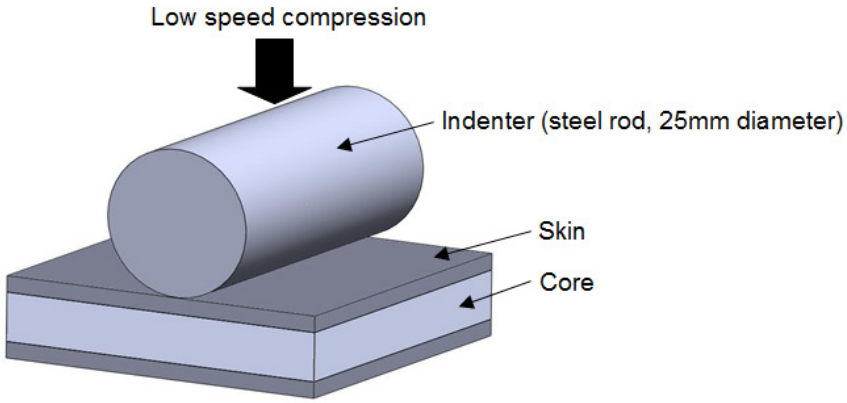

(b)

Figure 4-1: Indentation testing on sandwich specimens (a) spherical indenter and (b) cylindrical indenter

4.2.3 Impact Testing

Impact tests were performed by dropping a 25 mm diameter hemispherical steel tup (1.5 kg) on to the sandwich composites (Figure 4-2). Impact tests were performed at increasing incident energy levels up to 50 J, at which point the unpinned and z-pinned composites suffered extensive damage to the impact face skin and underlying core. The impact machine was instrumented with a laser photo/diode system to measure the inbound and rebound

velocities of the tup, and from this the amount of impact energy absorbed by the sandwich specimens was determined.

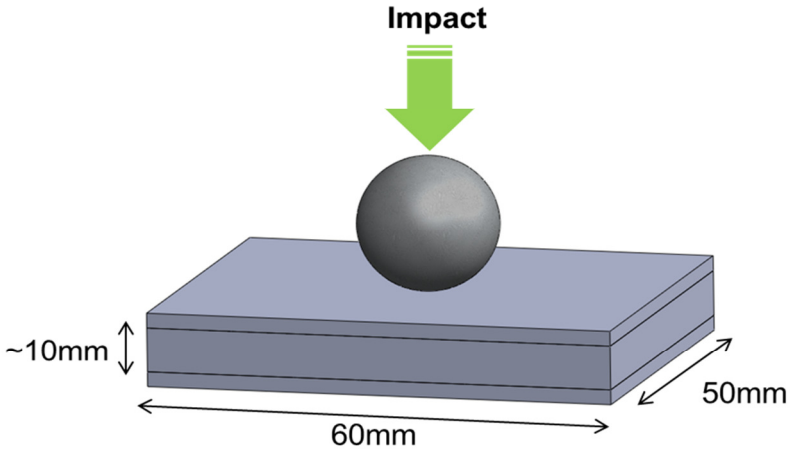

Figure 4-2: Impact testing

Following testing, the specimens were visually inspected to measure the size and shape of the impact damage region. Impacted specimens were also inspected using computed microtomography (SkyScan 1172) performed using an X-ray source voltage of 49 kV and current of 167 μA. The specimens were rotated through the X-ray beam in 0.2° steps with an exposure time of 1770 ms. Pixel size of the tomography images was set to 17 μm, and this gave adequate resolution to identify damage to the z-pins (which were 280 □m wide).

4.2.4 Post-Impact Compression Testing

The in-plane compression properties of the sandwich composites before and after impact were measured using the edgewise compression test specified in ASTM C364. The specimens were 60 mm long, 50 mm wide and 10 mm thick, and they were compressed in the lengthwise direction at a loading rate of 0.5 mm/min until final failure (Figure 4-3). Five samples of both the unpinned and z-pinned sandwich composites were tested under identical loading conditions. High speed photography (X-Stream XS-4) of the sandwich composites during testing was performed at a frame rate of 5000 per second to identify the failure process, which occurred within a very short period of time.

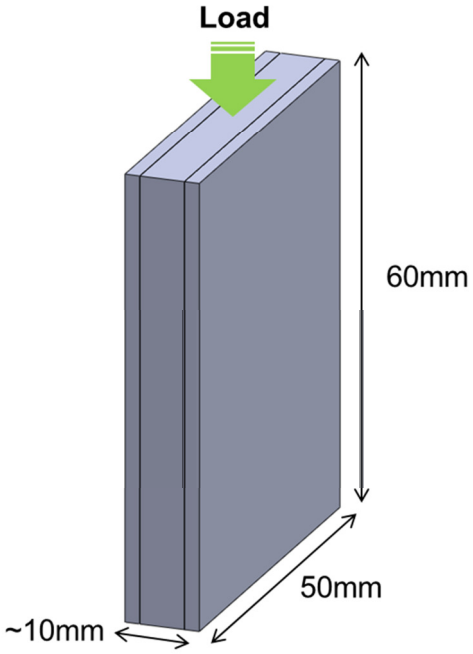

Figure 4-3: In-plane compression testing

4.3 INDENTATION RESISTANCE OF Z-PINNED SANDWICH COMPOSITES: RESULTS AND DISCUSSION

4.3.1 Indentation Properties

Figure 4-4 and Figure 4-5 show applied force against normalised displacement curves measured for the unpinned and z-pinned sandwich composites when indented using a sphere and cylinder, respectively. Multiple curves are presented for both materials to show the variability in the results. The displacement values were normalised to the through-thickness dimension (10 mm) of the sandwich composites. The loading response under a spherical indenter was similar to that measured by Long and Guiqiong [40].

The load-displacement curves show that the indentation stiffness, defined by the quasi-linear region during the initial phase of loading, was increased significantly by z-pinning. However, small load drops occurred during elastic loading of the z-pinned sandwich composite and this is attributed to damage to pins directly under the indentation point. As reported in chapter 3 for flatwise compression, load drops occur during elastic deformation of the foam core due to splintering and kinking of some pins.

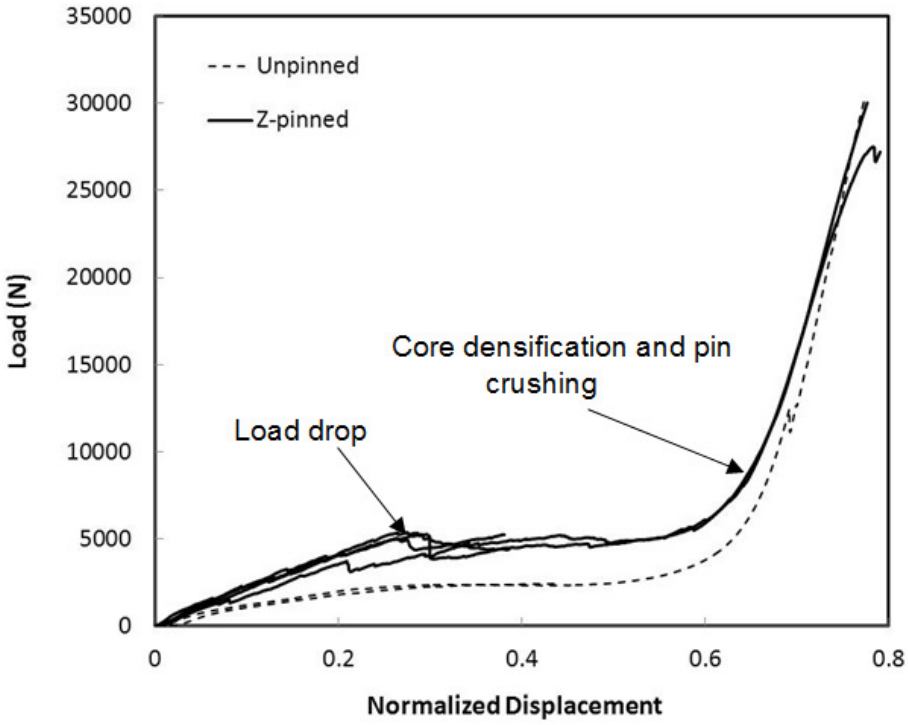

(a)

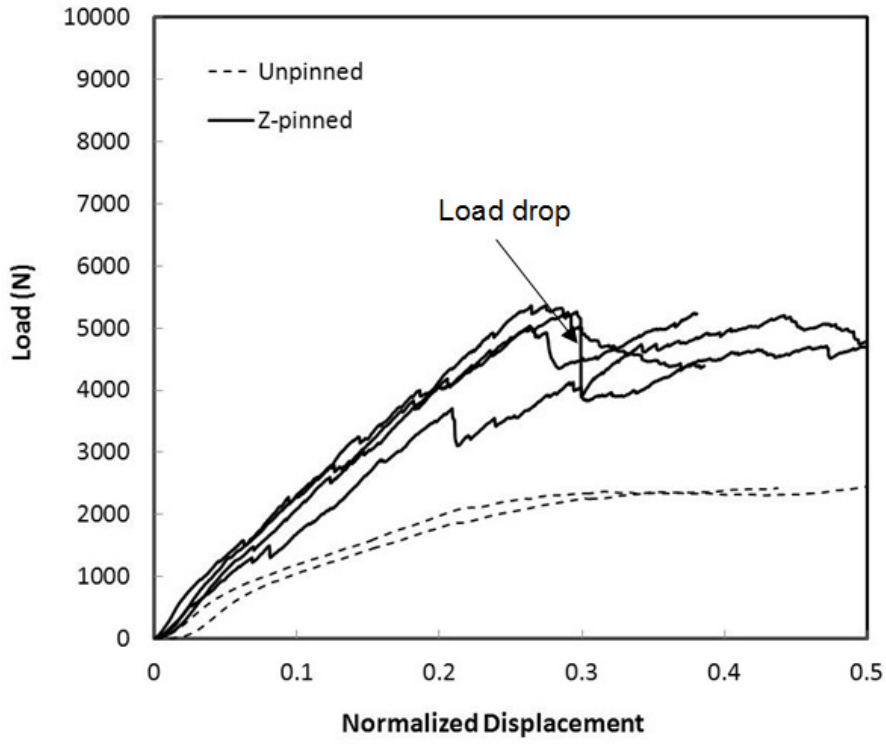

(b)

Figure 4-4: Load-normalised displacement curves for the unpinned and z-pinned sandwich composites indented by spherical steel tup: (a) full response and (b) elastic-plastic region

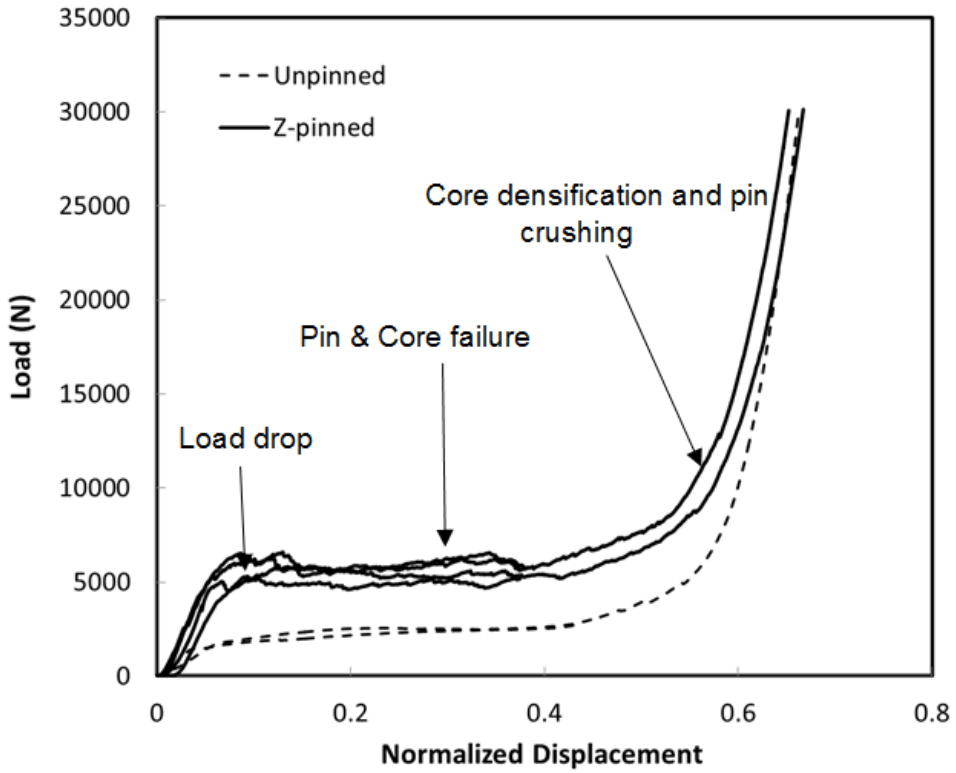

(a)

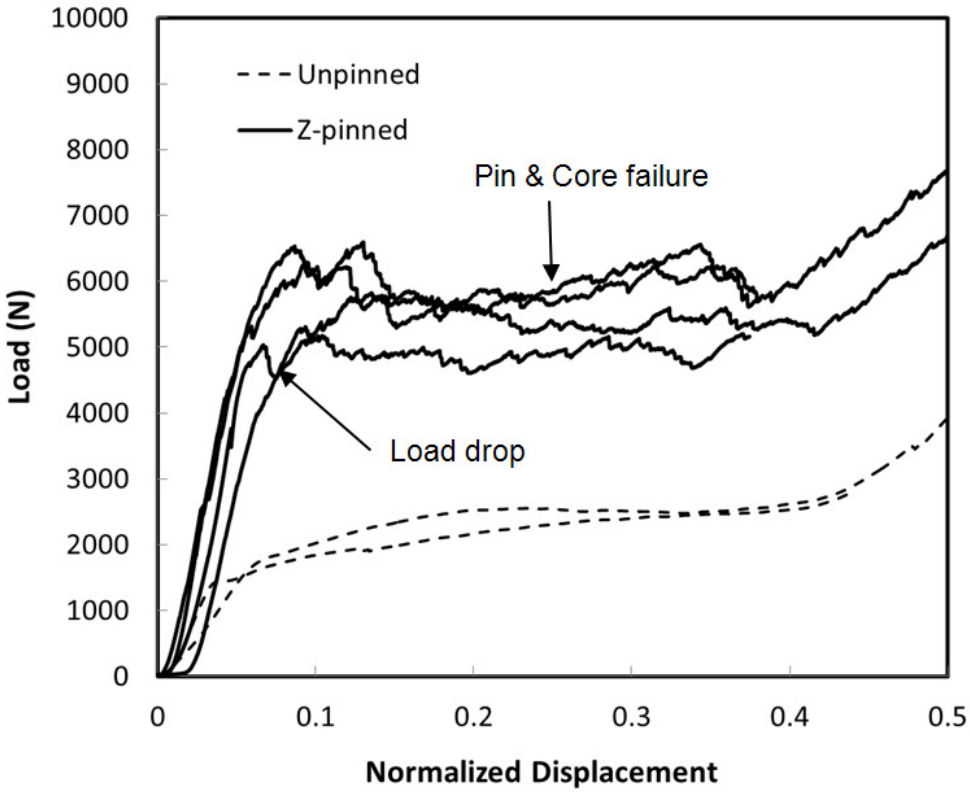

(b)

Figure 4-5: Load-normalised displacement curves for the unpinned and z-pinned sandwich composites indented by a cylinder: (a) full response and (b) elastic-plastic region

The elastic stress distribution within an isotropic material indented by a rigid sphere or cylinder can be calculated using Hertzian contact mechanics [109] and is shown schematically in Figure 4-6. The indentation pressure is highest under the indentation at point A in Figure 4-6, and is calculated using equation 4-1 and decreases with distance according to:

$$P_m = \left[\frac{4E^*}{3\pi}\right]\frac{a}{R} \qquad [4\text{-}1]$$

$$\text{where, } E^* = \left[\left(\frac{1-\nu_1}{E_1}\right)+\left(\frac{1-\nu_2}{E_2}\right)\right]^{-1} \text{ and } E_1 >> E_2. \qquad [4\text{-}2]$$

The internal stress below the indenter is calculated using;

$$\sigma_2 = -P_m\left(1+{z^2}/{a^2}\right)^{-1} \qquad [4\text{-}3]$$

This equation can be used to determine the stress field gradient below the indenter. Figure 4-7 shows the case of the σ_2 field in an isotropic solid having a Poisson's ratio of 0.26.

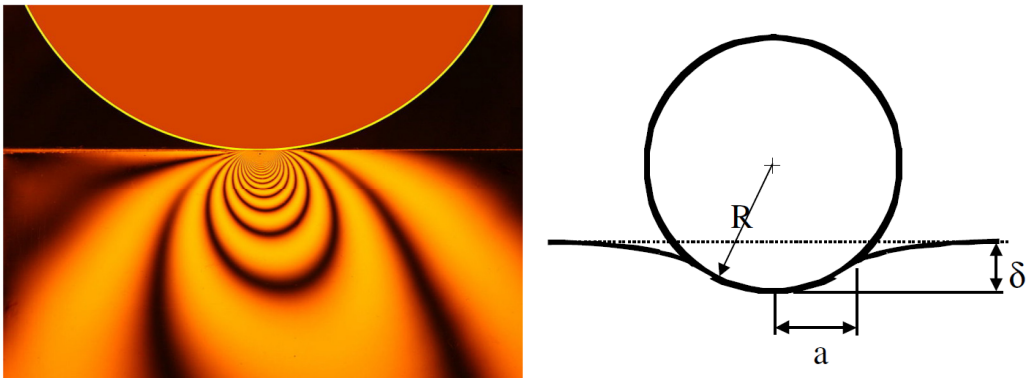

Figure 4-6: Two-dimensional representation of the stress distribution within an isotropic elastic medium subject to indentation loading by a rigid sphere. [110]

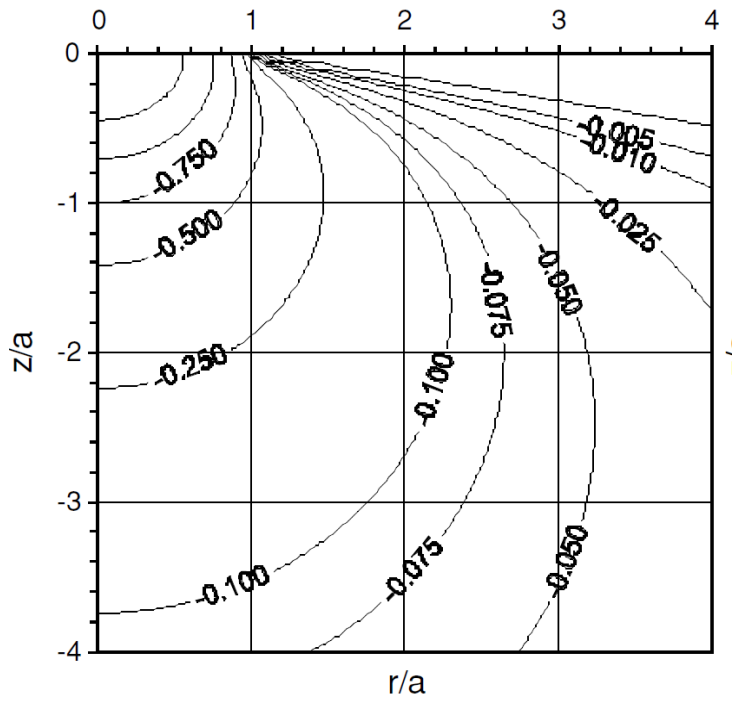

Figure 4-7: σ_2 field in an isotropic solid

Based on this analysis, the z-pins are not uniformly loaded when the sandwich composite is indented by the sphere or cylinder. Based on the stress distribution it is expected that the z-pins closest to the loading point will fail first because they are the most heavily loaded, as shown schematically in Figure 4-8. Pins further away will initially deform elastically, although with increasing loading the size of the stress field will expand resulting in a greater number of pins being over-loaded and failing.

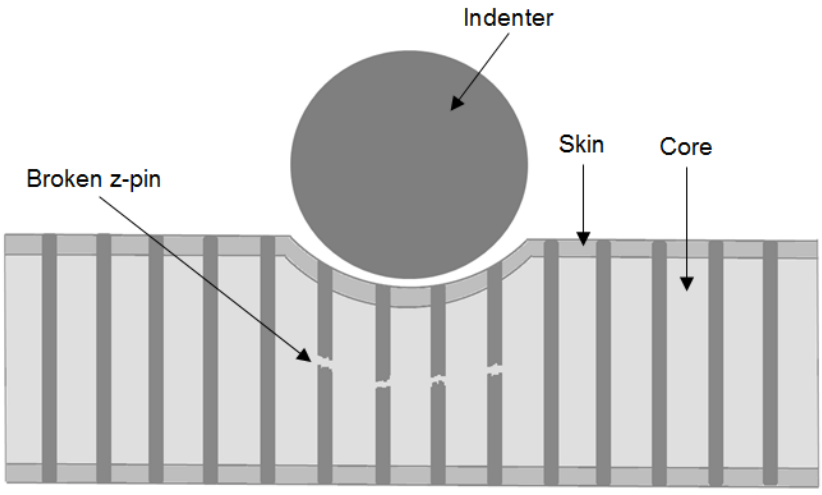

Figure 4-8: Schematic of damage of the z-pins due to non-uniform loading of the sandwich by a rigid sphere or cylinder.

The load-displacement curves for the unpinned sandwich material plateau following elastic loading, and this was due to irreversible (plastic) crushing of the foam core under the spherical and cylindrical indenters. The load remained constant until a high normalised displacement value (~0.55 for the sphere and ~0.45 for the cylinder) when the indentation resistance increased rapidly due to core densification. The z-pinned sandwich composite also displayed a quasi-static state load response following the elastic regime, although was subject to small load fluctuations due to discrete pin failure and pin crushing events. Over the entire displacement range the indentation load was much higher for the z-pinned sandwich composite compared to the unpinned material. Long and Guiqiong [40] assume that failure occurred at the skin-core or pin-skin interfaces during indentation loading, although they did not attempt to characterise the damage process. From the acoustic emission and x-ray tomography investigations reported in chapter 3, however, it is known the majority of z-pins fail immediately following the elastic regime by splitting and microcracking (and not by interfacial failure).

The indentation stiffness properties for the unpinned and z-pinned sandwich composites are given in Table 4-1. For comparison, the table also provides the measured stiffness values for these materials under flat-wise compression (in which the applied force is evenly distributed). Z-pinning more than doubled core stiffness regardless of whether the sandwich composite was locally loaded (sphere or cylinder) or uniformly loaded (plate). The percentage increase in stiffness due to z-pin reinforcement was approximately similar for the three loading conditions (within the range 100-170%). That is, z-pins were about equally effective at core stiffening under localised or distributed loading. Also given in Table 4-1 are the elastic energy absorption values for the unpinned and z-pinned materials, which were determined from the area under the elastic portion of the load-displacement curve (region before the curve plateaus). Despite significant scatter in the data for the z-pinned composite, it is apparent that the percentage increase to the elastic energy absorption due to z-pinning increases in the order: plate to cylinder to sphere. In other words, the efficacy of z-pins to increase the elastic energy absorption increases (on a percentage basis) with decreasing load contact area. The reason for this behaviour is discussed later in the chapter.

Table 4-1: Indentation stiffness and elastic energy properties of sandwich composites

Indenter	Stiffness N/mm Unpinned	Stiffness N/mm Z-pinned	% Improvement Stiffness	Elastic Energy Nmm Unpinned	Elastic Energy Nmm Z-pinned
Sphere	7610 +/- 396	17106 +/- 3094	125%	7 +/- 0.9	767 +/- 54
Cylinder	41151 +/- 8883	110041 +/- 110	167%	29 +/- 12	224 +/-54
Flat plate	135329 +/- 7337	279210 +/-52780	106%	43 +/- 3	179 +/- 132

Table 4-2 gives the yield load, plastic energy and total energy values for the unpinned and z-pinned sandwich composites for the three loading conditions. The yield load is the force needed to cause irreversible deformation of the foam core; the plastic energy quantifies the amount of strain energy needed to irreversibly deform the core and was measured using the area under the loading curve between the normalised displacements for the onset of plastic deformation and the deformation value before densification which is a normalized displacement value of 0.4; and the total energy defines the total elastic and plastic energies absorbed by the material and was determined from the total area under the load-displacement curve. The yield load of the foam core was increased by z-pinning for the three load conditions, with the average percentage improvement being 565% for the sphere, 328% for the cylinder and 132% for the plate. Z-pinning also increased the energy absorption of the foam core during plastic loading, with the percentage improvement increasing with the contact area of the indenter (i.e. in the order sphere, cylinder, plate). This trend is the reverse of the elastic energy absorption were it was found that the percentage improvement due to z-pinning decreases with increasing loading contact area. Because the energy absorbed during plastic deformation is much greater than that absorbed during elastic deformation, the percentage increase in the total absorbed energy due to z-pinning also increases with the loading contact area.

Table 4-2: Indentation yield load and energy properties of sandwich composites

Indenter	Unpinned	Z-pinned	% Improvement
	Yield Load (N)	Yield Load (N)	
Sphere	776 +/- 10	5161 +/- 192	565%
Cylinder	1505 +/- 181	6448 +/- 25	328%
Flat plate	3354 +/- 362	7781 +/- 475	132%
	Plastic Energy (Nmm)	Plastic Energy (Nmm)	
Sphere	645 +/- 38	505 +/- 105	-22%
Cylinder	802 +/- 51	1725 +/- 176	115%
Flat plate	1157 +/-68	3567 +/- 431	208%
	Total Energy (Nmm)	Total Energy (Nmm)	
Sphere	652 +/- 37	1364 +/- 141	109%
Cylinder	831 +/- 39	1949 +/- 227	134%
Flat plate	1200 +/- 71	3746 +/- 533	212%

This experimental study has proven for the first time that the efficacy of z-pins in the stiffening and strengthening of foam cores is dependent on the load conditions. The percentage improvement to the core properties gained by z-pinning are different for local indentation and distributed loading, and this can be explained via differences in the surface contact mechanics of z-pinned sandwich composites.

4.3.2 Contact mechanics

The results presented in tables 4-1 and 4-2 show that the percentage improvement to the sandwich composite properties due to z-pinning is dependent on the type of indenter. The contact mechanics of indentation have been investigated to explain this behaviour. The contact area between the spherical and cylindrical indenters and the face skin of the sandwich composites increases with the indentation depth. (The contact area of the plate, of course, is independent of the indentation depth). The contact area can be determined by first estimating the contact radius of the indenter and the sandwich composite, which is shown in Figure 4-9.

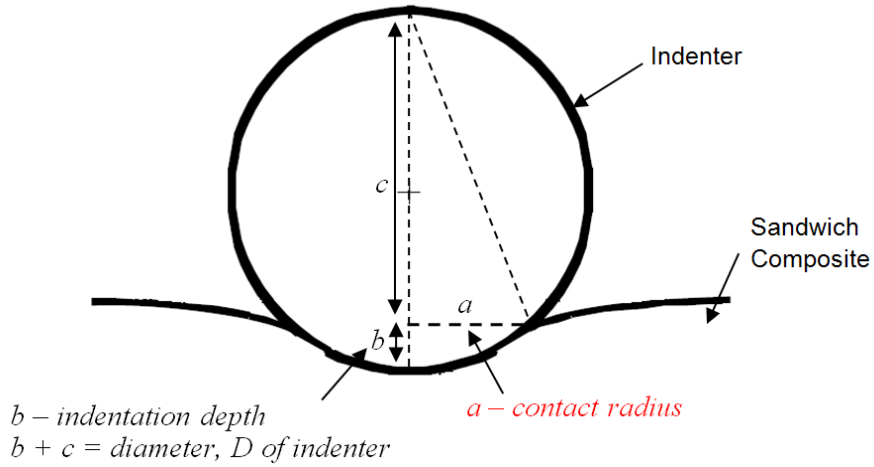

Figure 4-9: Estimating contact radius

Using the contact radius, equations for calculating the elastic contact area for a rigid sphere and cylinder are:

$$contact\ area\ sphere = \pi a^2$$

$$contact\ \ area\ \ cylinder\ = \pi a \times length\ of\ \ cylinder$$

Figure 4-10 shows the calculated increase in the contact area with increasing normalised indentation depth for the spherical and cylindrical indenters as well as the plate. As expected, the contact area for the sphere is much smaller than for the cylinder and plate, even at high indentation depths. Using this contact area data, it is possible to calculate the number of z-pins (based on the pin areal density) that are directly loaded for the three contact conditions. Figure 4-11 shows that the number of z-pins resisting indentation by the sphere and cylinder increases with the indentation depth. However, the total number of pins under load by the spherical indenter is relatively low due to the small contact area. This explains the dependence of total absorbed energy by the z-pinned sandwich composite on the type of loading. Table 4-2 shows that the percentage improvement to the total absorbed energy of the z-pinned material increased in the order of sphere, cylinder and plate. This trend occurs because the total number of z-pins available to absorb energy (via elastic deformation, splitting, kinking, crushing) increases with the contact area of the indenter.

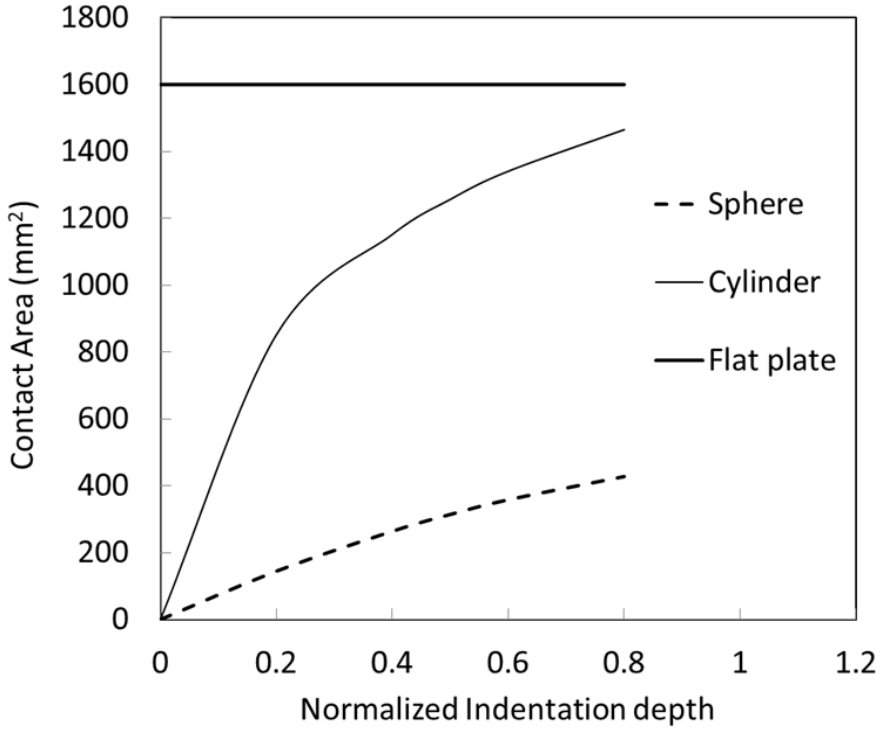

Figure 4-10: Effect of normalized indentation depth on the contact area

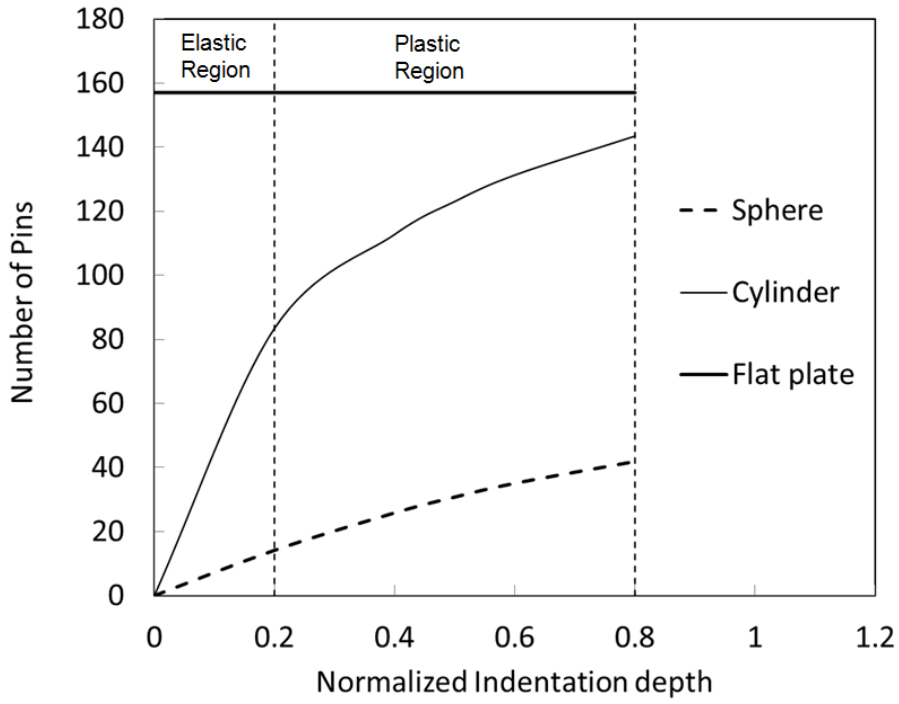

Figure 4-11: Effect of normalized indentation depth on the number of pins

The indentation loading response was analyzed further using an approximate analytical solution for z-pinned sandwich panels formulated by Long and Guiqiong [40]. The model assumes the sandwich panel is supported by a rigid base and is compressed using a spherical

indenter (Figure 4-12). It is assumed the indentation is confined to the region of the face skin and upper core immediately under the load point. It is also assumed that no bending is experienced during the indentation process because the sandwich composite is fully supported by a rigid substrate. In the Figure 4-12, F is the applied load, δ_0 is the indentation depth, ρ is the contact radius, and $2R_{el}$ and $2R_{pl}$ are the lengths of the elastic and plastic deformation zones in the core, respectively. An approximation is made where the spherical indenter is regarded as being a flat-nose indenter where the radius then becomes constant, R_{in}, and is assumed to be $R_{in} = 0.4R$.

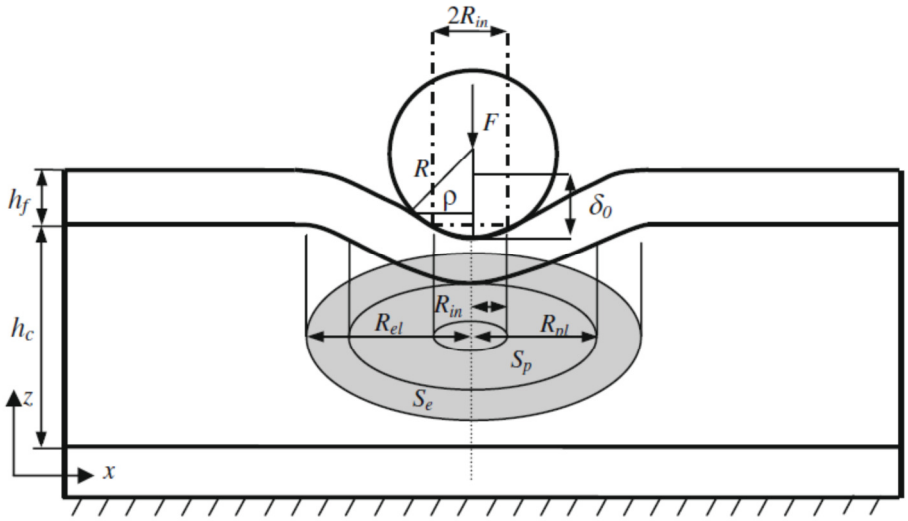

Figure 4-12: Quasi-static indentation of a sandwich composite (From Long and Guiqiong [40])

Long and Guiqiong [40] report that the plastic work (or absorbed plastic energy) in the indentation process is defined by:

$$D_{pl} = \int_{S_p} \sigma_c \delta dS_p = \pi\sigma_c\delta_0 R_{in}^2 + \frac{4}{9}\sigma_c\delta_0 (R_{el} - R_{in})^2 \left[1 - \left(1 - \frac{R_{pl} - R_{in}}{R_{el} - R_{in}}\right)^3\right]^2 \quad [4\text{-}4]$$

σ_c is the collapse stress of the foam core and R_{pl} is calculated using:

$$R_{pl} = R_{el} - \sqrt{\frac{\delta^*}{\delta_0}} \frac{R_{el} - R_{in}}{\left[1 + \frac{R_{in}}{R_{el} - R_{in}}\right]} \quad [4\text{-}5]$$

δ* is the displacement of the foam core, which is controlled by the physical and mechanical properties of the z-pins according to the expression:

$$\delta^* = \frac{\sigma_p h_c}{E_c \cos^2 \omega} = \frac{\pi^5 m^4 E_p d_p^4 + 64\beta l_p^4}{16\pi^3 m^2 \mu^2 E_p l_p d_p^2 \cos\omega} \quad [4\text{-}6]$$

where E_p is the pin modulus, σ_p is the pin strength, ω is the pin inclination angle, l_p is the pin length and d_p is the pin diameter.

It is assumed that under indentation loading all the z-pins fail at the same time by buckling (rather than splintering and kinking). Based on this assumption, the pin buckling stress, σ_p, is calculated using:

$$\sigma_p = \frac{\pi^2 E_p d_p^2 \cos^2 \omega}{16\mu^2 h_c^{\,2}} \left(m^2 + \frac{64\beta h_c^{\,4}}{m^2 \pi^5 E_p d_p^4 \cos^2 \omega} \right) \quad [4\text{-}7]$$

From this the compressive strength of the pin reinforced foam core is determined by:

$$\sigma_c = f\sigma_p \cos^2 \omega + \sigma_f \quad [4\text{-}8]$$

where,

$$\sigma_f = \frac{E_f \sigma_p}{E_p h_c \cos\omega} \quad [4\text{-}9]$$

This buckling model is based on the compressive strength model for pin buckling in a foam core sandwich composite developed by Cartié et al. [34]. (An assessment of this model for fibrous z-pins is presented in chapter 3).

Equation 4-4 was solved to determine the plastic energy absorbed in the indentation process, D_{pl}, of the z-pinned sandwich composite. The calculated plastic work defined by a normalized displacement range of about 0.2 to 0.4 (which is the region after the elastic regime and before the onset of densification) was much higher than the experimental values,

which were 89 Nm and 19 Nm respectively. The reason for the large discrepancy is attributed mostly to an accurate measurement of the size of the elastic region within the foam core (R_{el}). R_{el} cannot be calculated, and must be measured experimentally during indentation testing. However, visually measuring the R_{el} value is difficult because it is hard to identify the exact location of the elastic boundary, as shown for example in Figure 4-13 for a sandwich composite compressed using a cylinder. Furthermore, determining R_{el} for a spherical indentation is not possible because indentation occurs in the centre of the specimen, thus making the elastic region invisible.

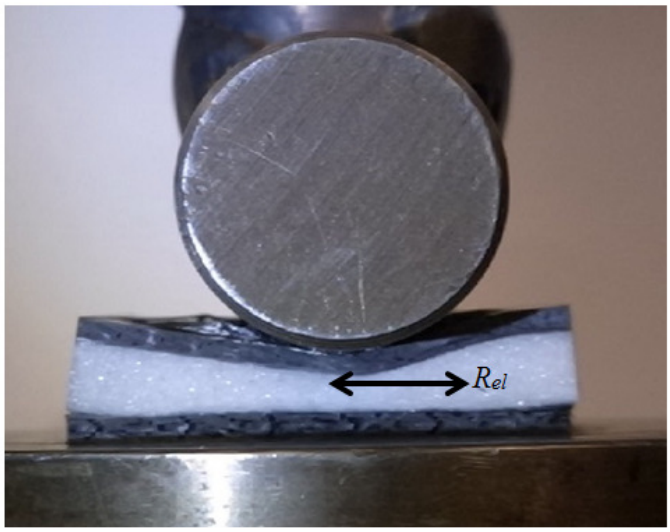

Figure 4-13: R_{el} estimate from experiment (cylindrical indentation)

Figure 4-14 shows the theoretical dependence of D_{pl} on R_{el} for the z-pinned sandwich composite calculated using equation 4-4. D_{pl} remains relatively constant with increasing R_{el} up to ~6 mm (which is the thickness of the pin reinforced foam core), and then increases rapidly in size with larger values of R_{el}. For R_{el} values greater than ~6 mm, a small change in R_{el} causes a large change in D_{pl}. Therefore, the inability to accurately measure R_{el} means that small inaccuracies in its measurement result in large inaccuracies in D_{pl}.

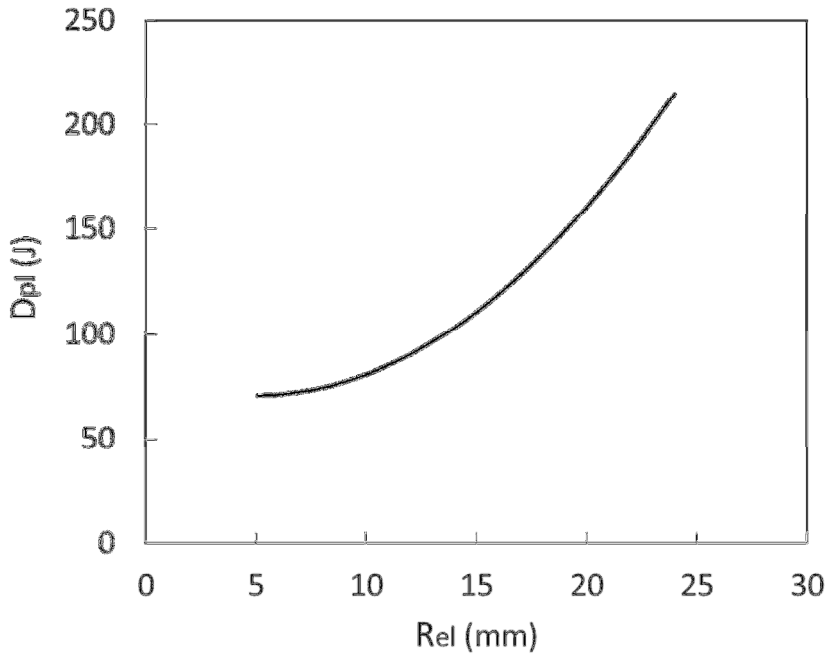

Figure 4-14: D_{pl} sensitivity to R_{el} for the z-pinned sandwich composite

The over-prediction of D_{pl} is also attributed to the invalid assumption that the z-pins fail by buckling under the indentation load. Chapter 3 discusses the stochastic nature of fibrous pin failure under compressive loading due to pre-existing flaws and misalignment of the pins. The z-pins in the sandwich composite failed randomly by splintering and kinking over a wide range of indentation depths whereas the model by Long and Guiqiong assume that all the pins fail in unison by Euler-type buckling supported by the core acting as a Wrinkler foundation. The inability of the model to analyse the stochastic failure processes of the z-pins is almost certainty a contributing factor to its inability to accurately predict the indentation plastic energy of the z-pinned sandwich composite.

Another factor affecting the accuracy of the indentation model is misalignment of the z-pins within the foam core (as shown in Figure 3-5). Figure 4-15 shows the dependence of D_{pl} on the pin offset angle. Based on equation 4-4, D_{pl} decreases gradually with increasing pin offset angle. Given that the average pin angle distribution in the foam core is between 0º (i.e. perfectly orthogonal) and 14º, whereas the model assumes all the pins are aligned at the same angle, it is not surprising that the calculated and measured D_{pl} values are different.

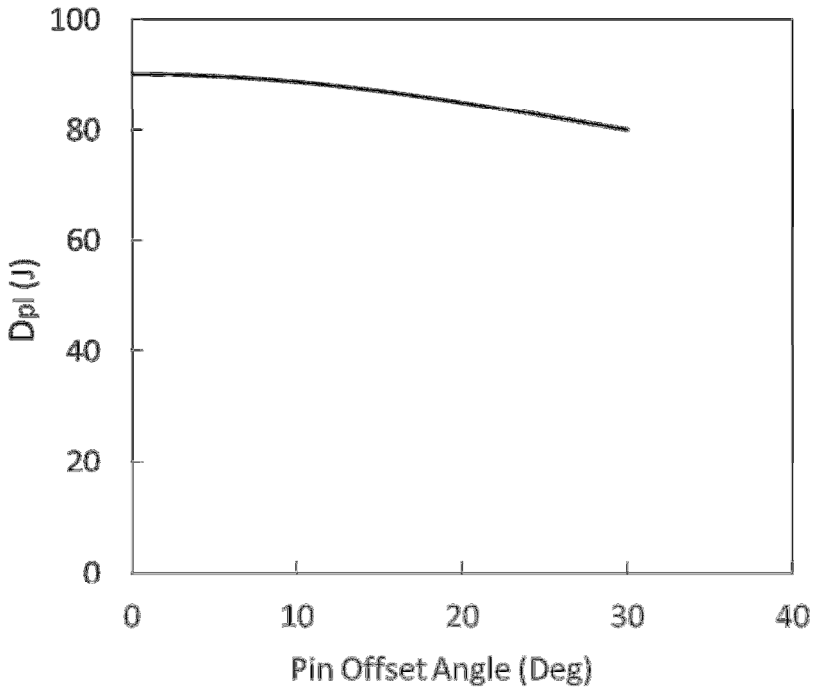

Figure 4-15: D_{pl} sensitivity to z-pin offset angle for the sandwich composite

This analysis reveals that the existing model by Long and Guiqiong for calculating the indentation resistance of z-pinned sandwich composites is not accurate for the material studied here. An improved model that is capable of analysing for the effects of variable pin strengths, failure modes and misalignment angles is needed to more accurately predict the effect of z-pin reinforcement on the indentation response of z-pinned sandwich composites such as the materials investigated here.

4.4 IMPACT RESISTANCE OF Z-PINNED SANDWICH COMPOSITES: RESULTS AND DISCUSSION

4.4.1 Impact Energy Absorption Properties

The effect of z-pinning on the impact response of the sandwich composite was quantified using the following properties: absorbed impact energy, impact damage area, and post-impact compression properties. This section presents the first investigation into the effect of impact loading on these properties for z-pinned sandwich composite structures.

Figure 4-16 shows the effect of increasing incident impact energy on the amount of energy absorbed by the unpinned and z-pinned sandwich composites. The absorbed energy was

determined by the difference between the incident energy of the impactor immediately before striking the sandwich composite and the rebound energy shortly after bouncing off the material. Two distinct impact energy regimes – low and high – are shown in the figure where the z-pins had different effects on the absorbed energy capacity of the sandwich composite. The low energy regime occurred when the incident impact energy was below ~25 J, and this regime was characterised by the unpinned and z-pinned sandwich materials having about the same impact absorption energy capacity (within the bounds of experimental scatter as indicated by the error bars).

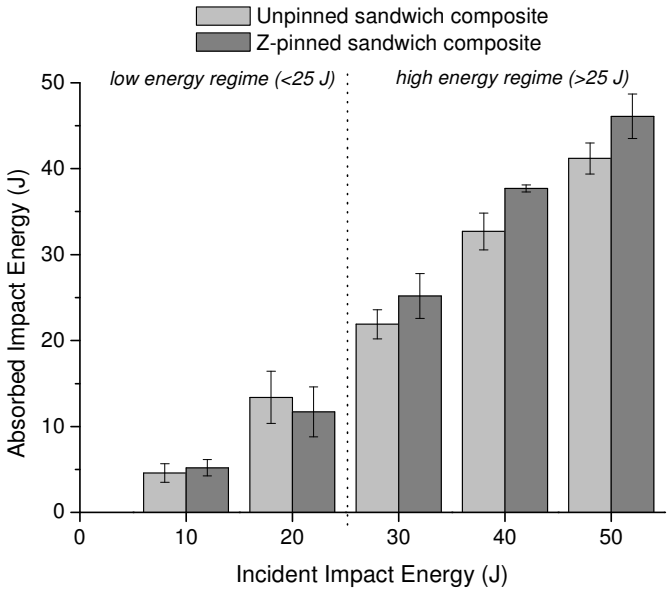

Figure 4-16: Effect of incident impact energy on the absorbed energy of the unpinned and z-pinned sandwich composites.

Examination of the sandwich specimens following impact loading up to 25 J (i.e. within the low energy regime) revealed that damage was confined mostly to delamination cracking in the face skin and debonding along the skin-core interface, as shown in Figure 4-17. This figure shows that the amount of delamination damage within the impacted face skin and the extent of skin-core debonding was less for the z-pinned composite. The smaller amount of cracking within the face skin was almost certainly due to the higher interlaminar fracture toughness of the carbon fibre-epoxy laminate due to bridging traction loads generated by the z-pins [9, 51, 66, 71, 111]. It is well known that bridging traction loads reduce the amount of impact damage to monolithic laminates reinforced with z-pins [32, 50, 69, 77, 82], and this study found a similar effect for the laminate skins to z-pinned sandwich composites. The smaller amount of skin-core debonding in the z-pinned sandwich material is attributed to

toughening of the interfacial region by the pins. Casari et al. [81] measured a large increase to the skin-core fracture load (~2 times higher) due to z-pinning of foam core sandwich composites. The pins generate traction loads across the skin-core interface (as well as within the skin) that increases the fracture load. This strengthening is believed to have increased the impact damage resistance of the skin-core interface to the z-pinned sandwich composite studied here. Figure 4-17 also shows that the core material to both the unpinned and z-pinned sandwich materials was not damaged significantly when impacted in the low energy regime.

X-ray microtomography revealed that most z-pins within the core were undamaged following low energy impact loading (Figure 4-18). A small percentage of the z-pins immediately below the impact point were damaged, and this is consistent with the observation made in the low-speed indentation that elastic loading of the core can cause some pins to fail due to the non-uniform stress distribution (Figure 4-6). It appears that under low incidence impact loads (up to 25 J) the foam core was elastically compressed and consequently the majority of z-pins were not damaged.

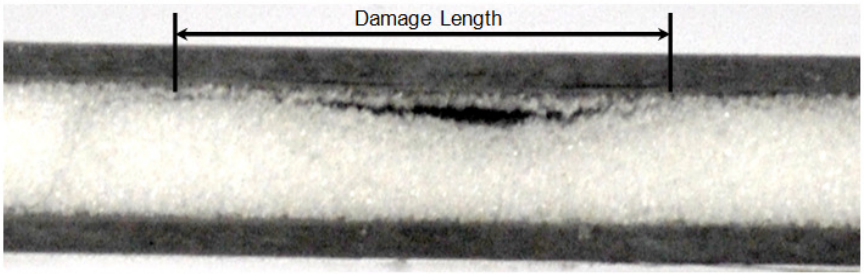

(a)

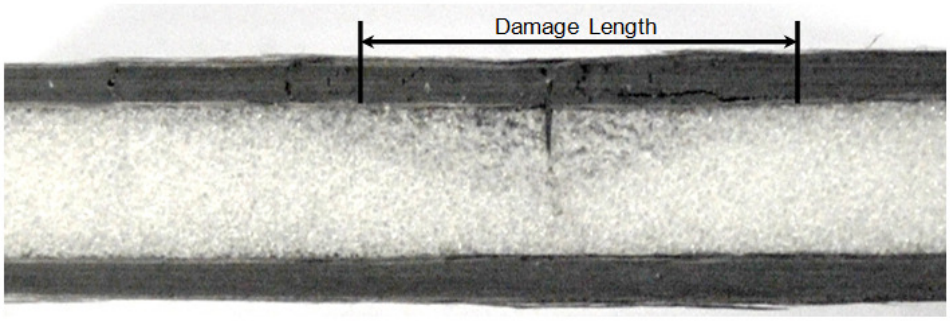

(b)

Figure 4-17: Cross-sectional images of the (a) unpinned and (b) z-pinned sandwich composites following low energy impact (20 J) which caused skin damage and skin-core debonding. The debond length between the skin and core is indicated.

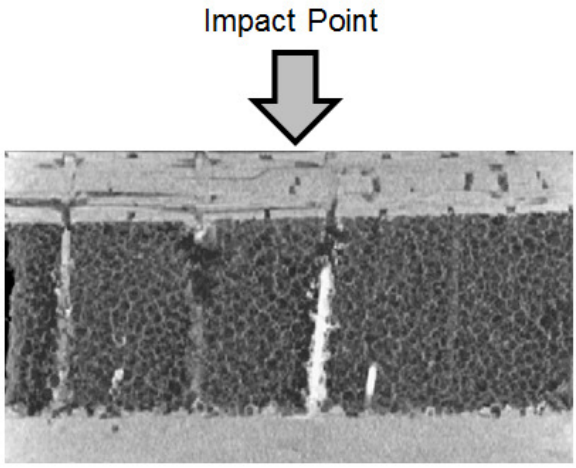

(a)

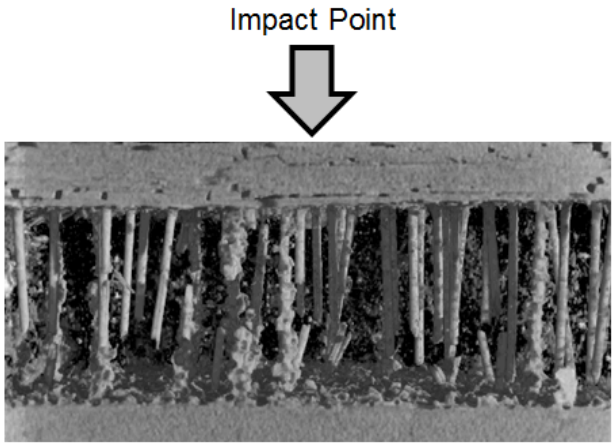

(b)

Figure 4-18: X-ray computed tomography image showing damage to the z-pinned sandwich composite following low energy impact (20 J). The foam core in (a) shows no crushing damage and the foam in (b) was digitally removed to reveal the z-pins, which are mostly undamaged.

Figure 4-16 shows that in the high impact energy regime (above 25 J) the amount of energy absorbed by the z-pinned sandwich composite was slightly higher (by an average of ~15%) than the unpinned material. The sandwich composites suffered crushing to the face skin and core in the high energy regime, as shown for example in Figure 4-19. The face skin was delaminated and, at the highest energies (approaching the maximum of 50 J), completely ruptured. The amount of delamination damage to the z-pinned face skin was less due to the high interlaminar fracture toughness promoted by the pins [51, 66, 71, 111], however the impact energy required to rupture the skin is expected to be about the same as the unpinned skin. Under high energy impact loading the face skin was compressed deep into the

underlying foam which caused core crushing (similar to that observed under low-speed indentation at a high depression depth). Microtomography revealed that all the z-pins immediately under the impact point were heavily crushed whereas many of the pins towards the edges of the impacted region where broken, as shown in Figure 4-20. The small increase in the absorbed energy of the z-pinned sandwich composite in the high impact energy regime was therefore attributed to the additional energy absorbed by breaking and crushing of the pins.

(a)

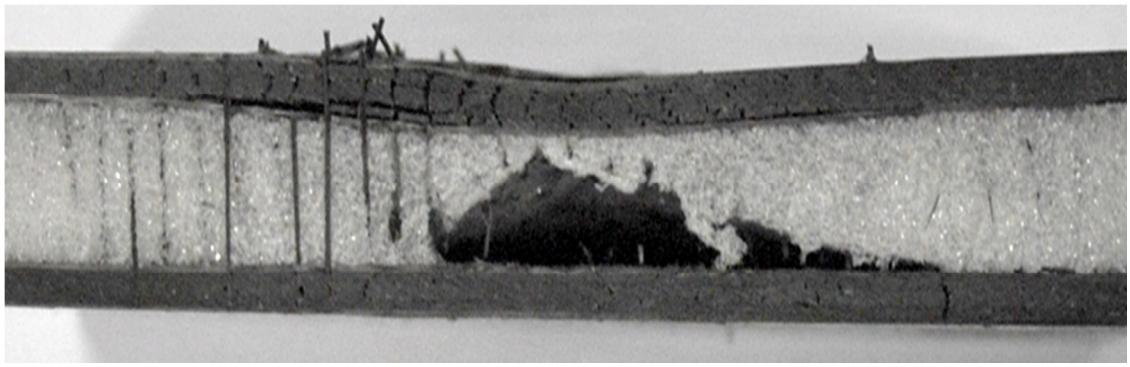

(b)

Figure 4-19**:** Cross-sectional images of the (a) unpinned and (b) z-pinned sandwich composites following high energy impact (40 J) which caused core crushing.

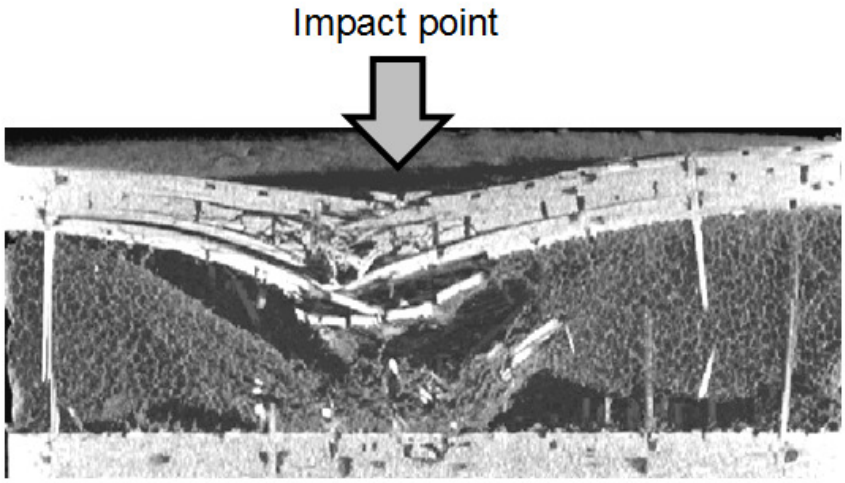

(a)

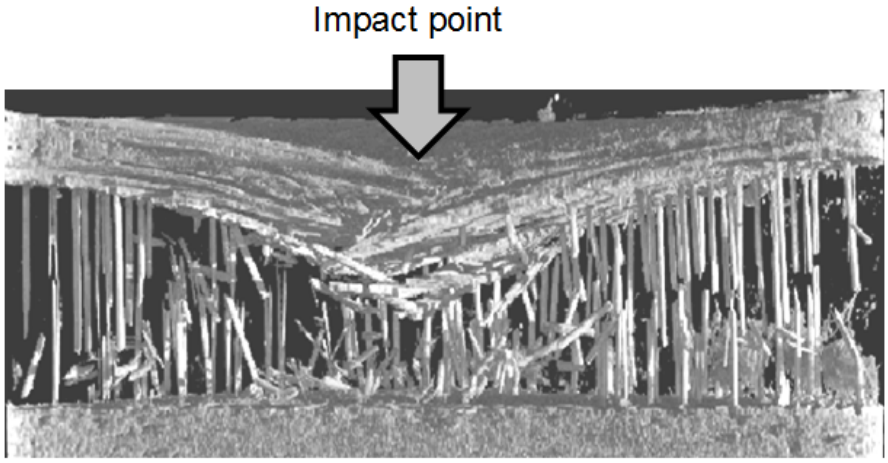

(b)

Figure 4-20: X-ray computed tomography image of the z-pinned sandwich composite following high energy impact (40 J) which caused crushing of the pins under the impact site. The foam core in (a) shows crushing damage and the foam in (b) was digitally removed to reveal the z-pins, which are also damaged.

The low-speed compression testing (as reported in chapter 3) revealed that the large increase to the energy absorption of the sandwich composite was due to strengthening and crushing of the z-pins. Similarly, z-pinning caused a large increase to the energy absorption under low-speed indentation by a sphere or cylinder, which again was due to the strengthening effect of the pins and the high amount of energy needed to break and crush them. It is expected, therefore, that the small increase to the energy absorption of the z-pinned sandwich material

under high energy impact loading (above 25 J) was almost certainly due to the energy absorbed in pin crushing. However, the increase to the absorbed energy capacity under impact loading (between 5 and 10%) was much less than under low-speed indentation. This difference is attributed to the short duration of the impact loading event, which was under several milliseconds. It is believed that the transient nature of the loading event resulted in less energy being absorbed by the pin and foam core than the continuous loading that occurs under quasi-static indentation.

4.4.2 Impact Damage Area

The effect of increasing incident impact energy on the size (expressed both as area and length) of the damaged region in the unpinned and z-pinned sandwich composites is shown in Figure 4-21. The damage size was measured visually from cross-sections of impacted samples. The samples were sectioned through the centre using a high speed cutting blade to observe the maximum extent of impact-induced damage. In addition, damage size was measured for a few, selected impacted samples using microtomography, and the measured size was in close agreement with the visual measurements. Figure 4-21 shows that the size of the damaged region increased with the impact energy for both materials, which is expected. However, the amount of damage sustained by the sandwich material for all energy levels (except the lowest of 10 J) was reduced by z-pinning. The increase to the damage resistance in the low energy regime (<25 J) was attributed to interlaminar toughening of the face skin and strengthening of the skin-core interface. It is well known that z-pinning reduces the amount of impact damage to carbon fibre-epoxy (and other) laminate materials due to bridging tractions generated by the pins [32, 50, 51, 66, 69, 71, 77, 82, 111]. As mentioned, Casari et al. [81] have shown that z-pinning also increases the fracture strength of the skin-core interface. For these reasons, it is believed that toughening of the face skin and skin-core interface by the z-pins resisted the growth of damage in the low impact energy regime. At the lowest energy (10 J), however, z-pins did not reduce the amount of damage, and this was attributed to the inability of z-pins to form bridging tractions in either the skin or skin-core interface. Interlaminar fracture toughness and impact testing of composite laminates has proven that z-pins cannot promote toughening until the damage size is sufficiently large to create a bridging traction zone along the crack [51, 66, 71, 111]. Studies performed on carbon fibre-epoxy laminates containing the same volume content of z-pins (2%) as the sandwich composite studied here reveal that the damage must be at least 10 mm long to

promote significant interlaminar toughening by crack bridging [51]. Similarities can be drawn from this study whereby the sandwich skins are reflective of the crack bridging seen in laminates. Figure 4-21 shows that at the lowest impact energy (10 J) the damage length was less than 10 mm, and therefore the cracks in the impacted face skin and skin-core interface were too short for z-pins to provide toughening. It was only when the impact damage length was longer than ~10 mm that the z-pins were effective at resisting damage growth in the low impact energy regime.

The amount of damage sustained by the sandwich composite in the high impact energy regime (>25 J) was reduced by z-pinning, as shown in Figure 4-21. The improved damage resistance was attributed to delamination toughening of the face skin, strengthening of the skin-core interface, and strengthening of the core by z-pins.

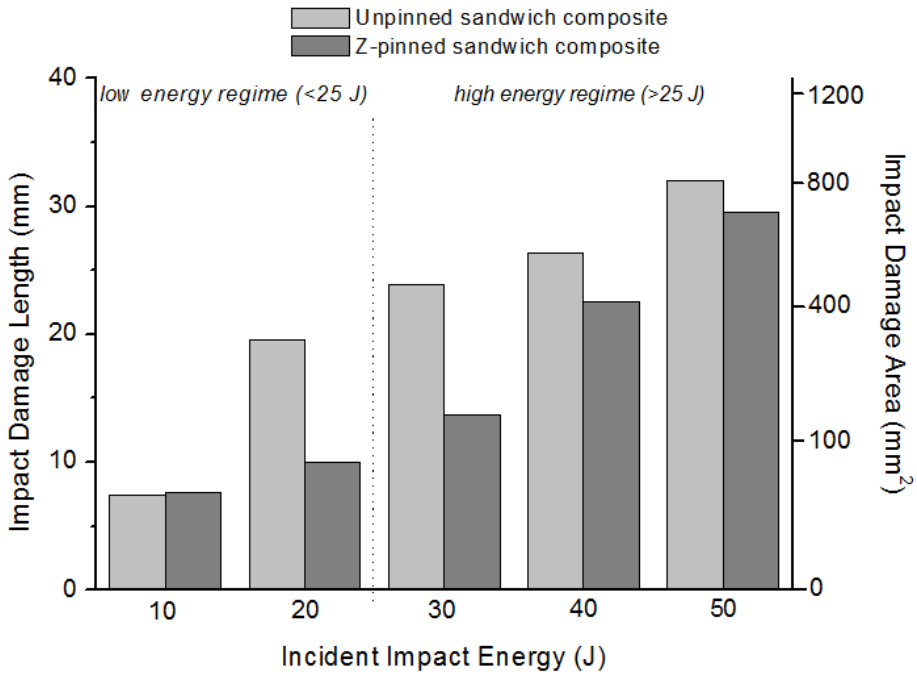

Figure 4-21: Effect of incident impact energy on the size of the impacted damage region for the unpinned and z-pinned composites.

4.4.3 Post-Impact Mechanical Properties

The post-impact mechanical properties of z-pinned sandwich composites have not been previously investigated. Therefore, an experimental investigation was conducted into their post-impact compression properties. The compression stiffness of the unpinned and z-pinned

sandwich composites without impact damage were virtually identical (i.e. 56.0 and 55.7 MN/m, respectively). This is consistent with studies that show no significant reduction to the compression modulus of laminates due to z-pinning [112, 113]. Similarly, the ultimate compression load was not changed significantly by z-pinning; 42.5 kN for the unpinned sandwich composite and 45 kN for the z-pinned material. However, z-pinning has been shown to reduce the compressive strength of laminates (typically by 5-20%) due to microbuckling failure of fibres crimped by the pins [77, 112-114]. The cause for the z-pins not lowering the compressive strength was investigated using high speed photography (5000 frames per second) of the failure process in the unpinned and z-pinned sandwich composites. Figure 4-22 shows the sequence of photographs of the two materials taken at intervals of 200^{-4}s in the short period leading up to and beyond failure. The failure sequence was the same for the unpinned and z-pinned composites, and initiated by core shear cracking which quickly led to out-of-plane buckling collapse. The pins did not suppress core shear cracking, and consequently the failure mechanism and ultimate load were not changed by z-pinning.

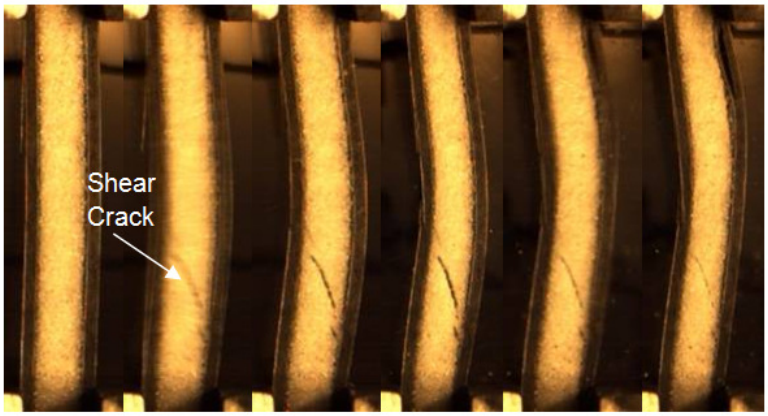

(a)

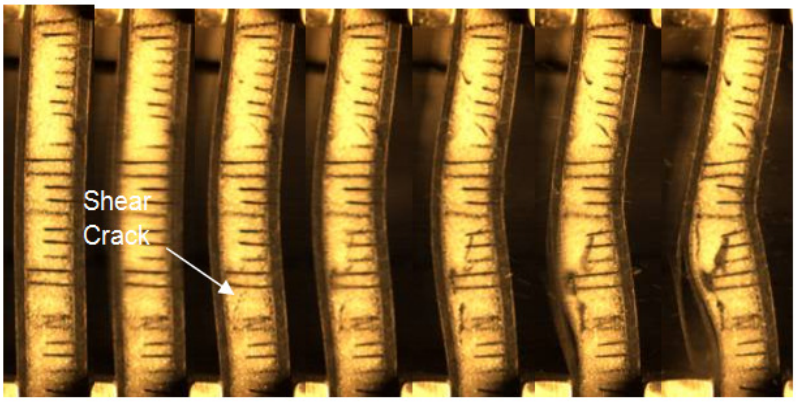

(b)

Figure 4-22: High speed photography (frame rate of 5000 s^{-1}) showing core shear failure of the (a) unpinned and (b) pinned sandwich specimens under in-plane compression loading

Figure 4-23 shows the effect of increasing incident impact energy on the in-plane compression stiffness and ultimate load of the unpinned and z-pinned sandwich composites. The in-plane compression properties are determined mainly by the properties of the laminate face skins, and not by the core material. While the post-impact mechanical properties reduced predictably with increasing incident energy, the post-impact properties of the two sandwich materials were virtually the same over the entire impact range from low energies (which caused face skin cracking and skin-core debonding) to high energies (which caused skin rupture and severe core crushing). While the z-pins reduced slightly the size of the impact damage region, the results presented in Figure 4-23 show that this does not translate into an improvement to the post-impact properties.

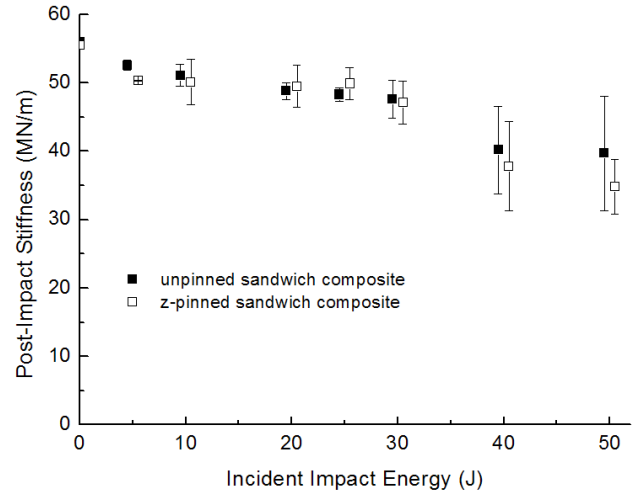

(a)

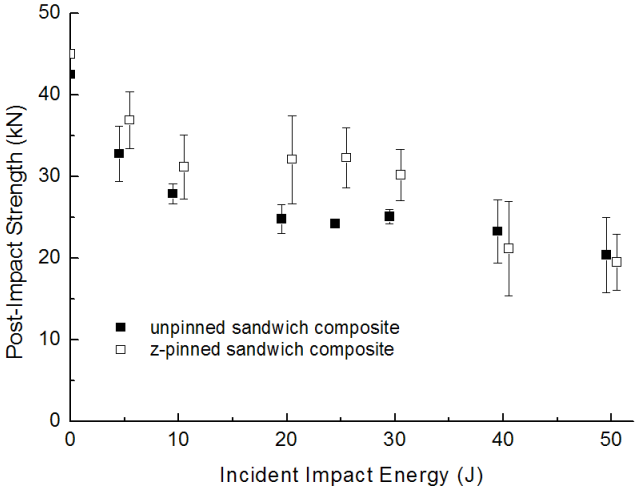

(b)

Figure 4-23: Effect of increasing incident impact energy on the post-impact (a) compression stiffness and (b) compression failure load of the unpinned and z-pinned sandwich composites.

The inability of z-pinning to increase the post-impact properties may be attributed to the modest reduction in the impact damage area due to the z-pins. The difference in the impact damage area between the unpinned and z-pinned sandwich composites was relatively small except over the energy level range of 20–30 J when the indentation damage condition changed from face skin and skin-core interfacial damage (at below 25 J) to face skin and core damage (above 25 J). Over this narrow energy range of 20–30 J, it is shown in Figure 4-21 that the damage area was reduced significantly by z-pinning, and there was a corresponding increase in the post-impact strength (Figure 4-23b). At energies below 20 J and above 30 J, the difference in the amount of damage between the unpinned and z-pinned materials was sufficiently small to not improve the post-impact properties.

4.5 CONCLUSIONS

The indentation resistance of sandwich composites was increased significantly by z-pinning. The stiffness, yield stress and strain energy absorption of z-pinned sandwich composites under an indentation load were increases by the z-pins resisting localised core deformation and crushing. The efficacy of z-pins to increase these properties is dependent on the indenter geometry and indentation depth. Increasing the load contact area increased the indentation resistance because of the greater number of pins. The existing model to predict the indentation energy absorption of z-pinned composites is inaccurate for the material studied here due to the assumption that z-pins fail via a buckling mechanism while in reality they fail via fragmentation, splitting and kinking. Also, the model is unable to analyse sandwich composites reinforced with z-pins of varying strength (due to pre-existing flaws) and inclined at a range of angles. Therefore, a modified model is required to accurately predict the behaviour of z-pinned sandwich composites under indentation loading conditions.

Through-thickness reinforcement of foam core sandwich composite structures with orthogonal z-pins can improve slightly the impact damage resistance. However, z-pins were only effective when impact-induced cracking within the face skin or along the skin-core interface was sufficiently large for the pins to create a bridging traction zone and at high impact energies when large-scale core crushing caused fracture of the pins. Low-speed indentation testing revealed that z-pin reinforcement was highly effective at increasing the

through-thickness stiffness, strength and energy absorption of the core. Such large increases were not achieved in the impact damage resistance and absorbed energy capacity. Despite the improved impact damage resistance of the z-pinned sandwich composite, its post-impact compression stiffness and strength properties were similar to the unpinned material. It can be concluded that z-pins are effective at improving the mechanical properties under a slow strain rate compression scenarios, however are not as effective in sustaining damage in high strain rate loading conditions.

Chapter 5 IMPROVING THE FRACTURE RESISTANCE OF SANDWICH COMPOSITE T-JOINTS BY Z-PINNING

ABSTRACT

This chapter presents an experimental and analytical study into the strengthening and toughening of sandwich composite joints by z-pinning. Cleats connecting the vertical stiffener and horizontal base panel to T-shaped sandwich joints were reinforced in the through-thickness direction with z-pins. Tensile (stiffener pull-off) tests revealed that z-pinning increased the ultimate fracture load and fracture energy by resisting crack growth along the cleat-skin and skin-core interfaces, which were the weakest points in the unpinned joint. It was found that z-pinning suppressed large-scale interfacial cracking in the T-joint due to high bridging traction loads, and this changed the fracture mode to rupture of the skin panel. Both the fracture load and fracture energy increased with the volume content of z-pins.

The strengthening and toughening effect of the z-pins was analysed using multiple pin pull-out tests performed on the sandwich composite panel. It is shown that elastic deformation, debonding and pull-out of the z-pins from the face skins is the primary toughening mechanism of the pinned T-joints. The pin pull-out process, which is the cause for the high strengthening and toughening of the T-joints, was analysed using pin bridging traction modelling. The mode I bridging law for z-pinned laminates was modified to analyse the pin traction mechanics for sandwich composites. The revised model was found to accurately predict the bridging forces generated during elastic stretching and pull-out of the pins from sandwich materials. A parametric analysis using the traction model for the various z-pin properties, including pin diameter, modulus, interfacial shear and friction stresses, on the toughening of sandwich composites was performed. It was found that the z-pin diameter had the biggest influence on the traction loads. This is the first study that proves z-pinning to be an effective toughening method for increasing the fracture resistance of bonded sandwich joints. This chapter also contains the first investigation in the bridging traction law for z-pinned sandwich materials, which can be used in the design of high toughness joints.

Part of the research presented in this chapter has been published in the following article:

Nanayakkara, A., Feih, S. and Mouritz, A. P., 'Improving the mechanical properties of sandwich composite T-joints by z-pinning', *Composite Structures*, Volume 96, pp. 207-2015, 2013.

5.1 INTRODUCTION

The joints connecting sections of sandwich panels are often the weakest link in sandwich composite structures. Various designs are used to maximise the fracture load limit of sandwich joints, including T-shaped joints, U-channel joints and other bonded fillet designs as well as bolted connections (e.g. [90-93]), as discussed in Chapter 2. Sandwich joints are susceptible to interfacial cracking along the skin-stiffener connection and the face skin/core interfacial region due to their low out-of-plane strength and fracture toughness properties. The usual method of increasing the interfacial fracture toughness is to use high-strength adhesive along the joint connections. An alternate approach that may be more effective in the strengthening and toughening of bonded sandwich joints is through-the-thickness reinforcement using z-pins, although this method has not been previously investigated.

Numerous research studies have shown that z-pinning is effective at increasing the structural properties (including the fracture load and toughness) of T-joints, L-shaped joints, stiffened panels and lap joints made of composite laminates [63, 66, 95-97, 99-101, 115, 116]. Z-pinning can also promote large increases in the fatigue life of laminate joints by resisting interfacial cracking between the adherends. For example, Koh et al. [99] recently reported that the ultimate load and fracture energy of carbon/epoxy laminate T-joints were increased respectively by up to 75% and over 600% with z-pinning. Chang et al. [95] measured a 40% increase in the fatigue strength of single lap joints when reinforced with z-pins. The properties were improved by the z-pins generating bridging traction loads which resisted large-scale crack growth along the polymer bond-line to the joints.

While the strengthening and toughening of laminate joints by z-pinning has been proven, it is not known whether pinning will significantly increase the fracture resistance of sandwich composite joints. The strengthening and toughening provided by z-pins is reliant on the formation of bridging traction loads along cracks within the joint [9, 63, 66, 95-97, 99, 100,

115], and it is not known whether the bridging response is different for sandwich composites due to the foam core and the skin-core interfaces.

In this chapter, the aim is to experimentally determine the effect of z-pinning on the structural properties and strengthening mechanics of sandwich composite joints. The joint type examined was a traditional fillet T-joint, which is one of the most common designs for joining sandwich composite panels. The joint was made with thin face skins of carbon fibre/epoxy laminate and a thick core of polymer foam, and this sandwich material is used in aircraft structures. The effect of increasing the volume content of z-pins on the ultimate fracture load and fracture energy of the sandwich composite joint was determined. Also, the effect of z-pinning on the development of damage and final fracture of the T-joint was assessed. The strengthening and toughening mechanics of the sandwich joint were analytically and experimentally studied using pin pull-out tests which provide key information on the bridging traction behaviour of z-pins in sandwich materials.

5.2 SANDWICH JOINTS AND EXPERIMENTAL METHODOLOGY

5.2.1 Fabrication of Sandwich T-Joints

The design and geometry of the sandwich T-shaped joint used to assess the effectiveness of pins to increase the structural and fracture properties are shown in Figure 5-1. The joint was constructed using two flat sandwich composite panels which formed the base and stiffener, and they were joined using two L-shaped laminate cleats. The cleats and face skins to the sandwich composite (base and stiffener) were made using eight plies of T700 carbon/epoxy prepreg (VTM264) arranged in a cross-ply stacking sequence $[0/90/0/90]_s$. The core material used in the base and stiffener panels was a closed-cell polymethacrylimid (PMI) foam (Rohacell Type 71RIST supplied by Evonik GmbH), which is the same core material used in the sandwich composites studied in chapters 3 and 4. The z-pins used were 0.28 mm diameter rods of pultruded T300 carbon/bismaleimide (Albany Engineered Composites Pty Ltd.).

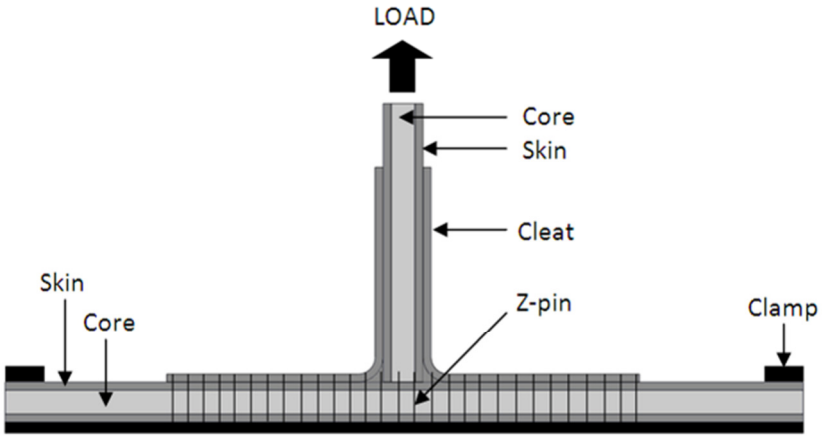

(a)

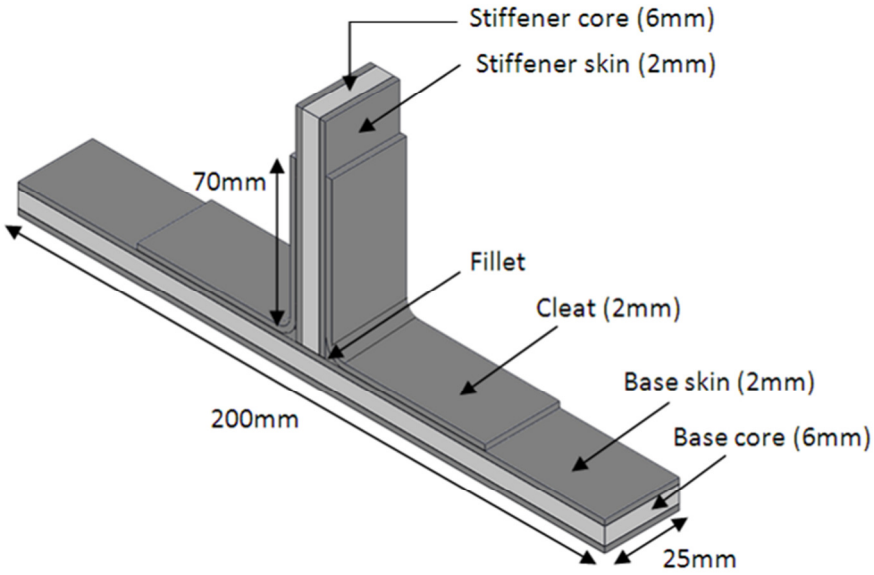

(b)

Figure 5-1: Schematic of the design and dimensions of the sandwich T-joint used in the structural pull-off test. The region that was reinforced with z-pins and the direction of applied loading is indicated in (a).

The T-joint manufacturing process involved several steps which are shown sequentially in Figure 5-2. The first step involved the fabrication of the base and stiffener panels. The stiffener skins were prepared separately and debulked on to the core to create the stiffener sandwich panel. The base sandwich panel was created in the same way whereby the skins were prepared and debulked on to the core material. However, with the base panel, one 0˚ ply (from the bottom skin) was left out of the process to be applied after the z-pinning process was completed.

Following preparation of the base and stiffener panels, the cleats were prepared on a pre-manufactured tool that was shaped to the required dimensions of the sandwich T-joint (as shown by step 2 in Figure 5-2. Plies were laid-up on the right angle tools (left and right) in a cross-ply stacking sequence to create the cleats. The cleats were then mounted upside down with the stiffener panel positioned in-between the cleat tool and secured using clamps. The base panel was then positioned on top of the assembly and joined to the cleats and stiffener. The local regions where the cleats, stiffener panel and base panel connect were filled with unidirectional prepreg to avoid the formation of weak resin-rich zones. Adhesive was not used to aid the bonding of the joint components.

Once the sandwich T-joint structure had taken shape and mounted securely, the z-pinning process was performed. The z-pins were inserted from the bottom surface of the sandwich T-joint. The bottom surface was first covered using protective film and a pre-cut panel of z-pins in preform was placed on the region requiring z-pinning and secured in place using adhesive tape. The pins were inserted using the Ultrasonically Assisted Z-Fiber® (UAZ®) process (described in Chapters 2 and 3), which basically involved driving the pins from a foam carrier preform into the uncured sandwich joint using high frequency (20 kHz) ultrasonic vibrations. The z-pins were inserted through the entire thickness of the horizontal section of the cleat and the sandwich base panel. Any excess length of pin protruding from the base of the sandwich T-joint is shaved off, resulting in the leading tip of the pin, which was forced into the sandwich material, being chamfered to ease the insertion process whereas the trailing end of the pin was blunt, as shown in Figure 5-3. Therefore, the bottom surface of the T-joint base panel consisted of blunt z-pin ends. Once the bottom surface of the base panel of the sandwich T-joint was cleaned post-z-pinning, the final $0^{\bullet}$ ply was laid up. The z-pinned sandwich panel was bonded by co-curing inside an autoclave operated at an overpressure of 276 kPa and temperature of 120°C for one hour (step 4). The geometry and fabrication of the unpinned T-joint was identical to the z-pinned joints.

The sandwich T-joint was reinforced with a low (0.5%) or high (2%) volume content of pins. Attempts were made to reinforce the joint with 4% z-pins, although the z-pinning device lacked sufficient power to insert the pins all the way through the base panel and cleats. Control T-joint specimens with no pins were prepared as the control to bench-mark any property improvement gained by z-pinning.

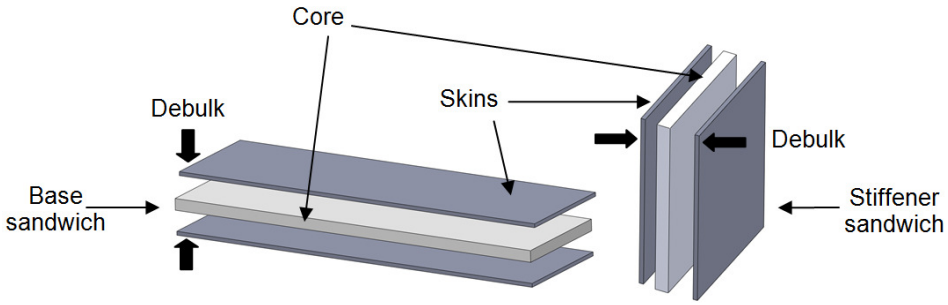

Step 1 Prepare base and stiffener panels by preparing the skins separately and debulking the skins on to core

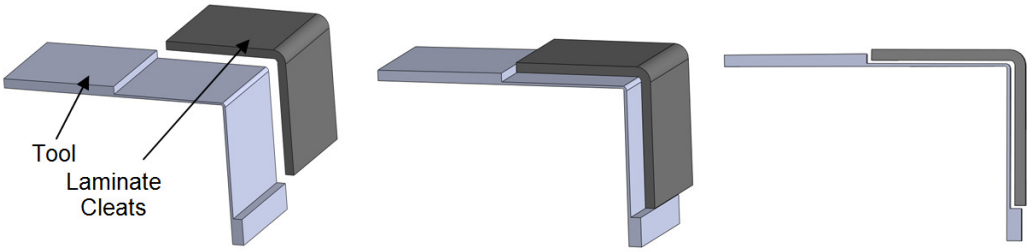

Step 2 Lay-up cleats on tool using prepreg plies in cross-ply stacking sequence. Plies are laid up incrementally with debulking between every two plies

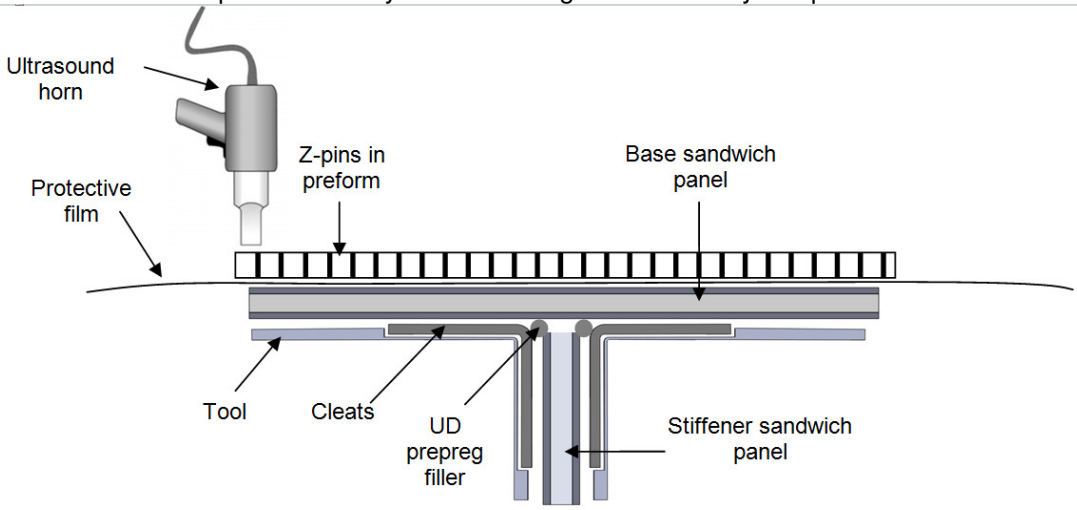

Step 3 Z-pinning of the assembled cleats, stiffener panel and base panel.

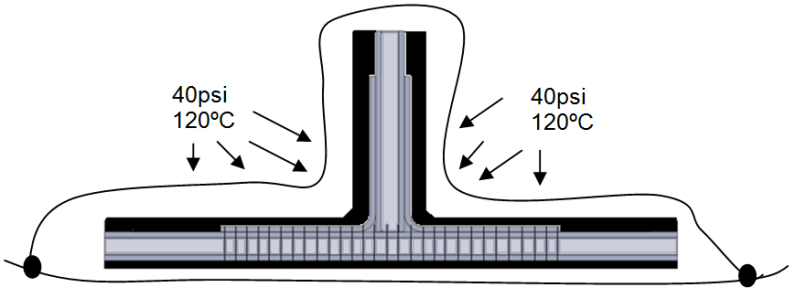

Step 4 T-joint co-cured in the autoclave. (Tooling is shown in black).

Figure 5-2: Manufacturing process of a z-pinned sandwich T-joint

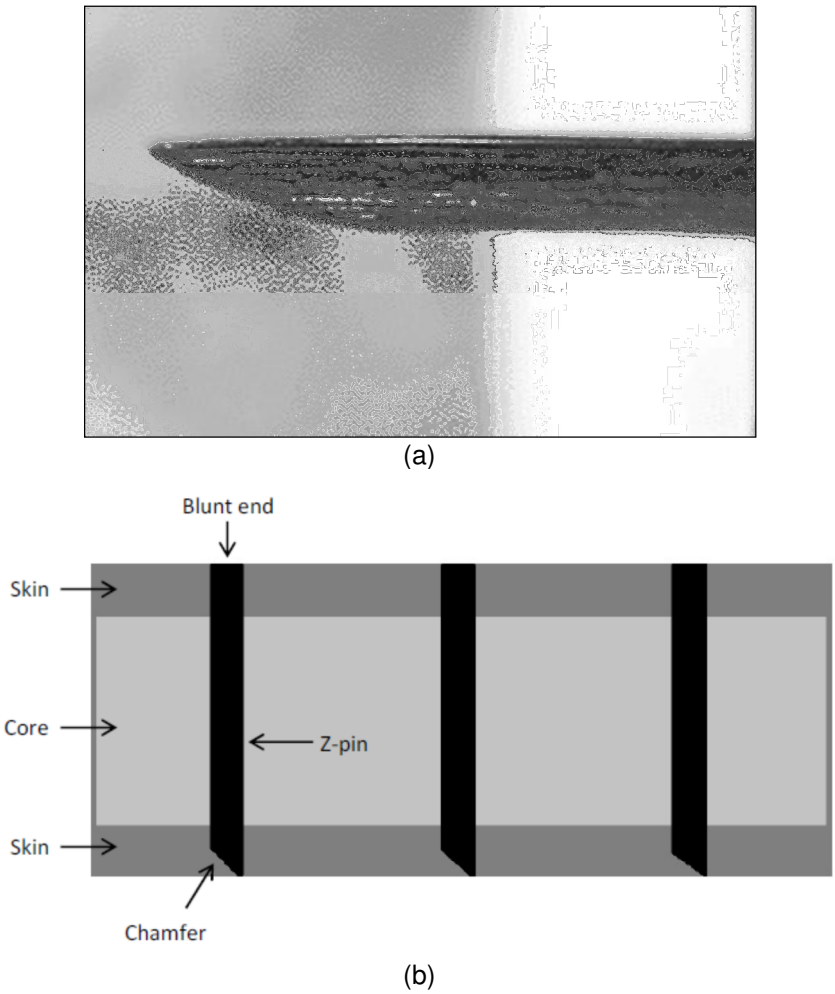

Figure 5-3: (a) Chamfer to the pin tip. (b) The pins in the sandwich composite (and base of sandwich T-joint) were all chamfered within one face skin and blunt in the other skin.

5.2.2 Structural Testing of Sandwich Joints

The structural properties of the unpinned and pinned sandwich T-joints were measured by applying a pull-off load parallel with the stiffener (as indicated by the arrow in Figure 5-4 and Figure 5-5) until final fracture, which is the catastrophic failure of the joint with multiple broken sections. The ends of the base panel were rigidly clamped, leaving an unrestrained length of 150 mm between the clamps. A tensile force was applied to the stiffener end using a 50 kN Instron loading machine operated at a constant displacement rate of 1 mm/min. From these tests the peak fracture load and fracture energy of the T-joints were measured.

Six specimens of each type of T-joint were tested under identical conditions to assess the variability in the fracture properties.

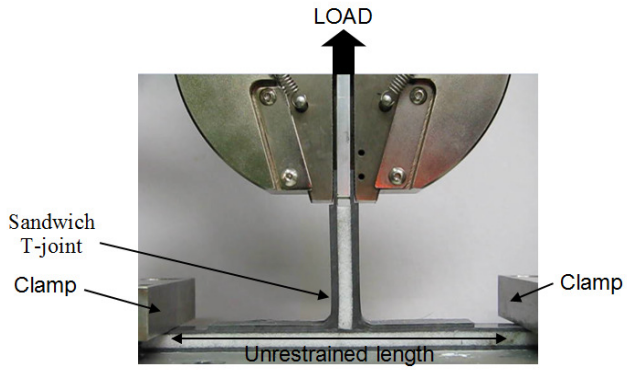

(a)

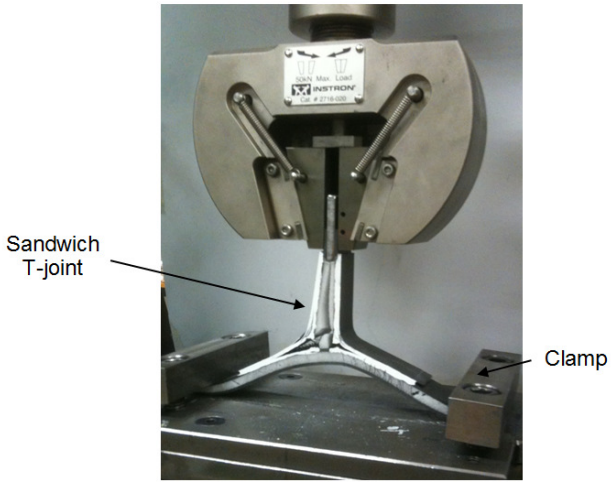

(b)

Figure 5-4: Structural testing of sandwich T-joints: (a) before testing and (b) final failure

5.2.3 Pin Pull-Out Tests on Sandwich Flat panels Composites

Multiple pin pull-out tests were performed on flat panels of the sandwich composite structure, as shown schematically in Figure 5-5. Specimens were manufactured using the z-pinning method outlined in Chapter 3. These tests were performed to determine the bridging traction load and traction fracture energy generated by a single pin under mode I loading, which is similar (but not identical) to the tensile loading on the pins along the cleat-base panel connection in the structural pull-off tests performed on the sandwich joints. The pins in the joint experienced mixed mode I/II interlaminar loading as opposed to pure mode I interlaminar loading as will be discussed later.

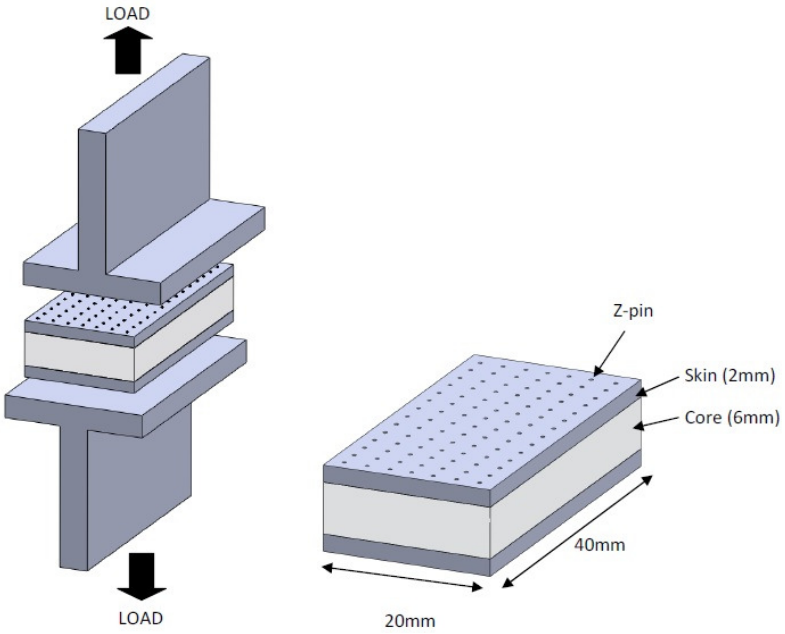

(a)

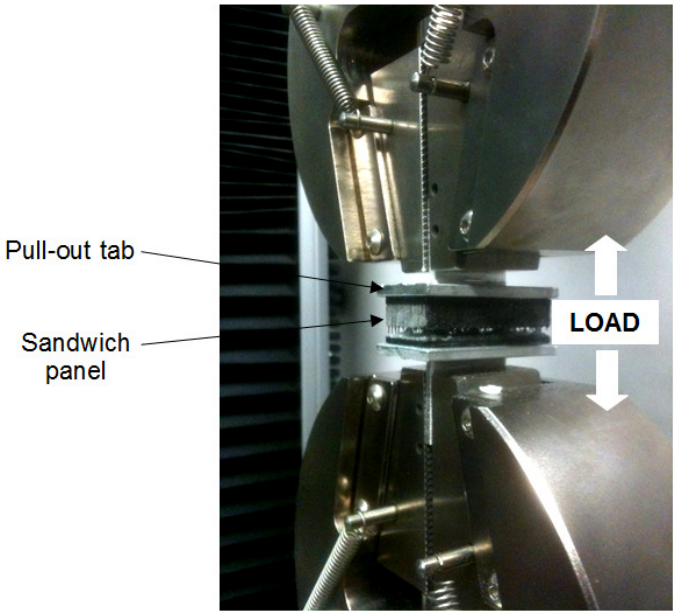

(b)

Figure 5-5: Pin pull-out tests on flat sandwich panels: (a) Specimen geometry and (b) test in progress.

The pin pull-out test specimen (measuring 40 mm x 20 mm) was reinforced with the same z-pins used in the joints. The entire area of the specimen was reinforced with about 80 or 260 z-pins, which is equivalent to the low and high volume pin contents, respectively. A tensile load was applied normal to the face skins of the sandwich composite at a displacement rate of 1 mm/min to final failure. Pull-out tabs were bonded to the face skins of the specimen

using a high strength epoxy (Araldite 420). The measured load was divided by the total number of z-pins in the sandwich sample to determine the average traction load generated by each pin. Three samples of the sandwich materials reinforced with the low and high pin contents were tested under identical conditions.

5.3 RESULTS AND DISCUSSION

5.3.1 Structural Properties and Fracture of Z-Pinned Sandwich Joints

Figure 5-6 presents typical applied load-displacement curves for the unpinned and z-pinned sandwich joints measured in the tensile pull-off test. The curves are characterised by multiple load spikes caused by progressive fracture of the joints, although the loads sustained by the z-pinned joints were higher over most of the displacement range up to final failure (which is the complete failure of the joint occurring at the displacement of 45-50 mm).

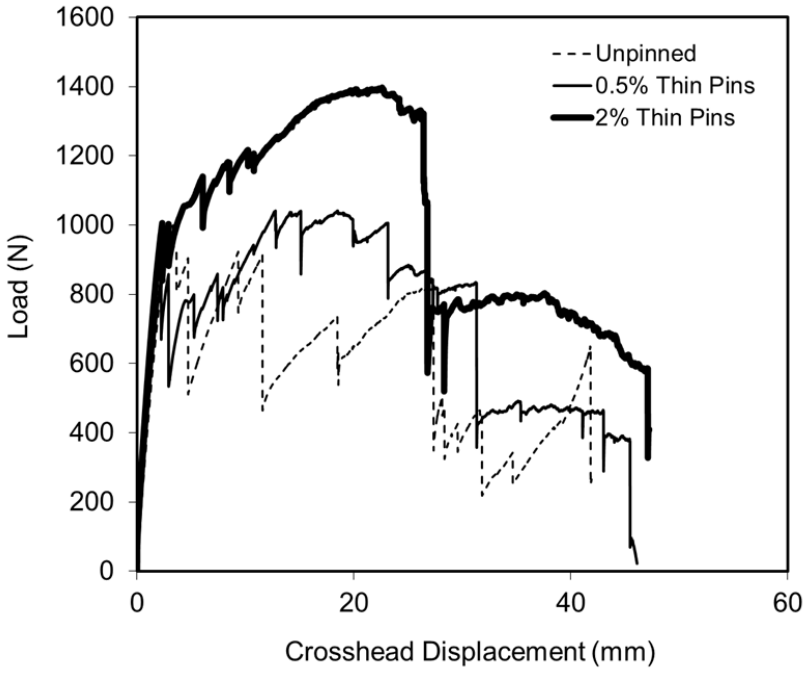

Figure 5-6: Representative load displacement curves for unpinned sandwich T-joint, T-joint reinforced with 0.5% z-pins and T-joint reinforced with 2% z-pins.

Using these curves the joint stiffness's, peak fracture loads and fracture energies of the joints were determined. The joint stiffness was calculated by determining the slope of the elastic region of the graph. Figure 5-7 shows the effect of z-pin content on the stiffness of the sandwich T-joint. It can be seen that stiffness increased steadily with increasing volume content of z-pins. The increase in stiffness may be caused by a stiffening of the base to the sandwich joint when z-pinned. The z-pins are expected to increase the shear modulus of the foam core which in turn will increase the flexural modulus of the sandwich material used for the base panel.

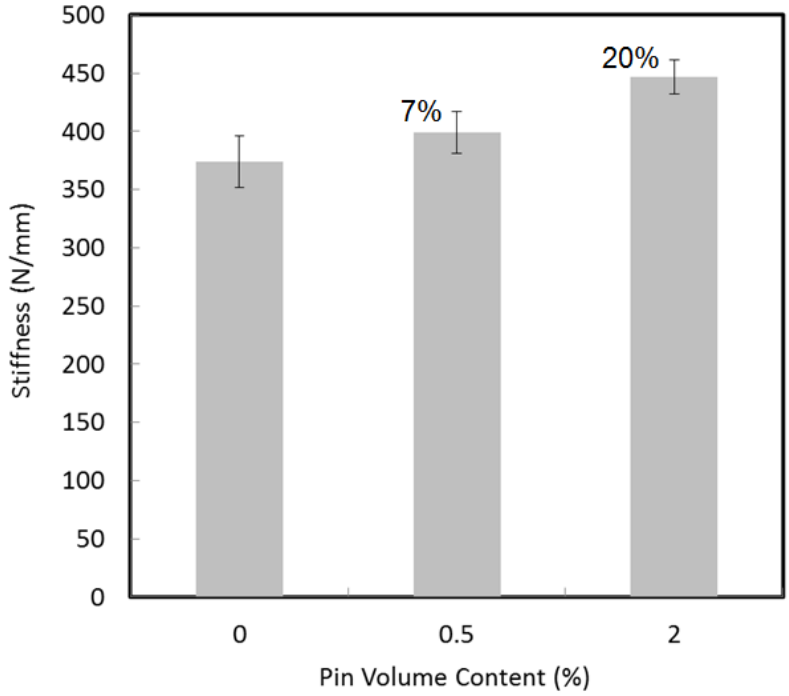

Figure 5-7: Effect of z-pin content on the stiffness of the sandwich T-joint.

The fracture load was defined by the maximum load sustained by the T-joint before final failure, and the fracture energy was determined from the total area under the applied load-displacement curve. It was found that increasing the z-pin content increased the peak fracture load and fracture energy, as shown in Figure 5-8, and at the highest pin content these properties were raised by an average of ~20% and over 50%, respectively. However, there is significant scatter in the measured property values, particularly for the 0.5% z-pinned joint, and the cause of this variability is discussed later in this chapter.

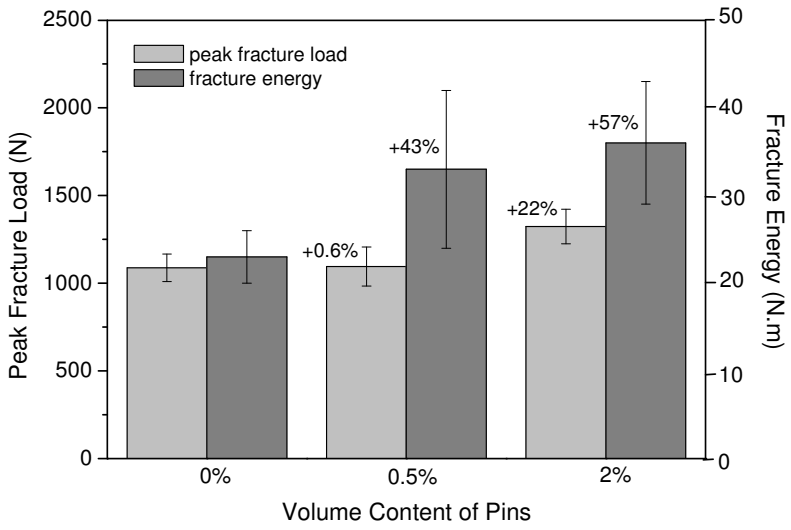

Figure 5-8: Effect of z-pin content on the peak fracture load and fracture energy of the sandwich T-joint. The percentage values show the average increase to the fracture properties of the pinned joints relative to the unpinned (control) joint.

Z-pinning also changed the damage and fracture mode of the T-joint. The unpinned joint initially failed by core cracking within the stiffener panel which was immediately followed by skin-core debonding in the base panel. Final fracture occurred by delamination cracking along the bonded interface between the cleat and base panel. This sequence of damage events occurred at increasing displacement values as indicated in Figure 5-9 and is shown in Figure 5-10 and Figure 5-11.

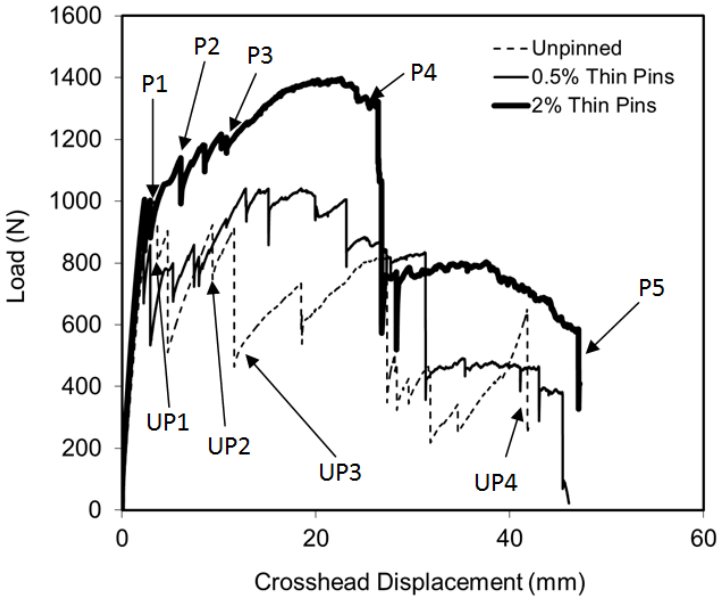

Figure 5-9: Typical load-displacements curves for the unpinned and z-pinned T-joints. The labels indicate when photos of the joints specimens shown in Figure 5-10 and Figure 5-11 were taken.

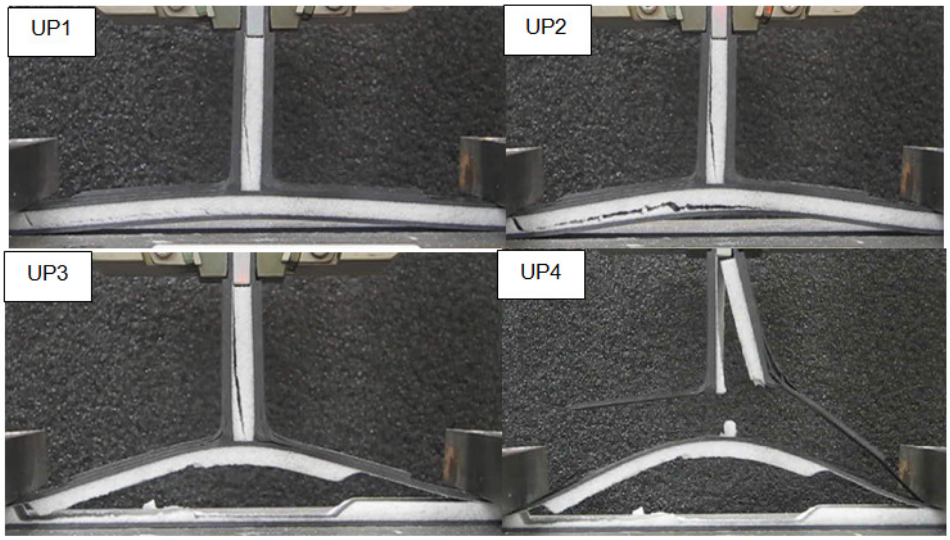

Figure 5-10: Failure of unpinned sandwich T-joint. The points labelled UP1 - UP4 are indicated in the load-displacement curves in Figure 5-9 when the photos were taken.

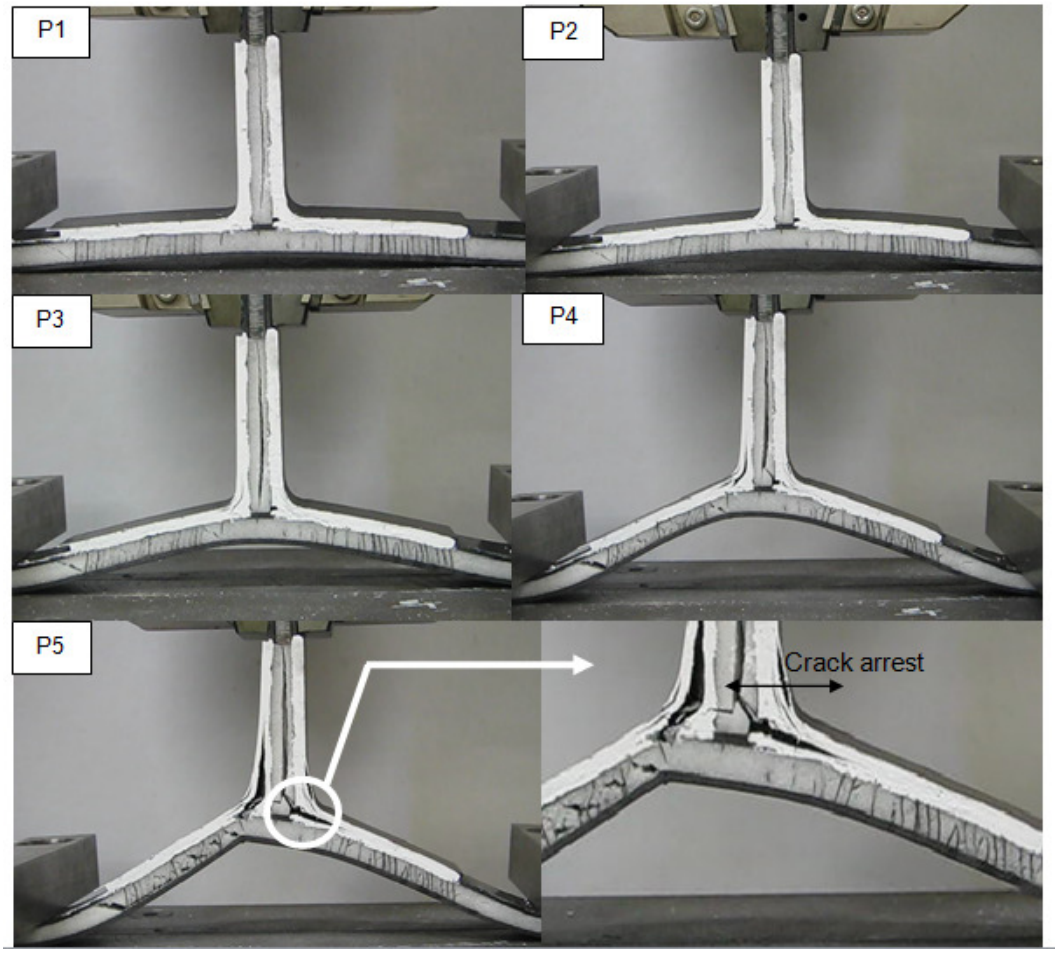

Figure 5-11: Failure of 2% z-pinned sandwich T-joint. The points labelled P1 – P5 are indicated in the load-displacement curve in Figure 5-9 when the photos were taken.

The z-pinned T-joints also initially failed by core cracking in the stiffener (which was not pinned), however skin-core debonding was arrested by the pins and cleat fracture did not occur. This represents a major change in the fracture behaviour of the joint due to pinning. The pinned joints fractured by skin rupture in the base panel, as shown in Figure 5-11. The strengthening and toughening mechanics responsible for the increases to the peak fracture load and fracture energy and the change to the fracture mode of the pinned joints were investigated by pin pull-out tests on the sandwich composite.

5.4 BRIDGING TRACTION PROPERTIES OF Z-PINS IN SANDWICH COMPOSITES

Figure 5-12 presents three examples of traction load-crack opening displacement (extension) curves for a single z-pin within the sandwich composite under through-thickness tensile loading. The curves were measured using the multiple pin sandwich specimens illustrated in Figure 5-5, with the traction load being the average force acting on a single pin (which is the total force divided by the number of pins in the specimen). The through-thickness tensile load applied on the pin pull-out specimens was similar to that experienced by the z-pins in the sandwich joints, although the pins along the cleat/skin bond-line also experienced an interlaminar shear stress induced by bending of the skin panel (i.e. mixed mode I/II loading).

The traction load curves in Figure 5-12 are similar in profile to those measured for laminates [17-19], and characterised by an initial elastic response of the pin followed by a sudden and large load drop, and then a more gradual load drop with increasing crack opening displacement to final failure. The initial linear increase in the traction load curve is due to elastic stretching of the z-pin, the large load drop is due to debonding of the pin from the sandwich material, and the gradual load drop is due to the loss in interfacial friction force as the pin is pulled out from the material.

While the profiles for the traction load-extension curves were similar for the z-pinned sandwich materials, there were large differences between nominally identical specimens. Figure 5-12 shows three curves measured for the sandwich composite test under the same conditions. While the profiles of the curves are the same, there is significant scatter and the cause of this is discussed later.

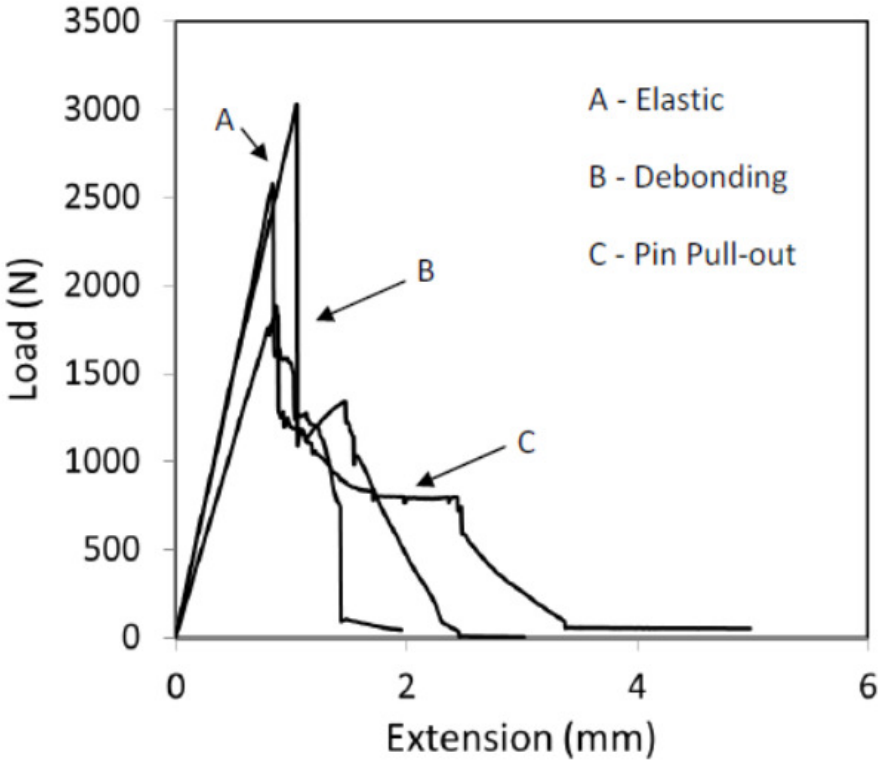

Figure 5-12: Traction load-extension curves for a single z-pin within three samples of the sandwich composite tested. The three stages of pin response to the loading are indicated.

The load reaction of a single z-pin under an applied tensile load during the elastic phase (i.e. before debonding and pull-out) is shown in Figure 5-12. The traction load generated by a z-pin within a sandwich composite can be estimated using a modified form of the mode I bridging traction laws for pinned laminates [20,21]. The elastic load generated by a z-pin up to the ultimate load point is due mainly to interfacial shear stress transfer across the bonded pin-sandwich composite interface, which includes the two face skins and core. The elastic load (P) is a function of the crack opening extension (δ) up to the ultimate load point (P_{max}) according to the following equation and illustrated in Figure 5-13:

$$P_{elastic}(\delta(h)) = 2(\tau_s \pi d_p h_s) + (\tau_c \pi d_p h_c) \qquad P_{elastic} \le P_{\max} \qquad [5\text{-}1]$$

The first and second terms represent the elastic traction loads generated by the interfacial shear stress between the z-pin and the two face skins and the z-pin and core, respectively. τ_s is the interfacial shear strength between the z-pin and face skin, τ_c is the interfacial shear strength between the z-pin and core, d_p is the pin diameter, and h_s and h_c are the original length portions of the z-pin in the skins and core, respectively. It is assumed with equation 5-1 that the z-pin is perfectly orthogonal and fully bonded to the face skins and core. It is also

assumed the residual cure stresses within the face skins do not alter the interfacial shear strength.

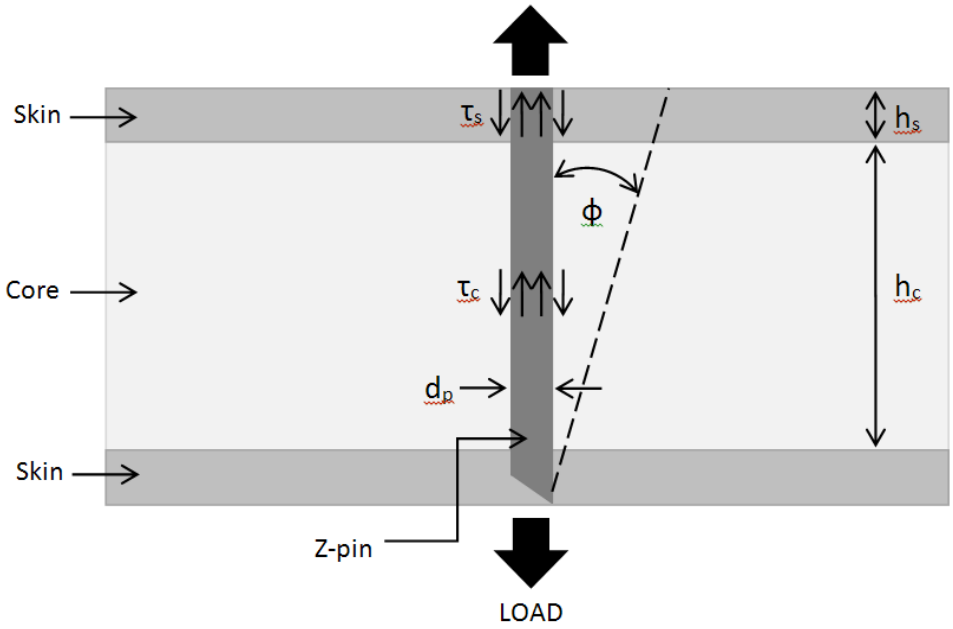

Figure 5-13: Traction stresses acting along the pin-sandwich composite interface under a through-thickness tensile load.

The interfacial shear stress generated at the pin-face skin interface is assumed to be much greater than the shear strength of the pin-foam core interface ($\tau_s >> \tau_c$). This is because the contact area between the z-pin and laminate skins is much greater than the area between the pin and core due to the porous cellular structure of the polymer foam. Therefore, the influence of the interfacial shear stress between the z-pin and core on the traction load can be ignored and equation 5-1 reduces to:

$$P_{elastic}(\delta(h)) \approx 2.\tau_s \pi d_p h_s \qquad [5\text{-}2]$$

The displacement is a function of the skin thickness (h_s) according to Jain [117]:

$$\delta(h_s) = \left[h - \frac{h_s}{r} \ln\left(\frac{h \times r}{h_s} + 1 \right) \right] \left[1 + \frac{h \times r}{h_s} \right] \qquad [5\text{-}3]$$

where r is the tensile extensibility ratio of the z-pin, which equals [117]:

$$r = \frac{\tau \pi d_p H_c}{A_f E_f} \qquad [5\text{-}4]$$

where A_f and E_f are the cross-section area and axial Young's modulus of the z-pin, respectively. H_c is the half-thickness of the sandwich composite.

The sudden drop in the traction load and then the further (more gradual) reduction in load with increasing crack opening displacement beyond the ultimate load point is due to debonding and pull-out of the z-pin, respectively. The traction load during the pull-out phase arises from friction stress generated between the z-pin and sandwich composite structure. When it is assumed that z-pin pull-out occurs along the mid-plane of the sandwich material (i.e. along the centre-line of the foam core as illustrated in Figure 5-14), then the bridging traction load can be calculated using:

$$P_{pull\text{–}out}(\delta(S)) = 2(H_s - S)\tau_{f(s)}\pi d_p + (H_c - S)\tau_{f(c)}\pi d_p \qquad [5\text{-}5]$$

It is assumed for this equation that the pull-out process of the z-pin is symmetric along the mid-plane of the core where tensile failure is considered to occur. The first term is the z-pin pull-out traction load caused by friction between the pin and two face skins while the second term is the traction load generated by sliding friction between the pin and core. H_s and H_c are the half-thickness values of the skins and core, respectively. $\tau_{f(s)}$ and $\tau_{f(c)}$ are the friction stress between the z-pin and face skins and the z-pin and core, respectively.

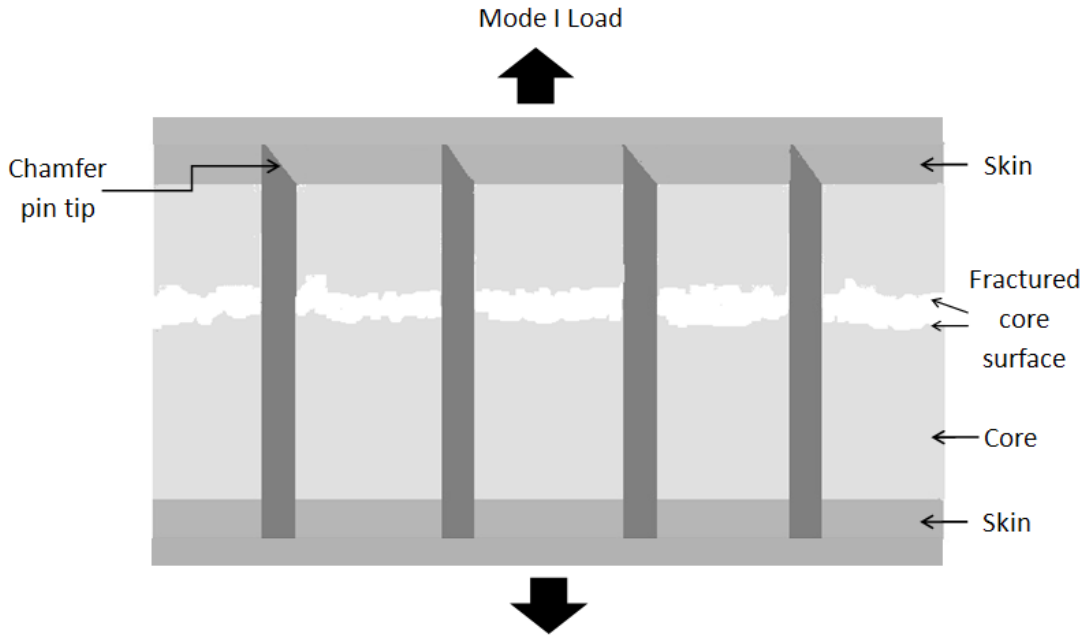

Figure 5-14: Z-pin pull-out along the mid-plane of the sandwich material (centre-line of the foam core)

The crack opening displacement during pull-out is a function of the slip length (S) of the pin according to Jain [117]:

$$\delta(S)=\left[H_c-\frac{H_c}{r}\ln\left(\frac{(H_c-S)r}{H_c}+1\right)\right]\left[1+\frac{(H_c-S)r}{H_c}\right] \qquad [5\text{-}6]$$

Equation 5-5 is valid when the sandwich composite breaks under tensile loading along the mid-plane of the core, and then the pin pull-out process occurs symmetrically from the two fractured halves of the material as shown in Figure 5-14. During pin pull-out testing, however, it was observed that this failure mode did not occur, and instead failure occurred at the interface between one of the face skins and foam core, as shown in Figure 5-15. The majority of the z-pins were completely pulled-out from one face skin whereas pin pull-out did not occur from the other skin. The pins were always completely pulled-out from the face skin containing the chamfered tip (Figure 5-3), and presumably failure occurred here because of the lower interfacial contact area between the pin and skin than at the opposite end where the pin was blunt (resulting in higher contact area).

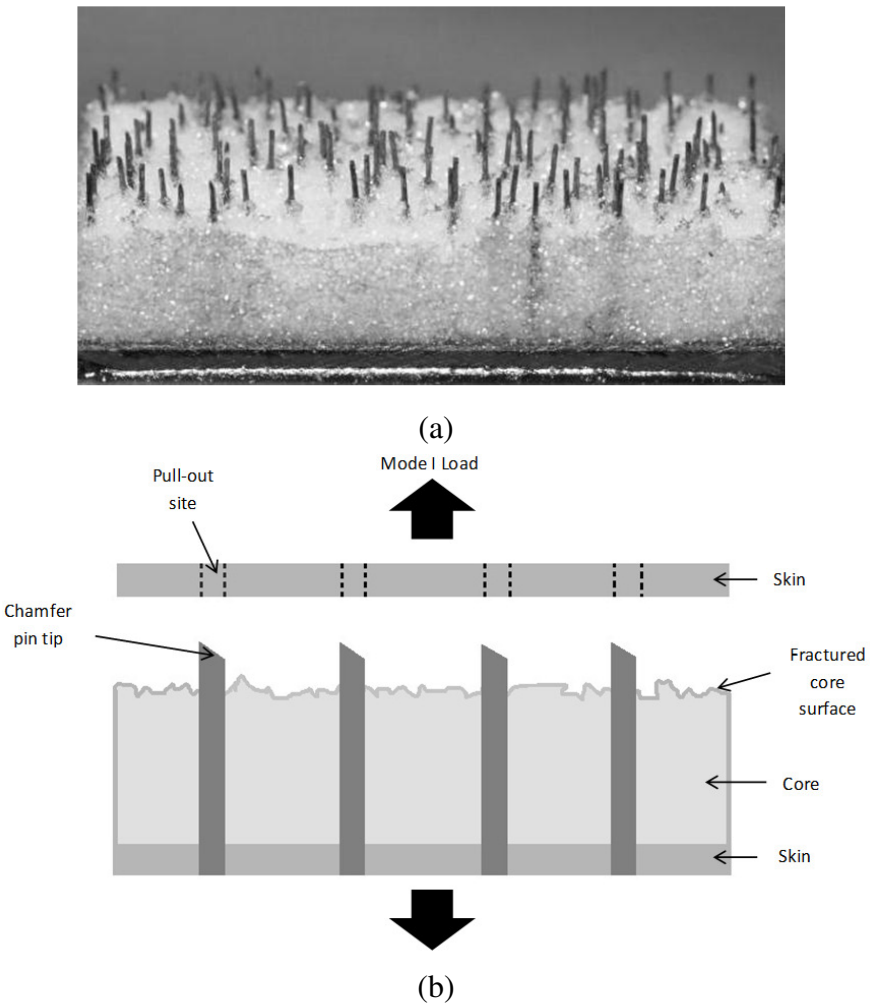

Figure 5-15: (a) Pin pull-out specimen which failed along the skin-core interface resulting in pin pull-out from the face skin. Shown are the z-pins remaining in the core and lower face skin after the upper skin has been pulled-off. (b) Schematic of the pin pull-out process from the sandwich composite.

When this failure mode occurs and when it is assumed that the interfacial friction between the z-pin and skin is much higher than between the pin and core (i.e. $\tau_{f(s)} >> \tau_{f(c)}$), then equation 5-5 can be reduced to:

$$P_{pull-out}(\delta(S)) \approx (H_s - S)\tau_{f(s)}\pi d_p \qquad [5\text{-}7]$$

The above is the first model to analyse the mode I bridging traction laws for z-pinned sandwich composites (based on the bridging mechanics of z-pinned laminates). Equations 5-2 and 5-7 were used to calculate the mode I bridging traction load due to elastic deformation and pull-out of the z-pin, respectively. Figure 5-16 compares the calculated bridging traction load curve for a single z-pin against an experimental curve when the analysis assumes that the pin is aligned in the orthogonal direction in the sandwich composite. The analysis gives a good prediction of the elastic bridging load, although the prediction of the pull-out load with increasing extension is less than the measured pull-out loads. One reason for the larger extension values in the experiment is due to some twisting motion which arises from the pull-out tabs not being perfectly aligned or parallel with the load direction.

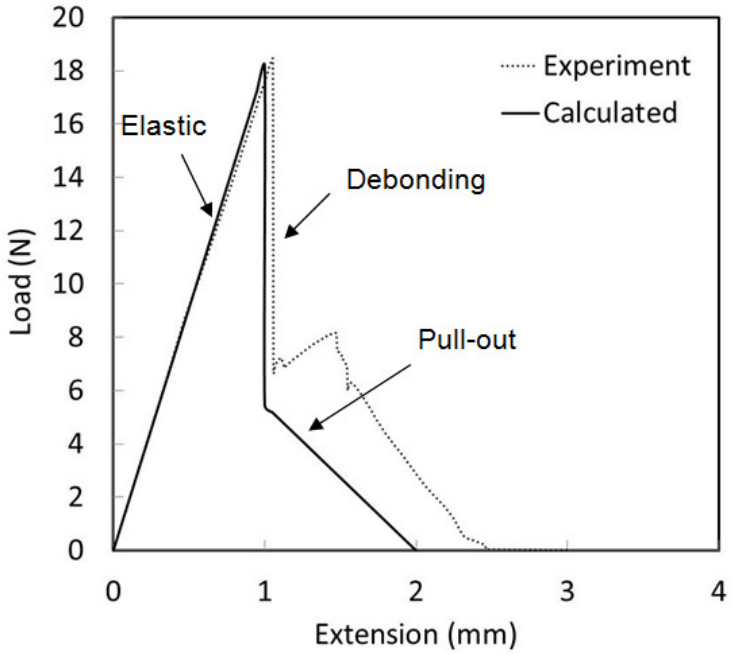

Figure 5-16: Comparison of the calculated and measured pin traction load-extension curve. The calculated curve assumes that the pin is perfectly orthogonal. Note the calculated curve is less than the measured curve during the pin pull-out phase.

An important factor influencing the pull-out traction load is the initial misalignment of the z-pins within the sandwich composite. The analysis (equations 5-1 to 5-7) assumes that the z-pin is perfectly orthogonal, although as discussed in chapter 3, most of the pins were offset over a range of inclined angles from the orthogonal direction. The offset of the z-pins will induce snubbing, which is the lateral deflection of the pin into the face skin as shown

schematically in Figure 5-17. The snubbing force increases with displacement as the skin resists deformation by the z-pins, and the mechanics of snubbing have been analysed for monolithic laminates under mode II interlaminar loading by Cox [74]. Snubbing increases the friction stress opposing pin pull-out from the skin.

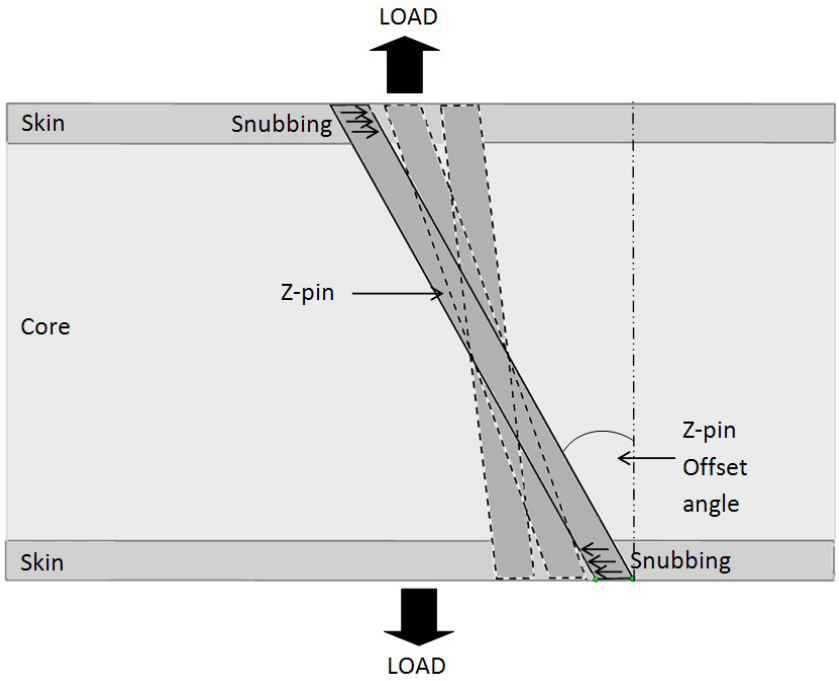

Figure 5-17: Snubbing process of offset z-pins in a sandwich composite under pull-out loads. The three pin angles represent the progressive straightening of the z-pin with increasing load.

Cartié and Fleck [71] report that the traction load for an inclined pin within a laminate during the pull-out phase is calculated using:

$$P(\phi) = \frac{4\pi d_p}{\phi}\left\{(h_s - S)\tau_f + z_o\tau_{e(s)}\right\} \qquad [5\text{-}8]$$

where z_o is the length of the pin deflected into the face skin (and is assumed to be $0.1H_s$) and $\tau_e(s)$ is the enhanced friction shear stress due to snubbing of the pin within the face skin. Cartié and Fleck [71] suggest that $\tau_e(s)$ is between 3 and 10 times higher than τ_f (i.e. the pull-out friction stress for a perfectively orthogonal z-pin for a carbon-epoxy laminate). The offset angle is assumed to be 2.1^o which is the average pin offset angle recorded for the 2% thin pin volume content category.

When the bridging traction load generated by pin pull-out (described mathematically by equation 5-7) and the effect of snubbing friction stress (equation 5-8) are combined, then an equation can be derived to analyse for the effect of snubbing on the pull-out traction load of a single pin from one face skin:

$$P_{pull-out}(\delta(S)) = \pi d_p \left[\left(\frac{H - S - z_o}{\cos\phi} \right) \tau_f + z_0 \tau_e \right] \quad \text{for} \quad 0 < S < z_o \qquad [5\text{-}9a]$$

where

$$P_{pull-out}(\delta(S)) \approx (H_s - S)\tau_{f(s)} \pi d_p \quad \text{for} \quad S > z_o \qquad [5\text{-}9b]$$

$$P_{pull-out}(\delta(S)) = 0 \quad \text{for} \; H = S \qquad [5\text{-}9c]$$

Equation 5-9a is valid for the range where the slip length of the pin (S) is between 0 and z_o, which is the active snubbing zone due to the pin inclination angle and is the pull-out region of the pin within the skin. A schematic of the pin pull-out process is depicted in Figure 5-18 showing the regions of slip length (S), pin length deflected in the skin (z_o), and skin thickness (H). Once S exceeds the length of z_o, snubbing is no longer experienced by the pin and equation 5-9b can be used to calculate the traction load in the pull-out phase. When the slip length of the pin reaches H, the traction load drops to zero because the pin has completely pulled-out from the skin.

Figure 5-19 shows calculations of the effect of friction snubbing stress on the pull-out traction load for a z-pin from the face skin of the sandwich composite. It was assumed that the depth of the snubbing zone was 0.1 mm, which is based on measured values for pins within a carbon-epoxy laminate under pure mode II loading [54]. It was also assumed that the pin offset angle was 2.1º, which is the average angle measured for the highest pin content (2% by volume). The different stages of the pin pull-out phase (represented by equations 5-9a to 5-9c) are calculated for a range of friction snubbing stresses; τ_e was assumed to be two, three and five times higher than τ_f, which was 6.8 MPa. Figure 5-19 shows that a value in the range of $\tau_e = 3\tau_f$ to $5\tau_f$ gives a good estimate of the pull-out traction load with increasing crack opening displacement.

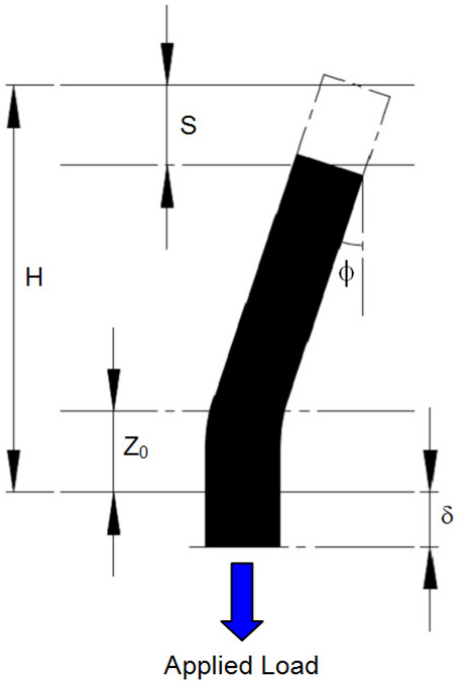

Figure 5-18: Schematic of pull-out process for a pin inclined at an angle (ϕ) from the orthogonal direction. Adapted from Cartié et al. [71]

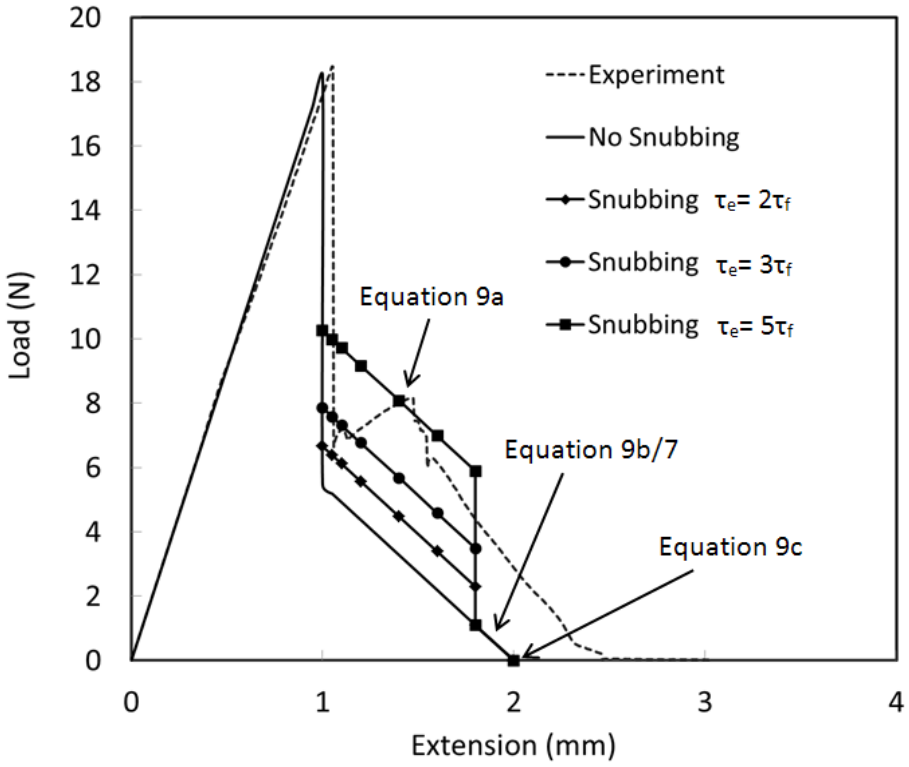

Figure 5-19: Comparison of the calculated pin traction load-extension curves and a measured curve. The calculated curves consider different magnifications of the enhanced friction (snubbing) stress caused by offset of the pin from the orthogonal direction.

The traction load analysis provides important insights into the causes for the variability in the mode I traction load response of the z-pins when pulled-out from the sandwich composite (as shown in Figure 5-19). For example, the analysis reveals that small variations in the z-pin offset angle can induce significant changes in the traction load generated during the pull-out phase. Another important factor contributing to the variability is debonding between the z-pins and face skins. Z-pins do not always fully bond to carbon fibre-epoxy laminates during the cure process, and cracks often exist along the interface between the pin and laminate. For example, Figure 5-20 shows radial and axial interfacial cracking within a z-pinned composite. These cracks are formed during the cool-down phase of the curing process when thermal stresses are generated due to the mismatch in the coefficients of thermal expansion of the z-pins and laminate.

Barrett [118] and Sweeting and Thomson [60] have shown via finite element analysis that the magnitude of the residual stresses can exceed the interfacial failure stress, resulting in cracking. It is important to note, however, that complete debonding of the z-pins rarely occurs, and instead partial cracking of the pin-laminate interface is more common. Chang [54] found that the amount of interfacial cracking varies significantly between z-pins, and this is due presumably to local variations in the residual stress due to the heterogenous microstructure of the laminate. The maximum traction load and the magnitude of the load drop immediately following the peak load is determined by the force needed to completely debond the z-pin from the laminate. Interfacial cracking will lower the maximum traction force and the subsequent load drop and differences in the amount of cracking between z-pins will induce variability in these two traction properties. For these reasons there were significant differences in the mode I traction load-displacement curves for the z-pinned sandwich composites, and similar behaviour has been reported for z-pinned laminates for the same reasons.

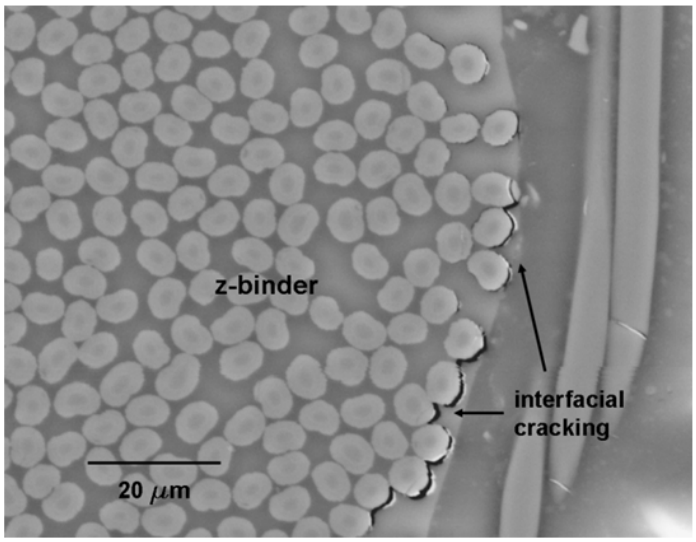

(a)

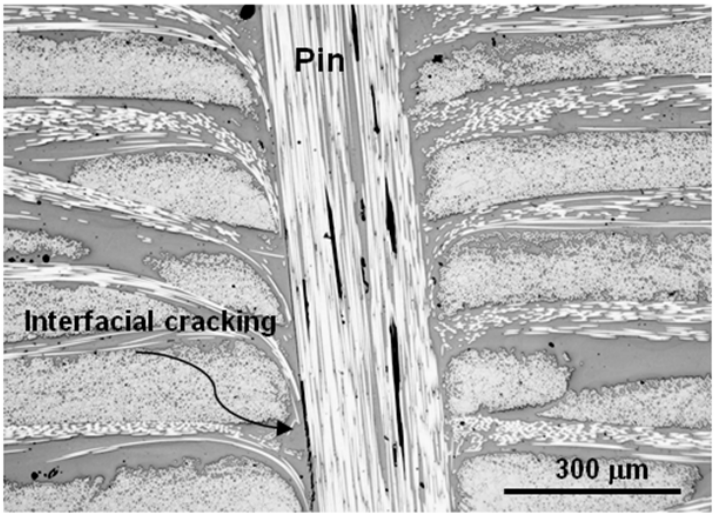

(b)

Figure 5-20: Photographs showing (a) radial interfacial cracking around a z-pin and (b) axial interfacial cracking along a z-pin in a carbon fibre-epoxy laminate. From Chang [54].

5.5 PARAMETRIC STUDY OF THE MODE 1 BRIDGING TRACTION PROPERTIES OF Z-PINNED SANDWICH COMPOSITES

The fracture process of the z-pinned sandwich joint specimens (shown in Figure 5-11) is more complicated than the failure process of the pin pull-out specimens under pure mode I loading. The fracture process of the z-pinned joint involved multiple damage modes, including centre-line splitting along the stiffener, core cracking within the skin, and skin-core interfacial cracking within the face skin. In contrast, the failure of the pin pull-out specimens

simply involved fracture along the skin-core interface. Despite these differences, the pin traction loads and traction energies can be used to qualitatively assess the strengthening and toughening effect of z-pins to sandwich T-joints. Based on the pin traction analysis, the peak fracture load and fracture energy of a z-pinned sandwich joint should increase with the volume content of pin, and this was proven by experimental testing of the joints. The analysis also revealed that following the onset of pin pull-out in the T-joint specimens, the snubbing effect induced by the pins being at inclined angles provides significant strengthening (high traction load) and toughening (high traction energy). The offset of the pin alignment from the orthogonal direction, which was inadvertently caused during manufacture, has a beneficial effect of the joint properties as the pins failed by pull-out.

The z-pin traction analysis reveals that the structural properties of the sandwich joints under stiffener pull-off loading should increase with (in addition to the volume content of z-pins) the diameter and inclination angle of the pins as well as the thickness of the face skins. Therefore, several approaches (e.g. z-pin content, z-pin diameter, z-pin angle, skin thickness) can be used in isolation or in combination to strengthen and toughen sandwich T-joints by pinning.

In light of the previous analytical study of the z-pin pull-out process in a sandwich composite structure, a further study was conducted to investigate the effect of individual pin properties on the mode I bridging traction properties. Using the pin traction model, a parametric analysis was performed into the influences of the Young's modulus (E_p) and diameter (d) of the z-pins and the friction stress (τ_f) and shear strength (τ) of the z-pin/sandwich skin interface. The analysis was performed assuming that the z-pins were perfectly orthogonal and fully bonded to the sandwich material.

Figure 5-21 shows the effect of z-pin modulus on the bridging traction load response. The z-pin modulus was varied from negative 20% to a positive 40% of the original pin modulus, which is 140 GPa. This range was selected as representative of the typical variation in the elastic modulus of fibrous z-pins due to changes in the type of carbon fibre or the carbon fibre content of the pins. It was found that changing the z-pin modulus does not have a significant effect on the bridging traction load. This implies that reinforcing sandwich T-joints with high stiffness z-pins will not induce a significant strengthening effect from the traction loads that are generated during the fracture process.

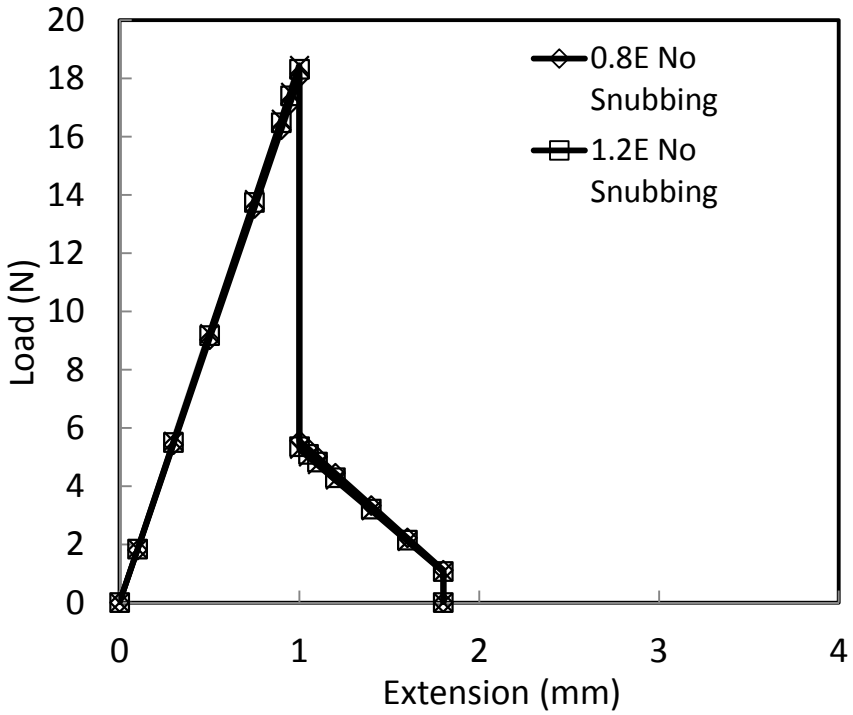

Figure 5-21: Effect of z-pin modulus on the bridging traction load-extension response for the sandwich composite

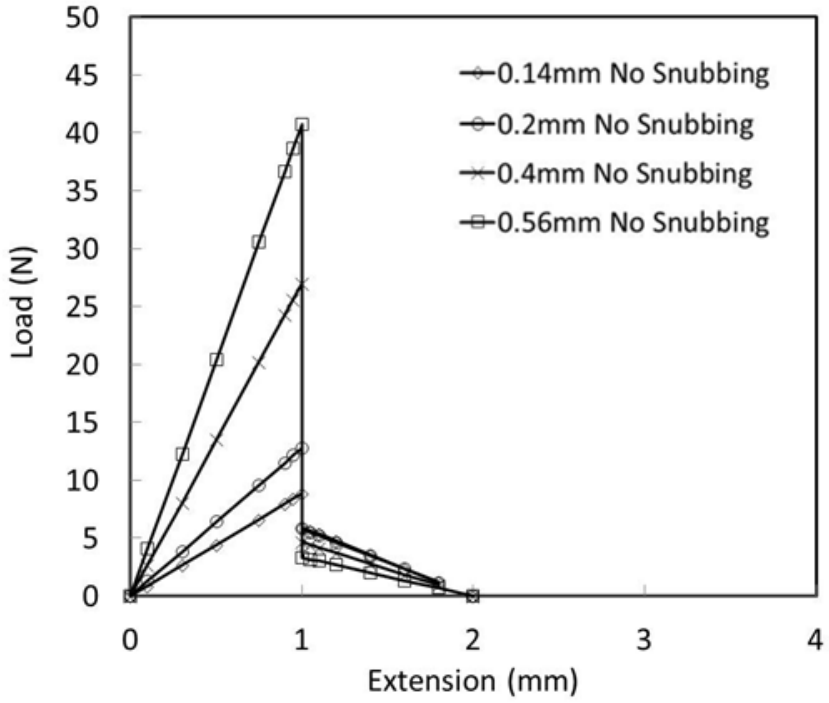

Figure 5-22: Effect of z-pin diameter on the bridging traction load-extension response for the sandwich composite

Figure 5-22 shows the calculated effect of z-pin diameter on the traction load response. The parameteric analysis was performed for a range of z-pin diameters ranging from 0.14mm to 0.56mm. It was found that the traction stiffness, maximum elastic load and frictional pull-out load were dependent on the pin diameter. These properties increased with the z-pin diameter due to the increased interfacial contact area with the sandwich composite which reduced the interfacial shear and frictional stresses during pin loading. Therefore, increasing the z-pin diameter should be an effective method for strengthening and toughening sandwich T-joints. However this needs to be verified experimentally.

Figure 5-23 shows the variation in pin traction loads with varying the shear strength and the frictional stress between the z-pin/sandwich skin interfaces, with and without snubbing. Figure 5-23a considers the complete pull-out process and Figure 5-23b considers the effect of snubbing in the pull-out region only. It can be seen that both parameters, shear strength and frictional stress were varied a negative 10% and a positive 10% and 20%. When the snubbing effect was ignored, the traction load shows a linear increase in the elastic region. The debonding traction load, just before pull-out, shows an increase but the load still converges to the thickness of the skin which is 2mm, supporting the theoretical model where extension cannot exist beyond the thickness of the skin from which the z-pin is pulling-out. With the inclusion of snubbing, the pullout phase shows an increase in the traction loads where the slip length, S, is between 0 and the active snubbing zone z0. The experimental traction loads show agreement with the theoretical 10% and 20% increase in the shear and frictional stresses.

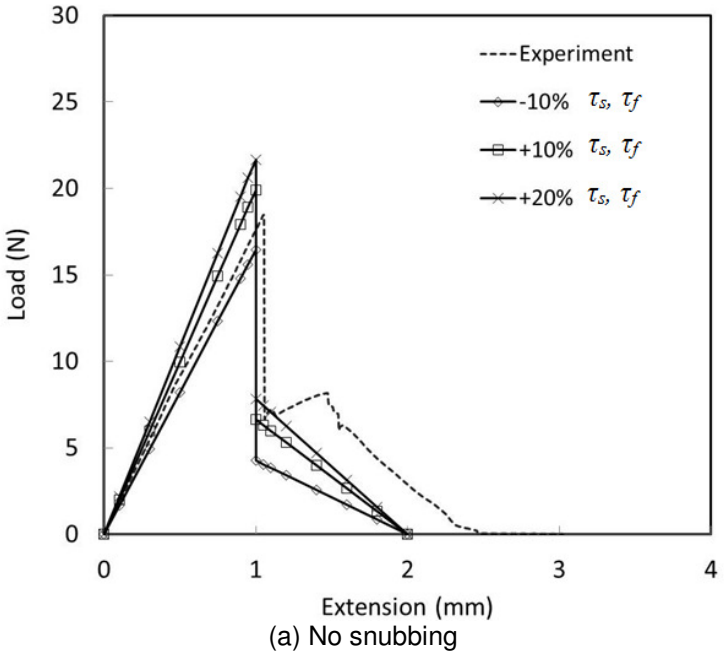

(a) No snubbing

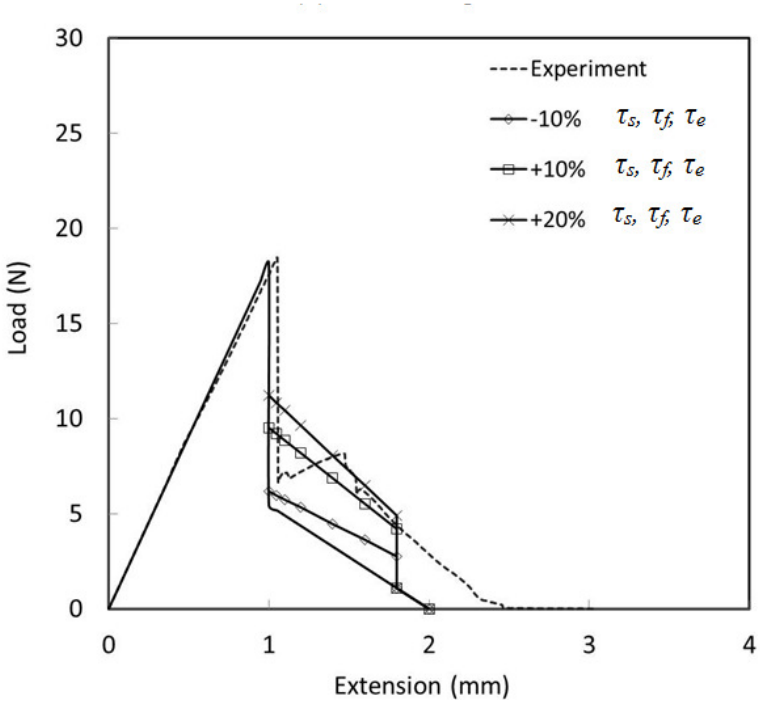

(b) Snubbing

Figure 5-23: Effect of interfacial shear and frictional stress on the bridging traction load-extension response for the sandwich composite

This parametric study reveals that the mode I traction loads are most sensitive to z-pin diameter, less sensitive to the shear and frictional stresses, and insensitive to the z-pin diameter over the range of values that were analysed. This is similar to the analytical study conducted by Koh et al. [70] which revealed a similar influence of z-pin diameter and shear and frictional stresses on the pull-out mechanics of z-pinned laminates. Due to the main failure mode of skin-core debonding, the bridging traction mechanics of z-pinned sandwich composites can be treated like a laminate. Any other failure mechanism would mean a modification of the analytical model. However, the study conducted in this chapter has concluded via theoretical and experimental validation that the pull-out behaviour of z-pin embedded in a sandwich composite can be predicted.

5.6 CONCLUSIONS

Through-thickness reinforcement of the T-shaped sandwich composite joints with z-pins increased the peak fracture load and fracture energy. The improvement to these properties increased with the volume content of z-pins, and at the highest (but still modest) content of

2% that was studied the fracture strength and fracture energy were increased by about 20% and over 50%, respectively. The fracture load increased with the z-pin content due to an increase in the traction load generated during elastic stretching and frictional pull-out of the pins. The high amount of energy absorbed by the z-pinned joints during elastic deformation and pull-out of the pins was partly responsible for the large increase to the fracture energy. The offset of the z-pins from the perfectly orthogonal direction (due to a lack of precise control of the pinning process) made a significant contribution to raising the pull-out friction stress and thereby the fracture energy to the joint. A mode I bridging traction law was formulated for z-pinned sandwich composites, which was based on the bridging mechanics of pinned laminates. The traction mechanics analysis revealed that the fracture resistance of T-joint can be improved by increasing the pin diameter, although this remains to be verified by experimental testing. The improvements to the structural properties of the joint due to z-pinning was accompanied by a change to the fracture mode; from bond-line delamination cracking for the unpinned joint to skin fracture (due to suppression of large-scale bond-line cracks) in the z-pinned joints, which demonstrates the high toughening effect of pin reinforcement.

Chapter 6 MAJOR CONCLUSIONS AND FUTURE WORK

6.1 COMPRESSION PROPERTIES OF Z-PINNED SANDWICH COMPOSITES

This PhD project has conducted an original and extensive research study into the mechanical properties of sandwich composites and bonded sandwich joints reinforced with z-pins. Z-pinning was shown experimentally to be an effective method for increasing the through-thickness compression properties of foam core sandwich composite structures. The compression modulus, strength and absorbed strain energy capacity were improved by z-pin reinforcement of the foam core. It was discovered that these compressive properties increased rapidly with the volume fraction of z-pins; and that only a small amount of pins (under 4%) is needed to improve the properties by several hundred percent.

In addition to investigating the effect of z-pin content, this project also investigated the effects of the diameter and the end restraint condition (built-in column or simply supported column) of z-pins on the through-thickness compression properties. Testing and analysis revealed that the improvement to the properties are controlled strongly by the z-pin content, and are not influenced significantly by the pin diameter (for the two sizes studied) or the pin end constraint (for the two conditions studied).

This PhD project characterised in detail the failure mechanisms of fibrous z-pins in sandwich composites under compression loading utilizing NDT technologies such as x-ray computed tomography and acoustic emission. It was found that fibrous z-pins fail during both elastic and plastic deformation of the foam core via a complex process involving splintering, kinking and fragmentation. It was also found that even after the z-pins have failed they retain significant load-bearing capacity because the foam core behaves as a Winkler elastic foundation which allows stress transfer with the damaged pins. Also, fractured ligaments of the z-pins are pressed into the foam core under increasing compressive strain which further strengthens the sandwich material.

Data and observations obtained from the experimental research were used to validate and assess the numerical accuracy of existing mechanical models for z-pinned sandwich composites. It was shown that existing models for calculating the through-thickness compression properties were not accurate for the type of z-pinned sandwich composite studied in this project. The models failed to accurately capture the complex strengthening mechanisms and failure modes of fibrous z-pins. The models used to calculate the through-thickness stiffness and strength assume crushing or buckling of the z-pins, which did not occur within the sandwich composites. The models do not account for the splintering and kinking of z-pins, and therefore a new model based on pin kinking was proposed to more accurately calculate the through-thickness compression strength of sandwich composites reinforced with fibrous z-pins.

6.2 INDENTATION AND IMPACT PROPERTIES OF Z-PINNED SANDWICH COMPOSITES

This project investigated the indentation resistance of z-pinned sandwich composites. The stiffness, yield stress and strain energy absorption properties under indentation loading were increased by the z-pins resisting localised deformation and crushing of the foam core. It was also found the effectiveness of z-pins to resist core indentation was dependent on the geometry of the indenter and the indentation depth. The indentation resistance increased with the load contact area due to an increased number of z-pins resisting the indentation load.

This PhD project assessed the accuracy of an existing model for calculating the indentation energy of z-pinned sandwich composites. The model was shown to be inaccurate for the z-pinned sandwich material investigated in this study due to the incorrect assumption that z-pins fail by buckling.

An experimental study into the impact properties revealed that z-pins can improve (albeit slightly) the impact damage resistance of sandwich composites. Z-pins were only effective at improving the impact damage resistance when impact-induced cracking within the laminate face skin and along the skin-core interface were sufficiently large for the pins to create a large-scale bridging traction zone. The traction loads generated by the z-pins resisted delamination cracking within the skin as well as cracking along the

interfacial region between the impacted skin and foam core. Despite the reduced amount of impact damage, the post-impact compression stiffness and strength properties measured in the in-plane direction were similar for the unpinned and z-pinned sandwich composites. Based on this work, it appears that z-pinning is not a highly effective method for increasing the impact damage resistance and post-impact compression properties of sandwich composites.

6.3 MECHANICAL PROPERTIES OF Z-PINNED SANDWICH COMPOSITE T-JOINTS

This PhD project investigated the effect of z-pinning on the mechanical properties of bonded T-joints made of sandwich composite structures. The stiffener/cleat region to the joint was reinforced with z-pins, and this represents the first investigation into the properties of z-pinned sandwich joints. Experimental testing proved that z-pins were effective at strengthening and toughening the bond-line between the base sandwich panel and cleat/stiffener panel of the joint. Z-pinning increased both the peak fracture load and fracture energy of the T-joint under tensile (stiffener pull-off) loading. These properties increased with the volume content of z-pins, and at the highest pin content (2% by volume) the fracture strength and fracture energy were raised by about 20% and over 50%, respectively. These improvements were due to strengthening and toughening induced by elastic stretching and pull-out of the z-pins. It was also found that z-pinning changed the failure mode of the T-joint. The unpinned joint failed by bond-line delamination cracking whereas the dominant fracture mode of the z-pinned joints was skin fracture (with large-scale bond-line cracking being resisted by the z-pins).

The mode I bridging traction laws for z-pinned laminates were adapted for z-pinned sandwich composites, and then applied to assess the parameters that would maximise the mechanical properties of T-joints. The analysis indicated that increasing the pin diameter and skin thickness will increase the joint properties, although this remains to be verified by experimental testing.

6.4 FUTURE WORK

The work presented in this PhD thesis contributes to the science and technology of z-pinned sandwich composites, although further research is needed to achieve an even greater understanding of these advanced materials. Described below are just three potential research topics which have been selected to promote the certification of z-pinned sandwich composites in aircraft structures.

6.4.1 Analytical Modelling of Z-Pinned Sandwich Composites

A comprehensive analysis of existing analytical models for calculating the through-thickness compressive properties revealed that they fail to accurately predict the stiffness and strength for sandwich composites reinforced with fibrous z-pins. This was attributed to the complex failure mechanism of the z-pins (involving kinking and splitting). A modification to the existing model was proposed, whereby the Budiansky-Fleck model for kinking of unidirectional fibre composites was used to predict the microbuckling failure stress of fibrous z-pins within the sandwich composite. However, this model was only able to capture one of several failure modes experienced by z-pins under compressive loading. Therefore, an analytical model that is able to capture every failure mode is required. Furthermore, given that the failure of metallic pins (involving buckling) is different to fibrous pins (kinking, splintering), the model should be able to analyse for both types of pins. In addition, the manufacturing quality of fibrous z-pins needs to be improved to achieve more consistent pin properties, which are currently variable due to porosity.

6.4.2 Finite Element Modelling of Z-Pinned Sandwich Composites

A finite element study into the elastic compression deformation of z-pinned sandwich composites was presented in chapter 3. Whilst the FE model was in agreement with analytical models in the prediction of the through-thickness properties, it was not an accurate representation of the actual response of z-pinned sandwich composites to compression loading. A finite element study that accurately represents the complex failure mechanism of fibrous z-pins is needed to be able to design aerospace sandwich composites. The finite element model should be able to capture the kinking, splitting and fracture of fibrous z-pins. This complex failure, being a result of pre-existing manufacturing flaws in the z-pins, needs to be accounted for in order to realistically

predict the compressive behaviour of z-pinned sandwich composites. As part of this work, the final production quality of fibrous z-pins needs to be investigated to determine the quantity, size and shape of pre-existing flaws to be able to accurately represent the anomaly of voids within z-pins.

6.4.3 Environmental Durability of Z-Pinned Sandwich Composites

Certification of z-pinned sandwich structures for aircraft requires a comprehensive study of their environmental durability, particularly under hot and moist conditions. Recent research has shown that the water absorption properties of carbon-epoxy laminates can be affected by z-pinning [119]. Thus far, a study on the environmental conditions such as heat, humidity and hot/wet conditions on the durability of z-pinned sandwich materials has not been performed. It is therefore recommended that the durability of z-pinned sandwich composites is investigated for various aviation environmental conditions. A detailed study into the physical changes and mechanical behaviour of z-pinned sandwich composites following conditioning in various environments should be conducted. An investigation into the damage tolerance of z-pinned sandwich composites under different environmental conditions should also be performed. It is also worthwhile investigating the performance of z-pinned sandwich T-joints under different operational environmental conditions.

6.4.4 Aircraft Certification of Composite Structural Components

Under FAR (Federal Aviation Regulations), certification of composite aircraft structural components requires a rigorous process whereby the materials and the manufacturing processes must undergo numerous trials and evaluation to finalize a repeatable and safe design. These criteria are specified under regulations §25.603, §25.605, §25.613 and §25.619. When certifying for material performance, environmental factors such as thermal and moisture analysis must be considered. Numerous static, dynamic and fatigue testing must be conducted at a coupon, component and structural level. Furthermore, the structural component must meet stringent requirements for damage tolerance and fatigue.

The introduction of z-pinned sandwich composites in primary aircraft structural components must therefore undergo the rigorous process of certification which includes testing, evaluation and improvements before z-pinned sandwich materials are used in aircraft. This PhD thesis provides a better understanding of the through-thickness properties and damage tolerance of z-pinned sandwich panels and joints. It finds the current models for predicting the through-thickness mechanical properties lacking and therefore makes suggestions for further improvement of these models. This thesis also investigates the potential for using z-pins to reinforce jointed structures as well, fulfilling a part of the research work needed to pave the way forward for these materials to be considered in future aircraft.

REFERENCES

1. Cutler, J. and J. Liber, *Understanding Aircraft Structures*. 3rd ed. 1998: Blackwell Science, USA.
2. Torres, M., W. Jonda, and J. Saporito, *Eurocopter Research in Composite Fuselage to Maintain the Production Cost Below the Target*, in *51st Annual Forum Proceedings – American Helicopter Society*. 1995, AHS, Alexandria: Fort Worth, TX, USA. p. pp. 1569-1584.
3. Evonik (2008) *ROHACELL® in Helicopter Rotor Blades for a Reliable Lift-Off*.
4. Huang, S.L., R.J. Richey, and E.W. Deska, *Cross reinforcement in a GR/EP laminate*, in *Annual winter meeting, American Society of Mechanical Engineers*. 1978.
5. Boyce, J.S., G.A. Freitas, C.L. Magee, T.M. Fusco, J.J. Harris, and E. Kunkel, *Ultrasonic Fastening System and Method*. 1998.
6. Krasnov, V.I., V.A. Kuznetsov, and A.Y. Maksokov, *Automated method of transverse reinforcement of composites by short fibres.* Mechanika Kompozitnykh Materialov, 1987. **3**: p. 449–504.
7. Tomashevskii, V.T., S.Y. Sitnikov, V.N. Shalgin, and V.S. Yakovlev, *A method of calculating technological regimes of transversal reinforcement of composites with short-fibre microparticles.* Mekhanika Kompozitnykh Materialov, 1989.
8. Tomashevskii, V.T., V.N. Shalgin, D.A. Romanov, and V.S. Sitnikov, *Transversal reinforcement of composite materials using ultrasonic vibrations.* Mekhanika Kompozitnykh Materialov, 1987.
9. Mouritz, A.P., *Review of z-pinned composite laminates.* Composites Part A: Applied Science and Manufacturing, 2007. 38(12): p. 2383-2397.
10. Baral, N., D.D.R. Cartié, I.K. Partridge, C. Baley, and P. Davies, *Improved impact performance of marine sandwich panels using through-thickness reinforcement: experimental results.* Composites Part B: Engineering, 2010. 41B: p. 117-123.
11. Davies, P., D. Choqueuse, and G. Bourbouze, *Microtomography to study high-performance sandwich structures.* J Sand Mat & Struct, 2011. 13: p. 7-21.
12. Engin, M.R. and H.R. Sami, *Material characteristics of 3-D FRP sandwich panels.* Const & Build Materials, 2007. 22: p. 1009-1018.
13. Grogan, J., S.A. Tekalur, A. Shukla, A. Bogdanovich, and R.A. Coffelt, *Ballistic resistance of 2D and 3D woven sandwich composites.* Journal of Sandwich Structures & Materials, 2007. 9: p. 283-302.
14. Judawisastra, H., J. Ivens, and I. Verpoest, *The fatigue behaviour and damage development of 3D woven sandwich composites.* Composite Structures, 1998. 43(1): p. 35-45.
15. Kunkel, E., E. Blaney, C. Magee, and D. Rich, *Sandwich structure and method of making same*, in *United States Patent US 6291049*. 2001: United States.
16. Lascoup, B., Khellil, M. Benzaggagh, Z. Aboura, and J. Maquet, *Stitched sandwich panel materials for resin infusion structures*. in *SAMPE J*. 2005.
17. Potluri, P., E. Kusak, and T.K. Reddy, *Novel stitch-bonded sandwich composite structures.* Journal of Composite Structures, 2003. 59: p. 251-259.
18. Preller, T., J. Brandt, and K. Dreschler. *Manufacturing and mechanical properties of new textile fiber preforms for structural sandwich applications,* . in *In Proceedings of Textile Composites in Building Construction*. 1990.
19. Raju, K.S. and J.S. Tromblin, *Energy absorption characteristics of stitched composite sandwich panels.* Journal of Composite Materials, 1999. 33: p. 712-728.
20. Sharma, S.C., M. Krisha, and H.N. Narasimha Murty, *Buckling response of stitched polyurethane foam composite sandwich structures.* Journal of Reinforced Plastics & Composites, 2004. 23: p. 1267-1277.

21. Stanley, L.E. and D.O. Adams. *Damage tolerance of stitched composite sandwich structures*. in *Proceedings of the SAMPE Technical Conference*. 2001. Long Beach CA.
22. Stoll, F. and R. Banerjee. *Measurement and analysis of fiber-composite-reinforced-foam sandwich core material properties*. in *Proceedings International SAMPE Symposium & Exhibition*. 2001. Long Beach, CA.
23. Stoll, F., R. Banerjee, S. Campbell, and S. Day, *Manufacture of fiber-reinforced-foam composite structures*. in *Proceedings of the. ASC 16th Annual Technical Conference*. 2001. Blacksburg, VA.
24. Sun, Q., X. Zhang, Y. Li, Y.N. Chai, and Z.H. Cao, *An experimental investigation on composites through-the-thickness stitched foam core sandwich panels.* Key Engineering Materials, 2007. 353-358(1443-1446).
25. Tekalur, S.A., A.E. Bogdanovich, and A. Shukla, *Shock loading response of sandwich panels with 3-D woven E-glass composite skins and stitched foam core.* Composite Science & Technology, 2009. 69: p. 736-753.
26. Vaidya, U.K., M.V. Kamath, M.V. Hosur, H. Mahfuz, and S. Jeelani, *Low-velocity impact response of cross-ply laminated sandwich composites with hollow and foam-filled z-pin reinforced core.* Journal of Composites Technology & Research, 1999. 21(84).
27. Van Vuure, A.W., J. Ivens, and I. Verpoest. *Sandwich panels produced from sandwich-fabric preforms*. in *Proceedings Symposium on Advanced Materials for Lightweight Structures*. 1994: ESTEC.
28. Verpoest, I., J. Ivens, A.W. Van Vuure, B. Gommers, P. Vandeurzen, S. Efstratiou, and D. Phillips, *New developments in advanced textiles for composites*. in *Proceedings 4th Japan Int. SAMPE Symposium*. 1995.
29. WebCore. *TYCOR® - a Superior Composite Core Solution*. 2011; Available from: http://www.webcoreonline.com/.
30. Xia, F. and X.-q. Wu, *Study on impact properties of through-thickness stitched foam sandwich composites.* Composite Structures. 92(2): p. 412-421.
31. Yang, X.T., J.F. Zhang, F. Yang, Y.N. Chai, and Y. Li, *Experimental and analytical study on the mechanical behaviour of stitched sandwich composite panel with a foam core.* Advanced Materials Research, 2008. 33-37: p. 477-482.
32. Zhang, X., L. Hounslow, and M. Grassi, *Improvement to low-velocity impact and compression-after-impact performance of z-fibre pinning*, in *13th International Conference on Composite Materials*. 2003: San Diego.
33. Zheng, X., L. Gou, X. Zheng, and J. Zhang, *Prediction of impact damage on stitched sandwich composite panels*. in *Proceedings of the 2nd International Conference on Smart Materials and Nanotechnology in Engineering*. 2009.
34. Cartié, D.D. and N.A. Fleck, *The effect of pin reinforcement upon the through-thickness compressive strength of foam-cored sandwich panels.* composite Science & Technology, 2003. 63: p. 2401-2409.
35. Steeves, C.A. and N.A. Fleck, *In-plane properties of composite laminates with through-thickness pin reinforcement.* International Journal of Solids and Structures, 2006. 43(10): p. 3197-3212.
36. Stringer, L.G. and M.J. Hiley, *Through-thickness reinforcement of composites : z-pinning, stitching and 3-D weaving*, in *14th international conference on composite materials*. 2003: San Diego.
37. Du, L., J. Guiqiong, and H. Tao, *Z-pin reinforcement on the core shear properties of polymer foam sandwich composites.* Journal of Composite Materials, 2009.
38. Mouritz, A.P., *Compression properties of z-pinned sandwich composites.* Journal of Materials Science, 2006. 41: p. 5771-5774.
39. Liu, T., Z.C. Deng, and T.J. Lu, *Analytical modeling and finite element simulation of the plastic collapse of sandwich beams with pin-reinforced foam cores.* International Journal of Solids and Structures, 2008. 45: p. 5127-5151.
40. Long, D. and J. Guiqiong, *Indentation study of z-pin reinforced polymer foam core sandwich structures.* Composites, 2009. 40A: p. 822-829.
41. Rice, M.C., C.A. Fleischer, and M. Zupan, *Study on the collapse of pin-reinforced foam sandwich panel cores.* Experimental Mechanics, 2006. 46: p. 197-204.

42. Tong, L., A.P. Mouritz, and M.K. Bannister, in *3D Fibre Reinforced Polymer Composites*. 2002, Elsevier Science: Oxford.
43. Partridge, I., T. Bonnington, and D. Cartié, *Manufacture and Performance of Z-Pinned Composites*, in *Advanced Polymeric Materials*. 2003, CRC Press.
44. Marasco, A.I., D.D.R. Cartié, I.K. Partridge, and A. Rezai, *Mechanical properties balance in novel z-pinned sandwich panels: out-of-plane properties.* Composites 2006. 37A: p. 295-302.
45. Palazotto, A.N., L.N.B. Gummadi, U.K. Vaidya, and E.J. Herup, *Low velocity impact damage characteristics of z-fiber reinforced sandwich panels – an experimental study.* Composite Structures, 1999. 43: p. 275-288.
46. Vaidya, U.K., S. Nelson, B. Sinn, and B., *Processing and high strain rate impact response of multi-functional sandwich composites.* Composite Structures, 2001. 52: p. 429-440.
47. Vaidya, U.K., A.N. Palazotto, and L.N.B. Gummadi. *Low velocity impact and compression-after-impact response of z-pin reinforced core sandwich composites*. in *ASME*. 2000.
48. Anon, L.K., *Z-Pins strengthen the Super Hornet, save weight and cost.* The Integrator, 2001. **3**: p. 1-2.
49. McBeath, S., *Safety pins. Racecar Engineering* 2002. p. 56-62.
50. Childress, J.J. and G. Freitas, *Z-Direction pinning of composite laminates for increased survivability*, in *AIAA aerospace design conference*. 1992: Irvine, California. p. 92–109.
51. Cartié, D.D.R. and I.K. Partridge, *Delamination Behaviour of Z-Pinned Laminates*, in *Proceedings of the 2nd European Structural Integrity Society Technical Committee 4 Conference*. 1999, Elsevier: Les Diablerets, Switzerland.
52. Cartié, D.D.R. and I.K. Partridge, *Delamination behaviour of z-pinned laminates*, in *Proceedings of the 12th International Conference on Composite Materials*. 1999: Paris, France.
53. Graftieaux, B., A. Rezai, and I. Partridge, *Effects of z-pin reinforcement on the delamination toughness and fatigue performance of unidirectional AS4/8552 composite*, in *ECCM-9*. 2000: Brighton, UK.
54. Chang, P., *The mechanical properties and failure mechanisms of z-pinned composites*. 2006, Royal Melbourne Institute of Technology.
55. Chang, P., A.P. Mouritz, and B.N. Cox, *Properties and failure mechanisms of z-pinned laminates in monotonic and cyclic tension.* Composites 37A, 2006. 1501-13.
56. Cox, B.N., M.S. Dadkhah, R.V. Inman, W.L. Morris, and J. Zupon, *Mechanisms of compressive failure in 3D composites.* Acta Metallurgica et Materialia, 1992. 40(12): p. 3285-3298.
57. Dickinson, L.C., G.L. Farley, and M.K. Hinders, *Prediction of effective three-dimensional elastic constants of translaminar reinforced composites.* Journal of Composite Materials, 1999. 33: p. 1002-29.
58. Steeves, C. and N.A. Fleck, *In-plane properties of composite laminates with through-thickness pin reinforcement.* Int J Solids Struct, 2006. 43: p. 3197–212.
59. Steeves, C. and N.A. Fleck, *In-plane properties of CFRP laminates containing through-thickness reinforcing rods (zpins)*, in *Proceedings of the 12th International Conference on Composite Materials*. 1999: Paris, France.
60. Sweeting, R.D. and R.S. Thomson, *The effect of thermal mismatch on Z-pinned laminated composite structures.* Composite Structures, 2004. 66(1-4): p. 189-195.
61. Freitas, G., T. Frusco, T. Campbell, J. Harris, and S. Rosenberg. *Z-fiber technology and products for enhacing composite design*. in *83rd Meeting of the AGARD SMP on "Bolted/Bonded Joints in Polymeric Composites"*. 1996. Florence, Italy.
62. Cartié, D.D.R., B.N. Cox, and N.A. Fleck, *Mechanisms of crack bridging by composite and metallic rods.* Composites Part A: Applied Science and Manufacturing, 2004. 35(11): p. 1325-1336.
63. Cartié, D.D.R., G. Dell'Anno, E. Poulin, and I.K. Partridge, *3D reinforcement of stiffener-to-skin T-joints by Z-pinning and tufting.* Engineering Fracture Mechanics, 2006. **73**(16): p. 2532-2540.

64. Cartie´, D.D.R., *Effects of z-fibres on the delamination behaviour of carbon fibre/epoxy laminates.* 2000, Cranfield University.
65. Cox, B.N., *Mechanisms and models for delamination in the presence of through-thickness reinforcement.* Advanced Composites Letters, 1999. 8: p. 249–56.
66. Rugg, K.L., B.N. Cox, and R. Massabo`, *Mixed mode delamination of polymer composite laminates reinforced through the thickness by z-fibres.* Composites, 2002. 33: p. 177–90.
67. Partridge, I.K., D.D.R. Cartie´, M. Troulis, M. Grassi, and X. Zhang, *Evaluating the mechanical effectiveness of z-pinning*, in *SAMPE technical conference*. 2004.
68. Troulis, M., D.D.R. Cartie, L. Bartattoni, and I.K. Partridge, *z-Pinned woven laminates: Interlaminar fracture results and pinning quality considerations*, in *Proceedings of the 6th international conference on deformation and fracture of composites*. 2001: Manchester, UK.
69. Rezai A, C.D., Partridge I, Irving P, Aston T, Negre P, Langer J., *Interlaminar damage resistance of z-fibre reinforced structural CFRP*, in *13th International Conference on Composite Materials*. 2001: Beijing.
70. Koh, T.M., S. Feih, and A.P. Mouritz, *Strengthening mechanics of thin and thick composite t-joints reinforced with z-pins.* Composites Part A, 2012. 43(8): p. 1308-1317.
71. Cartie´, D.D.R., B.N. Cox, and B.N. Fleck, *Mechanisms of crack bridging by composite and metallic rods.* Composites 2004. 35A: p. 1325–36.
72. Cox, B.N. and N. Sridhar, *A traction law for inclined fibre tows bridging mixed mode cracks.* Mechanics of Composite Materials and Structures, 2002. 9: p. 299-331.
73. Rugg, K.L., B.N. Cox, K.E. Ward, and G.O. Sherrick, *Damage mechanisms for angled through-thickness rod reinforcement in carbon-epoxy laminates.* Composites A, 1998. 29: p. 1603–13.
74. Cox, B.N., *Snubbing effects in the pullout of a fibrous rod from a laminate.* Mechanics of Advanced Material Structures, 2005. 12: p. 85-98.
75. Dai, S.-C., et al., *Experimental study on z-pin bridging law by pullout test.* Composites Science and Technology, 2004. 64(16): p. 2451-2457.
76. Zhang, A.Y., H.-Y. Liu, A.P. Mouritz, and Y.-W. Mai, *Experimental study and computer simulation on degradation of z-pin reinforcement under cyclic fatigue.* Composites Part A: Applied Science and Manufacturing, 2008. 39(2): p. 406-414.
77. Isa, M.D., S. Feih, and A.P. Mouritz, *Compression fatigue properties of z-pinned quasi-isotropic carbon/epoxy laminate with barely visible impact damage.* Composite Structures, 2011. 93(9): p. 2269-2276.
78. Grassi, M., *Numerical modelling of composite laminates with through-thickness reinforcements*. 2000, Cranfield University.
79. Grassi, M., X. Zhang, and M. Meo, *Prediction of stiffness and stresses in z-fibre reinforced composite laminates.* Composites Part A, 2002. 33: p. 1653-64.
80. Carstensen, T., D. Cournoyer, E. Kunkel, and C. Magee, *X-cor advanced sandwich core material*, in *Proceedings of the 33rd International SAMPE Technical Conference*. 2001: Seattle, WA.
81. Casari, P., D. Cartié, and P. Davies, *Characterization of Novel K-Cor Sandwich Structures.* Sandwich Structures 7: Advancing with Sandwich Structures and Materials, 2005: p. 865–874.
82. Freitas, G., C. Magee, P. Dardzinski, and T. Fusco, *Fiber insertion process for improved damage tolerance in aircraft laminates.* Journal of Advanced Materials, 1994. 25: p. 36-43.
83. O'Brien, T.K. and R. Krueger, *Influence of compression and shear on the strength of composite laminates with z-pinned reinforcement*. Appl Compos Mater 2006. 13: p. 173-89.
84. Steeves, C.A. 2001, University of Cambridge.
85. Chang, P., A.P. Mouritz, and B.N. Cox, *Flexural properties of z-pinned laminates.* Composites Part A: Applied Science and Manufacturing, 2007. 38(2): p. 244-251.
86. Mouritz, A.P., M.K. Bannister, P.J. Falzon, and K.H. Leong, *Review of applications for advanced three-dimensional fibre textile composites.* Composites Part A: Applied Science and Manufacturing, 1999. 30(12): p. 1445-1461.

87. Long, D., J. Guiqiong, and H. Tao, *Investigation of the effect of Z-pin reinforcement on the collapse of foam-cored sandwich panels.* Reinforced Plastics and Composites, 2008. 27: p. 1121-1224.
88. Türk, M.H. and M.S.H. Fatt, *Localized damage response of composite sandwich plates.* Composites Part B: Engineering, 1999. 30(2): p. 157-165.
89. Du, L., G.Q. Jiao, and T. Huang, *Investigation of the effect of z-pin reinforcement on the collapse of foam-cored sandwich panels.* Journal of Reinforced Plastics & Composites, 2008. 27: p. 1211-1224.
90. Guo, S. and R. Morishima, *Numerical analysis and experiment of composite sandwich T-joints subjected to pulling load.* Composite Structures, 2011. 94: p. 229-238.
91. Shenoi, R.A., P.J.C.L. Read, and C.L. Jackson, *Influence of joint geometry and load regimes on sandwich tee joint behaviour.* Journal of Reinforced Plastics & Composites, 1998. 17(8): p. 725-40.
92. Theotokoglou, E.E. and T. Moan, *Experimental and Numerical Study of Composite T-Joints.* Journal of Composite Materials, 1996. 30(190-209).
93. Turuga, U.V.R.S., *A study of Sandwich T-joints and Composite Lap Joints*. 2003, Purdue University.
94. Turuga, U.V.R.S. and T.C. Sun, *Failure Modes and Load Transfer in Sandwich T-joints.* Journal of Sandwich Structures & Materials, 2000. 2(225).
95. Chang, P., A.P. Mouritz, and B.N. Cox, *Tensile properties and failure mechanisms of z-pinned composite lap joints.* Composite Science & Technology, 2006. 66: p. 2163–76.
96. Chang, P., A.P. Mouritz, and B.N. Cox, *Elevated temperature of pinned composite laminate joints.* Journal of Composite Materials, 2008. 42: p. 741-769.
97. Grassi, M., B.N. Cox, and X. Zhang, *Simulation of pin-reinforced single-lap composite joints.* Composite Science & Technology, 2006. 66: p. 1623–38.
98. Owsley, G.S., *The effect of z-fibre™ reinforcement on fatigue properties of stiffened composite panels*, in *Proceedings of the 15th technical conference of the american society of composites*. 2000: Texas.
99. Koh, T.M., S. Feih, and A.P. Mouritz, *Experimental determination of the structural properties and strengthening mechanisms of z-pinned composite T-joints.* Composite Structures, 2011. 93(9): p. 2222-2230.
100. Koh, T.M., A. P. Mourtiz and S.Feih., *Improving the structural properties and damage tolerance of composite joints using z-pins.* Journal of Composite Materials, in press.
101. Park, Y.-B., Park, Y.-B., B.-H. Lee, J.-H. Kweon, J.-H. Choi, and I.-H. Choi, *The strength of composite bonded T-joints transversely reinforced by carbon pins.* Composite Structures, 2012. 94(2): p. 625-634.
102. Toral-Vazquez, J., B. Castanie, J.J. Barrau, and S. Didierjean, *Experimental analysis and modeling of z-pinned joints under pull-out, shear and flexure loadings*, in *Proceedings of the 4th international conference on composite testing and model identification*. 2008: Ohio.
103. Du, L., J. Guiqiong, and H. Tao, *The elastic properties of sandwich structures with z-pinned foam core.* Journal of Reinforced Plastics & Composites, 2008. 28: p. 318-831.
104. Kocher, C., W. Watson, M. Gomez, I. Gonzalez, and V. Birman, *Integrity of sandwich panels and beams with truss-reinforced cores.* Journal of Aerospace Engineering, 2002. 15: p. 111-117.
105. Budiansky, B. and N.A. Fleck, *Compressive failure of fibre composites.* Journal of the Mechanics and Physics of Solids, 1993. 41(1): p. 183-211.
106. Budiansky, B. and N.A. Fleck, *Compressive kinking of fiber composites: A topical review.* Appl Mech Rev, 1994. 47(6).
107. Argon, A.S., *Fracture of Composites*. Treatise of Materials Science and Technology. Vol. 1. 1972, New York: Academic Press.
108. Fan, X. and W. Xiao-qing, *Study on the impact properties of through-thickness stitched foam sandwich composites.* Composite Structures, 2010. 92: p. 412-421.
109. Johnson, K.L., *Contact Mechanics*. 1985: Cambridge University Press.

110. Cailletaud, G., S. Basseville, and V.A. Yastrebov (2010) *Contact mechanics 1: basics*. WEMESURF short course on contact mechanics and tribology.
111. Liu, H.-Y., W. Yan, X.-Y. TYu, and Y.-W. Mai, *Experimental study on z-pinned DCB mode I delamination*, in *Proceedings of the International Conference on Structural Integrity & Fracture* 2004: Brisbane, Australia.
112. Mouritz, A.P. and B.N. Cox, *A mechanistic interpretation of the comparative in-plane mechanical properties of 3D woven, stitched, and pinned composites.* Composites Part A, 2010. 41: p. 709-728.
113. Mouritz, A.P., *Compression properties of z-pinned composite laminates.* Composites Science & Technology, 2007. 67: p. 3110-3120.
114. O'Brien, T.K. and R. Krueger, *Influence of compression and shear on the strength of composite laminates with z-pinned reinforcement.* Applied Composite Materials, 2006. 13: p. 173-189.
115. Byrd, L.W. and V. Birman, *Effectiveness of z-pins in preventing delamination of co-cured composite joints on the example of a double cantilever test.* Composites 37B, 2006: p. 365-378.
116. Toral-Vazquez, J., J., B. Castanie, J.-J. Barrau, and N. Swiergiel, *Multi-level analysis of low-cost z-pinned composite joints Part 2: joint behaviour.* Composites, 42A, 2011: p. 2082-2092.
117. Jain, L.K. and R.C. Wetherhold, *The effect of fibre extensibility on the fracture toughness of short fibre/brittle matrix composites.* App Mech Reviews, 1992. 45: p. 377-389.
118. Barrett, D.J., *The mechanics of z-fibre reinforcement.* Composite Structures, 1996. 36: p. 23-32.
119. Mouritz, A.P., *Moisture absorption and degradation of z-pinned carbon fibre-epoxy laminate.* Composites Science and Technology, 2012. 72: p. 1568-1574.